

**A RATIONAL APPROACH TO ESTIMATE REASONABLE DESIGN  
VALUES OF SELECTED JOINTS BY USING LOWER  
TOLERANCE LIMITS**

by  
**Mesut Uysal**

**A Dissertation**

*Submitted to the Faculty of Purdue University  
In Partial Fulfillment of the Requirements for the degree of*

**Doctor of Philosophy**



Department of Forestry & Natural Resources

West Lafayette, Indiana

May 2019

**THE PURDUE UNIVERSITY GRADUATE SCHOOL**  
**STATEMENT OF COMMITTEE APPROVAL**

Assoc. Prof. Eva Haviarova, Chair

Department of Forestry and Natural Resources, College of Agriculture,  
Purdue University

Prof. Rado Gazo

Department of Forestry and Natural Resources, College of Agriculture,  
Purdue University

Assoc. Prof. Henry J. Quesada

Department of Sustainable Biomaterials, College of Natural Resources and  
Environment, Virginia Tech

Assistant Prof. Mo Zhou

Department of Forestry and Natural Resources, College of Agriculture,  
Purdue University

**Approved by:**

Prof. Robert G. Wagner

Head of the Graduate Program

*This dissertation  
dedicated to  
“GOODNESS”  
which always exists, never disappears,  
we have somewhere inside,  
we look for,  
we are looking for,  
and we will look for.*

## ACKNOWLEDGMENTS

I am grateful to all of those with whom I have had the pleasure to work during my Ph.D. degree at Purdue FNR. I would like to express wholeheartedly the deepest gratitude to my advisor and mentor Dr. Eva Haviarova, for her teaching in so many aspects, her enthusiasm, innovative ideas, assistance, easy cooperation and endless patience. Thanks to her, I was part of this project where I could expand my knowledge in the research area of my interest. I benefited tremendously from her rich pool of ideas. Furthermore, I would like to express deep appreciation to my Dissertation Committee members, Dr. Rado Gazo, Dr. Henry J. Quesada and Dr. Mo Zhou, who has provided me with extensive personal and professional guidance and taught me a great deal about scientific research and life in general.

I would like to extend a profound thank you to Dr. Carl A. Eckelman who was one of my academic mentor. Dr. Eckelman helped me to expand his initial ideas into my dissertation and his assistance during my experimental studies. Also, I would like to appreciate Dr. Derek S. Young from Department of Statistics at Kentucky State University and Tianyang Hu from Purdue Statistical Consulting Service for their help in this project. I would like to also acknowledge support of the Wood Research Lab Technician Dan Bollock, as well as clerical and business staff in the FNR department.

This work would not have been possible without the financial support from the Ministry of National Education in Republic of Turkey, Purdue University FNR and Billsland Dissertation Fellowship. These funding sources provided me with opportunities to expand my knowledge in academic field where I had a chance to interact with people in my research field around the world.

Also, I would like to thank Pike Lumber Company and Jasper Group which helped this project by providing wood materials and chair specimens.

I would like to thank my mother – my first teacher, my father – my role model, and my brother – my long-life friend. Their love and guidance are always with me in whatever I pursue and wherever I am.

I am also grateful to my friend and my officemate, Cagatay Tasdemir, who is always with me, supports me and encourage me to do better from the time we were in college. Besides, I appreciated my roommate, Aktan Alpsoy, who encourage me during my Ph.D. study. Also, I would like to thank my officemates – Logan Wells, Yue Zhao and Fanyou Wu who shared their experience and helped me during my Ph.D. study.

I would like to express my gratitude to Tulin Ece Tosun who is my friend and helped me to edit this dissertation.

Also, I would like to thank my friends – Buket Tasdemir, Aytakin Uzunoglu, Burak M. Koca, Mert M. Torunbalci, Ramazan Oduncu, Leyla N. Kahyaoglu, Tugba Yuksel, Hazal Turasan, Oguz K. Ozturk, Sena Agim, Aslihan Terzi, Irem Korucu, Ezgi Besikci, Burak Bal, Jinsha Li, Jared Sharp, Josh Roberts and Marc Dobbels who helped me socialize with their friendships during my Ph.D. study.

And finally, I would like to express my acknowledgment to everyone who I have been communicating scientifically and socially. It was great pleasure to share knowledge and experiences with all of you during last five years at Purdue.

## TABLE OF CONTENTS

LIST OF TABLES .....	10
LIST OF FIGURES .....	12
LIST OF ABBREVIATIONS AND SYMBOLS .....	17
ABSTRACT.....	19
CHAPTER 1. INTRODUCTION .....	22
1.1 General Overview .....	22
1.2 Statement of Problem.....	26
1.3 Aims and Objectives.....	29
1.4 Research Hypothesis.....	30
1.5 Significance of Study.....	30
CHAPTER 2. LITERATURE REVIEW .....	36
2.1 Structural Analysis of Chair Frames.....	36
2.1.1 Loads Consideration in Furniture Design.....	38
2.1.1.1 Static Loads in chair Frames .....	39
2.1.1.2 Cyclic Load of Chair Frames.....	42
2.1.1.2.1 Constant Cyclic Loads .....	42
2.1.1.2.2 Stepwise Cyclic Loads .....	42
2.1.1.2.3 Palmgren-Miner Rule to Predict Fatigue Life of Chairs.....	50
2.2 Joint Properties.....	51
2.2.1 Mortise and tenon joints .....	58
2.2.2 Dowel Joints .....	71
2.2.3 Screws.....	82
2.3 Load and Design Consideration.....	87
2.3.1 Load and Design Consideration in Wood Structural Engineering .....	88
2.3.1.1 Allowable Design Stress of Wood Structures .....	89
2.3.1.2 Load and Resistance Factor.....	91
2.3.2 Load and Design Consideration in Furniture Engineering.....	92
2.4 Recommended Standards for Chair Frames .....	94
2.4.1 Recommendations from American Library Association.....	94

2.4.2	Recommendation from Bureau and Institutional Furniture for Manufacturers.	94
2.5	Structural Reliability Analysis with Probabilistic Approaches	95
2.6	Statistical Tolerance Limits	100
2.7	Sample Size Determination for Tolerance Limits	104
2.7.1	Monte Carlo Sampling	105
2.7.2	Latin Hypercube Sampling	105
2.7.3	Faulkenberry-Weeks Methods	106
2.8	Determination of Confidence/Proportion Level for Tolerance Analysis	107
CHAPTER 3. LOWER TOLERANCE LIMITS FOR SELECTED FURNITURE JOINTS		108
3.1	Introduction	108
3.2	Materials and Methods	109
3.2.1	Materials	109
3.2.1.1	Wood Materials	109
3.2.1.2	Adhesive	112
3.2.1.3	Screws	112
3.2.2	Specimen Construction	112
3.2.3	Methods	115
3.2.3.1	Test Procedure	115
3.2.3.1.1	Determination of Some Mechanical and Physical Properties of Wood Materials	115
3.2.3.1.2	Joint Strength	117
3.2.3.2	Lower Tolerance Limits Method	119
3.2.3.2.1	Determination of Sample Size for Tolerance Intervals	119
3.2.3.2.2	Determination of Lower Tolerance Limits	120
3.3	Results and Discussion	126
3.3.1	Mechanical and Physical Properties of Wood Material	126
3.3.2	Determination of Minimum Sample Size Requirements for Univariate Tolerance Analysis	127
3.3.3	Joint Strength	133

3.3.3.1	Bending Strength of Rectangular Mortise and Tenon Joints.....	133
3.3.3.2	Bending Strength of Two-Pin Bending Resisting Dowel Joints .....	134
3.3.3.3	Screw Withdrawal Strength in Wood.....	135
3.3.3.3.1	Screw Withdrawal Strength in Wood from End-Grain.....	135
3.3.3.3.2	Screw Withdrawal Strength in Wood from Edge-Grain .....	135
3.3.3.3.3	Screw Withdrawal Strength in Wood from Face-Grain.....	136
3.3.4	Tolerance Analysis .....	137
3.3.4.1	Normality Assumption for Tolerance Analysis.....	137
3.3.4.2	Lower Tolerance Limits for Furniture joints.....	146
3.4	Conclusion .....	172
CHAPTER 4. DESIGN OF FURNITURE JOINTS .....		175
4.1	Introduction.....	175
4.2	Materials and Method .....	175
4.2.1	Structural Analysis of Chair Frame .....	175
4.2.2	Design of Joints .....	177
4.3	Results and Discussion .....	181
4.4	Conclusion .....	187
CHAPTER 5. PERFORMANCE TEST OF CHAIR FRAMES .....		189
5.1	Introduction.....	189
5.2	Materials and Methods.....	190
5.2.1	Specimen Construction.....	190
5.2.2	Test Procedure .....	191
5.2.2.1	Vertical Statically Load Test .....	191
5.2.2.2	Front-to-Back Cyclic Load Test.....	192
5.3	Results and Discussion .....	193
5.4	Conclusion .....	198
CHAPTER 6. SUMMARY AND CONCLUSION.....		200
6.1	Summary.....	200
6.2	Recommendations.....	203
6.3	Limitations .....	204
6.4	General Conclusion.....	205

APPENDIX A. TABLES FOR RATIONAL DESIGN OF JOINTS .....	207
APPENDIX B. SAMPLE PREPARATION AND TESTING .....	212
APPENDIX C. TABLES FOR K-TOLERANCE FACTOR DEPENDING ON SMAPLE SIZES AND ASSUMPTION.....	215
REFERENCES .....	231
VITA.....	246
PUBLICATIONS.....	247

## LIST OF TABLES

Table 1.1 1960-2015 Data on Wood in MSW by Weight .....	31
Table 2.1 Summary of Performance Test Load Schedule .....	49
Table 2.2 Calculation of The Fatigue Life for Red Oak Joint Using Palmgren-Miner Rule. .....	51
Table 2.3 Average Ultimate Withdrawal Strength of Dowels.....	74
Table 2.4 Experimental Average Ultimate and Predicted Bending Moment Capacity, and Moment-Rotational Coefficients of Dowel Joints at Various Rail Dimension and Dowel Spacing.....	75
Table 2.5 Average Ultimate Strength and Stiffness of Dowel Joints .....	76
Table 2.6 Screw Diameter and Suggested Pilot Hole Sizes .....	83
Table 2.7 Expressions to Predict Screw Withdrawal Strength in Wood and Wood Composite .....	83
Table 2.8 Some Test Types and Acceptable Load Levels for Chair Frames in Performance Tests .....	94
Table 2.9 Some Test Types and Test Procedure in ANSI/BIFMA X5.1-2017 .....	95
Table 3.1 Some Mechanical properties of Northern Red Oak and White Oak Wood at 12% Moisture Content .....	111
Table 3.2 Nomenclature of Sample Groups.....	118
Table 3.3 Error of Approximation Related to z-Score.....	124
Table 3.4 Some Mechanical and Physical Properties of Wood Material .....	126
Table 3.5 Bending Test of T-Shaped Joints.....	128
Table 3.6 Screw Withdrawal Strength of Wood.....	128
Table 3.7 Test Results for Bending Strength of RMT and Dowel Joints .....	133
Table 3.8 Test Results of Screw Withdrawal Strength in Wood .....	137
Table 3.9 Normality Test Results for RMT and Dowel Joints .....	138
Table 3.10 Normality Test Results for Screw Withdrawal Strength in Wood .....	138
Table 3.11 LTLs, Ratio of Mean and LTLs and, Number and Percentage of Values below LTLs Corresponding Confidence/Proportion Levels for RMT and Dowel Joints .....	155

Table 3.12 LTLs, Ratio of Mean and LTLs and, Number and Percentage of Values below LTLs Corresponding Confidence/Proportion Levels for Screw Withdrawal Strength in Wood.....	168
Table 3.13 continued LTLs, Ratio of Mean and LTLs and, Number and Percentage of Values below LTLs Corresponding Confidence/Proportion Levels for Screw Withdrawal Strength in Wood.....	169
Table 4.1 Dimensional Parameters for RMT Joints.....	182
Table 4.2 Dimensional Parameters for Dowel Joints.....	182
Table 4.3 Internal Stresses for RMT and Dowel Joints .....	183
Table 4.4 Factors in Equation and Joint Dimension for RMT Joints .....	185
Table 4.5 Factors in Equation and Joint Dimension for Dowel Joints .....	185
Table 4.6 Most Commonly Used Drill Bits Sizes .....	188
Table 5.1 Member Dimensions Used in Chair .....	190
Table 5.2 Performance Test Results of Chair Frames .....	195
Table 5.3 Evaluation of the Cyclic Front-to-Back Load Test Results Corresponding to ALA Specifications.....	197

## LIST OF FIGURES

Figure 1.1 History of Furniture Design.....	22
Figure 1.2 Similarity in Chair Structure .....	23
Figure 1.3 Quality Aspect of Furniture.....	24
Figure 1.4 Irregular Load History in Structure .....	25
Figure 1.5 First Crossing Concept in Fatigue Life of Structure. ....	27
Figure 1.6 Example of Recalls for Furniture .....	32
Figure 1.7 2017 data on recalls for children product.....	32
Figure 1.8 Impact of Reliability on Elaboration Cost and Operation Cost.....	33
Figure 1.9 The Relationship Between Product Reliability and Warranty Concept .....	34
Figure 1.10 2003-2017 Data on Furniture Warranty Claims Paid by 34 U.S. Based Companies .....	35
Figure 2.1 Degrees of Freedom in the A. Plane (2D) and B. Space (3D) System.....	37
Figure 2.2 Degrees of Freedom in A. Full Chair Frame and B. Side Chair Frame .....	38
Figure 2.3 Configuration of Some Possible Point Load Types in Side Chair Frame .....	39
Figure 2.4 Schematic Description of Simple Side Chair Frames .....	40
Figure 2.5 Bending Moment of Members and Deflected Shape on Statically Determinate Side Frame .....	40
Figure 2.6 Degrees of Freedom for Element Stiffness .....	41
Figure 2.7 Bending Moment Capacity of Members and Deflected Shape on Statically Indeterminate Side Frame.....	42
Figure 2.8 Configuration of Specimen for Joint Performance Test.....	43
Figure 2.9 Stepwise Load Model on Chair/Joint Specimen According to GSA .....	43
Figure 2.10 Configuration of Cyclic Vertical Load Test on Seats .....	44
Figure 2.11 Depiction of Cyclic Front-to-Back Load Test on Chair Frame.....	45
Figure 2.12 Depiction of Cyclic Back-to-Front Load Test on Chair Frame.....	46
Figure 2.13 Depiction of Cyclic Side-Thrust Load Test on Chair Frame .....	47
Figure 2.14 Depiction of Cyclic Front-to-Back Load Test on Chairs Backrest .....	48
Figure 2.15 Depiction of Cyclic Side-Thrust Load Test on Arm .....	49
Figure 2.16 M-N Curve from Constant Bending Test of Red Oak Joints .....	51

Figure 2.17 A wooden Chair Anatomy.....	52
Figure 2.18 Load Scheme of Joints in Diagonal Tension Test.....	53
Figure 2.19 Load Scheme of Joints in Diagonal Compression Tes.....	54
Figure 2.20 Load Scheme of Joints in Bending Test .....	55
Figure 2.21 Characteristics of the Stiffness of Joints .....	56
Figure 2.22 Mechanical Fasteners Used in Furniture Constructions.....	57
Figure 2.23 Classification of Furniture Joints Used in Furniture Construction.....	57
Figure 2.24 Schematic Depiction of Test Methods for Joint Tests.....	58
Figure 2.25 Depiction of Tight-Fitting Rectangular Mortise and Tenon.....	59
Figure 2.26 Depiction of Tight-Fitting Rectangular Mortise and Tenon with rounded Mortise .....	59
Figure 2.27 Depiction of Poor Matched Rectangular Mortise and Tenon.....	60
Figure 2.28 Effect of Tenon Length and Width on Joint Strength .....	61
Figure 2.29 Two Pin Moment Resisting Dowel Joint Configuration.....	72
Figure 2.30 Application of Monte Carlo Sampling in Tolerance Analysis .....	105
Figure 2.31 Application of Latin Hypercube Sampling in Tolerance Analysis .....	106
Figure 3.1 A. Northern Red Oak Wood and B. White Oak Wood .....	110
Figure 3.2 Configuration of Screw Used in Study.....	112
Figure 3.3 Configuration of RMT Joints .....	113
Figure 3.4 Configuration of Two Pin Moment Resisting Dowel Joints .....	114
Figure 3.5 Configuration of Specimens for Screw Withdrawal Strength in wood from, End-, Edge- and Face-Grain. ....	115
Figure 3.6 Delmhorst J-2000 Device to Measure MC in Wood.....	116
Figure 3.7 Configuration of Static Bending Test .....	117
Figure 3.8 Configuration of Bending Test Set Up.....	118
Figure 3.9 Configuration of Screw Withdrawal Test Set Up.....	118
Figure 3.10 Flow Chart for Calculation Process of LTLs .....	122
Figure 3.11 Curve Bell. a: One-Sided, b: Two-Sided.....	123
Figure 3.12 Load-Displacement Curves in Static Bending Test for Red Oak.....	127
Figure 3.13 Load-Displacement Curves in Static Bending Test for White Oak .....	127
Figure 3.14 Histogram, Density and Q-Q plots of RMT Joints Made of Red Oak .....	129

Figure 3.15 Histogram, Density and Q-Q Plots of RMT Joints Made of White Oak.....	129
Figure 3.16 Histogram, Density and Q-Q plots of Dowel Joints Made of Red Oak .....	130
Figure 3.17 Histogram, Density and Q-Q Plots of Dowel Joints Made of White Oak...	130
Figure 3.18 Histogram, Density and Q-Q Plots of Screw Withdrawal in Wood Made of Red Oak from End-Grain.....	130
Figure 3.19 Histogram, Density and Q-Q Plots of Screw Withdrawal in Wood Made of White Oak from End-Grain .....	131
Figure 3.20 Histogram, Density and Q-Q Plots of Screw Withdrawal in Wood Made of Red Oak from Edge-Grain.....	131
Figure 3.21 Histogram, Density and Q-Q Plots of Screw Withdrawal in Wood Made of White Oak from Edge-Grain.....	131
Figure 3.22 Histogram, Density and Q-Q Plots of Screw Withdrawal in Wood Made of Red Oak from Face-Grain.....	132
Figure 3.23 Histogram, Density and Q-Q Plots of Screw Withdrawal in Wood Made of White Oak from Face-Grain .....	132
Figure 3.24 Minimum Sample Size Requirement Given $\gamma/P$ Levels.....	133
Figure 3.25 Average Ultimate Bending Moment Capacity of RMT Joints.....	134
Figure 3.26 Average Ultimate Bending Moment Capacity of Two Pin Moment Resisting Dowel Joints.....	134
Figure 3.27 Average Ultimate Screw Withdrawal Strength in Wood from End-Grain (in N) .....	135
Figure 3.28 Average Ultimate Screw Withdrawal Strength in Wood from Edge-Grain.....	136
Figure 3.29 Average Ultimate Screw Withdrawal Strength in Wood from Face-Grain .....	137
Figure 3.30 Histogram, Q-Q plot and ECDF Plots for RMT Joints Made of Red Oak..	139
Figure 3.31 Histogram and Q-Q Plots for RMT Joints Made of White Oak.....	140
Figure 3.32 Histogram, Q-Q and ECDF Plots for Dowel Joints Made of Red Oak.....	141
Figure 3.33 Histogram and Q-Q Plots for Dowel Joints Made of White Oak.....	142
Figure 3.34 Histogram and Q-Q Plots for Screw Withdrawal Strength in Wood Made of Red Oak from End-Grain.....	142

Figure 3.35 Histogram and Q-Q Plots for Screw Withdrawal Strength in Wood Made of White Oak from End-Grain .....	143
Figure 3.36 Histogram and Q-Q Plots for Screw Withdrawal Strength in Wood Made of Red Oak from Edge-Grain.....	143
Figure 3.37 Histogram and Q-Q Plots for Screw Withdrawal Strength in Wood Made of White Oak from Edge-Grain.....	144
Figure 3.38 Histogram and Q-Q Plots for Screw Withdrawal Strength in Wood Made of Red Oak from Face-Grain.....	145
Figure 3.39 Histogram and Q-Q Plots for Screw Withdrawal Strength in Wood Made of White Oak from Face-Grain .....	145
Figure 3.40 LTLs for RMT Joints Made of Red Oak.....	146
Figure 3.41 LTLs in Data Chart and Histogram of RMT Joints Made of Red Oak .....	148
Figure 3.42 LTLs for RMT Joints Made of White Oak .....	149
Figure 3.43 LTLs in Data Chart and Histogram of RMT Joints Made of White Oak....	150
Figure 3.44 LTLs for Dowel Joints made of Red Oak .....	151
Figure 3.45 LTLs in Data Chart and Histogram of Dowel Joints Made of Red Oak .....	152
Figure 3.46 LTLs for Dowel Joints Made of White Oak.....	153
Figure 3.47 LTLs in Data Distribution of Dowel Joints Made of White Oak .....	154
Figure 3.48 LTLs for Screw Withdrawal Strength in Wood Made of Red Oak from End-Grain .....	156
Figure 3.49 LTLs in Data Chart and Histogram of Screw Withdrawal Strength in Wood Made of Red Oak from End-Grain .....	157
Figure 3.50 LTLs for Screw Withdrawal Strength in Wood Made of White Oak from End-Grain .....	158
Figure 3.51 LTLs in Data Chart and Histogram of Screw Withdrawal Strength in Wood Made of White Oak from End-Grain .....	159
Figure 3.52 LTLs for Screw Withdrawal Strength in Wood Made of Red Oak from Edge-Grain .....	160
Figure 3.53 LTLs in Data Chart and Histogram of Screw Withdrawal Strength in Wood Made of Red Oak from Edge-Grain.....	161

Figure 3.54 LTLs for Screw Withdrawal Strength in Wood Made of White Oak from Edge-Grain .....	162
Figure 3.55 LTLs in Data Chart and Histogram of Screw Withdrawal Strength in Wood Made of White Oak from Edge-Grain .....	163
Figure 3.56 LTLs for Screw Withdrawal Strength in Wood Made of Red Oak from Face-Grain .....	164
Figure 3.57 LTLs in Data Chart and Histogram of Screw Withdrawal Strength in Wood Made of Red Oak from Face-Grain .....	165
Figure 3.58 LTLs for Screw Withdrawal strength in Wood Made of White Oak from Face-Grain .....	166
Figure 3.59 LTLs in Data Chart and Histogram of Screw Withdrawal Strength in Wood Made of White Oak from Face-Grain .....	167
Figure 4.1 A. Chair Frame Obtained from Industry, B. Chair Model .....	176
Figure 4.2 Configuration of Structural Analysis on Chair.....	176
Figure 4.3 Configuration of RMT Joints in the Cross Section of Rail .....	178
Figure 4.4 Configuration of Dowel Pins on Rail Cross-Section.....	179
Figure 4.5 Tenon Dimensions.....	186
Figure 4.6 Dowel Dimensions .....	186
Figure 5.1 Relationship Between Load Steps and Chair Strength.....	189
Figure 5.2 Configuration of Chair Samples.....	191
Figure 5.3 Configuration of Vertical Statically Load Test Set-Up.....	192
Figure 5.4 Configuration of Front-to-Back Cyclic Load Test Set-Up.....	193
Figure 5.5 Average Failure Load of Chair Frames in Static and Cyclic Test.....	194
Figure 5.6 Individual Test Results for Failure Load of Chair Frames in Static and Cyclic Load Tests.....	195
Figure 5.7 Failure Stress in Joints.....	196

## LIST OF ABBREVIATIONS AND SYMBOLS

ALA – American Library Association  
 ANSI – American National Standard Institution  
 ASD – Allowable stress design  
 BIFMA – Business and Institutional Manufacturer Association  
 CLT – Central limit theorem  
 CoV – Coefficient of variation  
 CPSC – Consumer Product Safety Commission  
 DfE – Design for Environment  
 ECDF – Empirical cumulative distribution function  
 E-N – Strain-number of cycles  
 EPA – Environmental Protection Agency  
 GSA – General Service of Administration  
 LRFD – Load and design resistance factor  
 LTLs – Lower Tolerance Limits  
 LVL – Laminated veneer lumber  
 MC – Moisture content  
 MDF – Medium density fiber  
 MF – Melamine formaldehyde  
 M-N – Moment-number of cycles  
 MOE – Modulus of Elasticity  
 MOR – Modulus of Rupture  
 MPa - Megapascal  
 MSW – Municipal Solid Waste  
 MT – Mortise and tenon  
 OSB – Oriented Strand Board  
 PB – Particle board  
 PF - Phenol formaldehyde  
 PU - Polyurethane  
 PVA – Polyvinyl acetate  
 R - Reliability  
 RMT – Rectangular mortise and tenon  
 RoMRT – Round tenon and rectangular mortise  
 RoMT – Round mortise and tenon  
 SD – Standard deviation  
 TLs – Tolerance Limits  
 UF – Urea-formaldehyde

A- Area  
 $C_d$  – Design cost  
 $C_e$  – Elaboration cost  
 $C_m$  – Manufacturing cost  
 $C_o$  – Operation cost

cm - Centimeter  
E – Modulus of elasticity  
f,P – Force  
g - Gram  
in - inch  
kN – kilonewton  
L – Length  
lb – pound  
M - moment  
m – meter  
mm - millimeter  
n – Sample size  
N – Newton  
N.m – Newton-meter  
P – Proportion level  
psi – pound square inch  
rad – Radian  
s – Sample standard deviation  
 $\bar{X}$  - sample mean  
 $\alpha$  – Significance level  
 $\beta$  – Power  
 $\delta$  – relative content error, displacement  
 $\epsilon$  - Error  
 $\gamma$  – Confidence level  
 $\sigma$  – Stress, population standard deviation  
 $\mu$  - Population mean, displacement  
 $\rho$  – Specific gravity  
v – Poisson's ratio  
 $\phi$  – Moment rotation

## ABSTRACT

Author: Uysal, Mesut. PhD

Institution: Purdue University

Degree Received: May 2019

Title: A Rational Approach to Estimate Reasonable Design Values of Selected Joints by Using Lower Tolerance Limits

Committee Chair: Eva Haviarova

In this study, reasonable design values of selected joints were estimated by using the lower tolerance limits (LTLs) method. Although furniture members and joints can be designed if their strength capacities are known, design values of furniture joints have not been established. There are studies relating to the allowable design values of furniture joints that exist in literature review, but they have not been well-addressed. Another fact of information is that allowable design values for wood materials have been defined for building wood structure. However, wood materials used in furniture industry are smaller in size and primarily defect-free compared to those of wood structural material, so some mechanical properties of wood may differ from each other. Therefore, a determination of reasonable design values of furniture joint is needed.

Furniture joints are the weakest part of furniture structure. Increase in reliability of furniture joints provides lower failure probability for furniture structure during its service. Thus, furniture joints were selected to determine their reasonable design values in this study.

In the literature review, numerous studies have been conducted to determine strength capacities of furniture joints considering different wood species, joint sizes, adhesive types and tolerance fit of joints, etc. These studies were related to prediction interval or deterministic approach which does not satisfy the reliability of products. On the other hand, probabilistic approaches ensure reliability and safety of products. Tolerance intervals are one of the probabilistic approaches. Therefore, one-sided lower tolerance limits are used to determine reliability and safety of furniture joints.

Rectangular mortise and tenon (RMT) joints, two-pin moment resisting dowel joints, and screws, which are widely used joinery methods in furniture industry, were selected to study. All specimens were made of northern red oak and white oak wood. T-shaped RMT and dowel joints were examined in bending tests, while the screw withdrawal strength in wood from end-, edge- and face-grain were evaluated for screws. In order to determine sample sizes in tolerance analysis, reference data was used according to the modified Faulkenberry-Weeks method. According to test results, 220 specimens were used for each sample group to calculate lower tolerance limits of furniture joints.

In the tolerance analysis, randomness, homogeneity and normality assumptions were considered. If data was not normally distributed, one-sided LTLs were calculated for a non-normal data set. Firstly, the logarithmic normalizing transformation was sought. If the logarithmic data was normally distributed, LTLs were then obtained by using calculations for a normally distributed data set. The logarithmic value was then inverted. If the logarithmic data was not normally distributed, Weibull distribution was then used to calculate LTLs. Furthermore, non-parametric tolerance analysis was used if data did not fit the Weibull distribution. According to test results, data was normally distributed for six sample groups; namely, RMT joints made of white oak, dowel joints made of white oak, screw withdrawal strength in wood made of both red oak and white oak from end-grain, screw withdrawal strength in wood made of white oak from edge-grain, and screw withdrawal strength in wood made of red oak from face-grain. On the other hand, data was normally distributed for screw withdrawal strength in wood made of red oak from edge-grain and wood made of white oak from face-grain after logarithmic transformation. The data fitted Weibull distribution for both RMT joints made of red oak and dowel joints made of red oak. One of the 0.90, 0.95, and 0.99 levels were used for confidence/proportion levels in tolerance analysis. In order to obtain higher reliable products, LTLs for 0.99/0.99 confidence/proportion level were concentrated for design of joints.

In the design of joints, joint sizes were determined for RMT and dowel joints. In the first step, joints were considered as mechanical joints to calculate their cross-section dimensions. In the second step, length of joints was calculated by the rational design of joints.

According to LTLs for 0.99/0.99 confidence/proportional level, dimensions of RMT and dowel joints in chair construction were defined when subjected to a 2000 N load.

Performance testing of chairs of which joints designed by using the LTLs method was conducted. For this purpose, both the static vertical load test and the cyclic front-to-back load test were subjected to chairs. In the static vertical load test, chairs were expected to fail above 2000 N load level capacity. Test results showed that all chairs failed above this capacity. On the other hand, test results specifications in the cyclic front-to-back load test were benchmarked with American Library Association (ALA). According to test results, chairs met the acceptable load levels for light duty-household, restaurant, and library chair strength.

In conclusion, the LTLs method provides a systematic approach to estimate reasonable design values of furniture joints. Also, establishment of design values for furniture joints will increase joint reliability as well as simplify and reduce design process of furniture and its joinery. Overall, reliability of product has effects on (i) humans' health by reducing injury rate in case of falling on chairs, (ii) service life of product by increasing strength and durability of product, (iii) liability of products by ensuring safety of products, and (iv) cost by reducing rate of recalls and warranty costs.

## CHAPTER 1. INTRODUCTION

### 1.1 General Overview

Throughout history, furniture has improved the quality of humans' life. Even in primitive ages, humans used stones in their caves as furniture. The beginning of furniture history is based on the ancient Egyptian (3100-2890 B.C) but there are evidences to show that humans manufactured and used furniture in Paleolithic and Neolithic period [1]. Architectural finds also show that wood, stones, metal, and animal bones were used as furniture. At some point in time, humans recognized that wood was easy to cut and shape, and it became the most important material for furniture production.

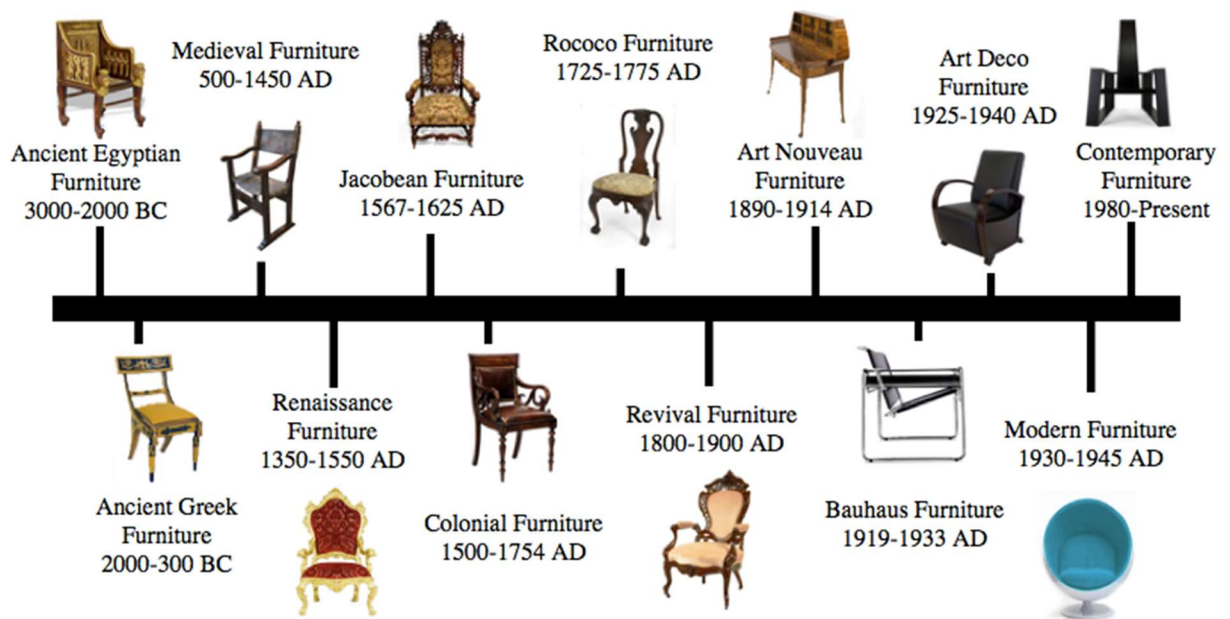


Figure 1.1 History of Furniture Design [1]

Furniture was not only used to serve human's needs but also affected by human culture. Figure 1.1 shows various types of furniture throughout the furniture history. Smardzewski classified furniture history [1] in the following categories:

1. *Antique furniture* – furniture of ancient Egyptian, Assyria, Persia, Greece and Rome,

2. *Furniture of middle ages* – Medieval furniture,
3. *Modern furniture* – Renaissance, Baroque, Rococo, Classical, Empire, Eclectic, Art Nouveau, Art Deco and Early twenty-century furniture.

Although furniture has evolved more rapidly than other forms of architecture, the design of the basic chair remains impeccable and timeless [1]. Figure 1.2 shows three chair designs from different eras and cultures. These chair designs are intuitively manufactured with stretchers which performs structural function in chairs and increase overall furniture strength. These stretchers reduce the bending moment capacity of the side rail to back post joint. By doing so, these stretchers also prevent the front leg and side rail from rotating as a unit [2].



Figure 1.2 Similarity in Chair Structure: A. Egypt 2800 B.C (British Museum), B. Finland around 1930 and Jasper, Indiana 2017

After the industrial revolution, furniture production greatly increased and became more available to all classes of the population – rather than only the elite – as production progressed from a craft-based to a machine-based industry. After simple needs of humans were met by development in the furniture industry, quality of the furniture came into prominence. During the early 1930s, engineering design practices of furniture were initiated. Evaluation of the furniture quality involves a detailed analysis of design, construction, functionality, ergonomics, safety for the environment, and usage. Fatigue life of furniture is evaluated from the stages of development and use, which are assessments of

furniture quality by using theory or sample testing, and furniture is subjected to dozens or hundreds of users, respectively. Therefore, furniture should be assessed by two groups in terms of quality; namely, by manufacturers and users, as shown in Figure 1.3 [1]. Moreover, it is indicated that furniture is expected to meet aesthetic, functional, and structural quality requirements [3].

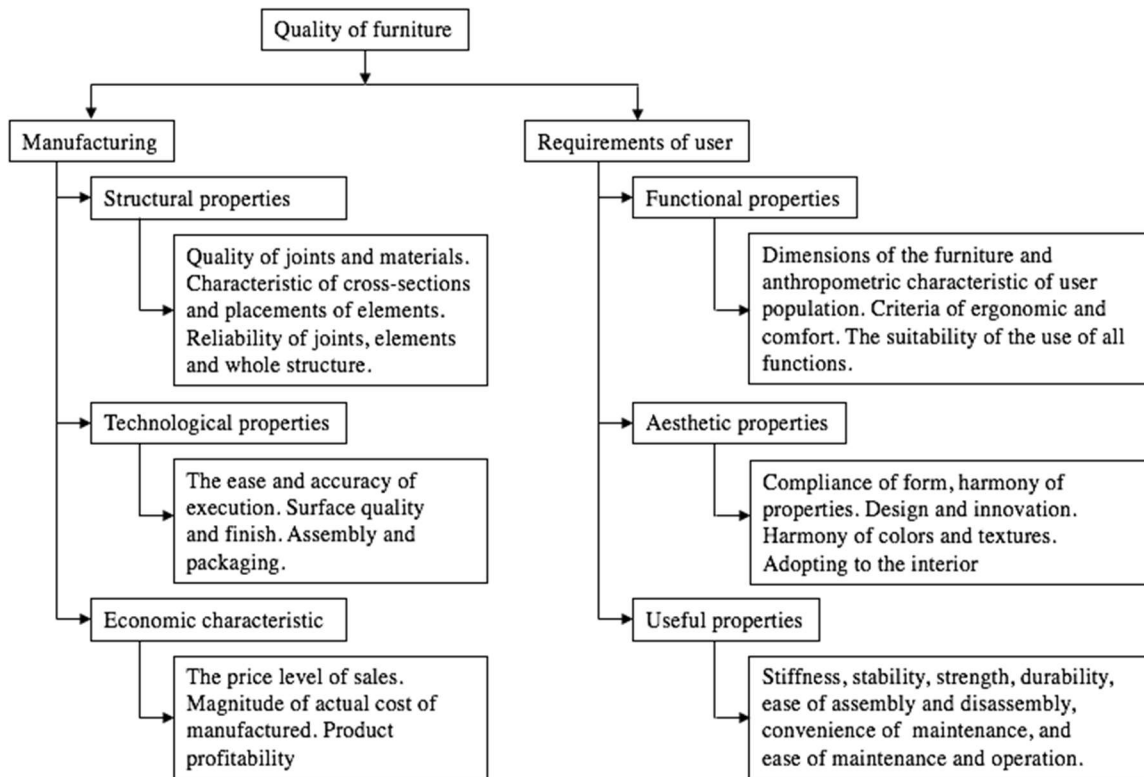


Figure 1.3 Quality Aspect of Furniture [1]

According to [4], there are three separate but related types of furniture design; namely, (i) *aesthetic design* – the artistic development of the furniture structure, (ii) *functional design* – design of furniture to meet its intended purpose, and (iii) *engineering design* – designing the furniture structure that will safely resist the load imposed on it in service. Structural engineering design has a major role to produce reliable furniture to ensure that joints and members will be able to carry the loads imposed on it while in service. The basic steps of engineering design according to Eckelman [4] are:

1. To determine the loads that will act on the structure.

2. To estimate the size of the members needed to carry the loads and draw up a trial furniture structure.
3. To determine the resulting magnitudes and distributions of the internal forces acting on the members and joints.
4. If necessary, to re-design the trial furniture structure until no-member is overstressed.
5. To design joints to carry the forces acting on them.

Overall strength of the furniture is reduced under the cyclic load, which is dozens and hundreds of loadings imposed on the furniture in the course of its lifespan, and prediction of such loadings in service is complicated (Figure 1.4) [5]. If the internal force on joint and members of furniture exceeds the capacity of the material strength, failure will occur. Therefore, the acceptable strength levels of joints and members should not be exceeded to ensure overall reliability of furniture.

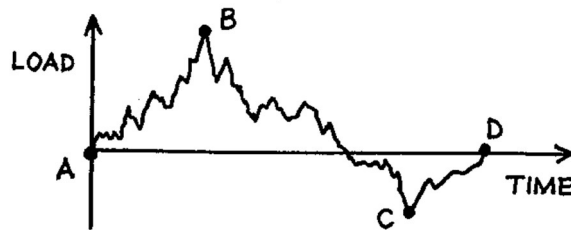


Figure 1.4 Irregular Load History in Structure [5]

Reliability of the furniture is ensured by describing its capacity to operate throughout required time and specified operational conditions by following reliability aspects [6]:

1. Reduction in number of components
2. Good fitting of components in construction
3. Appropriate material selection
4. Determining stress and strain on components and joints
5. Using probabilistic methods to determine optimal stress-strength distribution

6. Developing checklist in design, manufacturing, reliability, and maintainability application of products to catch design and manufacturing errors, and optimizing reliability as improving such application [7].

## 1.2 Statement of Problem

In order to produce durable furniture that is able to resist the loads imposed upon it in service, it is necessary to have rational estimates of the load capacities of the joints used in its construction [8]. Joints play major roles in the reliability of the furniture since failure may occur more often due to loose and failed joints rather than having fractured legs or rails. [9]. Thus, unreliable joints result in unreliable furniture [10].

The rational design values for various types of furniture joints constructed of either solid-wood or wood composite materials have been studied for various types of furniture constructions; namely, frame, case, and shell furniture. Although these studies provide strength capacities of the furniture joints, reasonable design values have not been established for them. In contrast, studies concerning allowable stress design of furniture joints, furniture members, and furniture frames do exist [8], [11]. On the other hand, standardization institutes, such as Business and Institutional Manufacturer Association (BIFMA), American Library Association (ALA), and American National Standard Institution (ANSI), recommend acceptance levels for performance testing of furniture. However, such recommended standards are considering the overall strength of the furniture structures but not considering individual furniture members and joints, whereas failures on furniture occurred mostly at these components since external loads exceed their resistance. Such external loads depend on the knowledge of the conditions which furniture would encounter in service. A piece of furniture is subjected to static and cyclic loading during its service. In the case of chair frames, the furniture is subjected to loads when sitting down, leaning backwards, and moving around while sitting. These loads are repeated dozens or hundreds of times in typical daily activities. Therefore, it comes into prominence to consider all possible conditions in use of furniture because it is not predictable how furniture would be utilized.

Allowable design values of static strength are stress (or strain) limits on structures under imposed loads. Furthermore, an allowable design value of fatigue strength is the minimum stress level under cyclic load until non-recoverable damage occurs. Based on test results and discussions with national and international institutions, allowable design stresses for materials and joints are painstakingly considered – and resolved. Allowable design values of members and joints represent characteristic and usage in furniture design and service. [12]. Although wood materials used in conventional structures have allowable stresses defined for their intended use, allowable design values for the woods used in furniture construction have not been defined, yet. Wood materials used in furniture construction behave differently from those used in the field of timber engineering, as furniture members and joints are in small sizes and made of defect-free wood material [8]. Hence, furniture members and joints must be tested to determine their structural capacities in furniture engineering practices but such design values are determined by designers' judgement and experience due to given paucity of information existing on the subject [13]. Importantly, variability must be considered with respect to not only service loads and material uniformity but also joint fabrication. Moreover, determination of the traditional design values are based on the safety coefficient and margin of safety to predict reliability of furniture construction, its components, and joints [10].

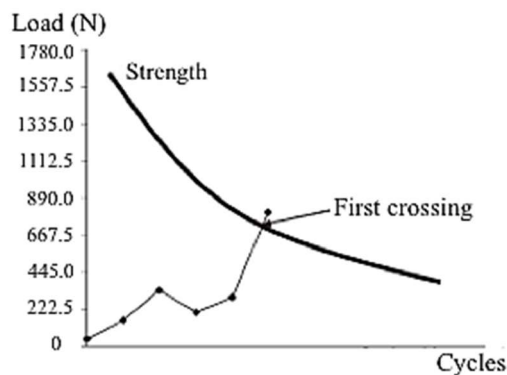


Figure 1.5 First Crossing Concept in Fatigue Life of Structure [14].

When a piece of furniture is new, it has ultimate strength capacity. Then, it is exposed to normal and abusive static or cyclic loading during its service. Therefore, its strength capacity would be expected to reduce as shown Figure 1.5 [3]. Knowing the strength

capacity of the joints is essential for the construction of reliable and durable furniture. In most furniture designs, the size of the joints does not meet engineering design requirements due to not only ignorance of structural requirements but also aesthetic design preferences [15]. Designers are developing slender and delicate shapes of furniture which are challenging for both engineers and manufacturers. The optimal size joints must be used in furniture to maximize overall strength of furniture and to minimize material cost. Such sizes must be obtained after determining a design value for furniture joints. Otherwise, under-sized joints would likely become overstressed as a result of imposed external loads upon furniture structure, whereas over-sized joints would increase material cost in a large-scale production. Another factor is that design and manufacturer errors reduce the length of the failure-free time of furniture in service. Such errors include sub-size members and joints, inappropriate joint types and adhesives, inappropriate wood species, etc. [16]. When large-scale production begins, the level of variation and occurrence of failure in construction of products would be expected to increase due to variability in material, design errors, and manufacturing errors. Determination of the allowable design values should measurably increase the reliability and safety of the structure [12]. Therefore, furniture joints must resist the external load as designed according to acceptable design values. In doing so, it becomes important to obtain what proportion of the ultimate strength is used to determine design values. At this point, the difficulties for designers and engineers are to predict failure probability of structure in service and to make appropriate reliability analyses [17]. Probabilistic approaches are useful methods to acquire uncertainties of different parameters and these approaches become more efficient in the course of time compared to experimental methods [18].

Intermediate procedure that could be used to develop rational values for design purposes is the use of statistical Lower Tolerance Limits (LTL) method. The LTL method is a probabilistic analysis which rationally suggests what proportion of the average bending strength for the furniture joint is used. The sample sizes and confidence/proportional levels are taken into consideration to determine such design values. Appropriate sample sizes must be used to make reliable tolerance analysis [19]. Determination of confidence/proportion levels requires a consideration of safety, as well as requiring

economic factors such as cost of replacement. Higher confidence/proportional levels may obtain severe restrictions in determining LTL values [8] whereas lower confidence/proportion levels may give unreliable LTL values.

### 1.3 Aims and Objectives

This study focused on issues associated with estimating design values of selected furniture joints; namely, rectangular mortise and tenon joints, two-pin moment resisting dowel joints, and screws. The primary purpose of the study is to propose a method by estimating reasonable design values for furniture joints used in chair frames by using lower tolerance limits. This study was intended to improve the methodology of joint design by using experimental and mathematical investigations for probabilistic approaches. The following objectives comprise the purpose of the study:

1. Determine minimum sample size requirements to make reliable tolerance analysis by using reference data set.
2. Determine internal forces of T-shaped rectangular mortise and tenon joints, and two-pin moment resisting dowel joints under static loading.
3. Determine screw withdrawal strength in wood from end, edge and face grain under static loading.
4. Examine statistical normality assumption for data sets to make reliable tolerance analysis. Then, calculate lower tolerance limit of both internal forces and screw withdrawal strength in wood by using either parametric or non-parametric tolerance limits; depending on normality of distributed data set or non-normally distributed data set, respectively.
5. Design joints based on given LTL values at desired confidence/proportion level.
6. Determine static load capacities of chair frames whose joints are designed based on LTL values.
7. Determine front-to-back cyclic load capacity of the chairs whose joints are designed based on LTL values.

#### 1.4 Research Hypothesis

*Null Hypothesis ( $H_0$ ):* The use of Statistical Lower Tolerance Limits provides a rational approach for the determination of reasonable design stresses for furniture joints.

*Alternative Hypothesis ( $H_a$ ):* The use of Statistical Lower Tolerance Limits does not provide a rational approach for the determination of reasonable design stresses for furniture joints.

#### 1.5 Significance of Study

In this study, the method is proposed to estimate reasonable design values for furniture joints by using statistical LTLs approach. In doing so, the intent is to increase the overall reliability of furniture by increasing the reliability of individual furniture joints. Reliability is of concern to furniture producers for sustainability, human safety and global competitive marketing, as furniture quality and reliability increase chances for higher market success [20].

A sustainable product aims for reduction of its environmental impact which can be reduced by extending its life span [21] through reducing post-manufacturing activities – products remanufacturing for reusing and recycling – and product disposal. Lagerstedt [22] and Hauschild [23] described the extension of a product life cycle to reduce its environmental impact and increase durability, reliability, and manufacturability in terms of Design for Environment (DfE) strategies. Table 1.1 shows data on wood in Municipal Solid Waste (MSW) [24]. Most of the generated wood waste in 2015 was landfilled and it amounts to 8% of total wastes in landfills that year. Besides, only 16.3% of the wood waste was recycled in 2015. After awareness of environmental impact of wood increased, recovery of the wood products from landfills was started but the majority of wood waste has been still discarded in landfills. Although wood is a biodegradable material, it takes around 13 years for wood to deteriorate in landfill. Finishes on wood products increased the degradation time and environmental impact of wood furniture [25]. Therefore, increasing furniture reliability is important for extension of its service life. Also, according to U.S.

Environmental Protection Agency (EPA), recovery of the furniture from landfills is difficult and furniture was accounted for 4.1% of the household waste [26].

Table 1.1 1960-2015 Data on Wood in MSW by Weight (in thousands of U.S. tons) [24]

Management Pathway	1960	1970	1980	1990	2000	2005	2010	2014	2015
<b>Generation</b>	3,030	3,720	7,010	12,210	13,570	14,790	15,710	16,120	16,300
<b>Recycled</b>	-	-	-	130	1,370	1,830	2,280	2,570	2,660
<b>Composted</b>	-	-	-	-	-	-	-	-	-
<b>Combustion</b>	-	10	150	2,080	2,290	2,270	2,310	2,540	2,580
<b>Landfilled</b>	3,030	3,710	6,860	10,000	9,910	10,690	11,120	11,010	11,060

According to [27], injury rate of a product must be reduced in its service. Similarly, [28] claims that a product cannot cause any danger for its user based on its nature of application; that is, reliability must have a direct impact on safety issues of product in service. Therefore, failure probability of the chair should be reduced by increasing the possibility of internal forces which do not exceed material strength.

Product liability is vital to avoiding failed furniture. According to U.S. Consumer Product Safety Commission (CPSC), a product is enforced to be recalled in the case of failure to meet the regulations and standards [29]. Therefore, a company should conduct a performance test of their products to evaluate product strength, durability, stability, flammability, etc. in order to prevent product recalls and any possible danger while in service. In the U.S. furniture industry, BIFMA provided standards to evaluate the performance of furniture. [30] stated that one of the largest causes of recalls is design defects. These defects result in manufacturing defects so that injury, accident, death or simply falling rate in furniture service increase. Figure 1.6 shows example of recalls for two wooden furniture because of failure. While folding chair had a seat failure, bar stool has joint failure [31]. Therefore, both products were recalled. KID Fighting for Product Safety reported (Figure 1.7) that children furniture accounted for 16% of recalled unit products which is the second largest rate in this category. In addition, 29% these recalls are owing to bodily injury such as falls, lacerations and tip-overs [32].



Figure 1.6 Example of Recalls for Furniture A. Folding Chair, B. Barstool [31]

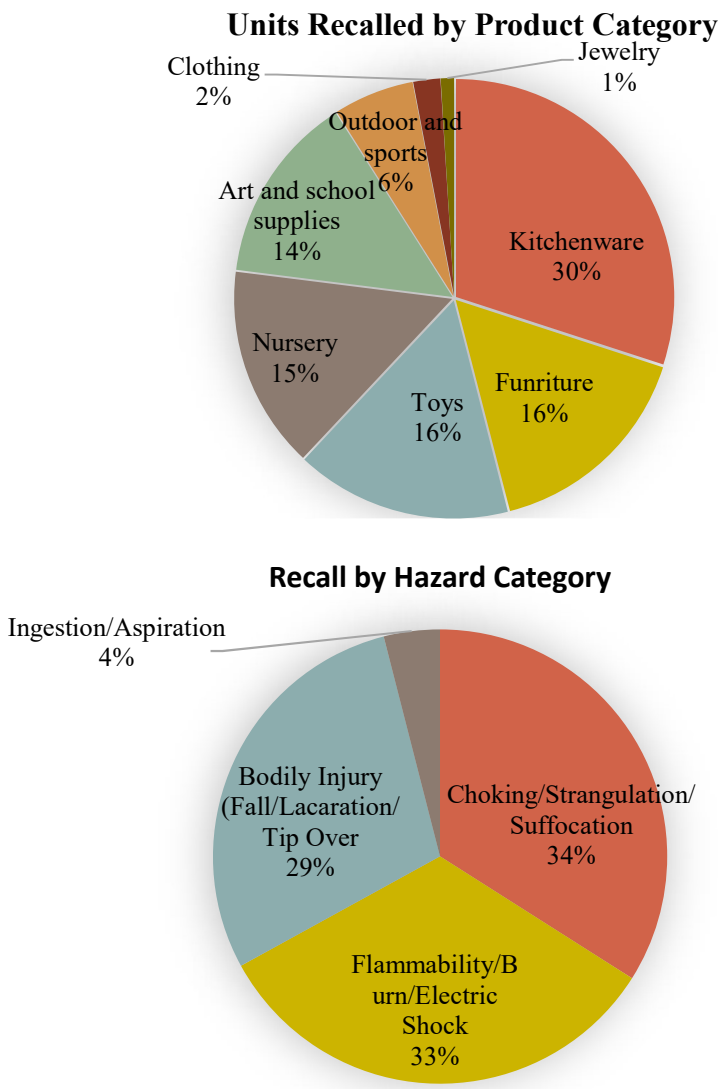


Figure 1.7 2017 data on recalls for children product [32]

In the US nationwide, the most frequent injuries are caused by chair failure while sitting down due to (i) a structurally unsound chair, (ii) manufacturing defect, and (iii) improper assembly [33]. According to CPCS, in 2003, 840 injuries were reported in hospitals as a result of furniture accidents, including collapsing furniture, entrapment, product fall, and laceration from sharp edge. 385 of these reported injuries caused death [34].

A strong relationship was found between product design and its quality because incorporation between the design process, manufacturing, and marketing increases product reliability [35]. Reliability of product does not only affect characteristics of the product but also reduces cost of operation; namely, stoppage cost, warranty cost, service cost, and repair cost [36]. Figure 1.8 shows the relationship between reliability ( $R$ ), operation cost ( $C_o$ ), and elaboration cost ( $C_e$ ) which includes manufacturing cost ( $C_m$ ) and design cost ( $C_d$ ). When the product reliability increases, probability of failure and costs of failure or unavailability obviously decrease while costs of investment increase [37]. Eventually, a designer must take into consideration the optimal reliability of a product to optimize total cost of the product. They must decide associated with durability and warranty time. Therefore, the designing process should address not only the products' aesthetic appearances but also its durability and utilization associated with reliability.

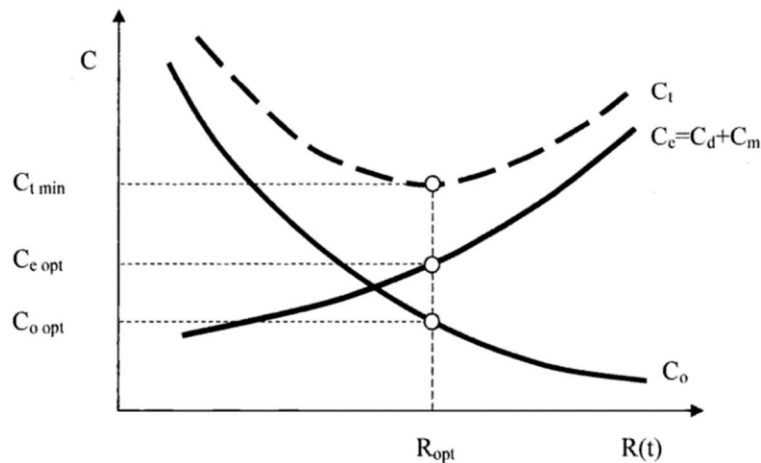


Figure 1.8 Impact of Reliability on Elaboration Cost and Operation Cost [36]

Increasing the reliability of a product is succeeded with a higher quality, which can be controlled by its design and manufacturing process. The cost of reliability improvements should be less than warranty cost in order to avoid any losses in profits, so that longer warranty provides better quality of products and commitment of producers as well as providing higher cost. Figure 1.9 shows the relationship between product reliability and warranty [38].

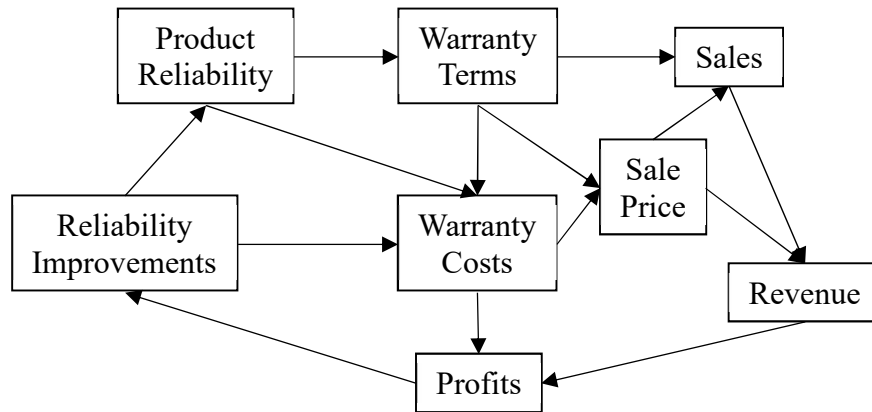


Figure 1.9 The Relationship Between Product Reliability and Warranty Concept [38]

Warranty cost consists of 2-10% of sale price depending on the types of product manufacturing, servicing, and storage time [39,40]. Figure 1.10 shows warranty claims paid by 34 U.S. nationwide furniture manufacturers between 2003 and 2017 [41]. Reliability of product has positive impacts on reducing warranty cost. Furthermore, more reliable products provide better/longer warranty times and greater insurance to customers [40].

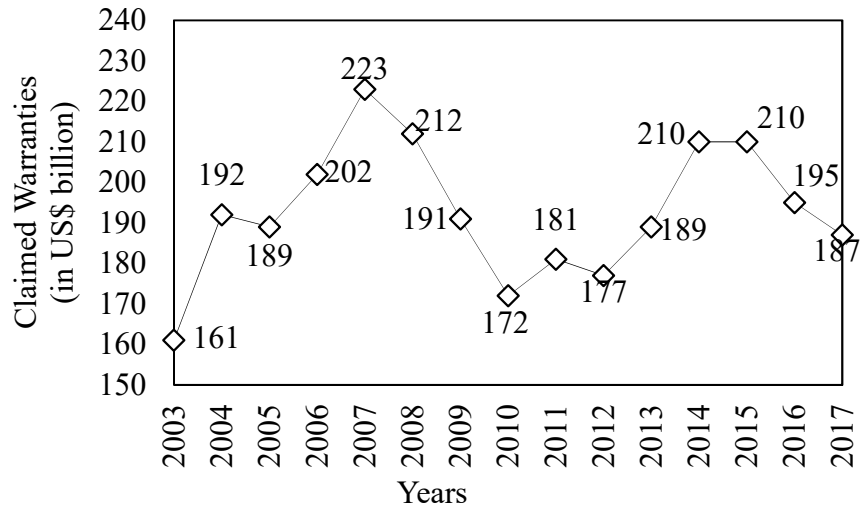


Figure 1.10 2003-2017 Data on Furniture Warranty Claims Paid by 34 U.S. Based Companies [41]

Consequently, determining a design value for furniture joints would increase both joint and construction reliability. Correspondingly, it will significantly influence the designing process and manufacturing cost.

## CHAPTER 2. LITERATURE REVIEW

In this chapter, the structural analysis of chair frames, joint properties, load and design consideration for wooden construction, national and international standards for furniture, probabilistic approach for structure, and tolerance limits are thoroughly discussed. The purpose of this chapter is to develop a comprehensive background for the dissertation. Literature review starts with a structural analysis of chair frames and understanding how it behaves under subjected loads. Joint properties are then discussed to understand its mechanical and physical behavior under different load types since this study is about estimating design values of furniture joints. Moreover, allowable stress design (ASD) and load resistance factor design (LRFD) phenomena are discussed in the field of wood construction. An overview of international and national standards for furniture (chair frames) is included. Reliability analysis for structures and use of probabilistic method and tolerance limits (TLs) are discussed as they provide the background for this dissertation.

### 2.1 Structural Analysis of Chair Frames

In the science of furniture strength design, it is necessary to be able to differentiate between structural elements and systems used in its construction. A piece of furniture is constructed in an infinite variety of ways by using such structural elements and systems, so it is difficult to recognize a basic structural system due to its form, strength, and rigidity [4]. Therefore, different types of furniture construction will have various joining systems and material geometry. Furniture construction are divided into groups; namely, (i) frame, (ii) panel, (iii) shell, and (iv) composite type furniture constructions [4]. In this study, frame-type furniture construction and its selected joint types will be thoroughly investigated.

Wood is an elasto-plastic material which means that its structure must have enough strength and stiffness to meet both serviceability and safety criteria in service. In the design process, appropriate materials selection and material geometry must be taken into consideration by analyzing structurally sound furniture construction. Frame-type furniture construction belongs to the group of statically indeterminate spatial system. Increasing the degree of

indeterminacy in a structure becomes complicated and structural analyses by hand are challenging. Therefore, structural analysis programs such as ABAQUS, ANSYS, SAP 2000, RISA 3-D, etc. have been developed. However, we need to understand the theoretical analysis of a structure before relying on structural analysis programs imprudently.

Degree of indeterminacy in a structure depends on the number of members, joints, and degrees of freedom [1]. A node has 3 and 6 degrees of freedom (Figure 2.1) if it is freely movable in a 2-D plane and 3-D space, respectively. An example regarding this concept for indeterminate structures shows that a simple stool has 30 degrees of indeterminacy whereas an armchair with armrests has 62 degrees of indeterminacy. The degree of indeterminacy is obtained by using following expression;

$$s = (r + h) - 3t \quad \text{Equation 2.1}$$

where,  $s$  is degree of indeterminacy,  $r$  is number of reaction forces in the system,  $t$  is number of members in the system and  $h$  is number of degrees of freedom in the system.

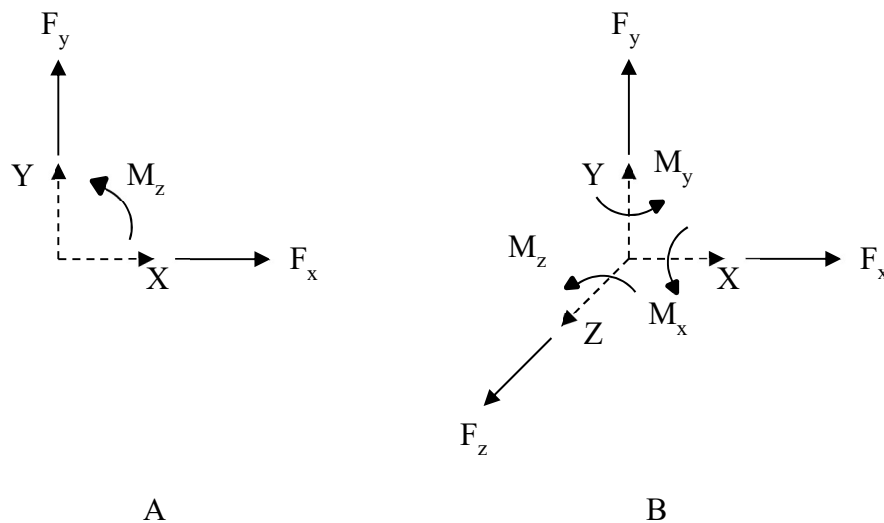


Figure 2.1 Degrees of Freedom in the A. Plane (2D) and B. Space (3D) System

In a spatial system, furniture frames are structurally analyzed by numerical methods. In addition, the structural analysis solution could be reduced to stiffness-strength calculation

of furniture side frames, owing to symmetry of the structure and load. In doing so, number of indeterminacies could be reduced to make easier calculation of internal forces depending on decreasing number of members, joints and degrees of freedom in the system [1]. Figure 2.2 shows a full chair frame and a side chair frame. There are 9 degrees of freedom in a joint for the full-frame chair (3D), while the side chair frame (2D) has only 6 degrees of freedom.

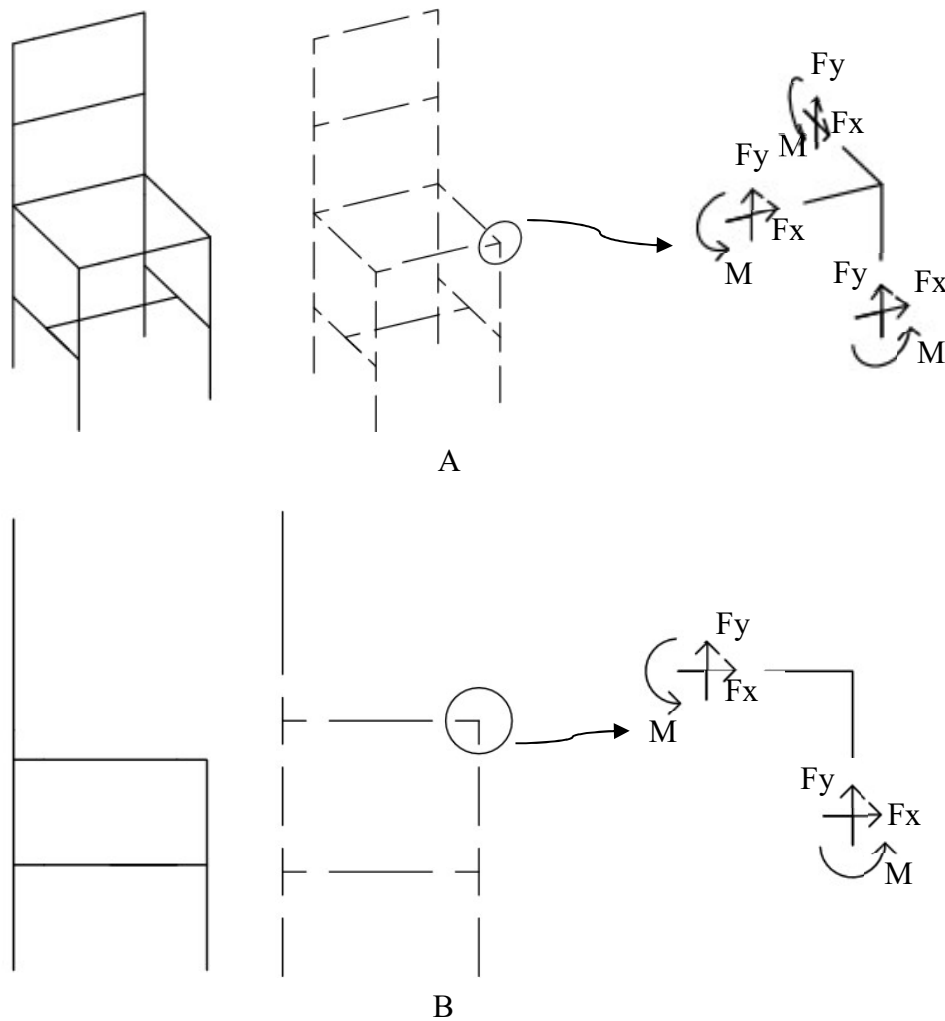


Figure 2.2 Degrees of Freedom in A. Full Chair Frame and B. Side Chair Frame

### 2.1.1 Loads Consideration in Furniture Design

The first step in the design procedure of chair frames is to determine magnitude, direction, and frequency of external loads and its occurrence in service. A typical chair frame is

subjected to static load –constant load, such as still object places on the chair, dynamic load – repeated load such as sitting down, standing up and leaning back, and impact load – sudden jump on a chair during its service [4]. It is unpredictable what type of loading would be imposed on a chair during its service.

A chair could be subjected to individual or a combination of loads during its service. Therefore, to make reliable chair frames, applied loads should be clearly defined in the design process. Ultimate load capacity levels of chair frames, ultimate internal loads of chair members, and joints corresponding to subjected external load must be known before designing a piece of furniture. In doing so, an indeterminate chair frame could be analyzed to obtain internal forces on members and joints by using structural analysis methods; namely, principle of energy and work (Castigliano's theorem), force-method, and displacement-method.

#### 2.1.1.1 Static Loads in chair Frames

A chair frame is subjected to vertical, horizontal, or inclined loading on seat and back during its service (Figure 2.3). Therefore, joints strength on both side rails and stretchers to back post must be high enough to resist these applied external loads.

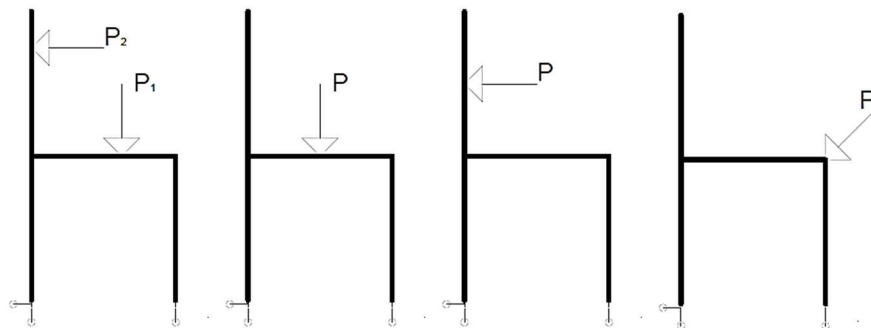


Figure 2.3 Configuration of Some Possible Point Load Types in Side Chair Frame

In the statically determinate structure, strength of the chair is less than those of statically indeterminate chair. Because adding a member (e.g. stretchers) to chair frame makes the structure stiffer, it also causes to have higher reliability and strength. In the case of a chair under simple loading, bending moment capacity on the side rail to back post joint is reduced

in half [2]. Figure 2.4 shows schematic depiction of side frames configuration for both, statically determinate and indeterminate structures. Bending moment capacity of side frame attached to back post in statically determinate chair frames is 400 N.m while those of indeterminate is 179.1 N.m shown in Figure 2.5 and 2.6, respectively.

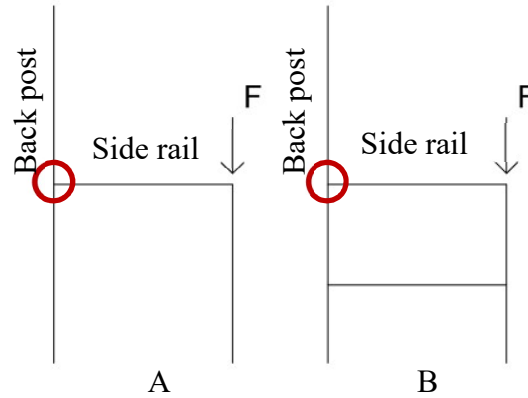


Figure 2.4 Schematic Description of Simple Side Chair Frames A. Statically Determinate and B. Statically Indeterminate

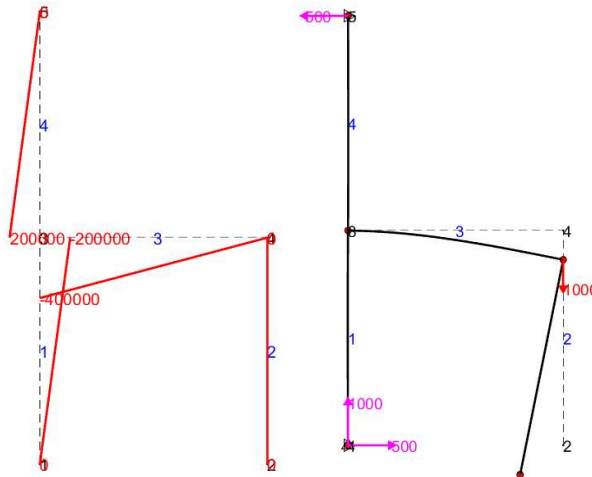


Figure 2.5 Bending Moment of Members and Deflected Shape on Statically Determinate Side Frame

In the case of statically determinate side chair frames, bending moment capacity on side rail to back post joint is calculated:

$$\sum M_A = 0$$

Equation 2.2

$$\sum F_x = 0 \quad \text{Equation 2.3}$$

$$\sum F_y = 0 \quad \text{Equation 2.4}$$

In the case of the statically indeterminate side frame analysis, internal forces were calculated by using stiffness method. A structure contains elements and nodes. A node has 3 degrees of freedom and an element has 6 degrees of freedom (Figure 2.6). Element stiffness is calculated by using equation 2.5 [42]. Stiffness matrix is constructed by adding element stiffness to each other. A statically indeterminate side frame is shown in Figure 2.4.B. In this figure, there are 7 elements and 21 degrees of freedom.

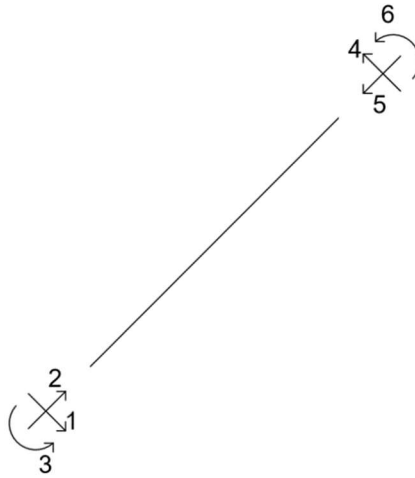


Figure 2.6 Degrees of Freedom for Element Stiffness

$$\{f\} = [K] \times \{u\} \quad \text{Equation 2.5}$$

$$\begin{Bmatrix} f_1 \\ f_2 \\ f_3 \\ f_4 \\ f_5 \\ f_6 \end{Bmatrix} = \begin{bmatrix} AE/L & 0 & 0 & -AE/L & 0 & 0 \\ 0 & 12EI/L^3 & 6EI/L^2 & 0 & -12EI/L^3 & 6EI/L^2 \\ 0 & 6EI/L^2 & 4EI/L & 0 & -6EI/L^2 & 2EI/L \\ -AE/L & 0 & 0 & AE/L & 0 & 0 \\ 0 & -12EI/L^3 & -6EI/L^2 & 0 & 12EI/L^3 & -6EI/L^2 \\ 0 & 6EI/L^2 & 2EI/L & 0 & -6EI/L^2 & 4EI/L \end{bmatrix} \times \begin{Bmatrix} u_1 \\ u_2 \\ u_3 \\ u_4 \\ u_5 \\ u_6 \end{Bmatrix} \quad \text{Equation 2.6}$$

where  $f$  is force vector,  $K$  is stiffness matrix,  $u$  is displacement vector,  $A$  is area of element cross-section,  $E$  is modulus of elasticity of element, and  $L$  is the length of element. The bending moment capacities and deflected shape of chair frame are given in Figure 2.7.

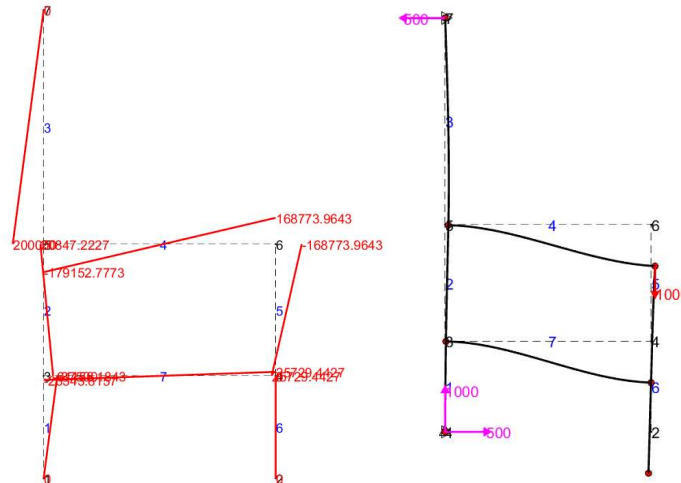


Figure 2.7 Bending Moment Capacity of Members and Deflected Shape on Statically Indeterminate Side Frame

### 2.1.1.2 Cyclic Load of Chair Frames

Although many methods are developed to evaluate performance of side chair frames, they have not provided tangible data to measure their performances which is needed for engineering design purposes. On the other hand, studies show that cyclic load testing of side chairs defines their performance and sets their acceptable levels [43].

#### 2.1.1.2.1 Constant Cyclic Loads

A certain strength level of modulus of rupture (MOR) of material or selected load level are applied on chair frames until desired load cycles are exceeded. (1,000,000 cycles) (Pass-Fail test) [15,44,45].

#### 2.1.1.2.2 Stepwise Cyclic Loads

According to General Service of Administration (GSA), tested frame members and joints (T-shaped joint specimen) are subjected to cyclic loading as shown in Figure 2.8. The test procedure begins with 222.5 N for joint load tests on arm outwards. After 25,000 cycles, load is increased by an increment of 111.25 N and another 25,000 cycles are completed. Rate of loading is 20 cycles per minute for all GSA performance testing. The cyclic load test is repeated until non-recoverable failure occurs, or desirable level of performance is achieved [43,45]. Figure 2.9 shows load level and load increments in each step.

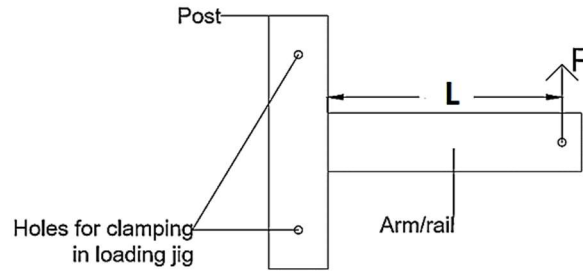


Figure 2.8 Configuration of Specimen for Joint Performance Test [45]

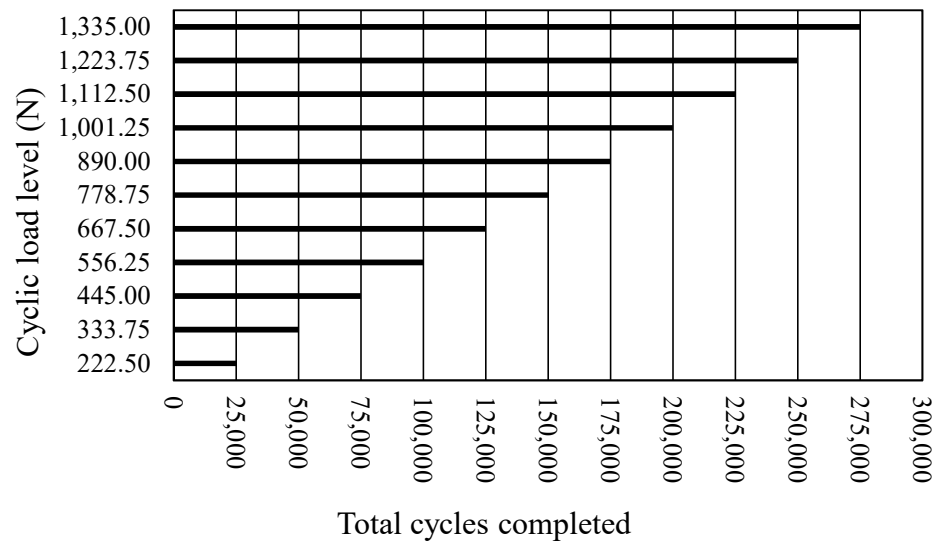


Figure 2.9 Stepwise Load Model on Chair/Joint Specimen According to GSA [43]

#### 2.1.1.2.2.1 Cyclic Vertical Load Test on Seat

In this test, the load is applied on a chair seat by pushing it vertically downward on the seat until chair fails or reaches desired load level (Figure 2.10). The purpose of the test is to evaluate strength and durability of the seat, as well as its supporting chair frame, by applying vertical load which occurs when someone sits down on a chair [43].

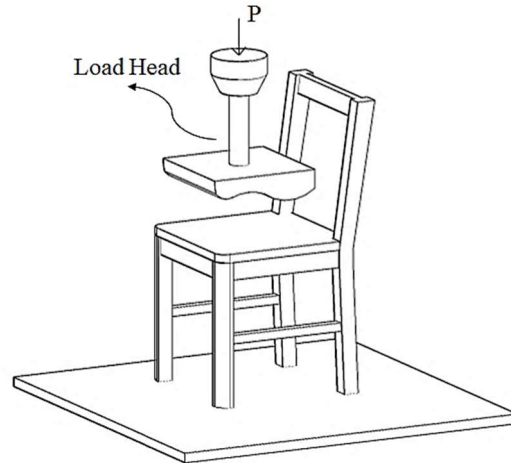


Figure 2.10 Configuration of Cyclic Vertical Load Test on Seats

The test procedure differs depending on what types of material is used for chair seats – solid wood seat and upholstered seats. In the case of applying vertical load on a chair frame with a solid wood seat, the initial load is 445 N at a rate of 20 cycles per minute. Load increments are 445 N after 25,000 cycles is completed at each preceding load level. On the other hand, a vertical load test is initiated with a load of 667.5 N at a rate of 20 cycles per minute on a chair with upholstered seat. Load increments are 166.875 N after 25,000 cycles is completed at each preceding load level [43].

According to American Library Association (ALA) [46], acceptable load levels of chair frames with solid wood seats are 2,670 N, 3,560 N and 4,450 N; correspondingly, it meets light, moderate and heavy-duty load capacities of chair seats, respectively.

#### 2.1.1.2.2.2 Cyclic Front-to-Back Load Test on Chair Frames

In this test, the load is applied on a chair frame from front to back until chair frame fails or reaches desired load level (Figure 2.11). The purpose of the test is to evaluate resistance of chair frame by applying load on the seat which occurs when someone sits down and tilts backward on a chair frame [43].

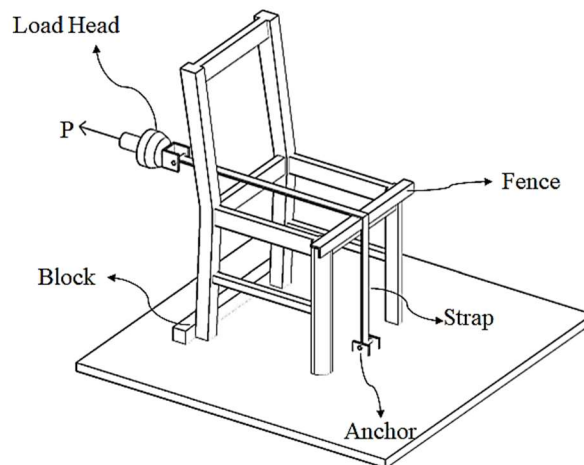


Figure 2.11 Depiction of Cyclic Front-to-Back Load Test on Chair Frame

The test procedure for cyclic front-to-back load is to apply horizontal load on a chair frame in a front-to-back direction with an initial load of 445 N at a rate of 20 cycles per minute. After 25,000 cycles is completed at each preceding load level until 1,112.5 N, loads are increased in increments of 111.25 N. Thereafter, load increments are 222.5 N until chair frame fails or reaches acceptable load level [43].

According to ALA specifications [46], these levels of chair performance used in libraries are 1,335 N, 1,557.5 N and 2,002.5 N, which are their light, moderate and heavy-duty load capacities, respectively. Those of light-duty load level for household chairs and restaurant chairs are 890 N and 1,001.25 N, respectively.

#### 2.1.1.2.2.3 Cyclic Back-to-Back Load Test on Chairs

In this test, load is applied on chair frame from back-to-front until it fails or reaches acceptable load levels. The purpose of this test is to evaluate strength of the front legs subjected to back-to-front force occurred when someone leans backwards on chair or slides it forward [43].

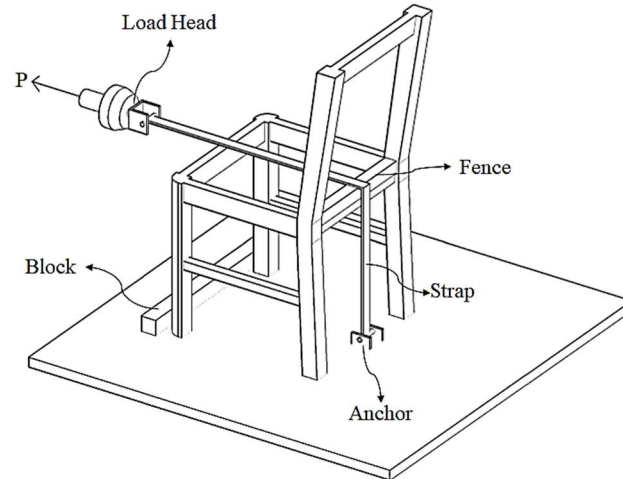


Figure 2.12 Depiction of Cyclic Back-to-Front Load Test on Chair Frame

The test procedure is similar with cyclic front-to-back load test on chair frames discussed in section 2.1.1.2.1.2 but loads are applied horizontally in a back-to-front direction.

According to ALA specifications [46], levels of performance for chairs used in libraries are 1,001.25 N, 1,446.25 N and 1,891.25 N which are light, moderate and heavy-duty load capacities, respectively.

#### 2.1.1.2.2.4 Cyclic Side-Thrust Load Test on Chair Frames

In this test, load is horizontally applied on a chair frame by pushing sideways until it fails or reaches acceptable load levels (Figure 2.13). The purpose of this test is to assess strength of the chair frames to side-thrust forces which occur when user tilts sideways or pulls on the arm of chairs to pull closer to another user. Such force resistances are not taken into consideration in design process so that arm failure on chairs is inevitable [43].

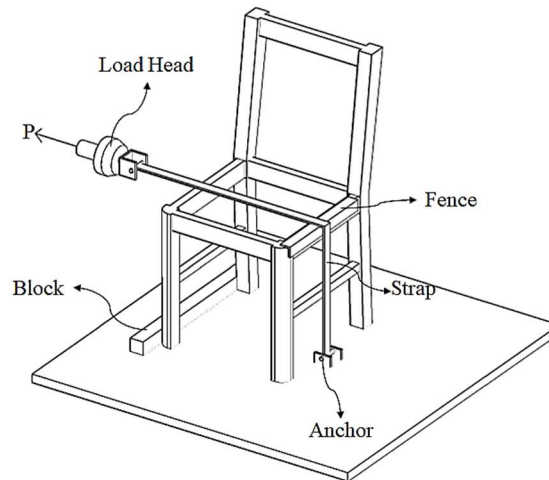


Figure 2.13 Depiction of Cyclic Side-Thrust Load Test on Chair Frame

The test procedure for cyclic side-thrust load is to apply horizontal load on the chair frame in a sideway direction with initial load of 222.5 N at a rate of 20 cycles per minute. After 25,000 cycles are completed at each preceding load level until 1,112.5 N, loads are increased in increments of 111.25 N. Thereafter, load increments are 222.5 N until chair frame fails or reaches acceptable load level [43].

According to ALA specifications [46], levels of performance for chairs used in libraries are 890 N, 1,112.5 N and 1,335 N which are their light, moderate and heavy-duty load capacities, respectively.

#### 2.1.1.2.2.5 Cyclic Front-to-Back Load Test on Chair Frames

In this test, loads are applied horizontally by pulling backward on backrest of chair until either backrest or its joint fails or reaches acceptable load level (Figure 2.14). The purpose of this test is to evaluate strength of backrest-to-back post [43].

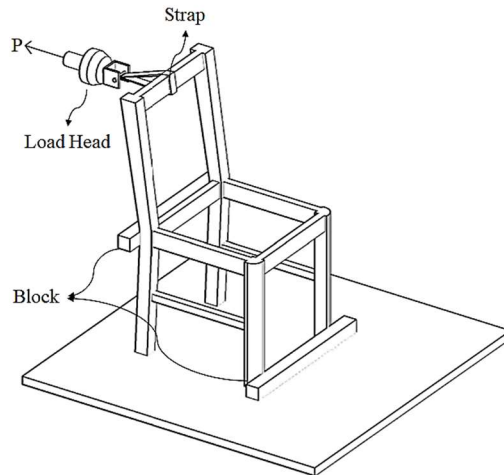


Figure 2.14 Depiction of Cyclic Front-to-Back Load Test on Chairs Backrest

The test procedure for this test is to apply load horizontally to backrest with initial load of 890 N at a rate of 20 cycles per minute. After completing 25,000 cycles at each preceding load levels, loads are increased at increment of 445 N [43].

According to ALA specifications [46], levels of performance for chair used in libraries are 1,335 N, 2,225 N and 3,115 N which are in light, moderate and heavy-duty load capacities, respectively.

#### 2.1.1.2.2.6 Cyclic Side-Thrust Load Test on Arm

In this test, loads are applied horizontally by pulling sideway (outward) on arms of chair until its joint fails or reaches acceptable load level (Figure 2.15). The purpose of this test is to evaluate strength of arm to side-thrust forces which occur when user pulls it sideways or pushes arms outward while sitting down or rising [43].

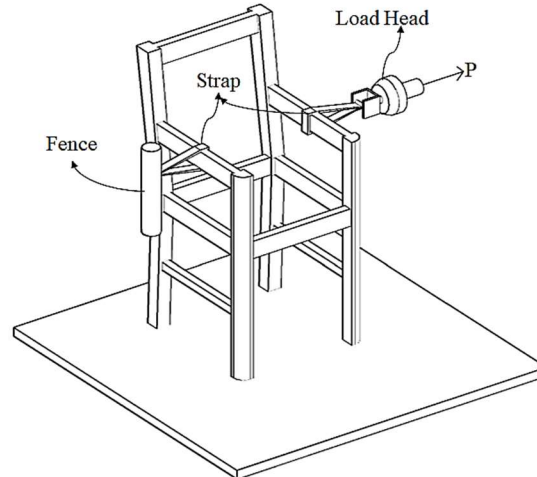


Figure 2.15 Depiction of Cyclic Side-Thrust Load Test on Arm

The test procedure for this test is to apply load horizontally to arm with initial load of 222.5 N at a rate of 20 cycles per minute. After completing 25,000 cycles at each preceding load levels, loads are increased at increment of 111.25 N [43].

According to ALA specifications (ALA 1995) [46], levels of performance for chair used in libraries are 667.5 N, 1,001.25 N and 1,335 N which are for light, moderate and heavy-duty load capacities, respectively.

Initial load and load increments for performance testing on chair were summarized in Table 2.1.

Table 2.1 Summary of Performance Test Load Schedule (Adopted from [4])

Cyclic performance test type		Initial load (N)	Load increment (N)
Vertical load test	Solid wood	445	445
	Upholstered	667.5	166.88
Front-to-back load test on chair frame		445	111.25 (222.5)
Back-to-front load test		445	111.25 (222.5)
Side-thrust load test on chair frame		222.5	111.25 (222.5)
Front-to-back load test on backrest		890	445
Side-thrust load test on arms		222.5	111.25

\* Values in parenthesis are load increments after 1112.5 N load level applied on chair.

### 2.1.1.2.3 Palmgren-Miner Rule to Predict Fatigue Life of Chairs

A concept was developed for ball bearing by [47] and beams by [48] to determine cumulative fatigue damage. This hypothesis was called Palmgren-Miner linear damage rule, which predicts fatigue failure of components when the summation of number of cycles applied at a stress level,  $N'_i$ , to number of cycles causing failure at each stress level,  $N_i$ , which equals to [47,49];

$$\sum_{i=0}^n \frac{N'_i}{N_i} = 1 \quad n: \text{number of applied stress level} \quad \text{Equation 2.7}$$

Zhang [45] showed that Palmgren-Miner rule could be applied to predict fatigue life of the furniture frame joints subjected to step loads. In this study, graded cyclic load test was applied on T-shaped two-pinned dowel joints constructed of Red Oak whereas 30, 50, 70, and 90 percent of the average ultimate bending moment attained from the static bending test of joints were applied on joints for constant cyclic load. All tests were conducted according to GSA recommendations. In the constant cyclic load test, results were shown on a log-linear plot for bending moment versus number of cycles to failure (M-N curves) and regression equation was obtained to predict number of cycles causing failure at the strength level. The regression equation is;

$$M = C + (D \times \log_{10} N_i) \quad \text{Equation 2.8}$$

where,  $M$  is bending moment, and  $C$  and  $D$  are fitting constant in regression analysis.

According to the results in this study, the M-N curve and regression equation for red oak specimens are given in Figure 2.16. By using the given regression equation and Palmgren-Miner rule, fatigue life of furniture frame joints is predicted in Table 2.2 (In this study, lb-in system was used. Therefore, prediction was made in the same system and then results were converted to metric system).

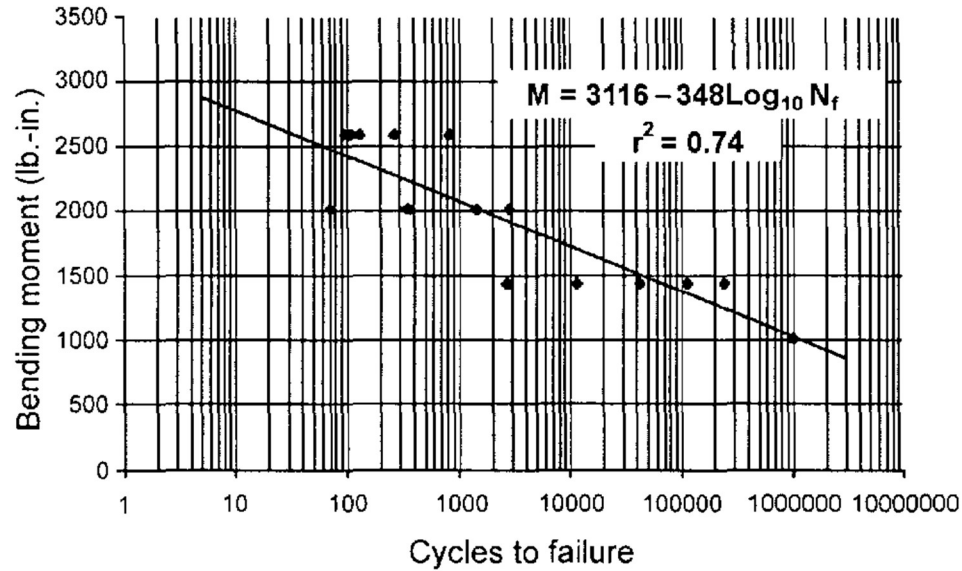


Figure 2.16 M-N Curve from Constant Bending Test of Red Oak Joints [45]

Table 2.2 Calculation of The Fatigue Life for Red Oak Joint Using Palmgren-Miner Rule (Adopted from [45]).

<b>i</b>	<b>M lb-in (N.m)</b>	<b>N<sub>i</sub></b>	<b>N'<sub>i</sub></b>	<b>N'<sub>i</sub>/N<sub>i</sub></b>
<b>1</b>	600 (68)	1.7E+07	25000	0.00147
<b>2</b>	900 (102)	2333548	25000	0.01071
<b>3</b>	1200 (136)	320627	25000	0.07797
<b>4</b>	1500 (170)	43652	25000	0.57271
<b>5</b>	1800 (204)	6025	N <sub>4</sub>	N <sub>4</sub> /6025
				<b>N<sub>4</sub>=102032</b>

According to results given in [45], fatigue life of red oak joints was 102,537 cycles in stepwise cyclic load test. The prediction of fatigue life from constant cyclic load of same type joint is 102,032 cycles with an error of 0.5%.

## 2.2 Joint Properties

A piece of furniture is a combination of furniture members, furniture joints, and reinforcements. The basic wood chair anatomy is shown in Figure 2.17. This typical household chair consists of (i) furniture members – legs (front and back legs), rails (side,

seat, back and crest rails), splats, and stretchers (side and cross stretchers), (ii) furniture joints – mortise and tenon joints (tenons for splats, crest rail and back rail, haunched tenons for seat rails, and loose tenons for side rails and stretchers), and (iii) reinforcements – corner blocks, pins, and screws. Furniture strength relies on the strength of furniture members and joints. If any of these furniture components fail, furniture itself fails. Therefore, the selection of material, size, and shape of furniture components come into prominence in the design process of reliable and durable furniture structures.

Joints are the weakest components of furniture structures. Most of the failure occurs due to loosen or failed joints rather than fractured legs or rails. Zhang stated that 61% of 172 outward arm tests showed joint failure whereas only 3% failed due to member material failures [45]. The strength and stiffness of joints determine strength and stiffness of furniture [50], and unreliable joints result in unreliable furniture [10]. Therefore, studies related to furniture engineering and strength design have been taken into consideration to estimate and determine joint strength of different types of joints.

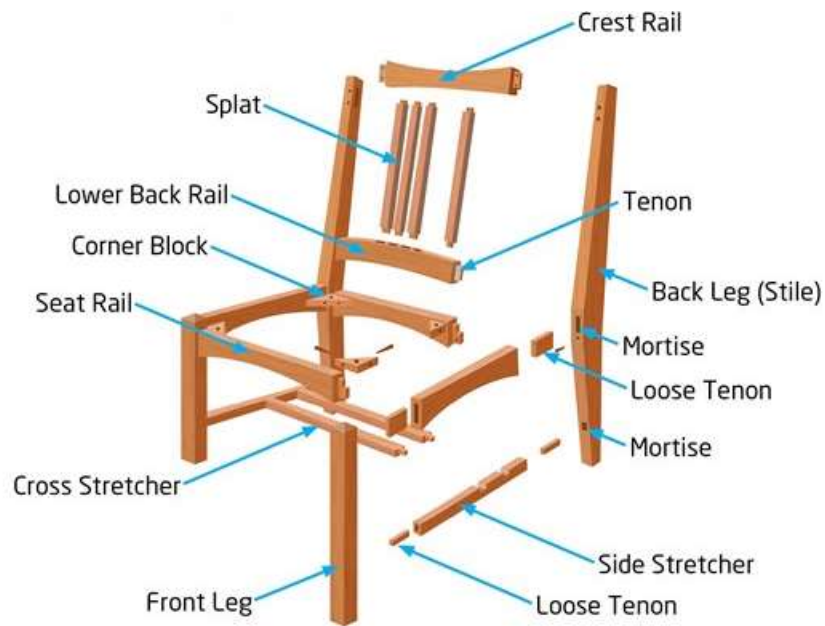


Figure 2.17 A wooden Chair Anatomy [51]

The quality of furniture joints is determined in terms of reliability, which is probability of failure of a joint in furniture structure, strength which is load resistance limit, and stiffness. Reliability of a furniture joint is directly influenced by strength and stiffness characteristics of a furniture joint. Individual behavior of furniture components under loading is not only affected by fundamental laws of Newtonian mechanics but also physical characteristics of materials used in furniture construction. Therefore, strength and stiffness of joints are characterized by using resistance limits with loads causing stress and strain. In here, resistance limit which occurs depending on maximum failure load of joints comes into prominence. If load imposed on a chair frame exceeds strength limit of joint, it fails after load is transferred on the system. In the design process, mechanical and physical behaviors of joints should be taken into consideration to make durable and reliable joints by selecting appropriate joint type, material type, joint geometry, and adhesive type if joint is classified as shape-adhesive joints [1].

The stiffness of L-shaped joints is determined by using following equations for L-shape joints [1]:

$$k = \frac{M}{\varphi} [Nm/rad] \quad \text{Equation 2.9}$$

where,  $k$  is stiffness coefficient,  $M$  is bending moment capacity, and  $\varphi$  is rotation angle of joints.

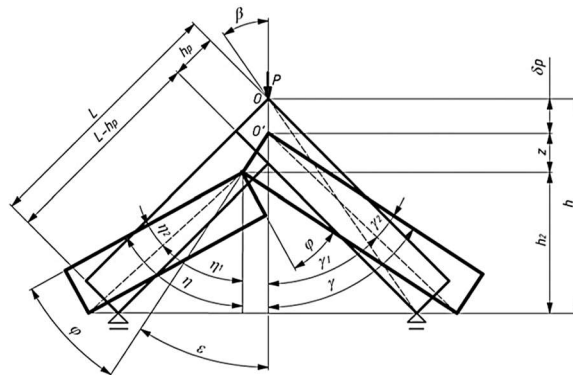


Figure 2.18 Load Scheme of Joints in Diagonal Tension Test [1]

In the case of diagonal tension test of L-shaped joints (Figure 2.18), stiffness of joint is calculated by using following equation:

$$k_R = \frac{M_R}{\varphi_R} \quad \text{Equation 2.10}$$

$$M_R = \frac{1}{2} P (L^2 + h_p^2)^{1/2} \sin \left( \arccos \frac{h - \delta_p}{(L^2 - h_p^2)^{1/2}} \right) \quad \text{Equation 2.11}$$

$$\varphi_R = \eta - \varepsilon \quad \text{Equation 2.12}$$

$$\eta = \eta_1 - \eta_2 \quad \text{Equation 2.13}$$

$$\eta_1 = \arccos \frac{L - h_p}{[(L - h_p)^2 + h_p^2]^{1/2}} \quad \text{Equation 2.14}$$

$$\eta_2 = \arccos \frac{h_2}{[(L - h_p)^2 + h_p^2]^{1/2}} \quad \text{Equation 2.15}$$

$$h_2 = \frac{\sqrt{2}}{2} (L + h_p) - h_p \cos(\varepsilon) - \delta_p \quad \text{Equation 2.16}$$

$$\varepsilon = 90^\circ - \gamma \quad \text{Equation 2.17}$$

$$\gamma = \gamma_1 - \gamma_2 \quad \text{Equation 2.18}$$

$$\gamma_1 = \arccos \frac{(L^2 + h_p^2)^{1/2} \left[ \frac{\sqrt{2}}{2} (L + h_p) - \delta_p \right]}{L^2 + h_p^2} \quad \text{Equation 2.19}$$

$$\gamma_2 = \arccos \frac{L \times (L^2 + h_p^2)^{1/2}}{L^2 + h_p^2} \quad \text{Equation 2.20}$$

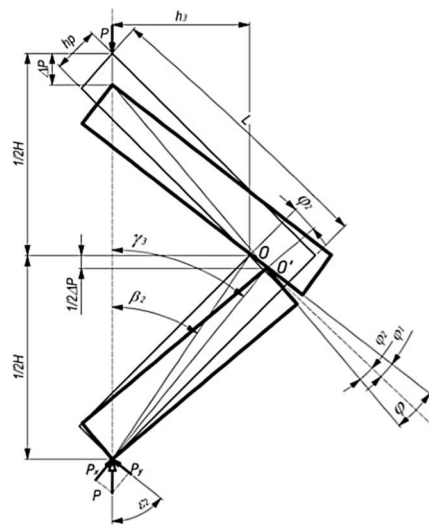


Figure 2.19 Load Scheme of Joints in Diagonal Compression Test [1]

In the case of diagonal compression test of L-shaped joints (Figure 2.19), stiffness of joint is calculated by using following equation [1]:

$$k_z = \frac{M_z}{\varphi_z} \quad \text{Equation 2.21}$$

$$M_z = P \cos(\Delta\varepsilon_2) [(L - h_p)^2 + h_p^2]^{1/2} \quad \text{Equation 2.22}$$

$$\varphi_z = \varphi_1 + \varphi_2 \quad \text{Equation 2.23}$$

$$\Delta\varepsilon_2 = 45^\circ + \arcsin \frac{h_p}{[(L - h_p)^2 + h_p^2]^{1/2}} - \varphi_2 \quad \text{Equation 2.24}$$

$$\varphi_2 = \gamma_3 - \beta_2 \quad \text{Equation 2.25}$$

$$\gamma_3 = \arccos \frac{\frac{1}{2}(a - \delta_p) [(L - h_p)^2 + h_p^2]^{1/2}}{(L - h_p)^2 + h_p^2} \quad \text{Equation 2.26}$$

$$\beta_2 = \arccos \frac{\frac{1}{2}a [(L - h_p)^2 + h_p^2]^{1/2}}{(L - h_p)^2 + h_p^2} \quad \text{Equation 2.27}$$

$$a = \sqrt{2}L \quad \text{Equation 2.28}$$

$$\varphi_1 = \varphi_2 \quad \text{Equation 2.29}$$

$$\varphi_z = 2\varphi_2 \quad \text{Equation 2.30}$$

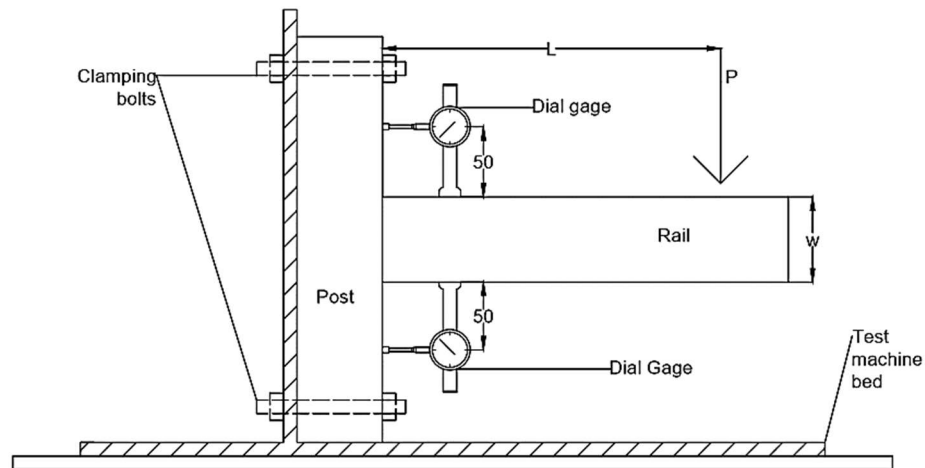


Figure 2.20 Load Scheme of Joints in Bending Test [52]

In the case of bending test of T-shape joints (Figure 2.20), stiffness of joint is calculated by using following equation [52]:

$$\frac{1}{k} = Z = \frac{y_1 + y_2}{2 + 2 + w} \times \frac{1}{M} [\text{rad}/\text{Nm}] \quad \text{Equation 2.31}$$

$$k = Z^{-1} [\text{Nm}/\text{rad}] \quad \text{Equation 2.32}$$

where,  $Z$  is semi-rigidity (semi-stiff) values,  $y_1$  and  $y_2$  are the absolute values on dial gage (m),  $w$  is width of the rail, and  $M$  is bending moment capacity of joint.

The stiffness of a joint varies depending on joint type, materials used in joint, and joint geometry. In Figure 2.21, if stiffness of joint exceeds stiffness quotient,  $k_1 = M_1/\varphi_1$ , joint is perfectly stiff. If it is less than  $k_3 = M_3/\varphi_3$ , joint has small stiffness and is considered as a pinned joint where its bending moment capacity is close to zero. On the other hand, if joint stiffness is between  $k_1$  and  $k_3$ , joint would be semi-stiff (semi-rigid) [1]. Each joint type has different stiffness (rigidity). Furniture joints are classified as semi-stiff (semi-rigid).

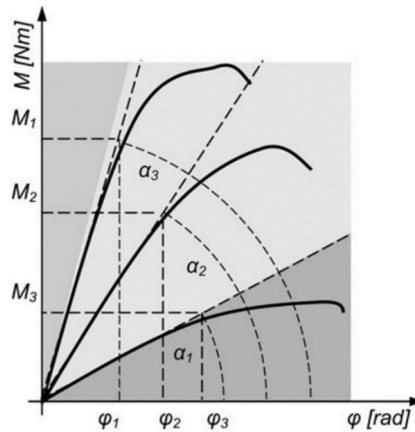


Figure 2.21 Characteristics of the Stiffness of Joints [1]

Furniture joints are divided into two groups; namely, mechanical fasteners and wood-adhesive joints. Mechanical fasteners are a large group of metal and plastic structural nodes; correspondingly, nail, wood screws, bolts, confirmat, and minifix are widely used in furniture construction. The advantage of mechanical fasteners is separable joints. In addition, they are used to reinforce wood-adhesive joints on structural nodes. Figure 2.22 shows mechanical fasteners for furniture construction. On the other hand, wood-adhesive joints are made of wood itself; correspondingly, mortise and tenon joint, dowel joints,

biscuits, and corner blocks. Wood adhesive joints are inseparable joints, but they provide higher strength and stiffness; correspondingly, better reliability compared to mechanical fasteners [1].

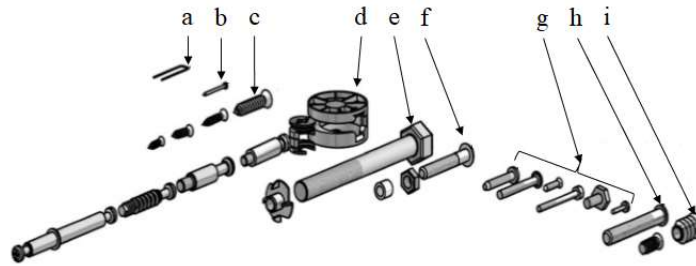


Figure 2.22 Mechanical Fasteners Used in Furniture Constructions [1]

Furniture joints are also classified in terms of connection types by [1]. The classification is shown in Figure 2.23.

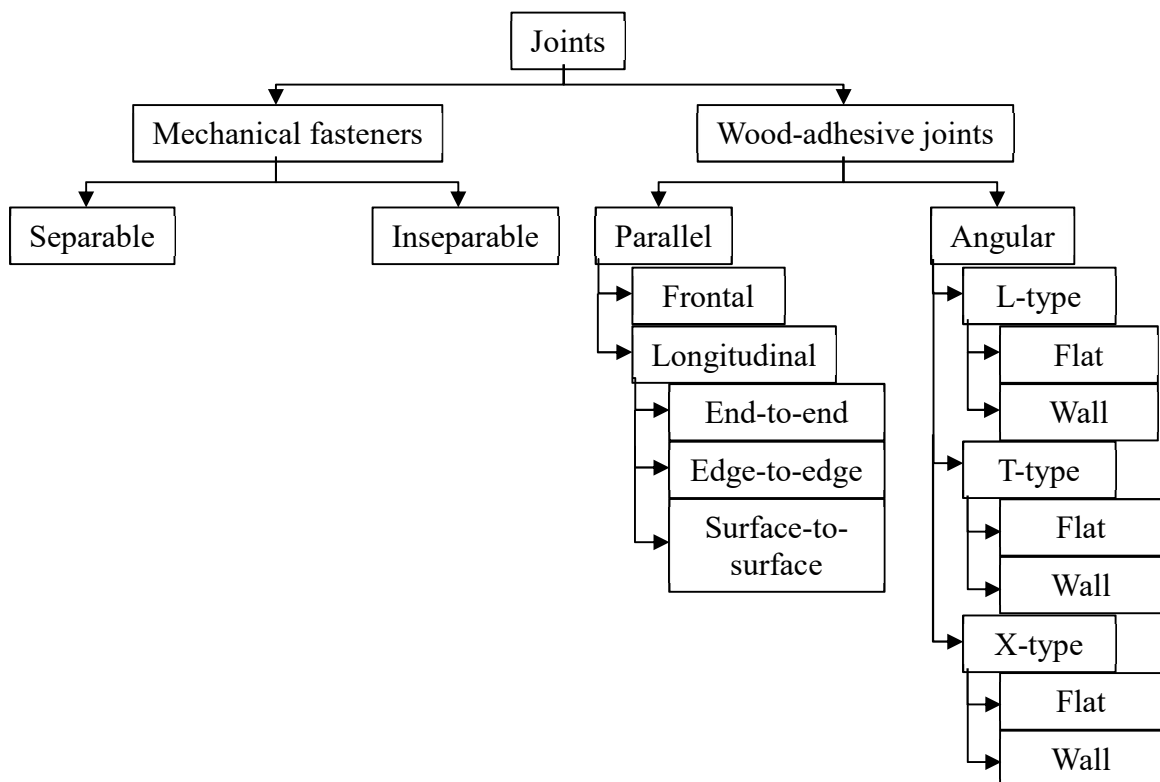


Figure 2.23 Classification of Furniture Joints Used in Furniture Construction [1]

In literature, different types of loads and joints specimens are defined. They are used to determine strength and stiffness of joints (Figure 2.24). Test methods in Figure 2.24a to c measure load capacity under compression loads while those of in Figure 2.24d measures load capacity under tension loading. Torsional strength can be derived by using test method in Figure 2.24e while Figure 2.24f and g shows test methods for shear strength in timber engineering. End withdrawal and face withdrawal test of joints are shown in Figure 2.24i and j.

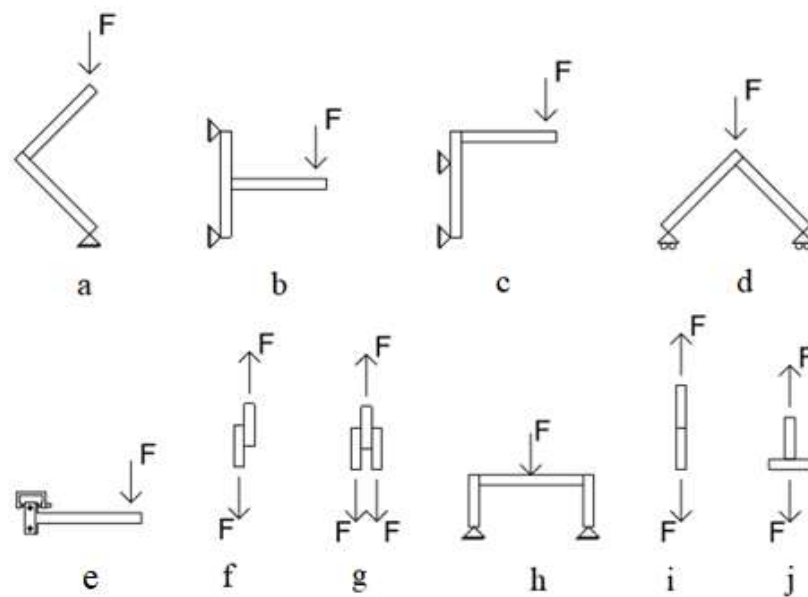


Figure 2.24 Schematic Depiction of Test Methods for Joint Tests: a) Diagonal Compression Test of L-Shaped Joint, b) Compression Test of T-Shaped Joint, c) Compression Test of L-Shaped Joint, d) Diagonal Tension Test of L-Shaped Joint, f) Torsion Test of L-Shaped Joint, g) Shear Test, h) Double-Shear Test, i) Lateral test of Joints, j) End Withdrawal Test and l) Face Withdrawal Test [53]

### 2.2.1 Mortise and tenon joints

Mortise and tenon (MT) joints are classified as rectangular or round mortise and tenon joints. Rectangular mortise and tenon (RMT) joints are the most common joints in frame-type of furniture construction. They provide higher strength and stiffness in construction depending on the type of wood materials used in joint and its geometry. Due to its favorable use in furniture construction, it has been widely studied in literature in the field of furniture

strength design and engineering. The structural behavior of moment-resisting rectangular mortise and tenon forces can be divided into three groups by [4]:

1. Tight fitting rectangular mortise and tenon (Figure 2.25) – top and bottom of tenons are supported by top and bottom of mortises. In the case of long tenon, joints behave as a mechanical joint, so strength of the joint can be calculated as strength of the tenon itself.

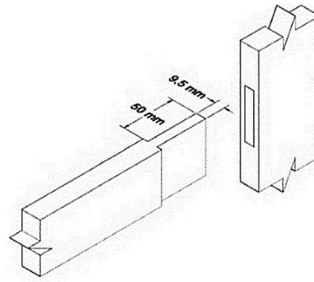


Figure 2.25 Depiction of Tight-Fitting Rectangular Mortise and Tenon [4]

2. Tight fitting rectangular mortise and tenon but top and bottom of mortise are rounded (Figure 2.26) – only sides of tenons are bonded with wall of mortise. The joint resists to torsional shear strength on glue line between walls of mortise and sides of tenon under bending force, so joint strength relies on tenon length and width but not thickness of tenon until it fails due to bending force.

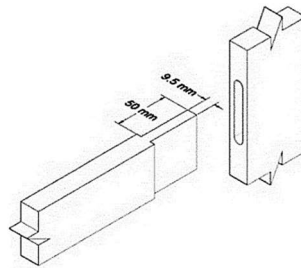


Figure 2.26 Depiction of Tight-Fitting Rectangular Mortise and Tenon with rounded Mortise [4]

3. Poor matched mortise and tenon joints (Figure 2.27) – joint strength depends on the glue line and joints fails due to withdrawal of tenon or insufficient support on top and bottom of mortise. In the case of using short tenons in joint, rectangular mortise and tenon joints behave as dowel joint until glue line failure. Then, its longitudinal axis is slightly stressed.

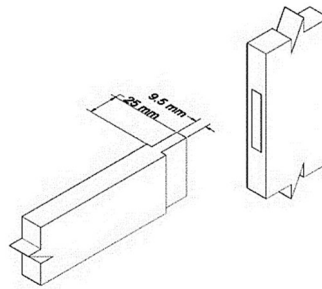


Figure 2.27 Depiction of Poor Matched Rectangular Mortise and Tenon [4]

Numerous studies have been conducted about strength and stiffness of MT joints which depends on their size, wood species, type, applied adhesive, etc. These studies are represented chronologically below:

Eckelman and Hill studied flexibility and bending strength of mortise and tenon joints [54]. The purpose of the study was to estimate strength of the mortise and tenon joints by regarding effects of joint size, wood species, and adhesives to derive an equation for their design calculation. This study shows that there was no linear relationship between bending strength of mortise and tenon joints, and tenon length as shown Figure 2.28. On the other hand, relationship between its bending strength and tenon width was linear. Also, the study indicates that larger tenon width and length provided stiffer mortise and tenon joints but tenon width had a higher impact on its stiffness compared to tenon length. Shoulder effects also increased stiffness of joints; namely, joint strength with shoulder was 20% greater than a joint with same size tenon without shoulder. Furthermore, the study expressed an equation by using linear regression analysis method to predict bending strength of rectangular mortise and tenon joints considering joint size, wood species, adhesive type,

and tenon fit factor in equations 33 and 34. The difference between actual joint strength and those predicted was at most 6.08% but was 29.45% for joints made of yellow poplar.

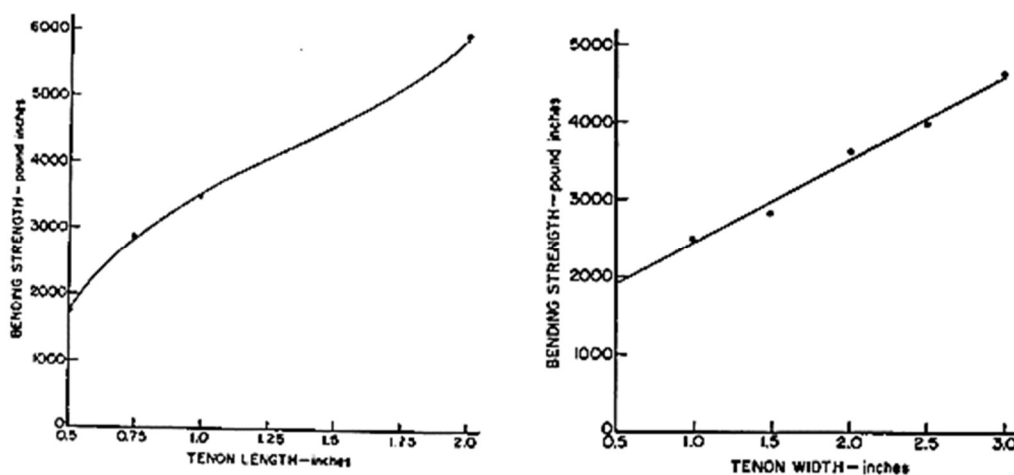


Figure 2.28 Effect of Tenon Length and Width on Joint Strength [54]

$$M = 0.7 \times S \times A \times B \times C \times D \quad \text{Equation 2.33}$$

$$A = (0.24 \times d) + (0.57 \times w) \quad \text{Equation 2.34}$$

where,  $M$  is bending strength,  $S$  is shear strength of wood species in joint,  $A$  is tenon-rail with factor,  $B$  is tenon length factor,  $C$  is adhesive factor,  $D$  is tenon fit factor,  $d$  is rail width, and  $w$  is tenon width. In the calculation of joint strength by using equations 2.33 and 2.34, pound-inch system should be used owing to correction factors. Otherwise, the calculations may give unreliable results. Equation factors are given in Appendix A.

Smardzewski stated that furniture design process is not only considered as drawing and standard requirements, but should also comprise of strength and rigidity of furniture construction [55]. Although furniture is constructed by neglecting or by completely overlooking these mechanical calculations, quality assurance with standards and certificates dictates that furniture manufacturers provide their appropriate strength certificates. Therefore, a mathematical model was developed to determine the strength of profile-adhesive joints used in skeleton (frame-type) furniture. While strength of a furniture construction depends on strength of joints subjected to bending, shear and tension, strength

of adhesive joint relies on shear strength of glue-line. The maximum shear stress is defined as:

$$\tau_{max}^2 = \tau_1^2 + \tau_{2max}^2 - 2\tau_1\tau_{2max} \cos\left(90^\circ + \arccot\frac{2z}{h} + \arccot\frac{T}{N}\right) \quad \text{Equation 2.35}$$

$$\tau_1 = \frac{(T^2 + N^2)^{0.5}}{nhl} \quad \text{Equation 2.36}$$

$$\tau_{2max} = \frac{c}{n} \left[ M - \frac{1}{3}(\sigma\delta l(l-z) - Tz - Nh) \right] \times \frac{1}{\int_{-(l-z)}^z \int_{-h/2}^{h/2} (\eta^2 + \xi^2) d\eta d\xi} \quad \text{Equation 2.37}$$

where,  $\tau_{max}$  is maximum shear strength on glue-line,  $\tau_l$  is shear stress caused by tension and shear force,  $\tau_{2max}$  is the highest shear stress caused by external moment,  $T$  is shear force,  $N$  is axial tension force,  $M$  is external moment,  $c$  is centerline of tenon,  $z$  is new position of centerlines after loading,  $n$  is number of tenons,  $h$  is width of tenon,  $l$  is length of tenon,  $\sigma$  wood compression strength, and  $\delta$  is thickness of tenon.

The rational design of furniture dictates that expressions are available to estimate bending strength of the joints [52]. Hence, T-shaped rectangular mortise and tenon joint specimens were constructed with different tenon and mortise size, rail width, wood species, and adhesives in the study. The purpose of this study was to express a prediction for bending moment capacity of these joints considering their variables. A linear regression analysis was used to evaluate bending strength and regression expression and is given in equation 2.38. In 15 sample groups, differences between actual joint strength and predicted strength was at most 7.7% but in their sample groups; namely, joints made of yellow poplar (50 mm-tenon wide and 25 mm-tenon long) adhered with phenol-resorcinol, sugar maple (50 mm-tenon wide and 12.5 mm-tenon long) adhered with urea-formaldehyde, and sugar maple (50 mm-tenon wide and 25 mm-tenon long) adhered with urea-formaldehyde, the differences were 21%, 15.4% and 10.1%, respectively. Furthermore, this study shows that joints become stiffer with an increasing of tenon length and width, and rail width, or any combination of them. Also, the change in tenon width is more effective on stiffness of joint than tenon length.

$$M = a \times [0.25 \times (W - D) + 0.78 \times D] \times L^{0.8} \times S \quad \text{Equation 2.38}$$

where,  $M$  is predicted bending moment capacity of joint,  $a$  is adhesive factor,  $W$  is rail width,  $D$  is tenon width,  $L$  is tenon length, and  $S$  is shear strength of wood.

Tankut and Tankut studied the dimension and edge-shape effects on bending moment capacity of rectangular mortise and tenon joints [56]. Edge-shape of mortises and tenons were separated into three categories: (i) round mortise and tenon (RoMT), (ii) rectangular mortise and tenon (RMT), and (iii) round mortise and rectangular tenon (RoMRT). According to results, joints strength with RMT was approximately 15% and 30% higher than those of RoMT and RoMRT, respectively. Moreover, this study shows that joint strength was getting greater while increasing effect of the shoulder on joints. On the other hand, in the study, tight and loose mortise and tenon joint were benchmarked. Tight joints provide 1% to 10% greater joints than loose joints but tight round tenon and mortise joints with 75 mm-rail thick and 65 mm-tenon thick had 0.5% less joint strength than those of loose joints.

Eckelman *et al.* studied shoulder effects of round mortise and tenon joints [57]. Joint strength increases in the presence of shoulder on joints owing to the change in neutral axis of tenon. In doing so, the loading of shoulder is altered from bending to tension. In the study, the joint specimen was constructed with different tenon diameters and rail width. T-shaped joints were tested under static loading and bending moment capacity of joints were attained. The test results were used to predict bending strength of joints with shoulder and without shoulder by using linear regression analysis. Prediction of bending moment capacity of round mortise and tenon joint with shoulder, those of without shoulder, and tenon withdrawal strength is given equation 2.39, 2.40, and 2.41, respectively.

$$F_S = 0.934 \times \frac{2w}{D^{1.66}} \times F_{NS} \quad \text{Equation 2.39}$$

$$F_{NS} = 1.18 \times \left( \pi \times \frac{D^3}{32} \right) \times S_4 \quad \text{Equation 2.40}$$

$$T = \frac{F_S}{0.894 \times w} \quad \text{Equation 2.41}$$

where,  $F_s$  is bending moment capacity of joint with shoulder,  $w$  is rail width,  $D$  is tenon diameter,  $F_{NS}$  is bending moment capacity of joint without shoulder,  $S_4$  is modulus of rupture of wood in tenon and  $T$  is tenon withdrawal resistance in tension.

Eckelman and Haviarova studied the strength of chair frames constructed with round mortise and tenon joints [58]. The load level of chairs was benchmarked to acceptable load levels specified for library chairs by the ALA. Service life of chairs is expected to be at least 2 years without failure if chair survives under 1001 N to 1112 N cyclic front-to-back load (light duty classification), but these load levels are satisfactory for household chairs. In the case of chairs' resistance to 1557 N cyclic front-to-back load (medium duty classification), their service life is expected to have many years. On the other hand, chairs that are designed according to 2002 N load level are provided greater strength than expected surviving time; that's why 1557 N load level can be accepted to have a long span of life for chairs. According to test results, the number of stretchers is significant in the increase chair strength. Strength of chair with 3 stretchers made of red oak is 26% and 81% higher than those of 2 stretchers and 1 stretcher, respectively. In the case of stretchers made of yellow poplar, these differences are 31% and 81%, respectively.

Prekrat and Smardzewski studied effects of glue line shape on strength of rectangular mortise and tenon joints [59]. In furniture industry, tenon gluing is processed poorly because only flat surfaces are adhered. Hence, they obtained two parallel bonds with the wall of mortises which has no interaction with each other. For this purpose, rectangular mortise and tenon joints were modeled with adhering polyvinyl acetate (PVA) on Algor which is a Finite Element Analysis software. In the first set of joints, sides of the tenon were only glued (poorly) whereas all surfaces were bonded (properly) in the second set. Results showed that properly glued joints had greater strength than those of poorly glued. Highest shear strength was also attained on the edges of tenon. Properly glued joints had the greatest normal stress due to bending, but their shear stress reduces due to an increase in effective cross-section of glue line.

Likos *et al.* studied effects of tenon geometry (rectangular mortise and tenon, round mortise and tenon, and diamond mortise and tenon joints), grain orientation, and shoulder (tight and loose) on bending moment capacity of mortise and tenon joints [60]. For this purpose, T-shaped mortise and tenon joints constructed of Loblolly pine tested under an edgewise static load. According to results in the case of tight shoulders, strength of joints which had 45° grain orientation was 8% and 11% greater than those of radial and tangential grain orientation, respectively. On the other hand, results in the case of loose shoulders shows these ratios were 8.2% and 4.5%. Furthermore, joints with tight shoulders provided higher strength (1.58 times greater) than those of loose shoulders. The length of the tenons had a significant effect on joint strength because joints with shorter tenon length failed probably due to adhesive failure, whereas those of longer length were expected to indicate primarily tenon fracture. In test results, in the case of tight shoulder, joint strength of 50.8-mm tenons had 34.7 and 43.7% greater strength than those of 38.1mm- and 25.4mm-. Moreover, joint geometry had a significant effect on joints strength as well. In the case of tight shoulder, diamond-shape mortise and tenon joints had higher strength with 25.4mm- and 38.1mm-tenons while rectangular mortise and tenon joint with 50.8 mm-tenon had greater strength compared to others. In the case of loose shoulder, rectangular mortise and tenon had higher strength owing to its section properties because only the joint cross-section was effective during testing.

Prekrat *et al.* studied the quality of a chair constructed with round mortise and tenon joints [61]. Durability of the joints under dynamic and static loading is an indicator for quality of products. For this purpose, a coefficient of bending moment capacities between dynamic and static were used to estimate reliability of the chair frames. According to test results, average static load capacity of specified chair test was 154.36 N.m. Correspondingly, bending moment capacities of chairs in dynamic test were recorded. Logarithmic relationship between a coefficient of moment capacity in dynamic load testing and static load testing, and number of cycles at failure were given. According to this relationship, an equation was found:

$$y = -0.077 \times \ln(x) + 0.8857$$

Equation 2.42

where  $y$  is coefficient of bending moment capacity in dynamic load and static load testing and  $x$  is number of cycles in failure. Also, the correlation between coefficient and number of cycles is dependent on each other and was high ( $R^2 = 0.91$ ). This study shows that fatigue life of chair frames could be estimated as long as both the bending moment capacity in static load test and the required number of cycles for chair frames are known.

Kasal *et al.* studied effects of tenon size and type of adhesive on joint strength [62]. For this purpose, tenons were cut at different lengths and widths. Furthermore, T-shaped rectangular mortise and tenon joints were glued with polyvinyl acetate (PVA) and polyurethane (PU), and then tested under actions of an in-plane static load. Test results show that joint strength and rigidity increased when tenon width and length increased. Strength of joints with PVA adhesive is slightly greater than those of PU. Bending moment capacities of joints were used to predict strength of joints by using non-linear regression analysis. This expression was fitted to data:

$$M = 0.003 \times \left(\frac{2WL}{3}\right) \times \left(\frac{W}{3} + d\right) \times S^{0.56} \times A \quad \text{Equation 2.43}$$

where,  $M$  is bending moment capacity of joint,  $W$  is tenon width,  $L$  is tenon length,  $d$  is shoulder width,  $S$  is shear strength of wood, and  $A$  is adhesive factor (1 for PVA and 0.95 for PU).

Likos *et al.* studied static and cyclic load carrying capacities of side chair frames constructed with rectangular, round, and diamond-shaped mortise and tenon joints [63]. Failure loads of chairs were benchmarked under both test types. Static load capacity of side chair frames with rectangular mortise and tenon joints are 14.8% and 11.1% greater than those of round and diamond. In the case of chairs in cyclic loading, ultimate failure loads of chair were 1.7 kN, 1.8 kN and 1.9 kN for rectangular, round, and diamond-shaped mortise and tenons, respectively. Also, the study showed that the cyclic load capacity of side chair frames was approximately 2/3 of their static load capacity.

Hajdarevic and Martinovic studied flexibility of mortise and tenon joints [64]. In this study, rotational stiffness and semi-rigidity of joints were investigated by using finite element methods. T-shaped joints were modelled with analogue of specimen in [52]. Test results were compared to the results of [52]. Differences between physical experiment and the finite element model varied 3.18% to 35.94%. A frame model was also defined according to transverse shear, based on Timoshenko beam theory, which was put together with rigid joints and semi-rigid joints with different tenon length. Rigid joints were 27% and 42% stiffer than semi-rigid joints with 50.8 mm and 12.7 mm tenon length, respectively.

Derikvand *et al.* studied bending moment capacity of mortise and loose-tenon joints, considering bottom shoulder width, tenon embedment on rail, tenon width, and wood species in tenons [65]. For this purpose, T-shaped joints constructed of oriental beech with tenons made of white oak, oriental beech, cottonwood, silver fir, and butternut were tested under in-plane static load. According to the results, the increase in shoulder width and tenon embedment enhanced joints strength significantly. Joints with tenons made of beech wood also had the highest bending moment capacity whereas those of fir wood had the lowest bending moment capacity. This study also indicated that there were no statistically significant differences between white oak, cottonwood, and butternut; correspondingly, shear strength of wood species has no linear relationship with bending moment capacity of joints. Furthermore, a nonlinear regression expression was fitted to test data:

$$M = 0.1 \times (W^{0.71} \times L) \times (W^{0.71} + Sh^{0.92}) \times (S_t^{0.63} + S_r) \quad \text{Equation 2.44}$$

where,  $M$  is bending moment capacity of mortise and loose-tenon joint,  $W$  is tenon width,  $L$  is tenon length,  $Sh$  is shoulder width,  $S_t$  is shear strength of wood in tenon, and  $S_r$  is shear strength of wood in rail. The coefficient of multiple determination of expression was 90%. The differences between bending moment capacity of joints in physical experiment and those in predicted were varied 0.1% to 12.7%.

Derikvand and Ebrahimi (2014) studied the effects of adhesive type (PVA and PU) along with tenon width and length on bending moment capacity of mortise and loose-tenon joints

constructed of oriental beech [66]. Loose-tenon joints are more economical and efficient compared to traditional mortise and tenon joints due to the fact that they are not cut from the end of rails. Another factor is that loose-tenon joint production required less time and ease of manufacturing than dowel joints. According to the test results, joint strength was greater when tenon embedment and thickness were increased. Joints adhered with PU also provided approximately 10% greater strength than those of PVA. The study proposed a non-linear regression expression for mortise and loose-tenon joints constructed of oriental beech wood;

$$M = 0.19 \times (L^{0.46} \times Th^{0.75}) \times (L^{0.46} + Th^{0.75}) \quad \text{Equation 2.45}$$

where,  $M$  is bending moment capacity,  $L$  is tenon length, and  $Th$  is tenon thickness. The correlation of multiple determination was 88% in this expression. Moreover, this study showed that the difference between bending moment in the experiment and predicted bending moment was at most 8.33%.

Oktaee *et al.* studied the determination of bending moment capacity of haunched mortise and tenon joints [67]. For this purpose, L-shaped rectangular mortise and tenon joints constructed of oriental beech wood were tested under diagonal compression and tension loads. In the study, 20-25-30 mm-tenon length x 7.5-10-15 mm-tenon thickness were used. In the first set of sample groups, tenon width was 50 mm without shoulder, while it was 37.5 mm and 25 mm with upper shoulder in the second set, and both upper and lower shoulder in the third set of sample groups, respectively. The fourth set of sample groups belonged to haunched rectangular mortise and tenon joints which had 37.5 mm- tenon width and 70% of haunch of tenon length (14-17-20 mm). According to the test results, the strength of joints with 37.5 mm-tenon width was 29.4% and was 46% greater than those of 25 mm and 50 mm. Joint strength with 50 mm-tenon width was lower since the top of the tenon was not supported with a mortise edge. To attain highest bending moment capacity, tenon width should be  $\frac{3}{4}$  of rail width. Moreover, joint strength with 10 mm-tenon thickness provided 8.6% and 13.3% higher strength than those with 7.5 mm and 15 mm. The study shows that tenon thickness should not exceed  $\frac{1}{3}$  of rail thickness; that's why,

joint strength with 15 mm-tenon thickness was lower than those of 10 mm. Furthermore, tenon length has a positive impact on bending moment capacity of joints. Joint strength with 30 mm-tenon length was 61% and 30.2% greater than those of 20 mm and 25 mm. The joint strength in compression testing was 50% higher than those in tension testing. In compression tests, joint strength with haunched mortise and tenon was 2.6%, 11.9% and 14.5% greater than those of second, third and first sample groups respectively. In the case of tension tests, joint strength was 13.4% and 23.1% higher than those of third and first sample groups respectively but 12.1% less than those of second sample group. The study shows that haunched rectangular mortise and tenon joints could provide greater strength or equal to traditional rectangular mortise and tenon joints' strength, considering enough joint size in both the compression and tension tests.

Kasal *et al.* studied the effects of wood species, adhesive type, and tenon size on bending moment capacity of L-shaped rectangular mortise and tenon joints in both diagonal compression and tension loadings [68]. To design furniture with rectangular mortise and tenon joints, it should be known that joints can resist imposing loads during their usage, ultimate capacity, and bending moment capacity. According to the test results, joints constructed of Turkish beech wood provided 25.1% and 13.9% greater strength than those of Scotch pine in compression and tension loading respectively. The strength differences between compression and tension loading were also 11.7% and -1.5% for Turkish beech and Scotch pine respectively. Joint strength increases when there is an increase in tenon length and width in both the compression and tension tests. A non-linear regression expression was fitted to test data to predict bending moment capacity of rectangular mortise and tenon joints considering tenon size, adhesive type, wood species, and loading type:

$$M = 0.00227 \times (W \times L) \times ((0.229 \times W) + d) \times S^{0.42} \times k_1 \times k_2 \quad \text{Equation 2.46}$$

where,  $M$  is bending moment capacity of joint,  $W$  is tenon width,  $L$  is tenon length,  $d$  is width of shoulder,  $S$  is shear strength of wood in tenon,  $k_1$  is coefficient of type of loading (1 for tension and 1.066 for compression loading), and  $k_2$  is coefficient of adhesive type (1 for PU and 0.85 for PVA). The correlation between average bending moment in

experiments and predicted bending moment capacity was 61.6%, which is lower compared to the other non-linear regression expression.

Kasal *et al.* studied the relationship between static front-to-back load capacity of a whole chair and the strength of individual chairs [69]. To produce reliable chair frames, joint strength, the mechanical behavior of wood used in joint, and improving the strength of joint should be taken into consideration. Therefore, joint sizes, adhesive type, shear strength of wood, tolerances between mortise wall and tenon sides, and gluing applications are set properly to increase the reliability of a product. For this purpose, a full-frame chair, individual T- and L-shaped rectangular mortise and tenon joints (for rail and post), and T-shaped round mortise and tenon joints (for stretcher and post) were tested under static loading. The bending moment of chair frame and joints with different tenon sizes were compared. The median of the ratio of bending moment of chair and joint was 1.4. The following equation was then used to estimate the load capacity of a full chair frame corresponding to bending moment capacity of an individual joint;

$$F_t = 2 \times \frac{[1.4 \times (T_m + L_m + 2T_{m2})]}{L_c} \quad \text{Equation 2.47}$$

where,  $F_t$  is load capacity of a full-frame chair,  $T_m$  is maximum bending moment capacity of T-shape rectangular mortise and tenon joints,  $L_m$  is maximum bending moment capacity of L-shaped rectangular mortise and tenon joints,  $T_{m2}$  is maximum bending moment capacity of T-shaped round mortise and tenon joints, and  $L$  is moment arm (height of the point where load applied). Results showed that average differences between load capacity of the full-frame chair and those estimated are 13%. The strength of full-frame chair is also 40% greater than the sum of the individual joint strengths. Hence, the proposed method provides prediction of load capacity level of chairs by using bending moment capacity of individual joints.

Zaborsky *et al.* studied the stiffness of rectangular mortise and tenon joints [70]. For this purpose, diagonal compression and tension loads were applied on L-shaped rectangular mortise and tenon joints with different wood species, joint sizes, adhesive type, and annual

ring deflection. The equation 2.9 was used to determine stiffness of joints. According to results, the highest stiffness (1,627 Nm/rad) was obtained in tension testing with joints made of beech, 12 mm-thick tenons, and PVA glue. On the other hand, the lowest stiffness (608 Nm/rad) was attained in tension testing with joints made of spruce wood, 8 mm-thick tenon, and PU adhesive. Joints made of beech wood were 38% stiffer than those of spruce wood. This study shows that annual ring deflection held significant effects on joint strength. Consequently, the joints were stiffer in compression testing and made of beech wood, 12 mm-thick tenons, PVA adhesive, and 90° annual ring deflection.

Acar *et al.* studied the effects of cross-sectional shapes on bending moment capacity in mortise and tenon joints [71]. Under ideal conditions, the strength of material in a round cross section with 1 mm<sup>2</sup>- area is 18% greater than those of rectangular. For this purpose, T-shaped rectangular and round mortise and tenon joints made of red oak, Scotch pine, yellow poplar, Caobilla, and Gmelina were tested under static loading. According to the test results, joints with circular cross section shape is 2%, 45 and 8% higher than those of rectangular; made of red oak, Scotch pine, and Gmelina respectively. On the other hand, joints made of yellow poplar and Caobilla with rectangular cross sections were 4% and 3% stronger than those with circular cross sections, respectively. The average difference between test values and tabulated modulus of rupture (MOR) in the Wood Handbook was 11.7%.

### 2.2.2 Dowel Joints

Dowel joints are favorable connectors in the furniture industry due to having simple design and construction for furniture. They utilize less material compared to mortise and tenon joints and are known to have high initial strength [1,4]. In furniture construction, dowel joints are expected to subject to axial, shear, bending and torsional forces but they are only subjected to axial and shear forces. Single dowel pins in furniture construction may be subjected to torsional force; this is why use of single pins in construction should be avoided to reduce torsional effect on failure [4].

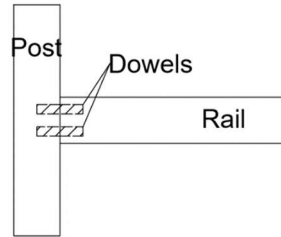


Figure 2.29 Two Pin Moment Resisting Dowel Joint Configuration

In furniture design, axial and shear forces are transferred to the dowels. Therefore, in furniture engineering, the strength of dowel joints depends on the size of joint, shear strength of wood materials used in both dowel pins and furniture members, type of glue, tolerance between dowel holes and dowel pins, and dowel surface. Eckelman studied how to predict withdrawal strength of dowel pins from side grain in solid wood by using the following equation [72]:

$$F_2 = 0.834 \times D \times L^{0.89} \times [(0.95 \times S_1) + S_2] \times a \times b \times c \quad \text{Equation 2.48}$$

where,  $F_2$  is ultimate withdrawal strength of dowels,  $D$  is diameter of dowels,  $L$  is depth of embedment of dowel in the members,  $S_1$  is shear strength of wood material in member parallel to grain,  $S_2$  is shear strength of wood material in dowel pins parallel to grain,  $a$  is adhesive factor,  $b$  is correction factor for dowel-hole clearance, and  $c$  is dowel surface factor. The equation 2.49 is a simplified version of equation 2.48 by using the tables in Appendix A:

$$F_2 = A \times [(0.95 \times S_1) + S_2] \times B \times c \quad \text{Equation 2.49}$$

where,  $A$  is factor for dowel diameter and dowel embedment in members, and  $B$  is factor for clearance of dowel hole, dowel pins, and adhesive type.

The studies showed that the ratio of dowel diameter and embedment in members should be at most  $\frac{1}{4}$  because there is no strength contribution on dowel joints if the ratio exceeds  $\frac{1}{4}$ . Moreover, studies indicated that higher strength for dowel joints was attained with 60%

solid content PVA adhesives. To obtain maximum dowel withdrawal strength, it is significant to apply adequate gluing [4].

Dozens of studies were conducted to determine strength and stiffness of dowel joints depending on material type, test method, number dowels, dowel diameter, depth of dowel embedment, adhesive types, dowel surface patterns, etc. These studies are presented below:

Eckelman studied to determine how dowel size, wood species, adhesive type, and clearance factor of dowel and dowel hole affect withdrawal strength from end-to-side grain and end-to-end grain of single-pin dowel joints [72]. The study was conducted by testing 400 specimens that were constructed of sugar maple, tulip poplar, and red oak with dowels (with diameter of 6.35 mm, 9.4 mm and 12.7 mm) made of white birch, sugar maple, tulip poplar, and red oak. By using test results, a non-linear regression analysis was made, and the following expression was attained to predict withdrawal strength of single-pin dowel joints from end-to-side grain shown equation 2.50. This equation was updated to equation 2.51 when considering rail width, dowel embedment, and dowel surface factor – smooth, multi-grooved or spiral dowel surfaces. For those of end-to-end grain, prediction of withdrawal strength was shown in equation 2.51. According to the results in the study, the difference between predicted and experimental strength varied from 0.2% to 28.31%. Although the prediction provided closer values to some experimental data, due to natural occurrence of wood the difference between them was high for specimens constructed of red oak owing to low density. Furthermore, it was suggested that expressions were used to predict ultimate strength rather than allowable design strength.

$$F_2 = 0.45 \times D \times L^{0.89} \times [(0.95 \times S_1) + S_2] \times a \times b \quad \text{Equation 2.50}$$

$$F_2 = 0.45 \times D \times L^{0.89} \times [S_1 + S_2] \times a \times b \quad \text{Equation 2.51}$$

Eckelman and Hill studied the effects of dowel surface on withdrawal strength of joints [54]. Although furniture manufacturers believe that spiral and multi-grooved dowels have higher strength rather than plain surface dowels in joints. Since glue is distributed in textures on the surface of dowel, the glued area on plain surface dowel increased their

strength more than spiral and multi-grooved dowels. However, the dowel joints are resisting shear and axial strengths. In the case of the cutting patterns on dowel surfaces, the cross-section area of dowel reduces; due to this factor, the shear and axial strengths are weakened. Under certain conditions, plain dowels should provide higher strength rather than patterned dowels. In the study, yellow birch dowels were used with diameters of 9.52 mm, 9.49 mm, and 9.47 mm: plain, spiral, and multi-grooved dowels respectively. The diameter of the dowel hole was 9.58 mm. The specimens were assembled into two different adhesive schedules; namely, (i) both dowel holes and walls were liberally coated with adhesive, and (ii) 0.2 cc adhesive were applied to bottom of each dowel hole by using urea-formaldehyde (UF), PVA with solid content of 40%, 42%, 42.5% and 60%, and liquid hide adhesives. According to the result of the study in the case of liberally adhesive coated, plain dowels are 10.5% and 15.2% stronger than multi-grooved and spiral dowels. On the other hand, plain dowels with 0.2 cc of adhesive are 16.5 % weaker than both multi-grooved and spiral dowels. Furthermore, dowels adhered with PVA with 60% solid contest adhesive give better results. Under ideal conditions and liberally coating, plain dowels provide better results.

Table 2.3 Average Ultimate Withdrawal Strength of Dowels (in N)

Adhesive	Plain	Multi-Groove	Spiral-Groove
<b>Liberally coated</b>			
<b>UF</b>	6488.1	5696	5842.9
<b>PVA-60</b>	6419.1	5927.4	5215.4
<b>PVA-40</b>	5478	5197.6	4516.8
<b>PVA-42.5</b>	5384.5	4694.8	4521.2
<b>PVA-42</b>	5482.4	4819.4	5064.1
<b>Liquid-hide</b>	5393.4	5033	4970.7
<b>0.2 cc. of glue</b>			
<b>UF</b>	3898.2	4828.3	5122
<b>PVA-60</b>	4543.5	5535.8	4752.6
<b>PVA-42.5</b>	3293	4005	4303.2
<b>Liquid-hide</b>	4018.4	4525.7	4677

Eckelman studied the bending strength and moment-rotation characteristics of T-shaped two-pin moment resisting dowel joints, which were constructed of sugar maple wood and

adhered with urea formaldehyde adhesive [50]. Bending strength and moment-rotational characteristic of joints at various rail dimensions and dowel spacing were determined and the result was compared the predicted bending moment capacity by using equation 2.51. Moment rotational characteristic was then determined by using equation 2.52. The least square regression analysis was made to estimate moment rotation on joints and the following equation was attained:

$$\varphi = a_0 + a_1 \times M \quad \text{Equation 2.52}$$

where,  $\varphi$  is rotation (rad),  $a_0$  and  $a_1$  are coefficient polynomials, and  $M$  is bending moment capacity (Nm). These coefficient polynomials should be considered as Z-values for semi-rigidity. Table 2.4 shows results of the study.

Table 2.4 Experimental Average Ultimate and Predicted Bending Moment Capacity, and Moment-Rotational Coefficients of Dowel Joints at Various Rail Dimension and Dowel Spacing [50]

Rail dimension (mm)	Dowel spacing (mm)	Average Ultimate bending Strength (N.m)		Error	Coefficient of polynomials	
		Experimental	Prediction		a <sub>0</sub>	a <sub>1</sub>
19.05x38.1	12.7	134.9	135.9	-0.70%	4.5x10 <sup>-4</sup>	1.1x10 <sup>-5</sup>
19.05x50.8	25.4	222.2	226.4	-1.90%	-6.2x10 <sup>-6</sup>	5.3x10 <sup>-6</sup>
19.05x63.5	38.1	316.2	317	-0.30%	-7.2x10 <sup>-5</sup>	3.1x10 <sup>-6</sup>
19.05x76.2	25.4	285	271.7	4.70%	5.6x10 <sup>-4</sup>	3.5x10 <sup>-6</sup>
19.05x76.2	38.1	361.4	339.6	6.00%	6.3x10 <sup>-5</sup>	3.2x10 <sup>-6</sup>
19.05x76.2	50.8	402	407.6	-1.40%	-2.1x10 <sup>-5</sup>	1.9x10 <sup>-6</sup>
19.05x88.9	63.5	462.4	498.1	-7.70%	-3.4x10 <sup>-5</sup>	1.5x10 <sup>-6</sup>

Eckelman studied the out-of-plane strength and stiffness of T-shaped dowel joints with members constructed of black walnut and dowels made of sugar maple [73]. In the study, withdrawal strength, in-plane bending strength and stiffness, out-of-plane bending strength and stiffness with tight and loose joints, and out-of-plane bending strength and stiffness with various rail thickness were determined. According to the results, in-plane bending

strength of joints is higher than those of out-of-planes. On the other hand, stiffness is greater in out-of-plane bending testing. Both out-of-plane stiffness and bending strength are reduced by increasing the gap between posts and rails, as well as decreasing rail thickness (Table 2.5). The study also provides an equation to predict out-of-plane bending moment capacity of joints:

$$F_4 = \left(\frac{\pi D^3}{16}\right) S_u + \frac{F_2(W+D)}{2} \quad \text{Equation 2.53}$$

where,  $F_4$  is bending moment (Nm),  $D$  is diameter of dowel (mm),  $S_u$  is modulus of rupture of wood for dowel (MPa –N/mm<sup>2</sup>),  $F_2$  is ultimate withdrawal strength of dowel (N), and  $W$  is rail thickness (mm).

Table 2.5 Average Ultimate Strength and Stiffness of Dowel Joints (adopted from [73])

Test Type	Average Ultimate Strength	Regression coefficient (Z-values) (rad/Nm)
Withdrawal	7,264.63 N	-
Bending in-plane	345.87 Nm	3.92E-05
Bending out-of- plane flush fit	102.68 Nm	5.59E-04
Bending out-of-plane with 1.5 mm gap	50.19 Nm	1.36E-03
Bending out-of-plane with 3 mm gap	44.22 Nm	1.63E-03
Bending out-of-plane with 25.4 mm rail thickness	118.68 Nm	3.07E-04
Bending out-of-plane with 31.25 mm rail thickness	137.40 Nm	2.40E-04
Bending out-of-plane with 38.1 mm rail thickness	155.57 Nm	1.84E-04

Zhang and Eckelman performed a study to determine bending moment capacity of L-shaped single-dowel corner joints in the case of construction [74]. Face and butt members were constructed of particleboard with a specific gravity of 0.71, internal bonding strength of 0.68 MPa, modulus of rupture (MOR) of 13.79 MPa, and modulus of elasticity (MOE) of 2,757.90 MPa while (multi-groove) dowels were made of yellow birch wood with diameters of 6.35, 7.9375, and 9.525 mm. In the study, the depths of dowel embedment on face members were 6.35 mm, 11.1125 mm, and 15.875 mm. Those of butt members were 19.05 mm, 25.4 mm, 31.75 mm, and 38.1 mm. The joints were subjected to both

compression and tension loads. The study was replicated with 10 specimens in each sample group (total specimen number is 360 - 3 dowel diameter x 3 face embedment x 4 butt embedment x 2 load x 5 replication). Results show that bending moment capacity of joints were strengthened by increasing dowel diameter and depth of dowel in face embedment in both compression and tension testing. Bending moment capacities of joints in tension test were higher than those of compression tests. The highest bending moment capacity (225.16 N.m) was attained for sample group of dowel diameter of 9.525 mm, face embedment of 15.875 mm, and butt embedment of 25.4 mm in tension testing. Increasing depth of dowel embedment in butt member did not have a significant impact on joint strength due to failure mode on joint specimens. A higher depth of dowel embedment in edge members did not provide higher strength of joints. However, to attain maximum bending strength of joints, the depth of dowel embedment in edge members should be 25.4 mm. Moreover, an equation was created at end of the study to predict bending moment capacity of L-shaped single pin corner joints by means of regression techniques. Equation 2.54 and 2.55 are bending moment of joint in compression and tension tests, respectively.

$$Y_c = 460.4 \times (D^{0.452}) \times (E^{1.14}) \quad \text{Equation 2.54}$$

$$Y_t = 614.4 \times (D^{0.591}) \times (E^{1.18}) \quad \text{Equation 2.55}$$

where,  $Y_c$  is bending moment in compression,  $Y_t$  is bending moment in tension,  $D$  is dowel diameter, and  $E$  is depth of dowel embedment in the face member.

Zhang and Eckelman studied the effects of number of dowels, dowel spacing, and length of specimens in tension and compression tests of L-shaped dowel corner joints in the case of construction [75]. Face and butt members were constructed of particleboard with dimensions of 158.75 by 19.05 mm and 139.7 by 19.05 mm in cross-section. Length of members were 171.45 mm, 228.6 mm, 279.4 mm and 355.6 mm. Multi-groove dowels were made of yellow birch with a diameter of 7.9375 mm and length of 41.275 mm. Depth of dowel embedment in face and butt members were 15.875 mm and 26.9875 mm respectively. The bending moment capacity of joints was determined under compression and tension loading. Number of dowels in construction have a positive effect on joints

strength, both in tension and in compression tests. In the case of specimen length, joint strength reduces by increasing specimen length. In the study, 70 specimens were used with 5 replications in each sample group. Maximum strength was attained when dowel spacing was 76.2 mm. In the case of specimen length, joint strength reduces by increasing specimen length. Furthermore, the study provides an equation to predict bending moment capacity of multi-dowel corner joints by using regression analysis. Equation 2.56 and 2.57 are predicted bending moment capacity of joints in compression and tension tests, respectively.

$$y_c = 558N^{0.95} \left[ \frac{1}{\left(\frac{W}{2N}\right)^{0.057}} \right] \times D^{0.5} \times L^{1.25} \quad \text{Equation 2.56}$$

$$y_t = 3800N^{0.75} \left[ \frac{1}{\left[\left(\frac{W}{2N}\right)-2\right]^2 +5} \right] \times D^{0.5} \times L^{1.25} \quad \text{Equation 2.57}$$

Zhang *et al.* studied the bending fatigue life of T-shaped two-pin dowel joints constructed of red oak, yellow poplar, plywood made of southern pine, engineered strand lumber (ESL) made of aspen, and particleboard with spiral groove dowels made of yellow birch [45]. All members of joints were measured 406.4 mm-long x 101.6 mm-wide x 9.525 mm-thick while nominal diameter and length of dowels were 9.525 mm and 50.8 mm respectively. All tests were conducted according to the General Service Administration (GSA) performance test procedure. In the first set of performance testing, 30%, 50%, 70% and 90% of bending moment capacities of dowel joints constructed with wood materials were applied in [50]. All joint specimens survived under a load level of 30% of bending moment until 1 million cycles. Number of cycles to failure for each joint specimen were below 1 million cycles at the 50%, 70% and 90% of bending moment levels. In order to predict fatigue life of joints, a logarithmic linear plot was plotted and number of cycles to failure were then obtained by using its equation with bending moment level of 813.8 N.m, 1,220.7 N.m, 1,627.6 N.m, and 2034.5 N.m. Second, Palmgren-Miner rule was applied which is given in equation 2.7. In the second set of performance testing, joint specimens were subjected to cyclic loading with an initial load of 813.8 N.m. After 25,000 cycles were completed, load increased by an increment of 406.9 N.m until non-recoverable failure occurred. Results showed that mean differences between average number of cycles to

failure and predicted number of cycles to failure by using Palmgren-Miner rule were from 0.5 % to 10.3%. The fatigue life of joints made with particleboard had lowest strength while statistical analysis presented that there was no significant difference among joints made of red oak, yellow poplar, plywood, and ESL. Those of static bending testing showed that there was no significant difference between red oak and plywood, and between yellow poplar and ESL. Furthermore, this study showed that Palmgren-Miner rule based on M-N (moment - number of cycles to failure) could be used to predict fatigue life of furniture joints.

Erdil and Eckelman studied face- and edge-withdrawal strength of single dowels in plywood made of southern pine, sweetgum, and Douglas fir, and oriented strand board (OSB) made of southern pine of different thicknesses [76]. Multi-groove dowels made of yellow birch were used with diameters of 6.35, 7.94- and 9.525-mm. Depths of dowel penetration in face were 9.525, 12.7, 14.288, 15.875, 19.05, and 22.225 mm while those of edge were 19.05, 25.4, and 31.75 mm. The result of this study showed that an increase in dowel diameter and depth of dowel embedment in face and edge, as well as density of board had a positive effect on withdrawal strength of single-pin dowel joints.

Zhang *et al.* studied the torsional strength of dowel joints constructed of plywood and OSB with different thickness [77]. Load was applied on edge of rail and face of rail in joint specimens with different dowel spacing. Load created higher torsional strength when load was applied on the edge of rails compared to those of face. Also, the increase in dowel spacing provided higher torsional strength on joints in both tests.

Altinok *et al.* found that dowel strength in tension and compression test of corner joints in case furniture slightly changed depending on the glue type; namely, PVA and polimarin were used [78]. In tension testing, dowel strength adhered with PVA (4.2 N/mm<sup>2</sup>) provided higher strength than those with polimarin (3.68 N/mm<sup>2</sup>). On the other hand, higher dowel strength in compression was attained for joint specimens with polimarin (0.52 N/mm<sup>2</sup>). Joint strength with PVA was 0.47 N/mm<sup>2</sup>.

Yerlikaya and Aktas studied the strength of corner joints in case furniture [79]. In this study, joints constructed of medium density fiberboard (MDF) were used with dowel, a combination of dowel and minifix, and a combination of dowel, minifix, and glass fiber fabric. Diagonal compression and tension tests were applied on the L-shaped corner joints. According to the test results, tension load capacity level of dowel joints (562.5N) was five times higher than those of compression test (107.2 N). In the combination of dowel and minifix joinery system, there was a 29% enhancement in joint strength in the compression test whereas those of tension test was 22%. Furthermore, enhancement was 75.7% in the case of dowel and glass fiber fabric in compression test but only 0.5% in tension test. In the combination of a-3 type of -joinery system, enhancement in strength of joint was 76% and 40% in compression and tension test, respectively.

Kasal *et al.* studied the shear force capacity of dowel joints by using various spacings between dowel and rail width [80]. In the study, all loads were applied in-plane and out-of-plane of T-shaped joints. According to the test result, strength of joints in-plane testing was higher than those of out-of-plane due to the fact that effective shear area was larger than in in-plane testing. Moreover, strength of joint was increasing while using wider rails with 25 mm-dowel spacing due to shoulder effects in joints. On the other hand, it was observed that the strength of joints reduced while increasing dowel spacing with 100 mm-rail thickness. Furthermore, by using regression analysis with test results, shear force of dowel joints could be predicted by using following equation:

$$F_s = -1825.4 + (925.2 \times t) + (2.34 \times S) - (0.00066 \times S^2) \quad \text{Equation 2.58}$$

where,  $F_s$  is shear force of joint (N),  $t$  is thickness of rail (mm), and  $S$  is shear strength parallel to the grain of wood used in rail (N/mm<sup>2</sup>).

Yerlikaya and Aktas studied the strength of dowel joints enhanced by using glass fiber fabric from edge and from both edge and surface [81]. Diagonal compression test was conducted on T-shaped joints. Load capacity level of joint specimen without any reinforcement were 287.16 N. In the case of 2 layers edge reinforcement with glass fiber,

strength of joint enhanced 43% whereas those of 4 layers was 67%. When 2 layer-glass fiber fabric applied on only surfaces, enhancement was 87%. In the case of 4 layer-glass fiber fabric applied on both edges and surfaces, enhancement in joints strength was 90%. The study showed that strength of dowel joints could be increased by using glass fiber fabrics.

Yerlikaya studied the optimum dowel spacing for corner joints in case-type furniture reinforced with glass fiber fabric [82]. Diagonal compression testing was applied on L-shaped joints made of medium density fiber board and particle board. 8 mm-diameter and 34 mm-long multi-groove beech dowels were used in joints adhered by polyvinyl acetate. Dowel spacings were 32 mm, 64 mm, 96 mm, and 128 mm. The distance between the edge of rail and centerline of dowel was 32 mm for each joint specimen. In joint specimens, 2 and 3 dowels were used. According to the results, in the case of that specimen had same dowel spacing, strength of joint enhanced from 12% to 42% while increasing number of dowels from 2 to 3. On the other hand, joint strength was increased through 15% to 65% in the case of that dowel spacing was increased but number of dowels was maintained. According to this study, optimum dowel spacing for MDF and PB were 96 mm and 128 mm with 3 dowels in joint, respectively.

Derikvand and Ebrahimi studied the effects of dowel diameter, dowel spacing, depth of dowel embedment, and number of dowels on rotational stiffness of L-type dowel joints constructed of 18 mm-thick MDF with multi-groove eastern beech dowels [83]. Diagonal compression tests were applied on all specimens. Rotational stiffness of joint was calculated by using equation 2.9. According to the test results, rotational stiffness of joints increased by the use of larger diameters and by the increase of dowel spacing. The results of finite element analysis also showed the same relationship between rotational stiffness, dowel diameter, and spacing with a difference from 2.45% to 11.46%. On the other hand, dowel diameter and depth of embedment had significant effect on rotational characteristics of dowel joints.

Podlena *et al.* studied the effects of adhesive type, surface pattern of dowel, and dowel manufacturer on strength of dowel joints [53]. In this study, straight multi-grooved, helical multi-grooved, and spiral single-grooved dowels were compared. Furthermore, three specimen groups of straight multi-grooved joints were examined: namely, pre-glued dowels with PVA from two different companies and non-pre-glued dowels from another company respectively. In the pre-gluing process, the moisture content of dowels were increased. In the case of different moisture contents in the PVA adhesives, strength of dowel joints reduced [84,85]. Strength of straight multi-grooved dowels, which were pre-glued, was lower than those of non-pre-glued dowels. The highest strength was obtained for helical multi-grooved dowels adhered with 1K-Holzkaltleim D4 (a product of PVA). Single-grooved dowel joints with any type of adhesives provided the lowest strength of dowel joints. Although joints with PU adhesive for straight multi-grooved and spiral single-grooved dowels had greater strength than those of PV, in the case of helical multi-grooved dowel with PU, joints performed the lowest strength.

### 2.2.3 Screws

Wood screws were started to be utilized in furniture construction in the first quarter of the 18<sup>th</sup> century to attach hinges to drop leaf tables [4]. Although screws are used nowadays as the main joinery system in furniture construction, they are also utilized as reinforcements to other joints to increase strength, durability, and reliability of furniture. Not only do material types and sizes of screws affect the strength of screws, but clearance and pilot holes can also hold a significant impact. Therefore, clearance holes should be drilled as large as the shank of screws. On the other hand, pilot holes should be equal to 70% of the root diameter of screws in order to attain maximum withdrawal strength [86]. However, pilot holes can be drilled larger for denser wood species. If clearance and pilot holes are not drilled, the wood material can split and cause damage to the product. On the other hand, if pilot holes are oversized, the withdrawal strength of screws reduces. Table 2.6 shows suggested pilot hole sizes compared to nominal screw diameters. In the literature review, several findings were indicated to predict screw withdrawal strength in solid woods and wood composites [87]. These predictions are shown in Table 2.7.

Table 2.6 Screw Diameter and Suggested Pilot Hole Sizes (in mm) (Adopted from [4])

Screw gage	Nominal screw diameters	Root diameter	Pilot hole
8	4.17	3.04	2.38
10	4.83	3.29	2.38
12	5.49	4.03	2.78
14	6.15	4.61	3.18
16	6.81	4.90	3.57
18	7.47	5.41	3.97
20	8.13	5.84	3.97

Table 2.7 Expressions to Predict Screw Withdrawal Strength in Wood and Wood Composite

Predicted strength	Expression
Withdrawal from side grain of solid wood	$F = 3.2 \times D \times L \times (L - D)^{3/4} \times S$
Withdrawal from end grain of solid wood	$F = 8.75 \times D^{7/4} \times (L - D)^{3/4} \times S$
Lateral strength of screws from solid wood	$F = 8782.3 \times D \times L^{1/2} \times S^{7/4} \times d^{0.306}$
Face withdrawal strength of screws from particleboard as a function of specific gravity	$F = 2655 \times D^{1/2} \times \left(L - \frac{D}{3}\right)^{5/4} \times S^2$
Edge withdrawal strength of screws from particleboard as a function of specific gravity	$F = 2055 \times D^{1/2} \times \left(L - \frac{D}{3}\right)^{5/4} \times S^2$
Face withdrawal strength of screws from medium density board as a function of specific gravity	$F = 3700 \times D^{1/2} \times \left(L - \frac{D}{3}\right)^{5/4} \times S^2$
Edge withdrawal strength of screws from plywood as a function of specific gravity	$F = 1950.1 \times D^{1/2} \times S^{3/2}$
Face withdrawal strength of screws from plywood as a function of specific gravity	$F = 3821.9 \times D \times S^{3/2}$
Edge withdrawal strength of screws from wood composite as a function of internal bond strength	$F = 18.4 \times IB^{0.85} \times D^{0.5} \times \left(L - \frac{D}{3}\right)^{1.25}$
Face withdrawal strength of screws from wood composite as a function of internal bond strength	$F = 39 \times IB^{0.85} \times D^{0.5} \times \left(L - \frac{D}{3}\right)^{1.25}$

where  $F$  is withdrawal strength,  $D$  is shank diameter of screws,  $L$  is embedment of screw,  $S$  is specific gravity of wood and  $IB$  is internal bond strength of wood composites.

Ultimate screw withdrawal strength of wood from side-grain is defined as [88]:

$$p = 108.25 \times G^2 \times D \times L \quad \text{Equation 2.59}$$

where,  $p$  is ultimate screw withdrawal strength of wood from side grain,  $G$  is specific gravity of wood at 12 % MC,  $D$  is shank diameter of screws, and  $L$  is length of penetration in wood.

Also, the outside ( $D$ ) and root ( $d$ ) diameters of screws are determined by using the following equations: screws with fine threads use equations 2.60 and 2.61 while screws with coarse threads use equations 2.62 and 2.63 [87]:

$$D = 1.524 + (3.302 \times N) \quad \text{Equation 2.60}$$

$$d = 1.083 + (0.242 \times N) \quad \text{Equation 2.61}$$

$$D = 1.547 + (3.322 \times N) \quad \text{Equation 2.62}$$

$$d = 1.14 + (0.241 \times N) \quad \text{Equation 2.63}$$

Ors *et al.* studied the withdrawal strength of screws from particleboard, MDF, werzalit, and beech wood, which are widely used in furniture production [89]. Rigidity of joints relies on screws and screw power holding capacity of wood used in the construction. For this purpose, edge- and face-withdrawal strength of screws were investigated considering the wood material type, screw type, and with or without adhesive in construction. In the face- and-edge screw withdrawal, beech wood had 9%, 56%, and 64% higher strength than werzalit, particle board, and MDF respectively. Screw face-withdrawal strength in beech wood and werzalit were 20% and 17% greater than those of edge-, respectively. While there was no significant difference between screw face- and edge-withdrawal strength owing to both homogenous structures in two directions, there was also a non-significant difference between specific gravity of surface and middle layers. On the other hand, in

particleboard, edge-withdrawal strength of screws was 38% higher than those of face- due to the fact that the edges of particleboard were reinforced with solid wood. Larger outer and root diameters increased screw withdrawal strength in wood material. In the case of using adhesives in pilot holes, withdrawal strength of screws increased between 9-45% and 7-39% compared to non-glued pilot holes in face- and edge-direction, respectively.

Semple and Smith studied the effects of density and internal bond strength of wood composite materials [90]. Test results were benchmarked against previously published predictive models of edge- and face-withdrawal strength of screws from particle boards. The study showed that if screw diameter and depth of embedment is taken into consideration to estimate withdrawal strength of screws, test results matched with the previously published models in a function of density and internal bond strength. However, there is no correlation between face- and edge-withdrawal strength of screws from particleboards and its density, but enough correlation between them and internal bond strength.

Efe and Demirci studied the effects of screw end-, edge-, and face-withdrawal strength in oak, beech, and Scotch pine wood [91]. The test results show that oak wood had the highest screw withdrawal strength compared to beech and Scotch pine wood, owing to higher density and better anatomical properties. Similarly, face-withdrawal strength of screws (in radial direction) is higher than those of edge- (tangential direction) and end- (longitudinal direction) because of annual ring growth in the radial direction, so that they hold the threads of screws.

Ozciftci studied the effects of pilot holes, screw types, and layer thickness on screw withdrawal strength in laminated veneer lumber (LVL) [92]. For this purpose, layers were cut from oak and Uludag fir woods with 4, 5, and 7 mm-thick material. These lumbers with 7-layers were then coated with phenol-formaldehyde (PF) and melamine-formaldehyde (MF). Oak wood provided 34% greater screw withdrawal strength than those of fir wood. Withdrawal strength of screws with smaller size diameter gave higher strength because of less wood splitting, although all pilot holes were 80% of root diameter of screws.

Withdrawal strength in LVL with PF was 5% higher than those of MF. Also, it was observed that glued pilot holes increased screw withdrawal strength. The highest strength for layer thickness was attained in veneers with 7 mm (14.5 MPa), while those of 5 mm and 4 mm had 13.76 MPa and 14.41 MPa, respectively. The relationship between screw withdrawal strength and layer thickness was not similar owing to effective length in wood materials rather than total length of embedment, which is total length of veneer thickness and glue line thickness.

Efe *et al.* studied the screw withdrawal strength in solid wood and LVL made of oak, Scotch pine and poplar wood [93]. LVLs were adhered with PVA and UF. Screw face-withdrawal strength in wood constructed of beech was higher than compared to those of Scotch pine and poplar wood. Besides, those of solid wood had higher strength rather than those of LVL with PVA and UF. Moreover, it was observed that screw face-withdrawal strength was higher than those of edge-.

Yuksel *et al.* studied the effects of panel type and thickness on bending moment capacity of L-shaped screwed corner joints, and deflection of four-member cabinets [94]. Stiffness and strength of panel type structures rely on torsional stiffness of its plates [95]. For this purpose, L-shaped joint and case furniture specimens made of particleboard, MDF (16 mm to 18 mm thickness), and plywood (15 mm to 18 mm) were subjected to diagonal compression and tension testing, and static moment resistance and stiffness testing, respectively. Screw edge-withdrawal strength in panels were 20% to 45% greater than those of face-. Panels made of plywood had higher face- and edge-withdrawal strengths than those of MDF and particleboard, owing to both its density and internal bond strength. There was no linear relationship between panel type and panel thickness; namely, while increasing panel thickness, (i) screw edge- and face-withdrawal strength in panels made of particleboards were reduced due to higher modulus of rupture, elasticity, and internal bond, (ii) those of MDF increased, and (iii) screw edge-withdrawal strength in plywood decreased but those of face-withdrawal increased. In the case of stiffness in four-member cabinets, panel thickness with 15 mm and 16 mm provided higher strengths rather than

those of 18 mm. The stiffness of cabinets made of plywood was higher than those of particleboard and MDF due to higher material properties.

Yorur *et al.* studied the effects of pilot holes, screw type, screw direction, water soak, and adhesive on the screw withdrawal strength in plywood made of beech wood [96]. For this purpose, screw face- and edge-withdrawal strength in plywood were tested while taking into consideration that (i) there was no pilot hole, (ii) pilot holes were 80% of major diameter of screws whether either PVA or PU were injected into pilot holes or not, and (iii) whether specimens were immersed in water for 2 hours or not. Screws used in the study had 3.5 mm- and 4 mm-major diameters. The results of this test showed that screw face-withdrawal strength in plywood was greater than those of edge-. Besides, specimens with pilot holes that were injected with PU provided higher withdrawal strength compared to others. Furthermore, it was observed that withdrawal strength of screws without pilot holes was higher than those with pilot holes due to the fact that the sample blocks did not have major splitting or cracks while driving screws, and they had larger contact area compared to samples with pilot holes. Moreover, specimens immersed in water provided less withdrawal strength of screws due to the fact that higher moisture contents would decrease material properties and internal bonding strength of wood material.

These studies relate to the strength and stiffness of mortise and tenon joints and dowel joints, as well as withdrawal strength of screws that pertain to rational designs of furniture joints in terms of determining their ultimate strength capacity. These studies provided tangible information on how to design joints in furniture frames, but they may not always result in the design of reliable furniture joints due to the fact that given information is based on sample means which is deterministic approach.

### 2.3 Load and Design Consideration

Wood material has been utilized in wood construction for centuries; namely, houses, ships, furniture, castles, towers, and other structures were using sawn lumber components or engineered wood products such as beams, headers, trusses, floor joist, decking, etc. Before designing a structure, resistance strength of materials used in construction and their

adjusting factors, also known as safety factors, must be known during their service. In this section, these factors would be briefly explained in both wooden structural engineering structures and furniture engineering structures [97].

### 2.3.1 Load and Design Consideration in Wood Structural Engineering

Wood as a material has been serving humankind in centuries of history as a crucial structural material. However, there was a lack of information about the fatigue behavior of wood material before the Second World War because it was not recognized in growing utilization of wood in aircraft. Creep and load duration were more significant design factors in civil engineering; that is why creep was accounted for safety factor rather than being accounted as fatigue of wood [98]. Therefore, studies concerning fatigue behavior of wood have been established during this time.

Kommers stated that Sitka spruce, Douglas fir, five-ply yellow birch and five-ply yellow poplar wood had bending fatigue at approximately 27% of their static strength under 50 million cycles in 1943 [99]. Dietz and Grinsfelder [100] studied the flexural fatigue strength of 2- and 3-ply birch plywood and found that fatigue strength was 25% of their static strength in bending testing under 2 million cycles in 1943. After these findings, a determination of fatigue behavior in wood materials under cyclic load was becoming popular leading to numerous studies being conducted with different wood material and loads. Tsai and Ansell provided comprehensive literature review on these studies [98].

As with many structural materials, the residual strength of wood materials varies depending on their mechanical properties and environmental conditions. Several studies have been conducted to indicate how fatigue behavior of wood changes depending on wood specific gravity, moisture content, temperature, and grain slope. Sekhar, Sukla and Gupta [101] indicated that an increase in moisture content of wood reduced the fatigue behavior of wood as static strength of wood. Lewis [102] studied the fatigue strength of air dried and green wood and found that fatigue strength of green wood was 50% of its static strength under 2 million cycles while those air-dried was 60%. Kommers indicated that increasing temperature during testing caused moisture loss of 1% so that it would influence fatigue

behavior of wood [98]. Sekhar and Sukla [103] reported that fatigue behavior of wood increased with increase of its specific gravity/density. Namely, fatigue strength increased 30% to 45% by an increase of wood specific gravity, as well as increasing the differences in specific gravity between sapwood and heart wood, and early and late wood. Lewis [102], Ibuku *et al.* [104] and, Maku and Sasaki [105] studied the effects of defects, notches, holes, and checks on fatigue behavior of wood and found that these defects reduced the static strength of wood, which resulted in the fatigue life of wood decreasing as well.

Wood as a structural material needs a design value in its construction as other structural materials because its strength would reduce over time, owing to its mechanical and anatomical properties, environmental conditions, and service life. Therefore, allowable design values and loads, as well as resistance factors were indicated in literature for wood constructions.

#### 2.3.1.1 Allowable Design Stress of Wood Structures

To design wood components in construction, design values are needed to be known; namely, bending strength, tension strength, shear strength parallel to grain, compression to both perpendicular and parallel to grain, and modulus of elasticity (MOE). The actual design value can be used in different circumstances, such as being used collectively, individually, or partially to design structural components in construction which depends on what component will be designed to do. In epitome, in a beam design, bending strength, shear strength, compression to perpendicular direction to grain and modulus of elasticity collectively. At the same time, compression parallel to grain and modulus of elasticity are used to design columns, and tension is used to design chords and trusses subjected to tensile forces. Given actual design values are affected by factors [97]:

1. *Temperature* ( $C_t$ ) – applicable when temperature is above 37°C,
2. *Moisture content* ( $C_M$ ) – an adjustment factor for wood components with moisture content above 19%,

3. *Load duration* ( $C_D$ ) – changes depending on how long wood components are subjected to load,
4. *Beam stability factor* ( $C_L$ ) – adjustment factor if beam is twisted, warped, rotated, or displaced under loading,
5. *Size factor* ( $C_F$ ) – is to adjust depth of the wood components
6. *Repetitive factor* ( $C_r$ ) – is 1.15,
7. *Incising factor* ( $C_i$ ) – is to account for notches in wood component which is filled with preservations,
8. *Column stability factor* ( $C_P$ ) – is used in designing column to adjust compression parallel to grain,
9. *Buckling stiffness factor* ( $C_T$ ) – is used in the case of combination of bending and compression of wood components for 50mm x 100 mm (or smaller) compression chords in wood trusses,
10. *Flat use factor* ( $C_{fu}$ ) – is to adjust wood components if they are loaded on the wide face (out-of-plane),
11. *Bearing area factor* ( $C_b$ ) – is used if bearing is less than 150 mm.

These factors are plugged into the equation of allowable design values of wood components in desirable construction.

In bending ( $F'_b$ ):

$$F'_b = F_b \times C_D \times C_F \times C_L \times C_M \times C_t \times C_{fu} \times C_r \times C_i \quad \text{Equation 2.64}$$

In tension ( $F'_t$ ):

$$F'_t = F_t \times C_D \times C_F \times C_M \times C_t \times C_i \quad \text{Equation 2.65}$$

In compression parallel to grain:

$$F'_c = F_c \times C_D \times C_F \times C_P \times C_M \times C_t \times C_i \quad \text{Equation 2.66}$$

In compression perpendicular to grain:

$$F'_{c\perp} = F_{c\perp} \times C_M \times C_t \times C_b \times C_i \quad \text{Equation 2.67}$$

In shear strength:

$$F'_v = F_v \times C_D \times C_M \times C_t \times C_i \quad \text{Equation 2.68}$$

In modulus of elasticity:

$$E' = E \times C_M \times C_t \times C_i \quad \text{Equation 2.69}$$

For practical use, ASD depends on maximum endurance stress and safety of factor which means internal stress should not exceed the maximum stress of wood components. Therefore, safety factor, including adjustment factors, is defined for wood components depending on what the component is designed to do. This practical approach is expressed as:

$$\sigma_{allow} = \frac{\sigma_{max}}{F.O.S} \quad \text{Equation 2.70}$$

where,  $\sigma_{allow}$  is allowable stress,  $\sigma_{max}$  maximum stress or modulus of rupture of wood components, and  $F.O.S$  is factor of safety.

### 2.3.1.2 Load and Resistance Factor

Load and resistance factor design (LRFD) method was implemented from ASD methods but is based on structural reliability calibration technique. The logic behind the LRFD is to evaluate the structure component by component assuming that the structure has linear elastic behavior to calculate the force. There are three essential requirements for LRFD:

namely, (i) statically stable structure, (ii) components must meet strength and stiffness requirements, and (iii) global deflections on components do not exceed limits [106]. LRFD is expressed by equation below:

$$\varphi \times R_n \geq \sum \gamma_i \times Q_{ni} \quad \text{Equation 2.71}$$

where,  $\varphi$  is the resistance factor,  $R_n$  is the nominal resistance,  $\gamma_i$  is load factor applicable to a specific load component, and  $Q_{ni}$  is specific nominal load component [107].

### 2.3.2 Load and Design Consideration in Furniture Engineering

In the field of furniture strength design, although many studies have been conducted to determine rational design values [8,15,44,108–111] such as ultimate bending moment capacity and withdrawal strength of furniture joints, studies on subject of allowable design values have been conducted very rarely.

Eckelman studied reasonable design stresses for wood used in furniture structures with 25 wood species and 800 specimens in total (sample sizes are not equal for each sample group) [8]. He stated that one-third of published ultimate bending stress [88] at 12% MC is used to estimate the bending strength of the wood used in furniture. In this study, statistical lower tolerance limits were also proposed and compared with one-third of published bending stresses. Results showed that the LTL values of two specimens were lower than one-third of ultimate bending stress, while the LTL values of seven specimens were slightly above such values and one specimen, yellow poplar, was substantially above it.

Bao and Eckelman [108] and, Bao *et al.* [109] studied fatigue life and design stresses of wood composite materials used in furniture construction. Specimens constructed of particle board, oriented strand board (OSB), medium density fiber board (MDF), and plywood were subjected to cyclic loading at 20%, 40%, 50%, 60%, and 70% of their ultimate bending stresses. Specimens survived over  $10^6$  cycles and 30% of published ultimate bending stresses. Specimens failed at those of 40%.

Ratnasingam and Ioras [110,112] studied the fatigue strength of the wood made of oil palm, rubberwood, particleboard, and fruit bunches particleboard (OPEFBP) used in furniture with one hundred species, respectively. Specimens were subjected to cyclic loading at 30%, 40% and 50% of their ultimate bending stress levels. At 40% of its ultimate bending stress, specimens began to fail almost at 500,000 cycles. BS 4875 [113] for chair and settees dictates that for reliable products, the number of cycles must be 200,000 cycles. Under the light of such information, they recommended that allowable design stresses for oil palm purposed to be used in furniture structure must not exceed 40% of its ultimate bending stress level.

Ratnasingam *et al.* [15] and, Ratnasingam and Ioras [44] studied fatigue strength of T-shaped mortise and tenon furniture joints constructed of palm oil and some Malaysian timbers with 25 specimens. Specimens were subjected to cyclic loading at 10%, 15%, 20%, 25% and 30% of bending strength given in static loading test. Results showed that number of cycles exceeded 200,000 cycles at the 20% of bending strength. They recommended that 20% of specimens' bending strength must be used for such furniture joints.

Studies above showed that specified percentage of ultimate bending stress/strength of wood were used to estimate design values of furniture components and joints. However, such studies are based on empirical knowledge. Such design values for furniture must be determined with reliability analyses while using probabilistic approaches and making statistical assumptions. Since sample sizes and confidence coefficients play key roles, analyzing proportions of future observation in experiments are critical to determine reasonable design values of products. Studies in the subject of allowable design stresses of furniture members and joints did not take into consideration such information. Therefore, stochastic approaches should be considered to determine reasonable design values in furniture engineering practices.

## 2.4 Recommended Standards for Chair Frames

### 2.4.1 Recommendations from American Library Association

American Library Association (ALA) was established in 1876 to provide leadership for the development, promotion and improvement of libraries. ALA provided test methods and the procedure for strength, durability and reliability of library chairs, tables and shelves. The acceptable load levels for chair performance testing are given in Table 2.8.

Table 2.8 Some Test Types and Acceptable Load Levels for Chair Frames in Performance Tests

Cyclic performance test type	Acceptable load levels (N)		
	Light-duty	Moderate-duty	Heavy-duty
Vertical load test	2670	3560	4450
Front-to-back load test on chair frame	1335	1557.5	2002.5
Back-to-front load test	1001.25	1446.25	1891.25
Side-thrust load test on chair frame	890	1112.5	1335
Front-to-back load test on backrest	1335	2225	3115
Side-thrust load test on arms	667.5	1001.25	1335

### 2.4.2 Recommendation from Bureau and Institutional Furniture for Manufacturers

Business and Institutional Furniture Manufacturers (BIFMA) is a non-profit organization which has been served to customers in terms of providing health, comfortable and productive workspace based on infrastructure engineering and materials standards for commercial furniture industry since 1973. In this section, *ANSI/BIFMA X5.1-2017 - General Purpose Office Chair-Test* will be explained slightly for frame-type chairs which is a defined standard Type III chair – fixed seat angle and fixed backrest. Some test types, along with its functionality and proof loads are given in Table 2.9. All acceptable levels do not have loss of serviceability in chair and sudden major changes in the structural integrity of the chair.

Table 2.9 Some Test Types and Test Procedure in ANSI/BIFMA X5.1-2017

No	Test type	Functional load (N)	Proof load (N)	No of cycles	Duration of load (sec.)
1	Backrest strength test - Static	667	1001	1	60
2	Drop test - Static	1001	1334.6	1	60
3	Seating durability test - Cyclic		445	100000	2 to 6
4	Arm strength test - Vertical - Static	750	1125	1	60
5	Arm strength test - Horizontal - Static	445	667	1	60
6	Backrest strength test - Cyclic		334 N	120000	2 to 6
7	Leg strength test - Front and side application	334	503	1	60
8	Arm durability test - Cyclic		400	60000	2 to 6
9	Structural durability test - Side to side- Cyclic		334	25000	2 to 6

## 2.5 Structural Reliability Analysis with Probabilistic Approaches

In engineering design, many uncertainties exist in loading, material properties, geometric size, and material strength. While determining maximum strength of the materials, such uncertainties are assumed deterministic that there isn't uncertainty in material strength. However, such values are not satisfied by reliability of material. Therefore, probabilistic approaches are developed to ensure their reliability. A deterministic approach uses safety factor or worst-case scenario and is not enough to address safety and reliability of the products. On the other hand, such concerns must be ensured by considering probabilities and statistic approaches in the design process. Although deterministic approached are successful in reducing cost and increasing product performance, uncertainties and variabilities in product are inevitable and must be considered in the product design process [114,115]. Deterministic approaches for furniture design is not reliable and cannot estimate warranty time and reliability of furniture [10].

In reliability analyses, the following issues must be considered:

1. Failure mode must be identified.
2. Variabilities in material properties and manufacturing that influence material strength must be identified.

Reliability analysis estimates probability of failure that predicts percentage of the material bending strength above its ultimate bending strength while considering uncertainties and variabilities mentioned above. Regardless of how to set safety factor by using deterministic approach, reliability analysis provides more precise and effective results than results obtained by safety of factor [115] but the failure probability never becomes zero [114]. In the case of reliability in the furniture structure, its construction parameters must be determined by appropriate stress and strength distribution on structure under imposed loading [10].

For probabilistic structural design purpose, several number of methods have been developed to support reliability analysis; namely, Monte Carlo Simulation, the first-order reliability method, the second-order reliability method, importance sampling [116], maximum likelihood, and tolerance analysis.

The approaches of structural reliability have been developed in the last few decades and related studies are available in literature [115]. Following studies are related to the subject of the reliability analysis in engineering design. In these studies, both structural reliability under static and fatigue loading were investigated using probabilistic approaches.

Das *et al.* used the first-order second-moment reliability analysis method to determine reliability of stringer-stiffened cylinders under axial loading [117]. Results showed that uncertainties due to loading were reduced from 20% to 10%; correspondingly, reliability of the materials increased up to two orders of magnitude.

Stewart developed a Human Reliability Analysis model to simulate the effects of the human error in design and structure since 75% of structural failures are due to human errors [118]. Results showed that human errors cause to undergo a significant reduction in structural reliability, but such errors could be controlled and the reduction in structural reliability could be prevented.

Yunis and Carney presented structural reliability techniques for aerospace application, which was the plume impingement loading of the Space Station Freedom Photovoltaic Arrays [119]. Probability distribution of the loading was determined by using Monte Carlo Simulation. Results showed that failure probability of design was insignificant when products were designed with proposed approaches.

Papadrakakis *et al.* examines the application of Neural Networks in the reliability analysis of complex structure about Monte Carlo Simulation [115]. Results showed that the prediction of probability of failure with Neural Networks was improved by using Monte Carlo Simulation with Importance Sampling.

Zureick *et al.* recommended a two-way Weibull distribution for modelling strength and stiffness properties [120]. Due to the small sample size in this study, tolerance limit was specified at 80/95 confidence/proportion level. The results showed that determining nominal strength and stiffness values for the design with given procedures increase the use of fiber-reinforced polymer composites in its structural area.

Smardzewski determined distribution of strain and strength for case furniture, failure probability of furniture joints, and probability of failure-free period of the furniture structure [10]. Results showed that usage of highly reliable joints in furniture structure could increase its overall reliability and prolong its service life.

Li *et al.* studied structural damage detection on an actual frame structure by applying statistical process control theory with a confidence interval [121]. Results showed that a moderate confidence interval gives moderate upper control limit for one-sided tolerance analysis and provides appropriate guidelines to illustrate undamaged and damaged nodes.

Klemenc and Fajdiga stated that prediction of the average fatigue strength of materials gives limited information about reliability but the prediction of structure reliability during service might provide tangible information about its reliability [122]. In this respect, they

presented an approach for strain-number of cycle (E-N) curves by using joint estimation method and its results showed well-reasoned estimates of parameters.

Echard *et al.* proposed a reliability analysis method for structures imposed to fatigue loading by using Monte Carlo Simulation and Kriging meta-model [17]. Results showed that the proposed method contributes to determining a robust, reliable design under fatigue loading.

Liao *et al.* proposed the method of reliability optimization design of rotor spindle involving confidence level of reliability based on central limit theorem and the stress-strength interference theory [123]. Results showed a theoretically meaning and engineering value for reliability design of the mechanical parts.

Yan and Yuen demonstrated the process of deriving a probabilistic-based blast design formula using site-specific vibration records with using Monte Carlo Simulation [124]. Results showed that the confidence interval of blast-induced vibrations are reliable with using proposed approaches.

Angelo and Nussbaumer studied fatigue reliability of the bridge in highway traffic [125]. They stated that probabilistic models must be established due to randomness of traffic loading and fatigue resistance, and the reliability analysis gives an effective way to perform fatigue reliability of the bridge.

Fink and Kohler studied probabilistic approach for modelling tensile strength and stiffness of timber board and finger joint connections as an estimation of strength values by using linear regression model [18]. Results for those of tensile strength and stiffness were compensated with required/recommended results in literature.

Klemenc presented the influence of material's fatigue-life-curve model on reliability of structure under a dynamic loading [126]. Probability density function was used for

reliability analysis in the study. It is recommended to use the proposed method with probability density function to calculate structural reliability accurately.

Piric studied reliability analysis method based on probability density function with using importance sampling and Monte Carlo Simulation [127]. Results showed that proposed method had wide acceptance with existing reliability analysis method in literature and was very demanding in a reliability-based design optimization environment.

Tolentino and Ruiz evaluated structural confidence factor and confidence level in a time interval after construction of the structure [128]. Results showed that construction factors were less than 5% in 50, 100 and 150 years and gives similarity between structural reliability evaluation of buildings and analyzed structures in the study.

Xu studied analysis of fatigue reliability with using a joint probability density evaluation [129]. Experimental results showed an accuracy compared to the proposed method. Xu also stated that fatigue life of a structure alongside using proposed failure probability could be predicted by using reliability isolines of fatigue damage.

Diller *et al.* studied a performance test of the chairs randomly obtained from different furniture producers in Turkey [130]. Results showed that there were variations between strength properties of the furniture structure due to lack of knowledge in research-development (R&D) application, and lack of performance testing of furniture structure before marketing.

Ning and Li used generalized likelihood uncertainty functions to determine the plastic hinge length by probabilistic approach [131]. Results showed that almost all observation remained below 90 percent confidence interval of predicted lengths.

Wang and Chen studied the equivalent stochastic process transformation approach for cost-effective prediction of reliability deterioration over the life cycle of an engineering design with using Monte Carlo Simulation [132]. Results showed that time evaluation of system

reliability was predicted accurately, and proposed approach provided less computational efforts compared to existing methods.

Zhao *et al.* studied how to improve the measurement of probabilistic fatigue limits with using deduced maximum likelihood approach and Monte Carlo Simulation [19]. Results show that the proposed approach gave minimum evaluation in standard deviation and appropriate evaluation on average value of fatigue limits compared to other approaches in literature.

The studies given above show that reliability analysis with probabilistic approach in field of structure have significance to determine design values and safety of the structure in engineering design practices and have started to come into prominence for furniture engineering practices. Therefore, such approaches could provide reasonable design values for furniture structure, its components, and joints.

## 2.6 Statistical Tolerance Limits

In a product design, three stages are essential: namely, (i) target setting, (ii) product design and development, and (iii) product quality validation stage. In a successful product design development, customers' demands must be satisfied and improved by product quality, reliability, and durability. Therefore, it would be vital to estimate design values for strength capacity of furniture joints. Practically, an entire population cannot be tested to estimate design values and hence random samples must be selected from the population. Two types of estimation are commonly used: namely (i) point estimation – infers a single number such as mean and variance, and (ii) interval estimation – calculates the region the true values of population parameters. Since population parameters are estimated based on finite samples, errors of estimation and variance are inevitable. Thus, such error cannot be reflected by point estimators [133].

Probability expressions are based on statistical interpretations. Such interpretations estimate characteristics and variability of the stochastically analyzed data set. Probability expressions are referred to [134]:

1. *Confidence intervals* are pertaining to parameters of population previously sampled.
2. *Prediction intervals* are pertaining to observations obtained from specific future sample randomly selected from a population previously sampled.
3. *Tolerance intervals* are pertaining some proportion of the possible future observation randomly selected from population previously sampled.

Confidence, prediction and tolerance intervals are random intervals. They are used to estimate a target population. Confidence interval is related to sample error while tolerance interval is related to both sample error and variation in future population; that's why, tolerance interval is wider than confidence interval. Furthermore, the idea of tolerance interval comes from prediction interval. In the prediction interval, a single random value is estimated by using regression analysis. On the other hand, tolerance interval takes as its subjected the potential outcome of a random variable [135].

In this chapter, tolerance intervals will be discussed thoroughly. Uncertainties such as failure load are quantified in conducted experimental testing [136]. In practice, the population parameters are unknown and are to be estimated from sample statistics, and thus uncertainty due to sampling cannot be ignored [137]. The data set in the experiment covers a wide range of load levels and gives predictions for overall performance of material, but it is optimistic to determine the design values without considering variability of the data set [138]. Therefore, lower tolerance limits are a recommended method to determine such design values. The statistical tolerance limits method has been known for the second half of the twentieth century [139] and used in quality control and engineering design to determine material specifications [138], because tolerance limits are related to an entire conceptual population rather than randomly selected samples from the population [134]. In many fields of engineering design, it is important that proportion of population lies within specified limits when using historical data set [140]. For product manufactured in large quantities, tolerance limits play fundamental roles for setting limits on the process capability [133,141]. Tolerance analyses in engineering design specifies outer limits of accessibility [114]. Moreover, tolerance analyses consist of two practical applications:

namely, population previously sampled and sample sizes of future sample from the same population [139]. The general definition of tolerance intervals is to denote previously sampled data to predict the  $\lambda$  confidence limits on the  $\beta^{\text{th}}$  proportion of the future observation [142].

Z-statistic is used to determine upper and lower limits in the tolerance analysis [143]. The probability expression for two-sided tolerance analyses is defined as  $Prob [z_{lower} < Z < z_{upper}] = \gamma$  and analyzed random variables  $Z$  either falls within intervals, or not. In the case of one-sided tolerance analyses, it is defined as  $Prob [z_{lower} < Z] = \gamma_{lower}$  and  $Prob [Z < z_{upper}] = \gamma_{upper}$  for lower tolerance limit and upper tolerance limit, respectively [134].

In many practices, tolerance analyses have been misunderstood and misused. Statistical tolerance limits arise with two natural cases: (i) more practically useful way than simple statement of mean and variance, and (ii) impossibility and impracticability of measurement and enumeration of all cases [144]. Before calculating tolerance limits, assumption for data set must be made whether distribution is continuous or discontinuous. If it is continuous, parametric tolerance analyses must be taken into consideration. Otherwise, non-parametric tolerance analyses must be done. Therefore, the variations in the samples obtained from population must be randomly selected and data distribution assumptions must be made carefully [139]. Moreover, during the experiment, the test set-up must be homogenous to have accurate assumptions and any heterogeneous in the experiment causes severe outcomes [134]. However, coherent methodology was proposed as integrating direct data – coming from experiment – and indirect data – coming from computational simulation/analysis – to calculate tolerance limits of heterogeneous sources and to give plausible estimates and tolerance limits close to nominal coverage probability [136].

When variabilities and uncertainties show a linear relationship, normality and independence assumptions allow for a simple calculation of tolerance analysis [145]. For any normal distribution, tolerance limits are calculated by using expression below;

$$\mu \pm (z_{P/2} \times \sigma)$$

Equation 2.72

where  $\mu$  is mean,  $z_{P/2}$  is z-score in given proportion, and  $\sigma$  is standard deviation if population parameters are known. However, in practice, population parameters are unknown and must be estimated from randomly selected samples from population [137]. In this case, let random variables be  $X_1, X_2, X_3, \dots, X_n$  obtained from  $N \sim (\mu, \sigma^2)$  and the tolerance limits are calculated by using expression below;

$$\bar{X} \pm (k_{(n, \gamma, P)} \times s) \quad \text{Equation 2.73}$$

where,  $\bar{X}$  is sample mean,  $k_{(n, \gamma, P)}$  is tolerance factor given sample size and confidence/proportional level, and  $s$  is sample standard deviation. In the regression model, overall variability is increased by residual error due to randomness of the study [146]. Assumption of reliable data source could be obtained from linear regression model [136] for tolerance analyses with normal distribution. The simple regression model is;

$$y_{ij} = \alpha + \beta x_i + \varepsilon_{ij} \quad \varepsilon_{ij} \sim N(0, \sigma_i^2) \quad (i, j = 1, 2, 3, \dots, k) \quad \text{Equation 2.74}$$

Tolerance limits are also used to make assumption for non-normal data sets [133]. In normal distribution, the skewness of data set plays a significant role since any violation on normality assumption causes erroneous results in tolerance analysis. In the case with normality assumption violations, other continuous distribution assumptions must be taken into consideration; namely, log-normal, Weibull distribution, etc. [133,139,145]. In this case, aforementioned simple calculations cannot be used and tolerance limits for non-normal distributions must be calculated by [145]. Rae and Subrahmaniam studied tolerance limits for moderately non-normal populations and found a pronounced effect of skewness and kurtosis of distribution on tolerance limits [147].

In industries, one-sided tolerance limits are generally used in design acceptance sampling plan of quality controls. While one-sided upper tolerance limits are used to determine acceptability of product characteristic, one-sided lower tolerance limits are used to determine reliability and safety of products [148] since it is appropriate to determine material specification in the case of uncertainties and variabilities damaging the credibility of the predictive analysis [134]. Material qualities, such as ultimate strength, are critical to

structural failures to ensure that imposed loads meet or exceed the design values specified by lower percentiles of the quality characteristics. For such percentiles, one-sided lower tolerance limits are widely used and give more conservative estimations [149].

For one-sided tolerance limits, let random variables  $C_L$  defined as;

$$C_L = \int_{L(x)}^{\infty} f(x; \theta) dx \quad \text{Equation 2.75}$$

$$\text{Prob}(C_L \geq P) = \gamma, \quad \text{Equation 2.76}$$

Confidence interval,  $\gamma$ , does not depend on the sample sizes. The objective of limit  $L(x)$  is to give a guaranteed assurance that at least  $100P\%$  of population is greater than  $L(x)$  [150].

## 2.7 Sample Size Determination for Tolerance Limits

To obtain reliable stochastic results, sample sizes' determination comes into prominence. Since k-tolerance factor depends on sample sizes, appropriate sample size must be determined to be able to perform tolerance analysis. Determination of appropriate sample sizes causes a reduction of unreliable statistical analysis, as well as reductions of sample cost and experiment time [151]. The accuracies of mean and standard deviation, for example, differ up to 0.012% and 60%, respectively, by using small sample sizes in the experiment [152]. Parametric tolerance limits need smaller sample sizes than non-parametric tolerance intervals [144,153]. Sample size determination for tolerance analysis is founded on a statistical comparison with a previously sampled historical data [142]. A suitable sample size depends on what type of tolerance analysis is done and what is evaluated in tolerance analysis [152]. For example, 50 specimens are enough to estimate the mean by using Latin Hypercube sampling method, but 200 specimens are needed to predict the standard deviation for the same population by using the same sampling method. In literature, even though there is a limited study on sample size determination by using historical data, sampling strategies were developed for tolerance analysis – Monte Carlo Sampling, Latin Hypercube Sampling, and Faulkenberry-Weeks method.

### 2.7.1 Monte Carlo Sampling

Monte Carlo Sampling is a method to calculate properties of the probability density function for random variables. The simulation process is [152]:

1. All random variables must be identified, and the most important variable must be chosen.
2. Probability distribution of input variables must be defined.

The major advantage of Monte Carlo sampling is to describe functional behavior with analytical equations, so its process could be performed rapidly. In Figure 2.30, Monte Carlo sampling process is given [152].

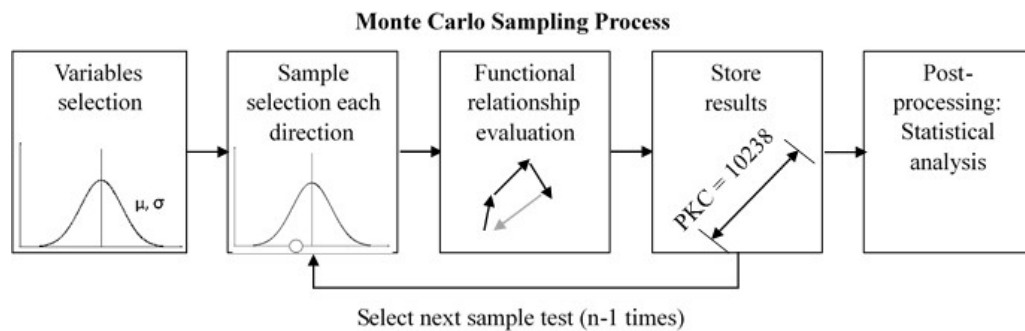


Figure 2.30 Application of Monte Carlo Sampling in Tolerance Analysis

### 2.7.2 Latin Hypercube Sampling

Latin Hypercube sampling method was proposed by [154] for the first time. In the Monte Carlo sampling method, each variable must be identified, and suitable probability distribution of such random variables must be selected. In Latin Hypercube sampling method, this information is used to generate input parameter combinations by dividing the probability distribution into  $n$  sections of equal probability and its outline is given in Figure 2.31. A point in subsections is selected randomly. Then, each input variables are mapped to a vector with  $n$  discrete input values resembling the specified distribution. All input parameter vectors are joined  $n \times n$  matrix. Then, the  $n$  rows matrix contains  $n$  simulations input parameter sets for computation of functional relationship [152].

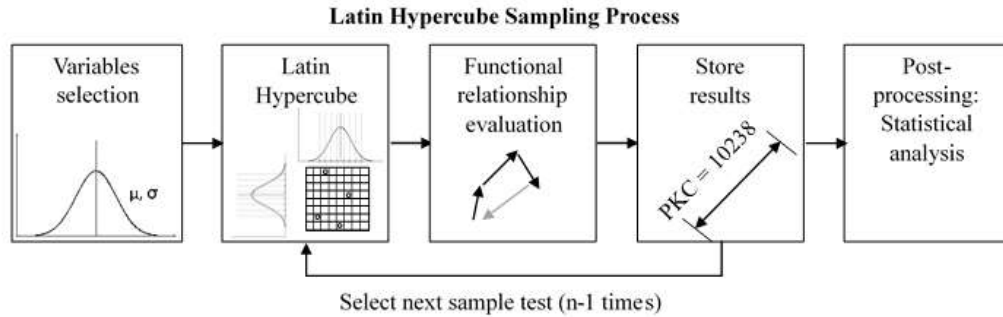


Figure 2.31 Application of Latin Hypercube Sampling in Tolerance Analysis

Although both Monte Carlo sampling and Latin Hypercube sampling methods are complicated and tedious processes with given outlines, they are easily cooperated with by utilizing MATLAB codes which are given for both sampling methods by [152].

### 2.7.3 Faulkenberry-Weeks Methods

Faulkenberry – Weeks method was proposed in 1968 to address the problem of sample size determination for univariate normal distributions and to determine sample size based on specified tolerance intervals [150]. In this approach, precision quantities,  $\delta$  and  $P$ , are specified to characterize tolerance interval. However, this approach was modified by [151] and a *R-software tolerance* package was developed by [155]. Therefore, modified approach is discussed since it more current information.

When an experiment is designed, safety margins are specified with historical data to guide future experiments but such data must meet practical requirements as shown below [150];

1. Previously set-up experiment and future experiment must be identical.
2. Previously sampled material and future sample material must be identical.
3. The process of previously sampled data must be stable.

Minimum sample size determination with Faulkenberry – Weeks method will be discussed in Chapter 3 since it would be used for determining sample sizes of furniture joint samples for tolerance analysis.

## 2.8 Determination of Confidence/Proportion Level for Tolerance Analysis

According to literature review, there is not sufficient information on the subject how to determine acceptable confidence/proportional levels. Several studies provided how to determine confidence intervals [124,156–158] reasonably. However, appropriate confidence/ proportion levels could be inferred to obtain reliable tolerance analysis. Such information is given that numbers of observation below LTL value does not exceed more than  $(1-\gamma)\%$  of total observations in the experiment [139]. Moreover, in the proposed Faulkenberry – Weeks approach, minimum sample size requirements are given related to confidence/proportion levels. Consequently, the acceptable confidence/proportional level might be determined under the light of previously given information. However, in order to determine design value, confidence/proportion levels must be specified in each tolerance analysis.

## CHAPTER 3. LOWER TOLERANCE LIMITS FOR SELECTED FURNITURE JOINTS

### 3.1 Introduction

Contemporary, sustainable, and eco-friendly furniture is aiming to be designed as strong, durable, and reliable with long-service life and should meet expectations for stress-strain limits. Eco-friendly furniture is easy to repair, allowing for reusability and recyclability of the furniture itself or its component that reduces the amount of new material needed for future furniture production. Important features of eco-friendly or so called sustainable furniture include durability, long service life, and joints that retain structural sound during its service life [159]. Since joints are the weakest component of furniture structure, higher reliability in joints result in more reliable furniture structure. Due to the lack of information mentioned previously about allowable design values for furniture itself and furniture components, designers rely on their experiments and experimental results with point estimation which is based on deterministic approaches. Therefore, if reasonable design values of furniture joints are known, more reliable joints can be designed and service life of furniture can be increased. For this purpose, the lower tolerance limits (LTL) method, which is one of the probabilistic approaches, is used to estimate reasonable design values of selected furniture joints – rectangular mortise and tenon joint (RMT), two-pin moment resisting dowel joint, and screws. The initial questions are to determine (i) what sample size should be used to make a reliable tolerance analysis and (ii) what should be concluded with selection of different LTL levels.

The first study on reasonable design values of furniture members by using the LTLs method was conducted by [8]. Since then, there was study about LTLs for neither furniture member nor its joints. Eckelman *et al.* studied on LTLs of RMT joints with an assumption that data met normality, homogeneity, and randomness [13]. The results of his study provided a tangible outcome about how a systematic procedure can be proposed to estimate design values for furniture joints. Eckelman *et al.* studied the LTLs approach to equation-based rational design values for T-shaped [160] and L-shaped RMT joints [161]. In the construction of tolerance intervals, homogeneity of data was not considered. LTLs were

sought for ratio of test results and predicted results. Furthermore, Uysal and Haviarova studied the LTLs of the dowel joint and its design [162]. In this study, minimum sample size requirements for LTLs of furniture joints were defined by using modified Faulkenberry-Weeks methods.

## 3.2 Materials and Methods

### 3.2.1 Materials

#### 3.2.1.1 Wood Materials

Northern red oak (*Quercus rubra* L.) wood is a widely used material for furniture construction owing to its beautiful grain pattern, color characteristic, warm tone, good machining, and easy finishing. It is also a dense and strong wood. Northern red oak is a ring porous wood species. Open large diameter pores are produced in the spring wood whereas very small diameter thick-walled pores are present in late wood. This is a wood species with visible texture and distinguishing characteristics. Therefore, red oak wood has a dramatic appearance [163].

White oak (*Quercus alba* L.) wood is also a widely used material in furniture production. It is also a ring porous species, but large pores have the presence of tyloses, which block liquid movement in the vessels, making the wood impenetrable to preservatives and harder to stain. Moreover, this wood also works great in machining – planing, shaping, and boring [164].



Figure 3.1 A. Northern Red Oak Wood and B. White Oak Wood [165]

Mechanical properties of northern red oak and white oak at 12% MC are given in Table 3.1 [88].

Table 3.1 Some Mechanical properties of Northern Red Oak and White Oak Wood at 12% Moisture Content [88]

<b>Wood species</b>	<b>Specific gravity</b>	<b>Modulus of rupture (MPa)</b>	<b>Modulus of elasticity (MPa)</b>	<b>Compression parallel to grain (MPa)</b>	<b>Compression perpendicular to grain (MPa)</b>	<b>Shear parallel to grain (MPa)</b>	<b>Tension perpendicular to grain (MPa)</b>	<b>Side Hardness (N)</b>
<b>Red oak</b>	0.63	99	12,500	46.6	7	12.3	5.5	5,700
<b>White oak</b>	0.68	105	12,300	51.3	7.4	13.8	5.5	6,000

### 3.2.1.2 Adhesive

In this study, 40% solid content polyvinyl acetate (PVA) adhesive was used. PVA is a thermoplastic adhesive and water-based emulsion. It is often used as an adhesive for porous materials such as wood [166]. PVA is a non-structural purpose adhesive type and appropriate for interior applications. It has high-dry strength but low resistance to moisture [88]. Mechanical properties of PVA adhesive decrease with high temperature; namely, its bonding strength capacity loses at 70°C [167]. Use of an adequate glue amount in joint has significant effects on joint strength [54]. It is recommended to use 200g/m<sup>2</sup> of PVA adhesive on surface [167]. In this study, glue was liberally applied on the surface of the tenons and wall of the mortises for RMT joints, and surface of the dowels and dowel holes for two-pin moment resisting dowel joints [50].

### 3.2.1.3 Screws

In this study, #12 coarse thread wood screws were used for screw withdrawal strength of wood. Figure 3.2 shows screw and schematic depiction of screw configuration used in the study. All screws used in the test were 4.82 mm in major diameter (3.60 mm in diameter without thread) by 50.8 mm long (5.75 mm length of screwhead) with 2.08 mm distance between threads.

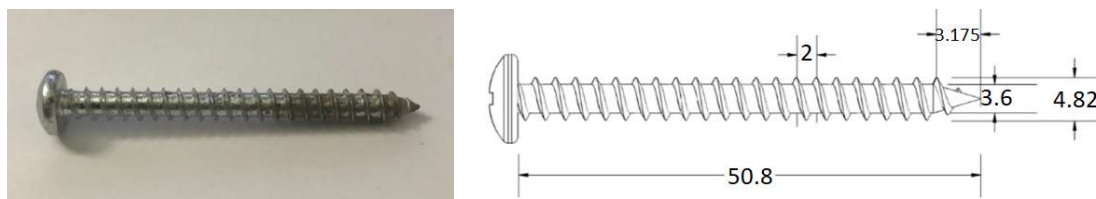


Figure 3.2 Configuration of Screw Used in Study (in mm)

### 3.2.2 Specimen Construction

All northern red oak and white oak boards were obtained from a local sawmill in Northeast Indiana. Material was firstly conditioned to and then maintained at 7% moisture content. All boards were subsequently machined to a thickness of 22 mm; and then cut to visually

defect-free 63.4 mm wide by 304.8 mm long blanks. Afterwards, all rails and posts for test specimens were randomly selected among these blanks.

*Rectangular mortise and tenon (RMT) joints* – tenons, 31.75 mm long by 38.1 mm wide by 9.525 mm thick, were cut with tenoning machine. Matching mortises were cut with a multi-chisel router. Average gap between wall of the mortise and surface of the tenons were 0.127 mm. The faces of the tenon and the walls of mortise were coated with PVAc adhesive and the full length of the tenon was inserted into the mortise and clamped in place. Specimens were remained clamped for 24 hours. Then, they were kept in conditioning room for at least one week at 7% MC before testing. Figure 3.3 shows configuration of RMT joints.

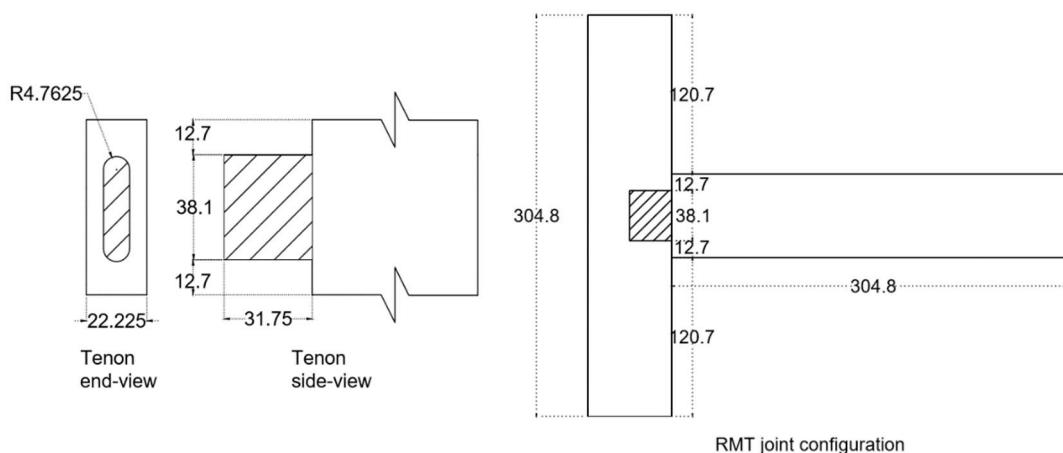


Figure 3.3 Configuration of RMT Joints (in mm)

*Two-pin moment resisting dowel joints* – holes for dowels were drilled into the rails and posts to a depth of 25.4 mm using a 9.525 mm diameter router bit. The average gap between dowel surfaces and dowel hole was 0.127 mm. The hole walls in the rails and half of the length of each corresponding dowel were coated with PVAc adhesive. Coated dowels were then inserted into the accompanying dowel holes to a depth of 25.4 mm and excess glue was wiped off to keep end of rails clean while maintaining perfect alignment with the edge of posts. After the rail components were cured for at least 8 hours in a conditioning room set at 7% MC, dowel holes were bored into posts and the exposed dowel surfaces were

coated with adhesive. These dowels were then inserted into the dowel holes at the edge of posts. The resulting assemblies were clamped for at least 8 hours. All specimens were subsequently maintained at 7% moisture content. At least one week elapsed before specimens were tested. Figure 3.4 demonstrated configuration of dowel joints.

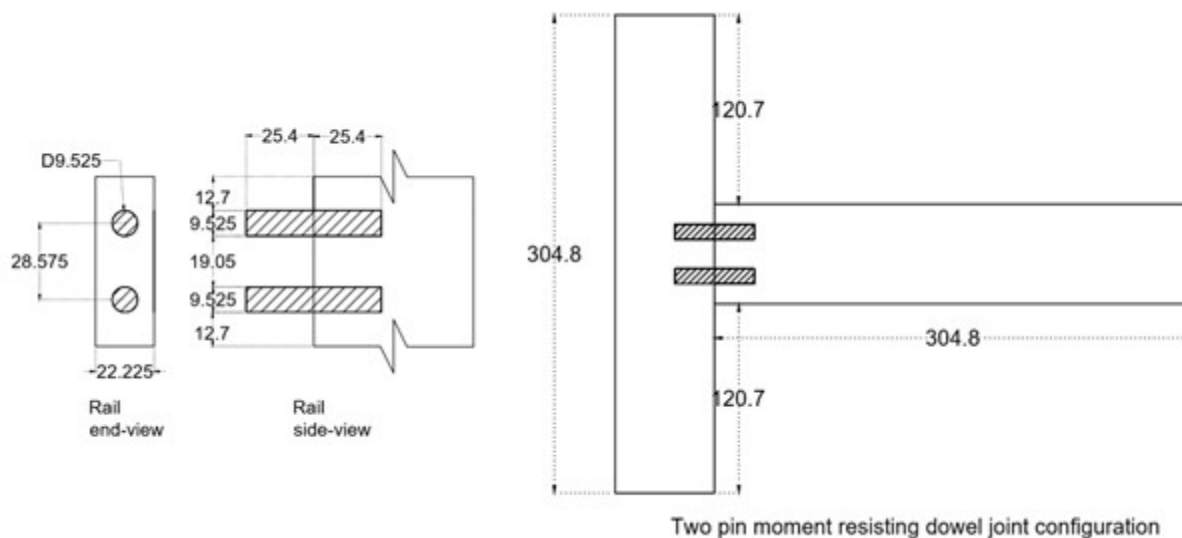


Figure 3.4 Configuration of Two Pin Moment Resisting Dowel Joints (in mm)

*Screws* – each blank remaining from posts and/or rails used in RMT and dowel joints were utilized for screw withdrawal strength in wood from end-, edge- and face-grain. Depth of penetration of screws in the end- and edge-grain was 25.4 mm while initial effective length of screws in withdrawal test from face-grain was 22.225 mm owing to 3.175 mm distance between screw tips and bottom face of the specimens after screws were driven 25.4 mm. After insertion of the screws, the specimens were stored in a conditioning room to maintain 7% MC for at least 1 week. Figure 3.5 depicts configuration of screw withdrawal test specimen from end-, edge- and face-grains.

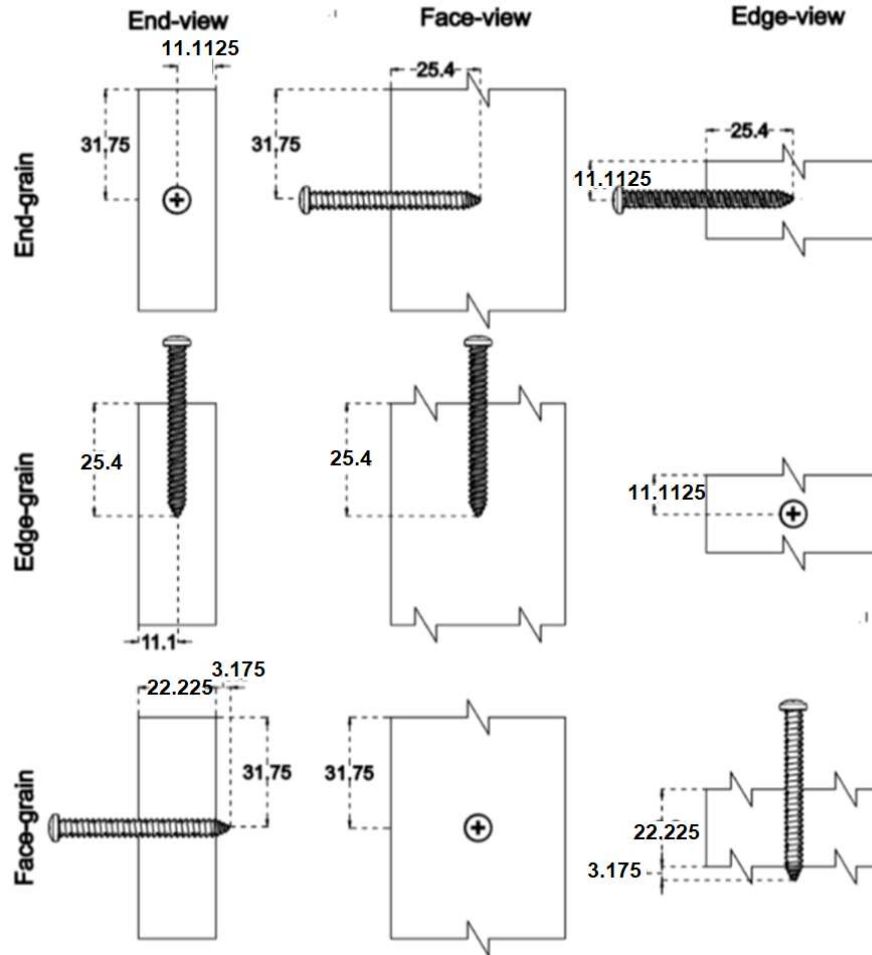


Figure 3.5 Configuration of Specimens for Screw Withdrawal Strength in wood from, End-, Edge- and Face-Grain.

### 3.2.3 Methods

#### 3.2.3.1 Test Procedure

##### 3.2.3.1.1 Determination of Some Mechanical and Physical Properties of Wood Materials

*Moisture content (MC)* – A Delmhorst J-2000 device was used to measure MC of specimens shown in Figure 3.6. MC was measured from several spots of specimens. Average of MCs were used in the study.



Figure 3.6 Delmhorst J-2000 Device to Measure MC in Wood

*Specific gravity* – 25 by 25 by 50 mm specimens were prepared at 7% moisture content. The density of specimens was calculated by using equation 3.1. Specific gravity of specimens was determined by measuring ratio of density of specimens as compared to water ( $1 \text{ g/cm}^3$ ) [168].

$$d = \frac{W}{V} \quad \text{Equation 3.1}$$

where  $d$  is density of wood ( $\text{g/cm}^3$ ),  $W$  is weight of wood specimen (g), and  $V$  is volume of wood specimen ( $\text{cm}^3$ ).

*Static bending test* - According to ASTM D 143 – 94 standards [169], 25 by 25 by 410 mm specimens were prepared for tests. A three-points bending test was conducted with the rate of 25 mm per minute depicted in Figure 3.6. Tests were continued until the specimens failed. During the testing process, loads and deformations on specimens were recorded to calculate modulus of rupture (MOR) and modulus of elasticity (MOE) shown in equation 3.2 and 3.3, respectively.

$$MOR = \frac{3 \times F \times L}{2 \times b \times d^2} \quad \text{Equation 3.2}$$

$$MOE = \frac{(F_1 - F_2) \times L^3}{4 \times (\delta_1 - \delta_2) \times b \times d^2} \quad \text{Equation 3.3}$$

where,  $\sigma$  is MOR of wood ( $\text{N/mm}^2$ ),  $F_{max}$  is ultimate failure load in testing (N),  $L$  is span between supports (mm),  $b$  is width of specimen (mm),  $d$  is height of specimen (mm),  $F_1$  is load in elastic region of load-deflection curve (N),  $F_2$  is load in elastic region of load-deflection curve (N),  $\delta_1$  is deflection corresponding to  $F_1$  (mm), and  $\delta_2$  is deflection corresponding to  $F_2$  (mm).

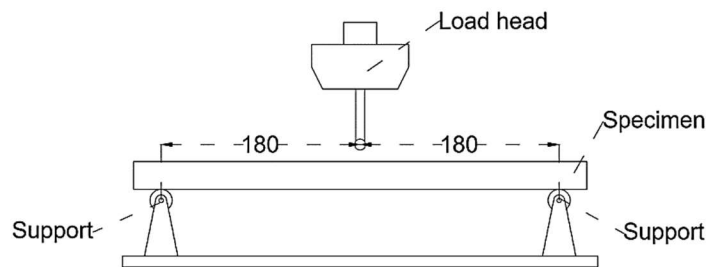


Figure 3.7 Configuration of Static Bending Test (in mm)

#### 3.2.3.1.2 Joint Strength

All tests were conducted on a MTS universal test machine. Test set-up is given in Figure 3.10. The vertical load head movement was 12.7 mm/min. In the bending test of T-shaped joints, an edge-wise load was applied on the rail with a 254 mm-long moment arm. Loading for each test method was continued until non-recoverable failure occurred [170]. Afterwards, the bending moment capacities of RMT and dowel joints were calculated with equation 3.4. In tensile test for screws, ultimate failure load gives screw withdrawal strength in wood from end-, edge-, and face-grain.

$$M = F \times L \quad \text{Equation 3.4}$$

where,  $M$  is bending moment capacity of joints (N.m),  $F$  is ultimate failure load of joints (N), and  $L$  is moment arm (m).

Table 3.2 Nomenclature of Sample Groups

Sample group	Wood species	Joint type	Test method
I	Red oak	RMT	Bending test of T-shaped joints
II	White oak	RMT	Bending test of T-shaped joints
III	Red oak	Dowel	Bending test of T-shaped joints
IV	White oak	Dowel	Bending test of T-shaped joints
V	Red oak	Screw	Withdrawal test from end-grain
VI	White oak	Screw	Withdrawal test from end-grain
VII	Red oak	Screw	Withdrawal test from edge-grain
VIII	White oak	Screw	Withdrawal test from edge-grain
IX	Red oak	Screw	Withdrawal test from face-grain
X	White oak	Screw	Withdrawal test from face-grain

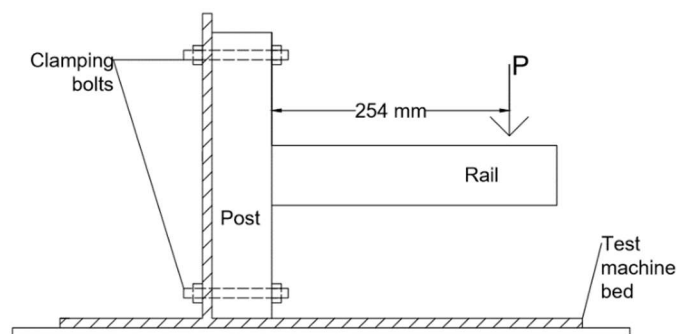


Figure 3.8 Configuration of Bending Test Set Up

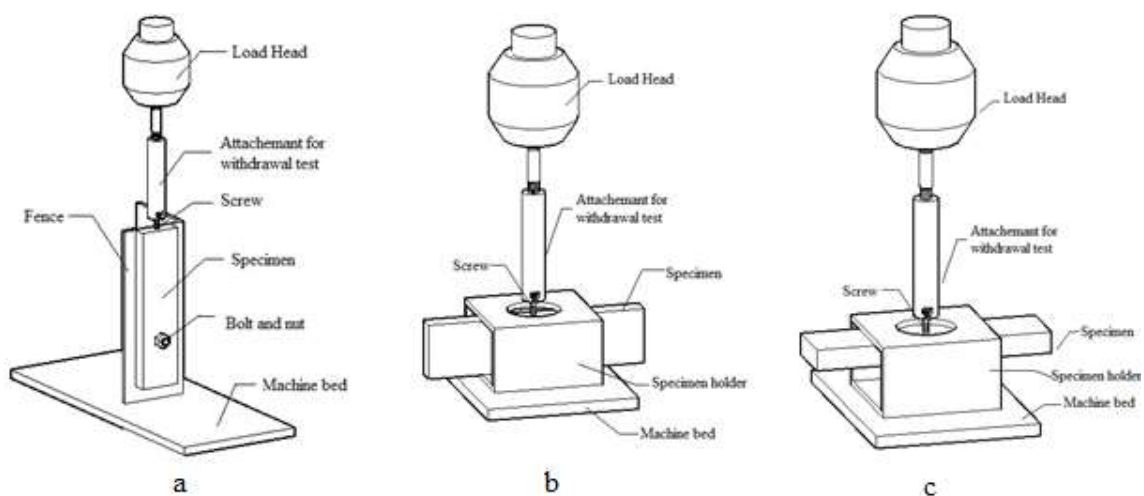


Figure 3.9 Configuration of Screw Withdrawal Test Set Up.

### 3.2.3.2 Lower Tolerance Limits Method

#### 3.2.3.2.1 Determination of Sample Size for Tolerance Intervals

To make a reliable tolerance analysis, sample size must be determined because a statistical tolerance interval is constructed based on some proportion ( $P$ ) of previously sampled data with a confidence level ( $1-\alpha=\gamma$ ) [151]. An *R-package tolerance* was developed to determine minimum sample size requirements for univariate (normally distributed) data sets modifying Faulkenberry-Weeks method [154,170]. The R-code is given below to obtain minimum sample size to construct 0.95/0.90 confidence/proportion level for two-sided tolerance intervals to show that process meets the specification limits.

```
norm.ss(x = milk, alpha = 0.05, P = 0.90, side = 2, spec = c(0.900, 1.100),
method = "YGZO", hyper.par = list(mu.0 = 0.994, sig2.0 = 0.002))
```

The given R-code is for two-sided tolerance intervals. This code is not fit for one-sided tolerance analysis because confidence level ( $1-\alpha$ ) changes depending on either two-sided or one-sided tolerance intervals; for example,  $\alpha$  is equal to 0.025 at 0.95 confidence level for two-sided tolerance intervals, while it is 0.05 for those of one-sided. Therefore, the R-code is modified as given below:

```
norm.ss(x = data, alpha = 1- $\gamma$ , P = P, side = 1, spec = c( $\bar{X}$  - 3s), method =
"YGZO", hyper.par = list(mu.0 =  $\bar{X}$ , sig2.0 =  $s^2$ ))
```

where,  $\bar{X}$  is sample mean,  $s$  is sample standard deviation, and  $s^2$  is sample variance.

Construction of specification limits come into prominence at that point. The rule-of-thumb is to set the specification limits as -3 standard deviations from the mean of reference data. When reference data is obtained, future samples can be characterized based on how it should closely follow specification limits. If tolerance intervals exceed the specification limits, this is an indication that the process is out of statistical control. It is somewhat related to the use of +/-3 standard deviation as a threshold when one determines if an observation is a possible outlier when analyzing residuals from regression fit [151]. Therefore,

specification limits for one sided lower tolerance limits were constructed as -3 standard deviations.

Shapiro-Wilks tests were conducted for each sample group to check normality of data set. The test does not reject the null hypothesis ( $H_0$ : Dataset is normally distributed) when it is insignificant ( $p\text{-value} > 0.05$ ). Therefore, the test allows to indicate that data fits the normal distribution with 95% confidence [172].

After determining the minimum sample size requirements for tolerance intervals, if sample size in reference data is large enough then the data set is used as is, and tolerance analysis is then made at desired confidence/proportional levels. Otherwise, sample size is increased as homogenous and randomness assumptions in experiment are taken into consideration.

#### 3.2.3.2.2 Determination of Lower Tolerance Limits

To make a reliable tolerance analysis, normality assumptions must be checked. If data is normally distributed, following expression [174] or R-code is used to calculate one-sided LTLs for data set [154,170]:

$$\bar{X} - (k(n, \gamma, P) \times s) \quad \text{Equation 3.5}$$

$$\text{normtol.int}(x = \text{data\_name}, \text{alpha} = 1 - \gamma, P = P, \text{side} = 1)$$

where,  $\bar{X}$  is sample mean,  $k(n, \gamma, \beta)$  is tolerance factor for specified sample size and confidence/proportional level, and  $s$  is sample standard deviation. On the other hand, if data set is not normally distributed, the following methods are used [175]:

1. Logarithmic normalizing transformation is sought. The normality of data set is then checked. If data set is normally distributed, LTL is calculated by using equation 3.5 or R-code for normal tolerance limits. Afterwards, transformed LTL values are inverted to get real value.
2. If data is not normally distributed after transformation, other distributions such as Weibull distribution are used. LTLs are then calculated by using the

following R-code for data set fitted to Weibull distribution [155]. Kolmogorov-Smirnov test is conducted to check whether data fits to Weibull distribution or not.

```
exttol.int(x = data_name, alpha = 1-γ, P = P, dist = "Weibull", NR.delta = 1e-8)
```

3. If data does not fit the Weibull distribution, non-parametric tolerance analysis is used by using binomial probability in equation 3.6 [176] or provided R-code [155].

$$P(X_i < \xi) = \binom{n}{x} \times p^x \times q^{n-x} \quad \text{Equation 3.6}$$

```
nptol.int(x = data_name, alpha = 1-γ, P = P, side = 1, method = "WILKS", upper = NULL, lower = NULL)
```

Calculation of LTLs with R-code is recommended rather than utilizing binomial probability, although this method is more conservative when compared to other methods. In the case of binomial probability, LTL values at a higher confidence/proportional level may be the minimum value in the data set. If there is an outlier in the data set, it will be an LTL value for higher confidence/proportion levels. In doing so, this may damage the construction of reliable tolerance analysis. Figure 3.10 demonstrates a logical flow chart for the calculation process of LTL values, considering all possible methods.

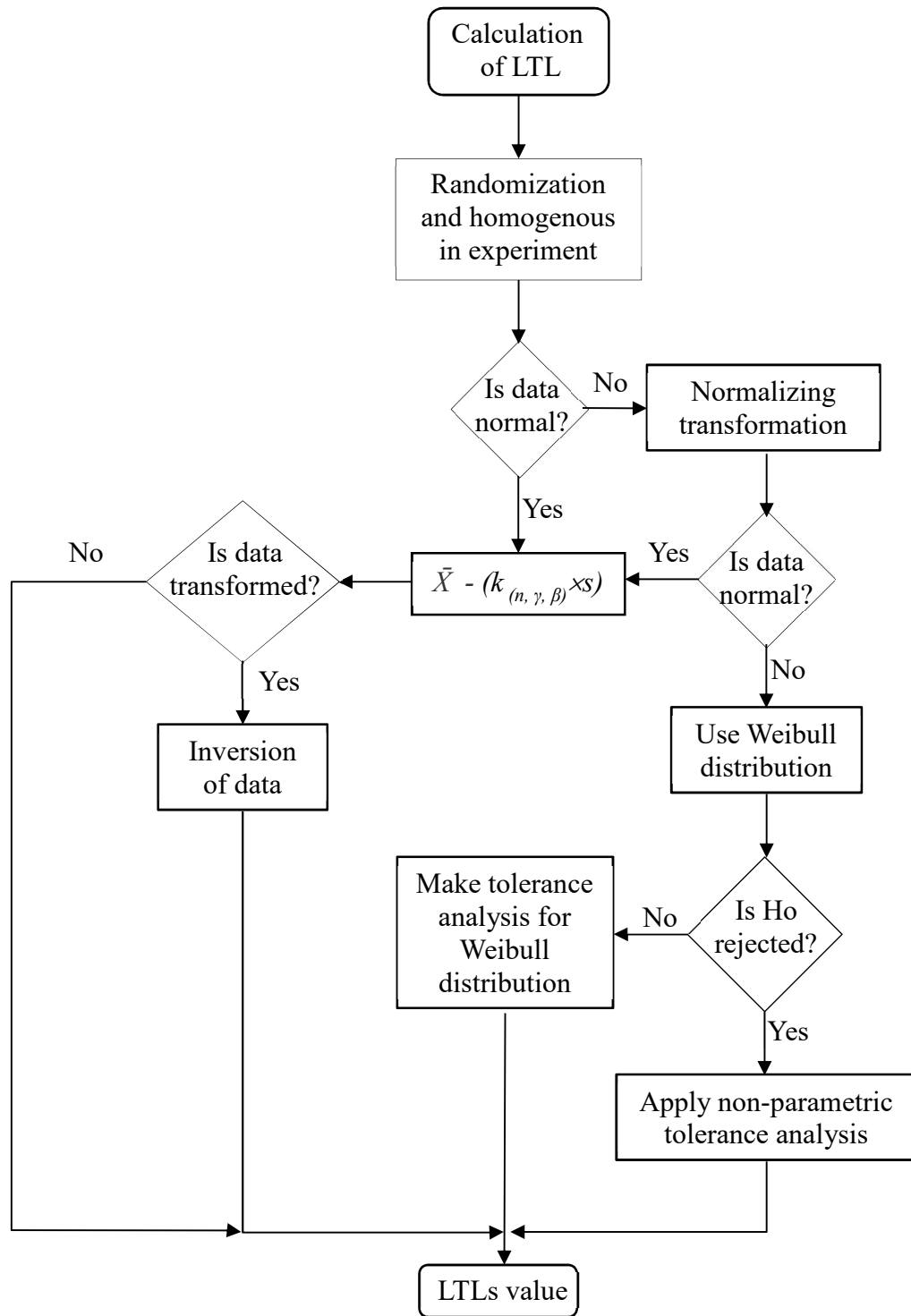


Figure 3.10 Flow Chart for Calculation Process of LTLs

### 3.2.3.2.2.1 Construction of k-Tolerance Factor

k-tolerance factor for tolerance limits changes depending on the sample size ( $n$ ), confidence level ( $\gamma$ ), and proportion level ( $P$ ). In the literature review, k-tolerance factors for one-sided tolerance limits and two-sided tolerance limits are calculated by using different equations. Since probability coverage area represents different areas on the curve-bell (Figure 3.11), z-scores for both  $\gamma$  and  $P$  differ for one-sided and two-sided tolerance limits.

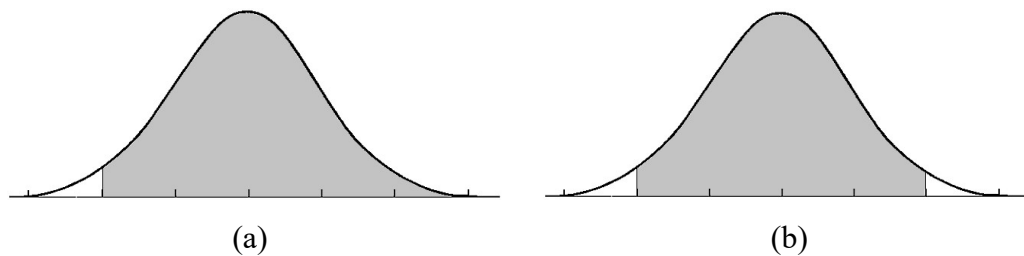


Figure 3.11 Curve Bell. a: One-Sided, b: Two-Sided

Ireson gave equations 3.7 to 3.9 to calculate k-tolerance factor for one-sided tolerance limits [148] and tabulated such values for different sample sizes in Appendix C.

$$k = \frac{z_p + \sqrt{z_p^2 - ab}}{a} \quad \text{Equation 3.7}$$

$$a = 1 - \frac{z_\gamma^2}{2(n-1)} \quad \text{Equation 3.8}$$

$$b = z_p^2 - \frac{z_\gamma^2}{n} \quad \text{Equation 3.9}$$

where,  $k_{(n,\gamma,P)}$  is tolerance factor given sample size and confidence/proportional level,  $n$  is sample sizes,  $z_p$  is z-score for proportion level, and  $z_\gamma$  is z-score for confidence level. Furthermore, equations for  $z_p$  and  $z_\gamma$  are needed in order to be calculated. Zelen and Severo [177] proposed an approximation for these quantities in 1972.

$$z_{\gamma} \approx t_{\gamma} - \frac{c_0 + c_1 t_{\gamma} + c_2 t_{\gamma}^2}{1 + d_1 t_{\gamma} + d_2 t_{\gamma}^2 + d_3 t_{\gamma}^3} + \varepsilon(\gamma) \quad \text{Equation 3.10}$$

$$z_P \approx t_P - \frac{c_0 + c_1 t_P + c_2 t_P^2}{1 + d_1 t_P + d_2 t_P^2 + d_3 t_P^3} + \varepsilon(P) \quad \text{Equation 3.11}$$

$$t_{\gamma} = \sqrt{\ln\left(\frac{1}{(1-\gamma)^2}\right)} \quad \text{Equation 3.12}$$

$$t_P = \sqrt{\ln\left(\frac{1}{(1-P)^2}\right)} \quad \text{Equation 3.13}$$

where,  $c_0 = 2.515517$ ,  $c_1 = 0.802853$ ,  $c_2 = 0.010328$ ,  $d_1 = 1.432788$ ,  $d_2 = 0.189269$ , and  $d_3 = 0.001308$ .

The error of the approximations of  $z_{\gamma}$  ( $\varepsilon(\gamma)$ ) and  $z_P$  ( $\varepsilon(P)$ ) must be less than  $4.5 \times 10^{-4}$  in absolute value. In addition, z-scores could be calculated as using “*normsinv (probability)*” formula in MS Excel. Based on equations, an application was created in MS Excel to calculate k-tolerance factors with various  $n$ ,  $\gamma$ , and  $P$ . The k-tolerance factors are tabulated in Appendix C. Furthermore, ratios of error (%) between tabulated k-tolerance factors and calculated k-tolerance factors by using equations 7 to 13 are shown in Appendix C.

#### 3.2.3.2.2.1.1 Effect of Error in the Approximation

The effect of error in the approximation may be smaller but should not be negligible. Such effects are shown in Appendix C. When  $(\gamma, P)$  level increases, effect of error on k-tolerance factor increases too. On the other hand, when sample size increases, these effects decrease. Table 3.3 shows changes in the error of approximation. It was found from the subtraction of z-score obtained by using rational approximation without error from z-score obtained by using MS excel formula and

Table 3.3 Error of Approximation Related to z-Score

<b>z-score</b>	<b>Error</b>
<b>0.75</b>	0.000301
<b>0.9</b>	-0.000177
<b>0.95</b>	-0.000358
<b>0.99</b>	-0.000437
<b>0.999</b>	-0.000290

### 3.2.3.2.2.1.2 Effect of Sample Size

Lieberman [178] proposed the equation to calculate k-tolerance factor (equation 3.7). However, this equation is used for sample sizes larger than 50. Link proposed an equation 3.17 [179] to solve k-tolerance factor by using Guttman [180] theorem given in equations 3.14 and 3.15, and non-central t- distribution (equation 16) approximated by standard normal distribution,  $z$ , shown by [177]. Assumption for normal distribution is poor for small sample sizes owing to underestimation. Therefore, the t-distribution must be used when sample size is less than 30.

$$P[P(X \geq t_0) \geq 1 - \beta] = P[T_{n-1} \times (\sqrt{n} \times z_\beta) \leq \sqrt{n} \times k] \quad \text{Equation 3.14}$$

$$P[T_v \times \delta \leq t] \approx P \left[ Z \leq \frac{t(1 - \frac{1}{4v}) - \delta}{\sqrt{1 + \frac{t^2}{2v}}} \right] \quad \text{Equation 3.15}$$

$$k = \frac{z_\beta(1-f) + \sqrt{z_\beta^2(1-f)^2 - (a' \times b)}}{a'} \quad \text{Equation 3.16}$$

$$a' = (1 - f)^2 - \frac{z_\beta^2}{2(n-1)} \quad \text{Equation 3.17}$$

$$f = \frac{1}{4(n-1)} \quad \text{Equation 3.18}$$

where,  $P$  is probability,  $X$  is random variables,  $T$  is t-score,  $t$  is non-centrality parameter for t-distribution,  $v$  is degree of freedom, and  $\delta$  is non-centrality parameter.

Lieberman's formula ignores  $f$  factor in calculating k-tolerance factor. Such  $f$ -factor is negligible when sample size is larger. However, ignoring this factor would damage k-tolerance factor when sample size is small ( $n \leq 50$ ). Therefore, equation 3.17 is used to recalculate k-tolerance factor without ignoring  $f$ -factor. In addition, ratio of error between tabulated k-tolerance factors and calculated k-tolerance factors by using equation 3.17 is shown in Appendix C.

Young *et al.* used a k-tolerance factor equation for one-sided lower tolerance limits which computed the inverse cumulative distribution function for the non-central t-distribution (Student's t-distribution) [151]:

$$k_1(n, \alpha, P) = \frac{1}{\sqrt{n}} t_{(n-1, 1-\alpha, \delta)} \quad \text{Equation 3.19}$$

$$\delta = \sqrt{n} z_P \quad \text{Equation 3.20}$$

where,  $t_{(n-1, 1-\alpha, \delta)}$  is t-score for non-central t-distribution,  $n$  is sample size,  $\alpha$  is significance level, and  $\delta$  is non-centrality parameter. Unless sample size is  $n \leq 10$ , the difference in the methods do not have much of practical effect. k-tolerance factor is re-calculated by using equation 3.20 when sample sizes is  $n \leq 10$  since calculating k-tolerance factor by using equation 3.20 may give more conservative results for small values. Ratios of error between k-tolerance factor by using equation 3.7 and equation 3.20 are shown in Appendix C. Results show that there is a significant similarity with k-tolerance factors according to study in [148].

### 3.3 Results and Discussion

#### 3.3.1 Mechanical and Physical Properties of Wood Material

Result of bending tests are given in Table 3.4, as well as Figure 3.12 and 3.13. According to the test results, specific gravities at 7% MC of red oak and white oak were 0.70 and 0.79, respectively. The MOR of red oak were 111.47 MPa while those of white oak were 159.58 MPa. Besides, MOE of red oak and white oak were 12,576.75 MPa and 15,756.50 MPa, respectively. In bending test of clear specimens, most of the failure (7 specimens) occurred because of simple tension, while 4 specimens failed because of cross-grain tension and 1 specimen failed owing to splintering tension.

Table 3.4 Some Mechanical and Physical Properties of Wood Material

Wood species	Specific gravity	MOR (MPa)	MOE (MPa)
Red Oak	0.70	111.47	12,576.75
White Oak	0.79	159.58	15,756.50

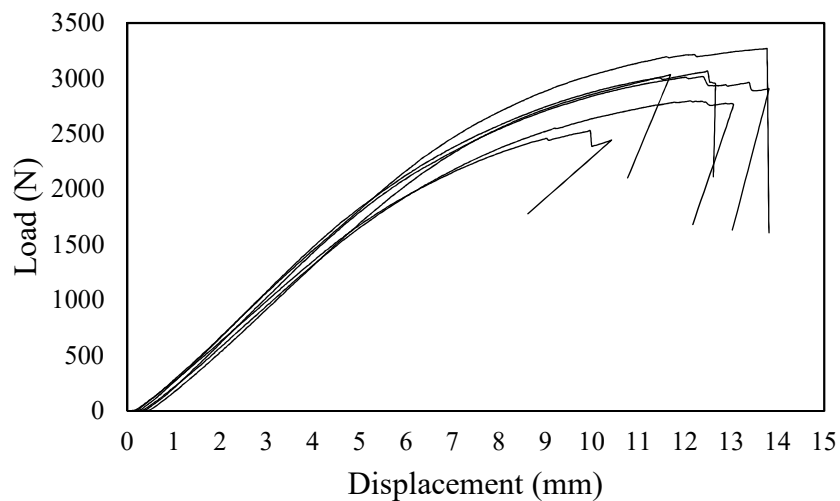


Figure 3.12 Load-Displacement Curves in Static Bending Test for Red Oak

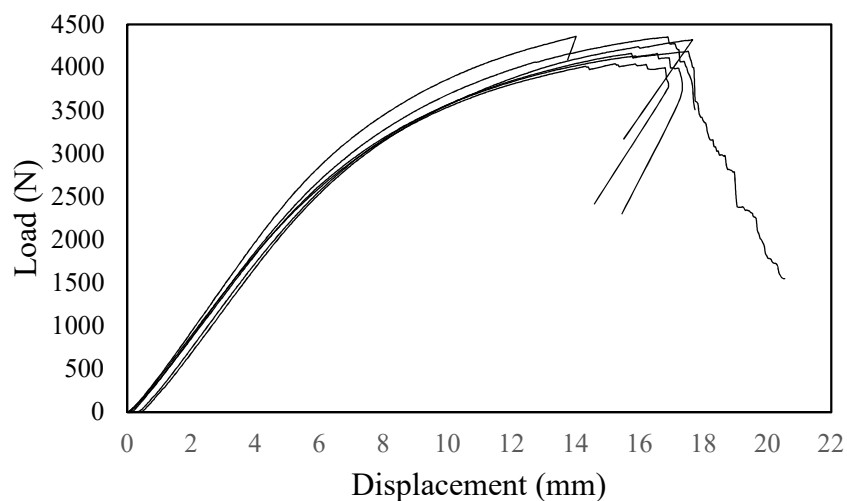


Figure 3.13 Load-Displacement Curves in Static Bending Test for White Oak

### 3.3.2 Determination of Minimum Sample Size Requirements for Univariate Tolerance Analysis

A reference data was used to determine minimum sample size requirement for univariate tolerance analysis. For this purpose, 30 specimens (based on Central Limit Theorem (CLT)) for each sample group were tested. Test results are given in Tables 3.5 and 3.6. According to the test results, specimens made of white oak provided stronger joints compared to those of red oak since the mechanical properties and specific gravity of white oak wood are

higher than those of red oak. In bending testing, RMT joints are stronger than dowel joints. In screw withdrawal strength in wood, the screw withdrawal from edge-grain have the highest strength while those of end-grain have less strength. The reason for higher tensile strength in wood from edge- and face-grain than end-grain is that screws may conjoin to wood rays at edge- and face-grain orientation so screw withdrawal may endure these screw orientations effectively [91].

Table 3.5 Bending Test of T-Shaped Joints

Joint Type	Wood Species	Average (N.m)	SD (N.m)	CoV (%)	Power ( $\beta$ )	p-value
RMT	Red Oak	350.55	46.36	13.23	0.996	0.5253
	White Oak	362.79	63.34	17.46	0.944	0.3902
Dowel	Red Oak	231.85	22.36	9.64	1	0.061
	White Oak	249.02	40.17	16.13	0.999	0.2365

Table 3.6 Screw Withdrawal Strength of Wood

Screw Orientation	Wood Species	Average (N)	SD (N)	CoV (%)	Power ( $\beta$ )	p-value
End	Red Oak	5981.88	1012.7	16.99	1	0.8652
	White Oak	6646.11	948.79	14.28	1	0.3396
Edge	Red Oak	6777.41	973.66	14.37	1	0.9254
	White Oak	7314.93	1112.54	15.21	1	0.4089
Face	Red Oak	6577.79	919.38	13.98	-	0.4504
	White Oak	6687.75	938.42	14.03	-	0.0991

Power testing was conducted to make reliable design of experiment and to assess whether sample size is large enough or not. The power test results are given in Tables 3.5 and 3.6. Delta ( $\delta$ ) in the power test were determined by subtracting average strength values of joints calculated from predictive equations given in Chapter 2. Power of all tests were above acceptable levels at 80% with the 30 specimens. However, 40 specimens were used for sample group of RMT joints made of white oak because power of this test was 64%, which is not acceptable so, sample size was not enough for test. Furthermore, p-values for Shapiro-Wilks normality test are given in Tables 3.5 and 3.6. To check normality of the data sets, Shapiro-Wilks tests were conducted for the sample groups. According to

normality test, all p-values are above 0.05 significance level which means that  $H_0$  is not rejected and the datasets are normally distributed. Also, histogram, density, and Q-Q plots, which also express normality of datasets, are given through Figures 3.14 to 3.23. In here, all Q-Q plots look close to normal (45° line) while plots for screw withdrawal strength of white oak wood from face grain are relatively less close to normal.

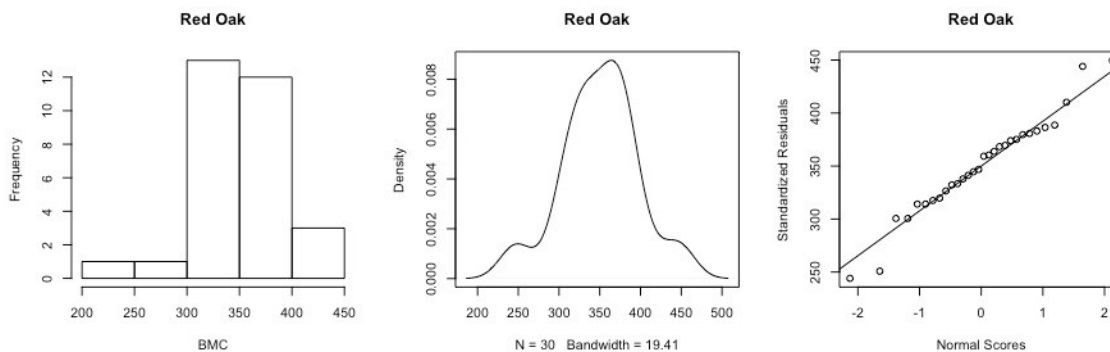


Figure 3.14 Histogram, Density and Q-Q plots of RMT Joints Made of Red Oak

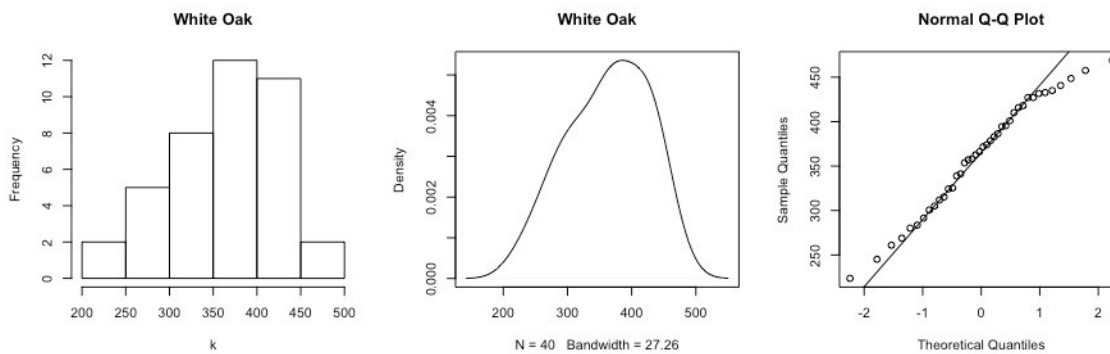


Figure 3.15 Histogram, Density and Q-Q Plots of RMT Joints Made of White Oak

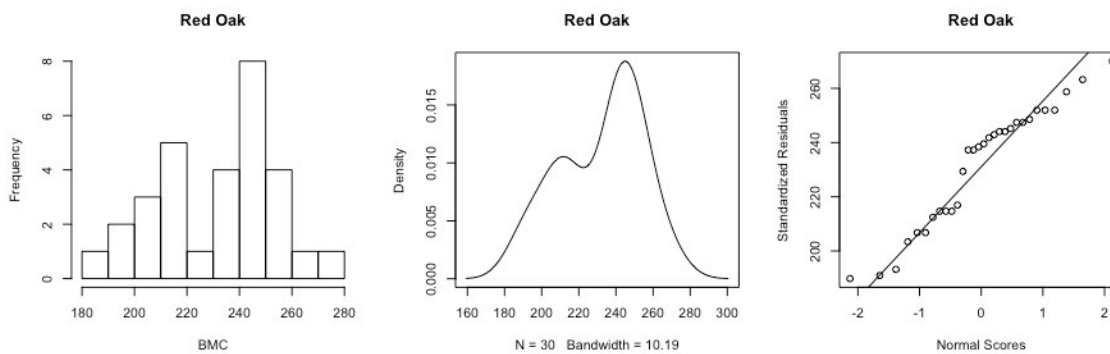


Figure 3.16 Histogram, Density and Q-Q plots of Dowel Joints Made of Red Oak

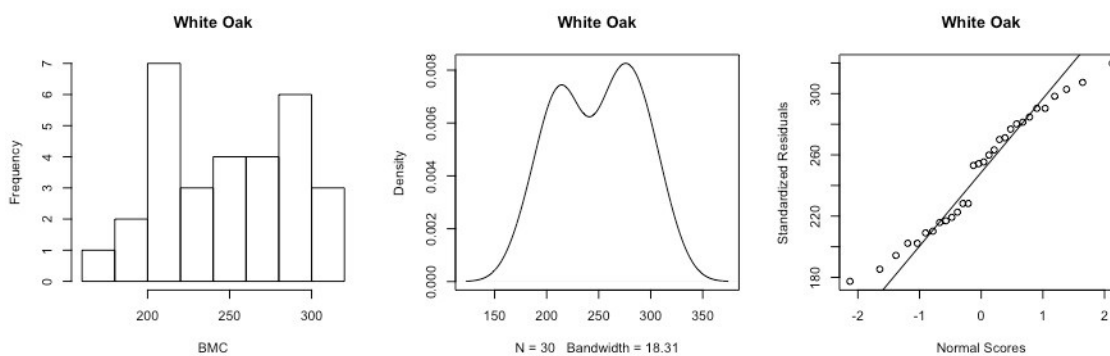


Figure 3.17 Histogram, Density and Q-Q Plots of Dowel Joints Made of White Oak

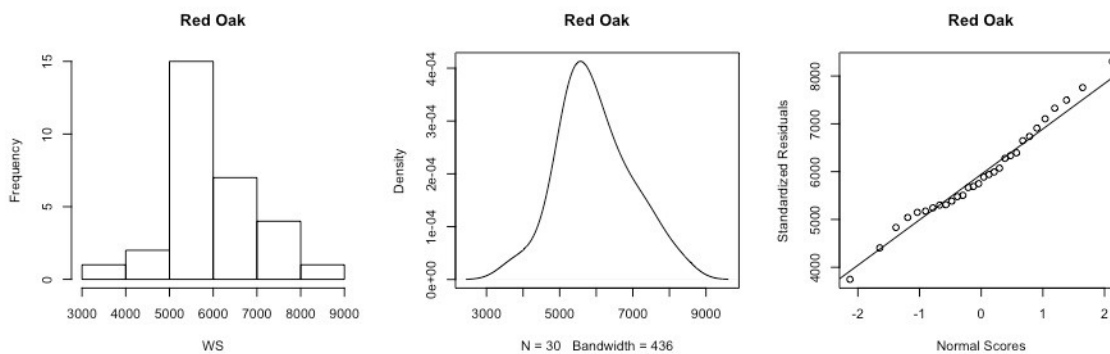


Figure 3.18 Histogram, Density and Q-Q Plots of Screw Withdrawal in Wood Made of Red Oak from End-Grain

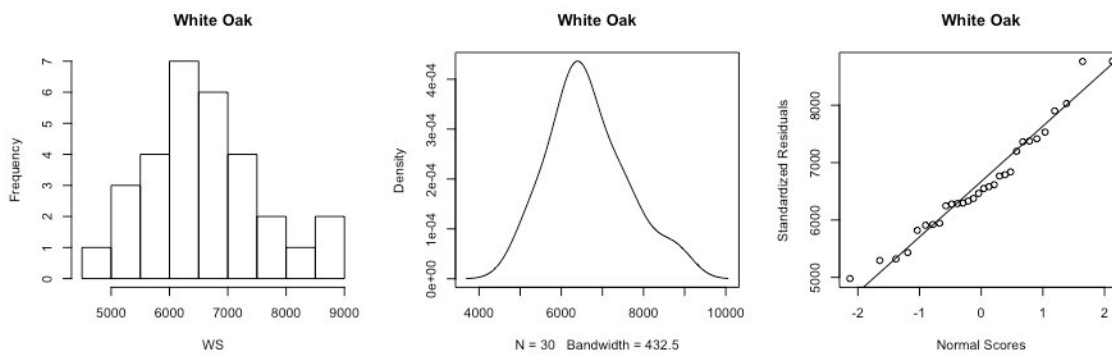


Figure 3.19 Histogram, Density and Q-Q Plots of Screw Withdrawal in Wood Made of White Oak from End-Grain

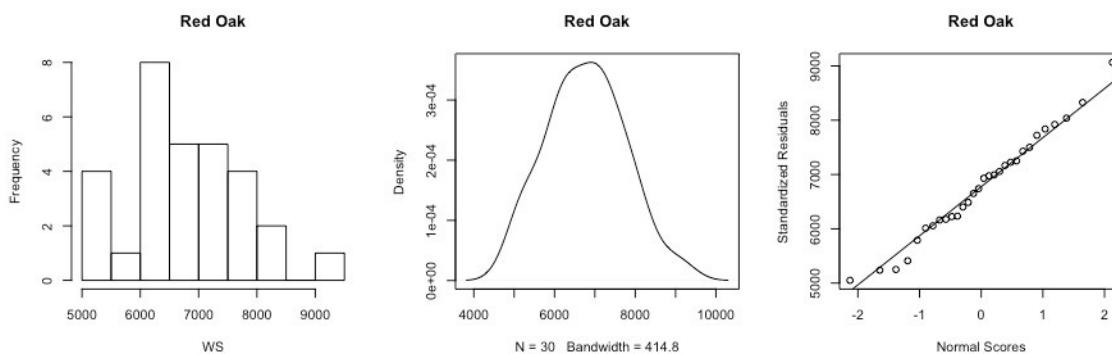


Figure 3.20 Histogram, Density and Q-Q Plots of Screw Withdrawal in Wood Made of Red Oak from Edge-Grain

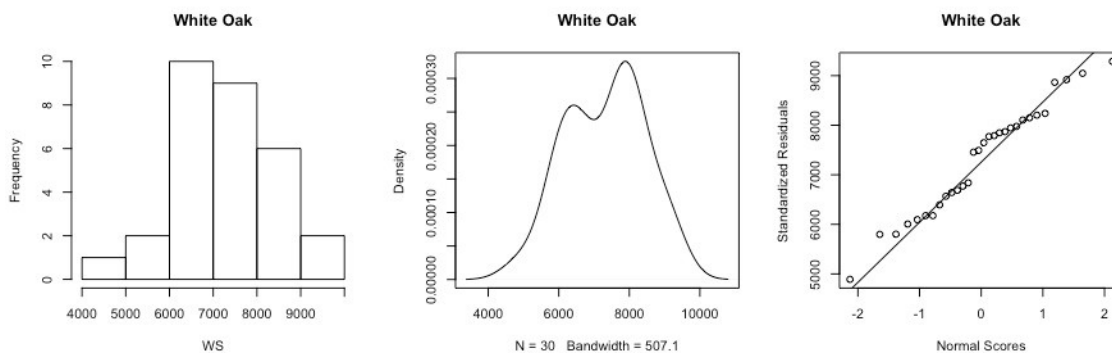


Figure 3.21 Histogram, Density and Q-Q Plots of Screw Withdrawal in Wood Made of White Oak from Edge-Grain

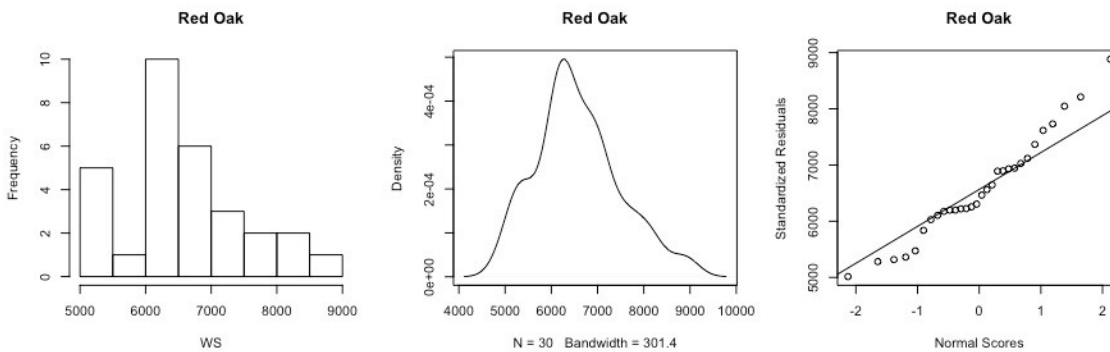


Figure 3.22 Histogram, Density and Q-Q Plots of Screw Withdrawal in Wood Made of Red Oak from Face-Grain

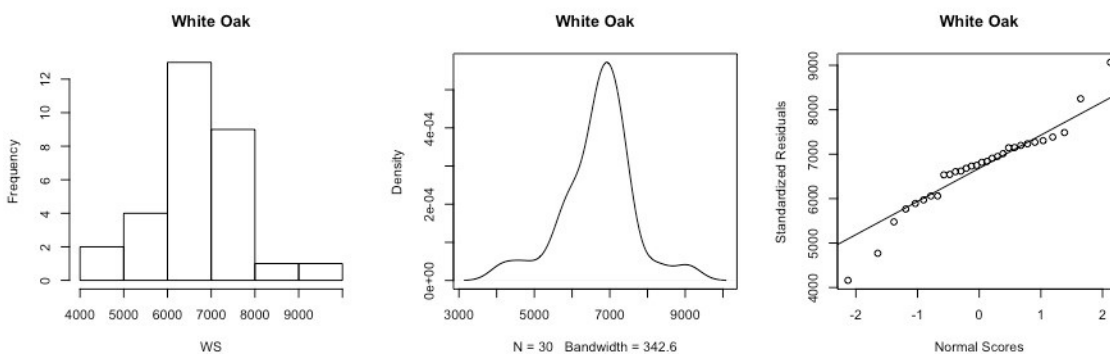


Figure 3.23 Histogram, Density and Q-Q Plots of Screw Withdrawal in Wood Made of White Oak from Face-Grain

To determine minimum sample size requirements from reference data, both confidence levels ( $\gamma$ ) and proportion levels ( $P$ ) were used from one each of 0.90, 0.95, and 0.99 levels. Minimum sample size requirements for sample groups are given in Figure 3.24 corresponding to each  $\gamma/P$  level. To make a tolerance analysis at 0.99/0.99  $\gamma/P$  level, minimum sample size requirement is 215 for each sample group but sample groups with RMT joints made of white oak and dowel joints made of red oak are required minimum 216 specimens. 220 specimens were constructed for each sample group to eliminate any error during experiment and tolerance analysis.

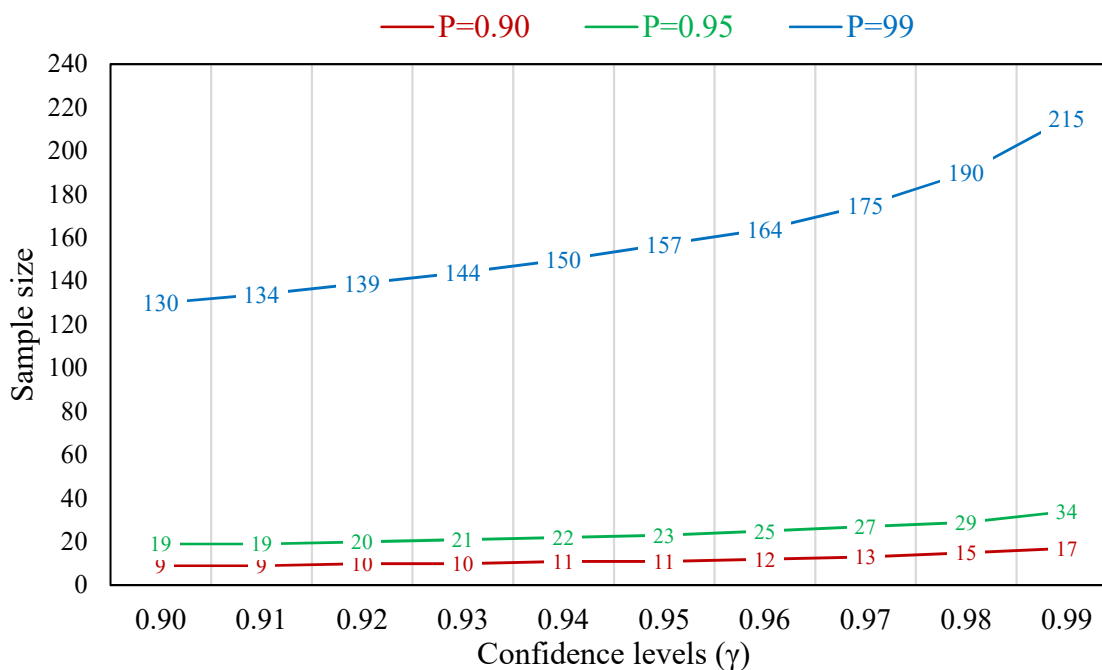


Figure 3.24 Minimum Sample Size Requirement Given  $\gamma$ /P Levels.

### 3.3.3 Joint Strength

#### 3.3.3.1 Bending Strength of Rectangular Mortise and Tenon Joints

Test results for T-shaped joints are shown in Figure 3.25 and Table 3.7. Average bending moment capacity of RMT joints made of red oak is 350.57 N.m with a standard deviation of 50.03 N.m while those of white oak is 341.17 N.m with a standard deviation of 60.25 N.m.

Table 3.7 Test Results for Bending Strength of RMT and Dowel Joints

Joint Type	Wood Species	Mean (N.m)	SD (N.m)	CoV (%)
RMT	Red Oak	350.56	50.03	14.27
	White Oak	341.17	60.25	17.66
Dowel	Red Oak	240.81	30.65	12.72
	White Oak	243.44	37.12	15.24

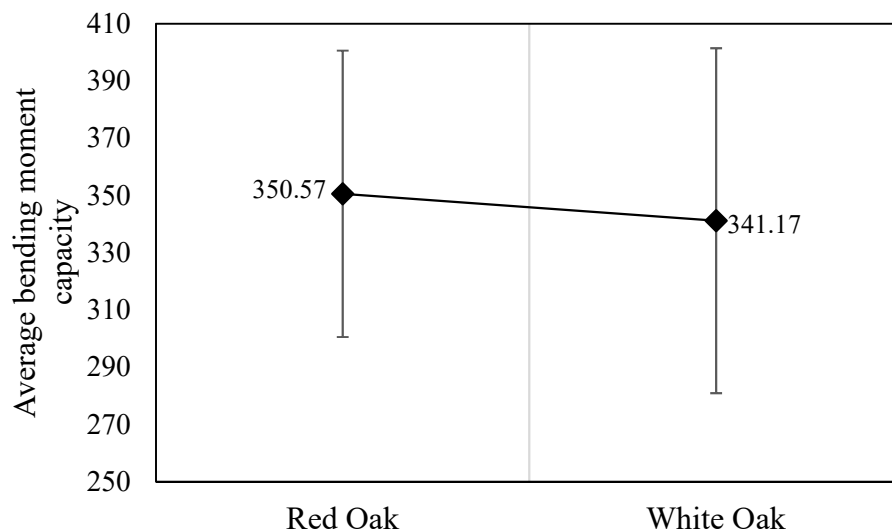


Figure 3.25 Average Ultimate Bending Moment Capacity of RMT Joints (in N.m)

### 3.3.3.2 Bending Strength of Two-Pin Bending Resisting Dowel Joints

Test results for two-pin moment resisting dowel joints are shown in Figure 3.26 and Table 3.7. Average bending moment capacity of joints made of red oak wood is 240.81 N.m with a standard deviation of 30.65 N.m, while those of white oak is 243.44 N.m with a standard deviation of 37.12 N.m.

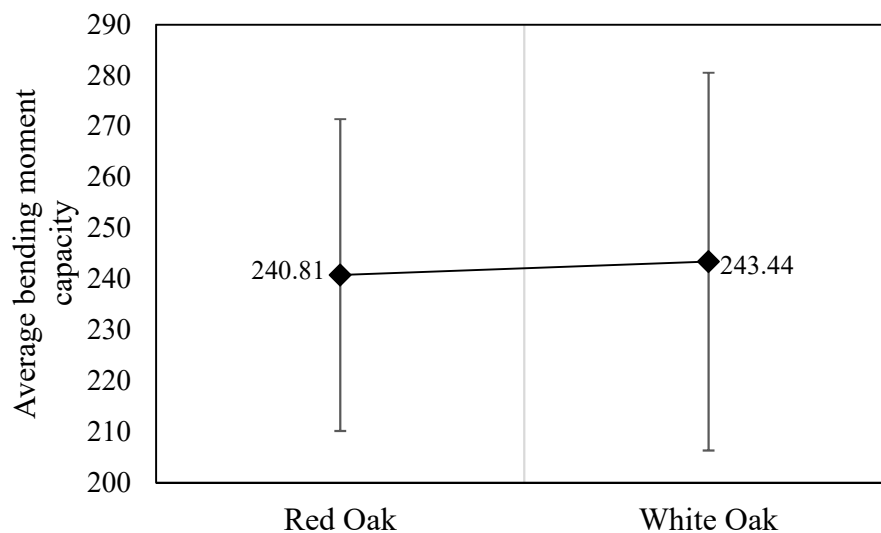


Figure 3.26 Average Ultimate Bending Moment Capacity of Two Pin Moment Resisting Dowel Joints (in N.m)

### 3.3.3.3 Screw Withdrawal Strength in Wood

#### 3.3.3.3.1 Screw Withdrawal Strength in Wood from End-Grain

Test results for screw withdrawal strength in wood from end-grain are shown in Figure 3.27 and in Table 3.8. Average screw withdrawal strength in wood from end grain made of red oak wood is 5780.50 N with a standard deviation of 916.64 N, while those of white oak is 6291.04 N with a standard deviation of 967.36 N.

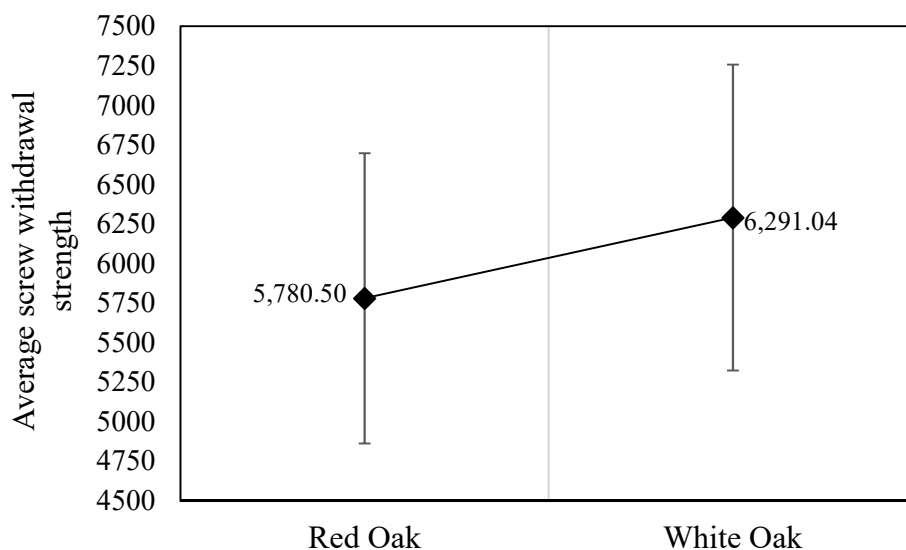


Figure 3.27 Average Ultimate Screw Withdrawal Strength in Wood from End-Grain (in N)

#### 3.3.3.3.2 Screw Withdrawal Strength in Wood from Edge-Grain

Test results for screw withdrawal strength in wood from edge-grain are depicted in Figure 3.28 and in Table 3.8. Average screw withdrawal strength in wood from edge-grain made of red oak wood is 5780.50 N with a standard deviation of 916.64 N, while those of white oak is 6291.04 N with a standard deviation of 967.36 N.

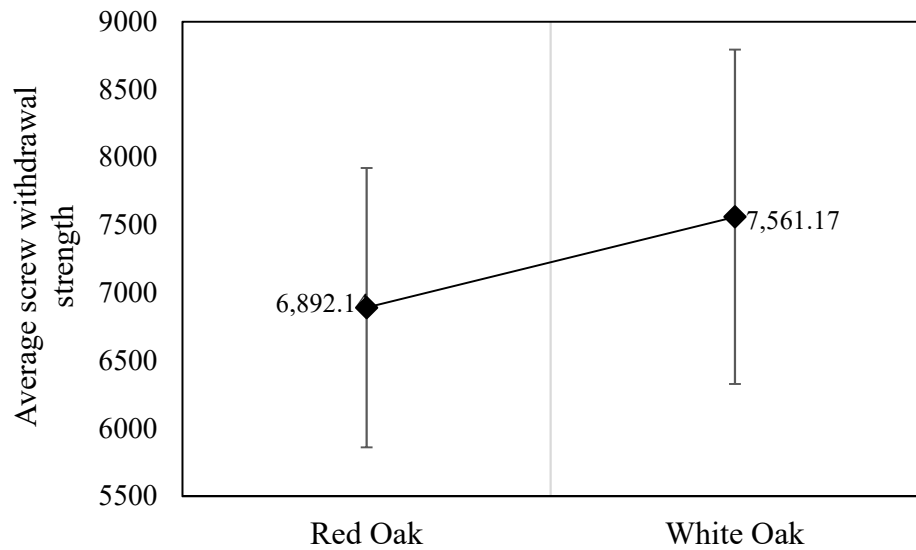


Figure 3.28 Average Ultimate Screw Withdrawal Strength in Wood from Edge-Grain (in N)

### 3.3.3.3.3 Screw Withdrawal Strength in Wood from Face-Grain

Test results for screw withdrawal strength in wood from face-grain are demonstrated in Figure 3.29 and Table 3.8. Average screw withdrawal strength in wood from edge-grain made of red oak is 5,780.50 N with a standard deviation of 916.64 N, while those of white oak is 6,291.04 N with a standard deviation of 967.36 N.

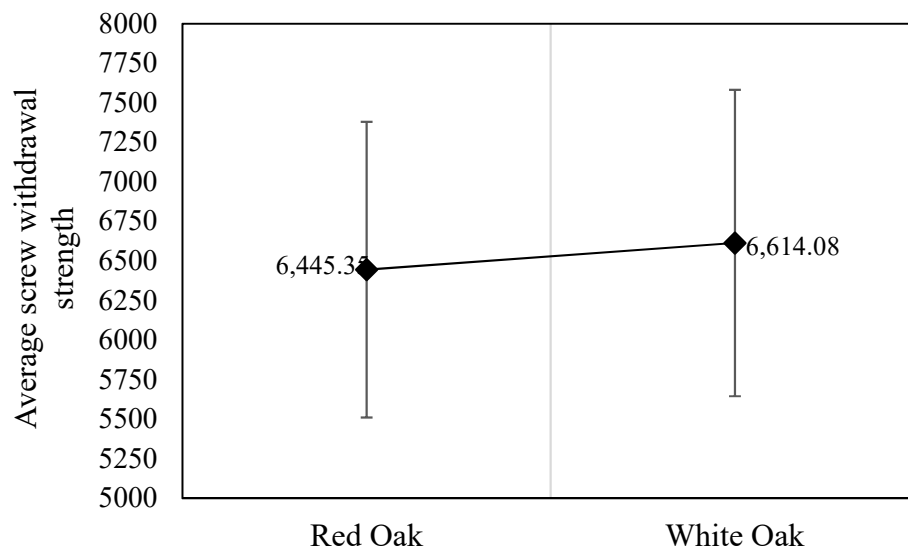


Figure 3.29 Average Ultimate Screw Withdrawal Strength in Wood from Face-Grain (in N)

Table 3.8 Test Results of Screw Withdrawal Strength in Wood

Screw Orientation	Wood Species	Mean (N)	SD (N)	CoV (%)
End	Red Oak	5780.51	916.64	15.85
	White Oak	6291.04	967.36	15.38
Edge	Red Oak	6892.14 (8.82)	1030.05 (0.15)	14.94
	White Oak	7561.17	1232.89	16.31
Face	Red Oak	6445.35	934.46	14.49
	White Oak	6614.08 (8.78)	967.88 (0.14)	14.63

\*Values in parenthesis are test results after data set are transformed logarithmic values.

### 3.3.4 Tolerance Analysis

#### 3.3.4.1 Normality Assumption for Tolerance Analysis

Lower tolerance limits (LTLs) of selected furniture joints were determined by considering randomness, homogeneity, and normality assumptions in the experiment. Randomness assumption was considered while selecting specimen parts from the material pool before testing. Homogeneity assumption was considered during selection of specimen parts, specimen construction, and specimen testing, so that identical specimens in the same

sample groups were tested according to same test procedures. Normality assumption was considered during data analysis. According to this assumption, data sets in six sample groups were normally distributed ( $p\text{-value} > 0.05$  in Shapiro-Wilks test) while two sample groups were log-normally distributed after logarithmic transformation of data ( $p\text{-value} > 0.05$  in Shapiro-Wilks test for transformed data) and those of two sample groups fitted to Weibull distribution ( $D\text{-value} < 0.0917$  in Kolmogorov-Smirnov test). The results of normality assumption test for bending strength of RMT and dowel joints are given in Table 3.9 while those of screw withdrawal strength test are given in Table 3.10.

Table 3.9 Normality Test Results for RMT and Dowel Joints

Joint Type	Wood Species	p-value for normal data set	p-value for log-normal data set	D-value of Kolmogorov-Smirnov test	Distribution of data set
RMT	Red Oak	3.02E-06	3.72E-13	0.0651	Weibull
	White Oak	0.5172	-	-	Normal
Dowel	Red Oak	0.0081	0.0002	0.0858	Weibull
	White Oak	0.5991	-	-	Normal

Table 3.10 Normality Test Results for Screw Withdrawal Strength in Wood

Screw Orientation	Wood Species	p-value for normal data set	p-value for log-normal data set	D-value of Kolmogorov-Smirnov test	Distribution of data set
End	Red Oak	0.3553	-	-	Normal
	White Oak	0.2683	-	-	Normal
Edge	Red Oak	0.0041	0.2718	-	Log-normal
	White Oak	0.3362	-	-	Normal
Face	Red Oak	0.1920	-	-	Normal
	White Oak	0.0053	0.8485	-	Log-normal

In *RMT joints made of red oak*,  $p\text{-value}$  in Shapiro-Wilks normality test is  $3.08\text{e-}06$  which violates normality assumption for this sample group. In Figure 3.30, histogram, Q-Q and 1 Q-Q plot, and empirical cumulative distribution function (ECDF) plots for their bending moment capacity are shown. The histogram is skewed left as well as that normal Q-Q plot is left-tailed due to two outliers. After a logarithmic transformation of data sets, it does not get closer to normal and its histogram is skewed left ( $p\text{-value}=3.72\text{e-}13$ ). The data sets fit

into the Weibull distribution because D-value in Kolmogorov-Smirnov test is 0.0651, which is lower than 0.0917. In the ECDF plot, approximately 85% of data is between 300 N.m and 400 N.m. Besides, Q-Q- plots for Weibull distribution look normal. Therefore, a tolerance analysis for RMT joints made of red oak was done according to Weibull distribution.

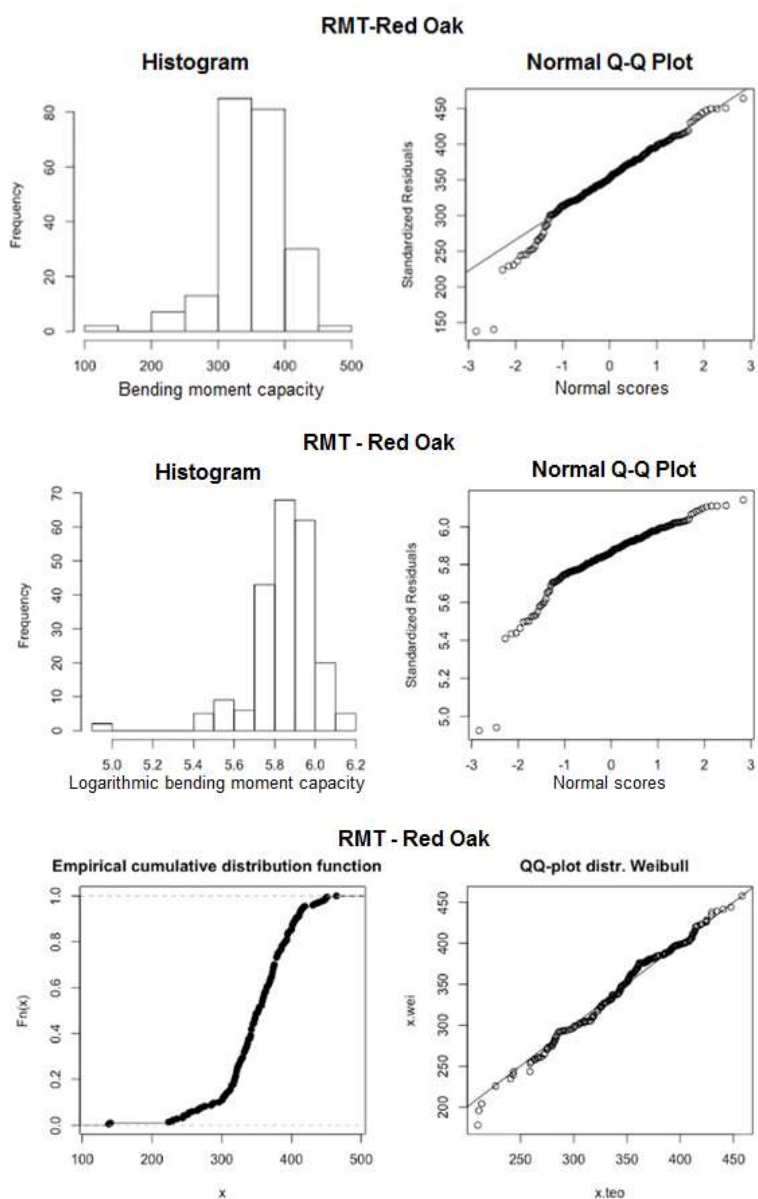


Figure 3.30 Histogram, Q-Q plot and ECDF Plots for RMT Joints Made of Red Oak

In *RMT joints made of white oak*, p-value in Shapiro-Wilks normality test is 0.5172 which does not violate normality assumption. Moreover, histogram looks symmetric and normal Q-Q plot looks normal because its line is close to 45° (Figure 3.31). Thus, tolerance analysis for RMT joints made of white oak was done according to a normally distributed data set.

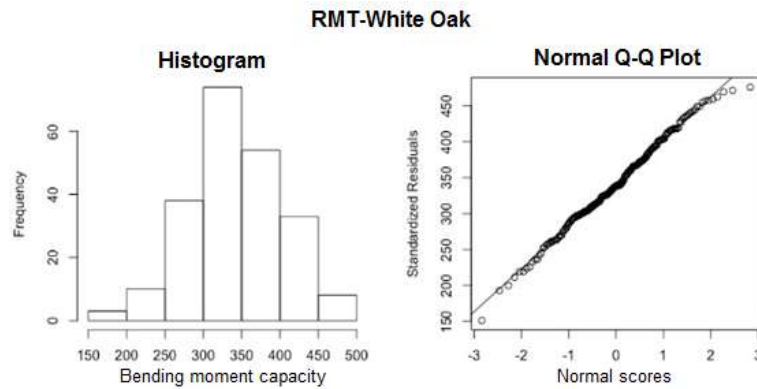


Figure 3.31 Histogram and Q-Q Plots for RMT Joints Made of White Oak

In *dowel joints made of red oak*, p-value in Shapiro-Wilks normality test is 0.0081 which violates normality assumption. Its histogram, Q-Q and ECDF plots are demonstrated in Figure 3.32. The histogram is slightly skewed left, but normal Q-Q plot looks normal. Yet, other methods should be tried not to damage tolerance analysis. After logarithmic transformation of data set, its p-value is 0.0002 which still violates normality assumption. After logarithmic transformation, its histogram is skewed left and its Q-Q plot is light-tailed. The data still fits to Weibull distribution because D-value in Kolmogorov-Smirnov test is 0.0858, which is less than 0.0917. Furthermore, ECDF says that approximately 85% of data is between 200 N.m and 275 N.m. Although Q-Q plot in Weibull distribution looks light-tailed, a tolerance analysis for dowel joints made of red oak can be made according to Weibull distribution owing to the result of the Kolmogorov-Smirnov test.

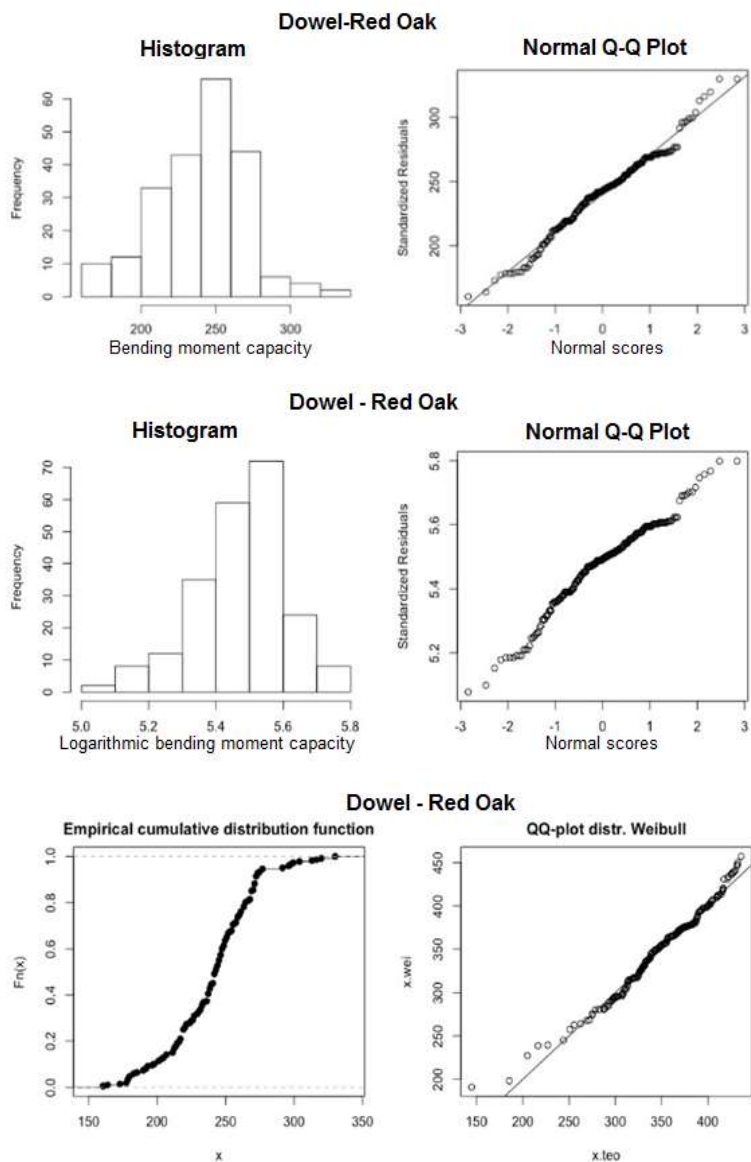


Figure 3.32 Histogram, Q-Q and ECDF Plots for Dowel Joints Made of Red Oak

In *dowel joints made of white oak*, p-value in Shapiro-Wilks normality test is 0.5991 which does not violate normality assumption. Its histogram looks symmetric and its normal Q-Q plot is light-tailed but still looks normal given in Figure 3.33. Thus, the tolerance analysis for dowel joints made of white oak was done according to a normally distributed data set.

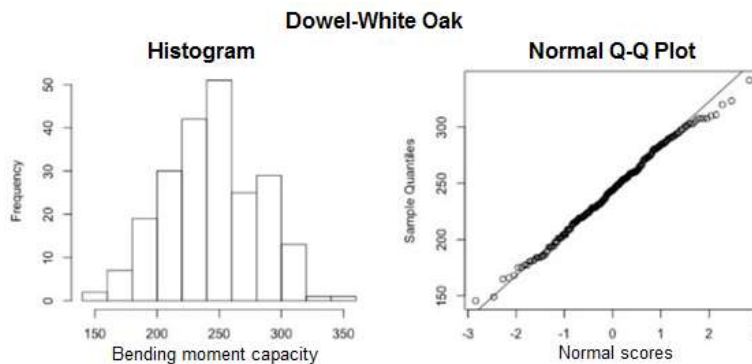


Figure 3.33 Histogram and Q-Q Plots for Dowel Joints Made of White Oak

In *screw withdrawal strength in wood made of red oak from end grain*, p-value in Shapiro-Wilks normality test is 0.3553 which does not violate normality assumption. Its histogram looks symmetric and its normal Q-Q plot is light-tailed but looks normal shown in Figure 3.34. Thus, the tolerance analysis for screw withdrawal strength in wood made of red oak from end grain was done according to a normally distributed data set.

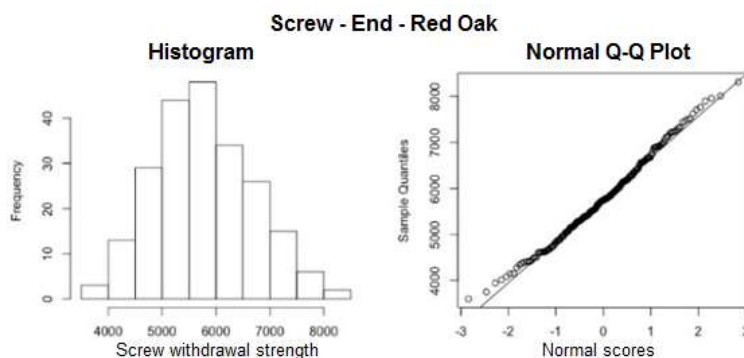


Figure 3.34 Histogram and Q-Q Plots for Screw Withdrawal Strength in Wood Made of Red Oak from End-Grain

In *screw withdrawal strength of wood made of white oak from end grain*, p-value in Shapiro-Wilks normality test is 0.2683, which does not violate normality assumption. Its histogram looks symmetric and its normal Q-Q plot is light-tailed but looks normal demonstrated in Figure 3.35. Thus, the tolerance analysis for screw withdrawal strength in wood made of white oak from end orientation was done according to a normally distributed data set.

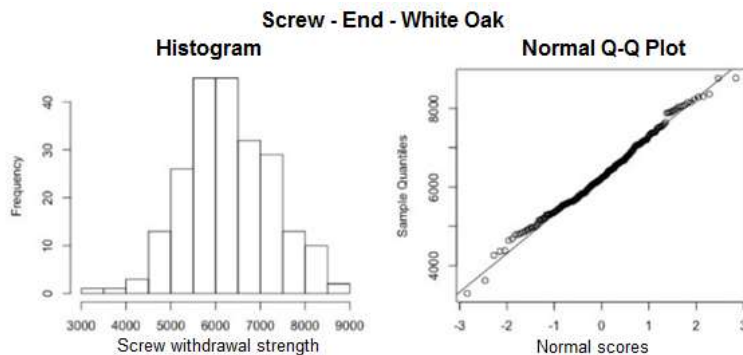


Figure 3.35 Histogram and Q-Q Plots for Screw Withdrawal Strength in Wood Made of White Oak from End-Grain

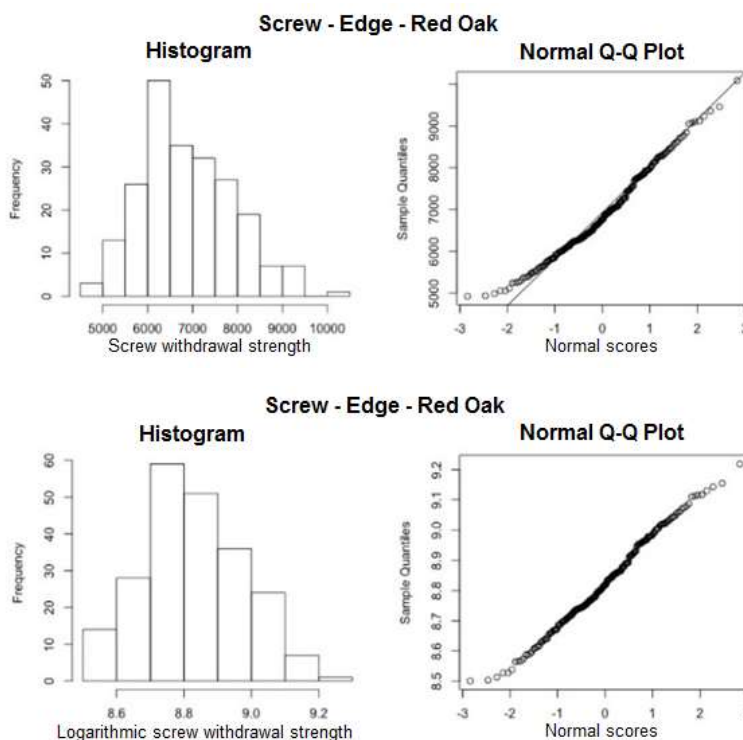


Figure 3.36 Histogram and Q-Q Plots for Screw Withdrawal Strength in Wood Made of Red Oak from Edge-Grain

In *screw withdrawal strength of wood made of red oak from edge grain*, p-value in Shapiro-Wilks normality test is 0.0041 which violates normality assumption. Its histogram is skewed right, and its normal Q-Q plot is light-tailed depicted in Figure 3.36. After logarithmic transformation of data set, its p-value is 0.2718 which does not violate

normality assumption. Although its histogram is slightly skewed right, its normal Q-Q plot looks normal in Figure 3.36. Thus, the tolerance analysis for screw withdrawal strength in wood made of red oak from edge orientation was done after normalizing transformation.

In *screw withdrawal strength in wood made of white oak from edge grain*, p-value in Shapiro-Wilks normality test is 0.3362 which does not violate normality assumption. In Figure 3.37, its histogram is slightly skewed right, and its normal Q-Q plot is light-tailed but looks normal. Thus, the tolerance analysis for screw withdrawal strength in wood made of white oak from edge orientation was done according to a normally distributed data set.

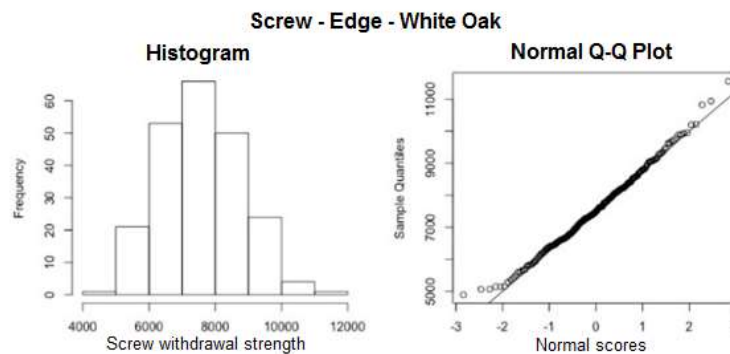


Figure 3.37 Histogram and Q-Q Plots for Screw Withdrawal Strength in Wood Made of White Oak from Edge-Grain

In *screw withdrawal strength in wood made of red oak from face grain*, p-value in Shapiro-Wilks normality test is 0.1920 which does not violate normality assumption. Its histogram is slightly skewed right, and its normal Q-Q plot is light-tailed but looks normal given Figure 3.38. Thus, the tolerance analysis for screw withdrawal strength in wood made of red oak from face *grain* was done according to a normally distributed data set.

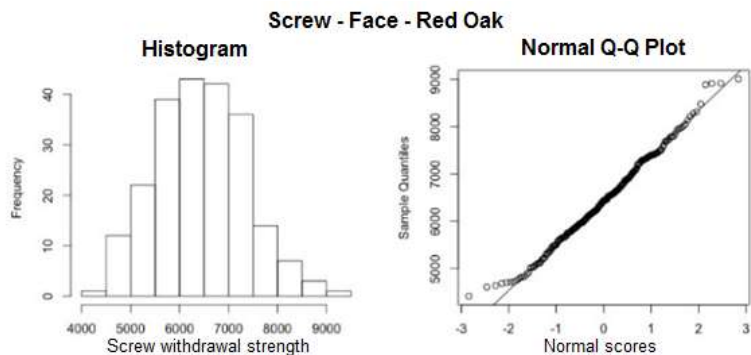


Figure 3.38 Histogram and Q-Q Plots for Screw Withdrawal Strength in Wood Made of Red Oak from Face-Grain

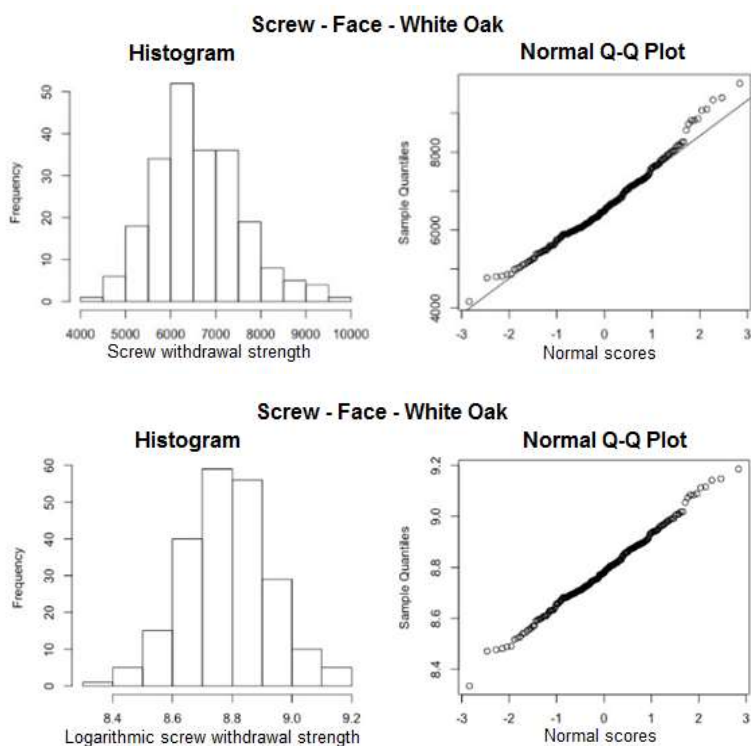


Figure 3.39 Histogram and Q-Q Plots for Screw Withdrawal Strength in Wood Made of White Oak from Face-Grain

In *screw withdrawal strength of wood made of white oak from face grain*, p-value in Shapiro-Wilks normality test is 0.0053 which violates normality assumption. In Figure 3.39, its histogram is skewed right, and its normal Q-Q plot is light-tailed. After logarithmic transformation of data set, its p-value is 0.8485 which does not violate normality

assumption. Although its histogram looks symmetric and Q-Q plot looks light-tailed, it is still close to normal in Figure 3.39. Thus, tolerance analysis for screw withdrawal strength in wood made of white oak from face grain was done after normalizing transformation.

### 3.3.4.2 Lower Tolerance Limits for Furniture joints

After normality assumption was made for all sample groups, LTLs values were attained at the 0.90/0.90, 0.95/0.90, 0.99/0.90, 0.95/0.90, 0.95/0.95, 0.95/0.99, 0.99/0.90, 0.99/0.95, and 0.99/0.99 ( $\gamma/P$ ) levels. The reason for choosing higher confidence proportional levels is to increase reliability of furniture joints by constructing higher confidence levels and including more future products with higher proportion levels. The increase in proportion levels affects tolerance limits higher than the increase in confidence levels. Confidence level is related to sample error while proportion level pertains to variance in the population, so the gap between tolerance limits for proportion level is higher compared to those of confidence levels [155].

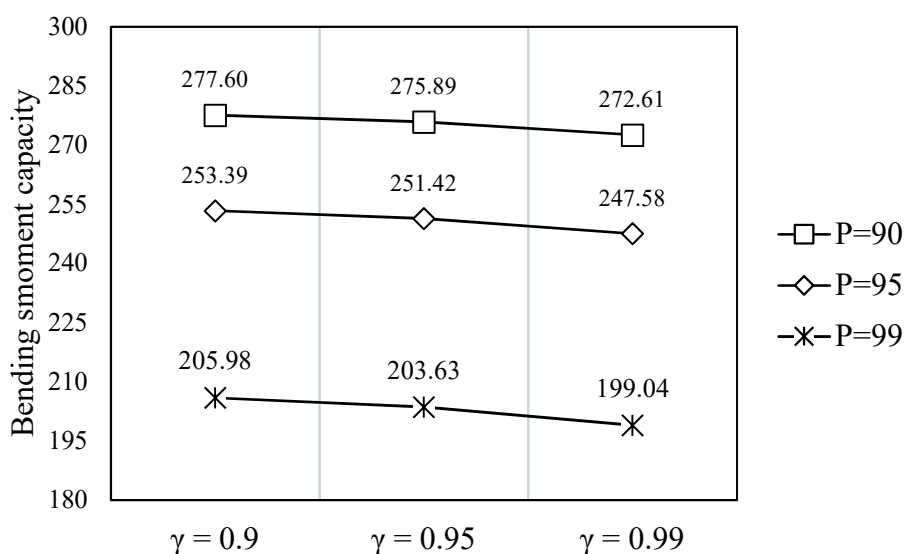


Figure 3.40 LTLs for RMT Joints Made of Red Oak

LTLs values for *bending strength of RMT joints made of red oak* are given in Figure 3.40. Its data distribution and histogram corresponding to LTLs values are shown in Figure 3.41 and the ratio of LTL value, average bending moment capacity, and percentage of number

of values below LTLs values are shown in Table 3.11. According to the test results, LTLs values for the 0.90/0.90, 0.95/0.90, 0.99/0.90, 0.95/0.90, 0.95/0.95, 0.95/0.99, 0.99/0.90, 0.99/0.95 and 0.99/0.99  $\gamma/P$  levels are 277.60, 275.89, 272.61, 253.39, 251.42, 247.58, 205.98, 203.63, and 199.04 N.m, respectively.

There is no violation in the tolerance analysis of RMT joints made of red oak but the ratio of numbers of values below LTL value for 0.95/0.90  $\gamma/P$  level is 5.45%, which must be less than 5%. The closest value above LTL at 0.95/0.90 (253.39 N.m) is 257.61 N.m (error is 1.7%). Only two values (140.10 and 137.84 N.m) are below LTL values for 0.99/0.99  $\gamma/P$  levels because they were outliers for its data set. These outliers may cause that ratio of number of values below LTL value is higher than 5% LTL value (199.04 N.m) for 0.99/0.99  $\gamma/P$  level is 56.78% of average bending moment capacity of RMT joints made of red oak.

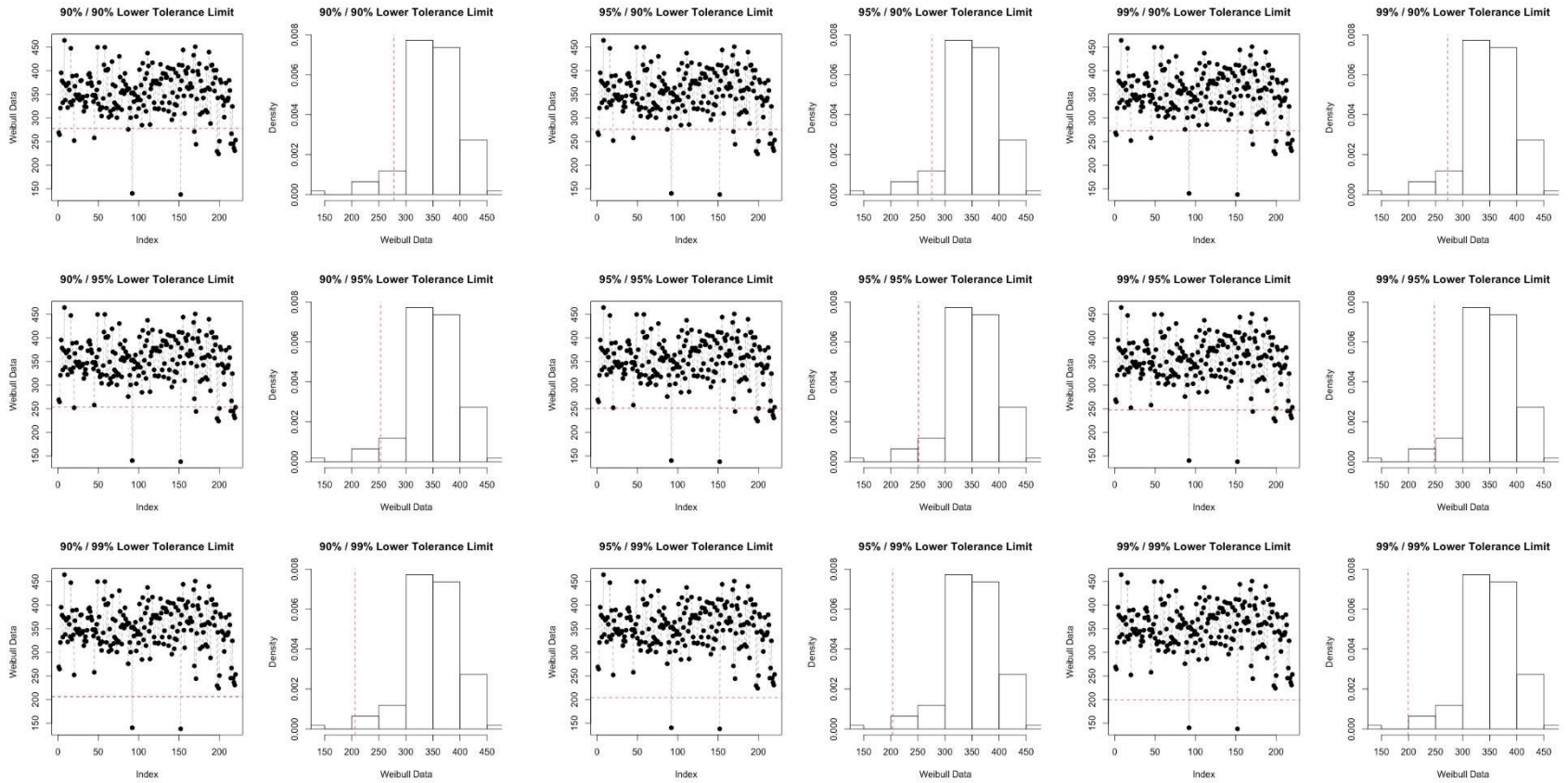


Figure 3.41 LTLs in Data Chart and Histogram of RMT Joints Made of Red Oak

LTLs values for *bending strength of RMT joints made of white oak* are given in Figure 3.42. Its data distribution and histogram corresponding to LTLs values are demonstrated in Figure 3.43. The ratio of LTL value, average bending moment capacity, and percentage of number of values below LTLs values are tabulated in Table 3.11. According to test results, LTLs values for the 0.90/0.90, 0.95/0.90, 0.99/0.90, 0.95/0.90, 0.95/0.95, 0.95/0.99, 0.99/0.90, 0.99/0.95, and 0.99/0.99  $\gamma/P$  levels are 256.53, 254.34, 250.09, 233.57, 231.06, 226.18, 190.27, 187.09, and 180.88 N.m, respectively.

As it can be seen in Figure 3.43 and Table 3.11, there is no violation for the ratio of number of values below LTL value in tolerance analysis of RMT joints made of white oak. Besides, only one value (151.39 N.m) is below LTL value for 0.99/0.99  $\gamma/P$  level. LTL value (180.88 N.m) for 0.99/0.99  $\gamma/P$  level is 53.02% of average bending moment capacity of RMT joints made of white oak.

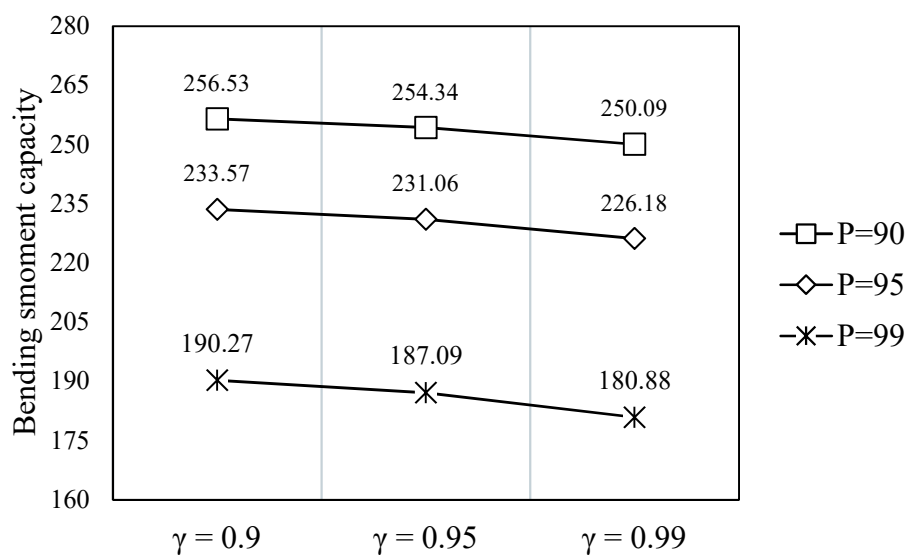


Figure 3.42 LTLs for RMT Joints Made of White Oak

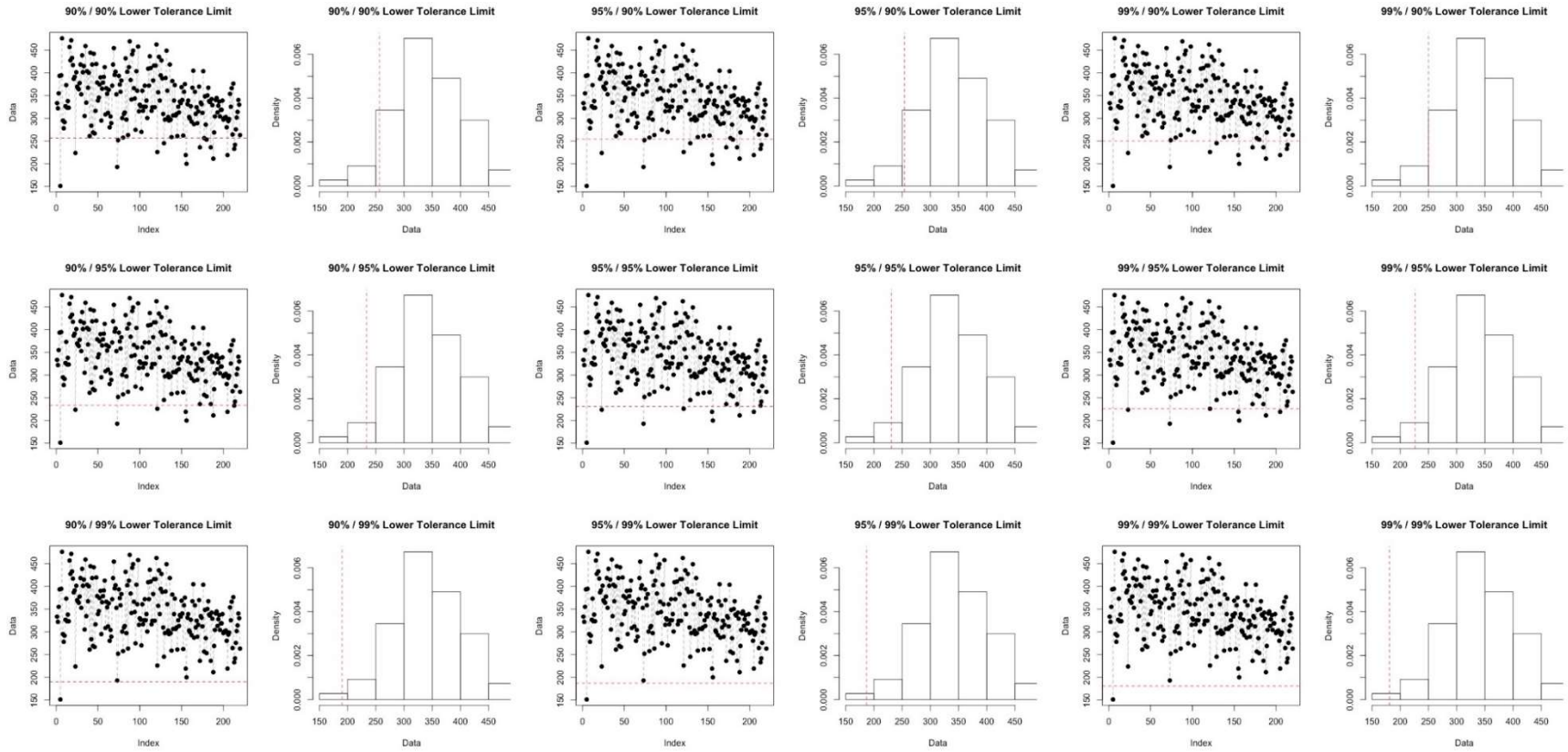


Figure 3.43 LTLs in Data Chart and Histogram of RMT Joints Made of White Oak

LTLs values for *bending strength of dowel joints made of red oak* are given in Figure 3.44, and its data distribution and histogram corresponding to LTLs values are shown in Figure 3.45. The ratio of LTL value and average bending moment capacity and percentage of number of values below LTLs Values are tabulated in Table 3.11. According to the test results, LTLs values for the 0.90/0.90, 0.95/0.90, 0.99/0.90, 0.95/0.90, 0.95/0.95, 0.95/0.99, 0.99/0.90, 0.99/0.95, and 0.99/0.99  $\gamma/P$  levels are 190.04, 188.86, 186.61, 173.42, 172.07, 172.07, 169.43, 140.89, 139.28, and 136.14 N.m, respectively.

As it can be seen in Figure 3.45 and Table 3.11, there is no violation for the ratio of number of values below LTL value in tolerance analysis of dowel joints made of red oak. There is also no value below LTL value for 0.99/0.99  $\gamma/P$  level. LTL value (136.14 N.m) for 0.99/0.99  $\gamma/P$  level is 56.53% of average bending moment capacity of dowel joints made of red oak.

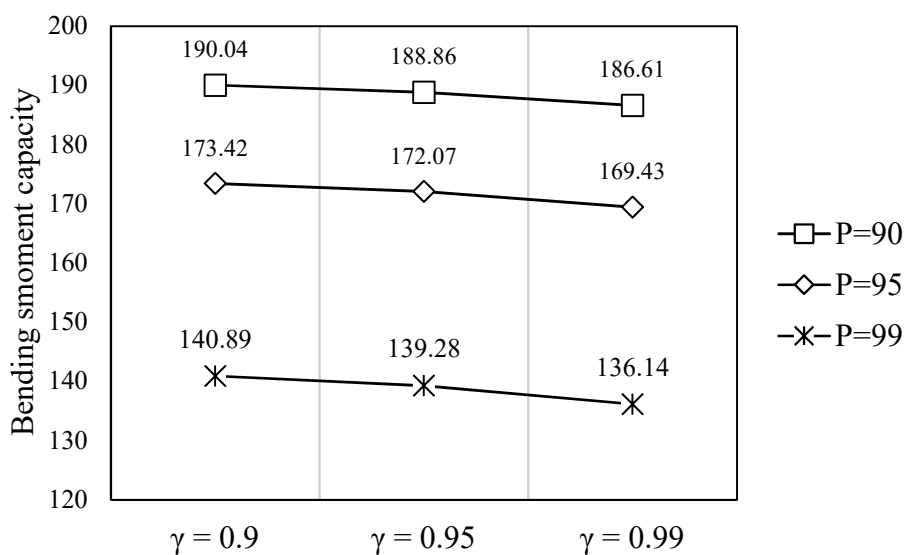


Figure 3.44 LTLs for Dowel Joints made of Red Oak

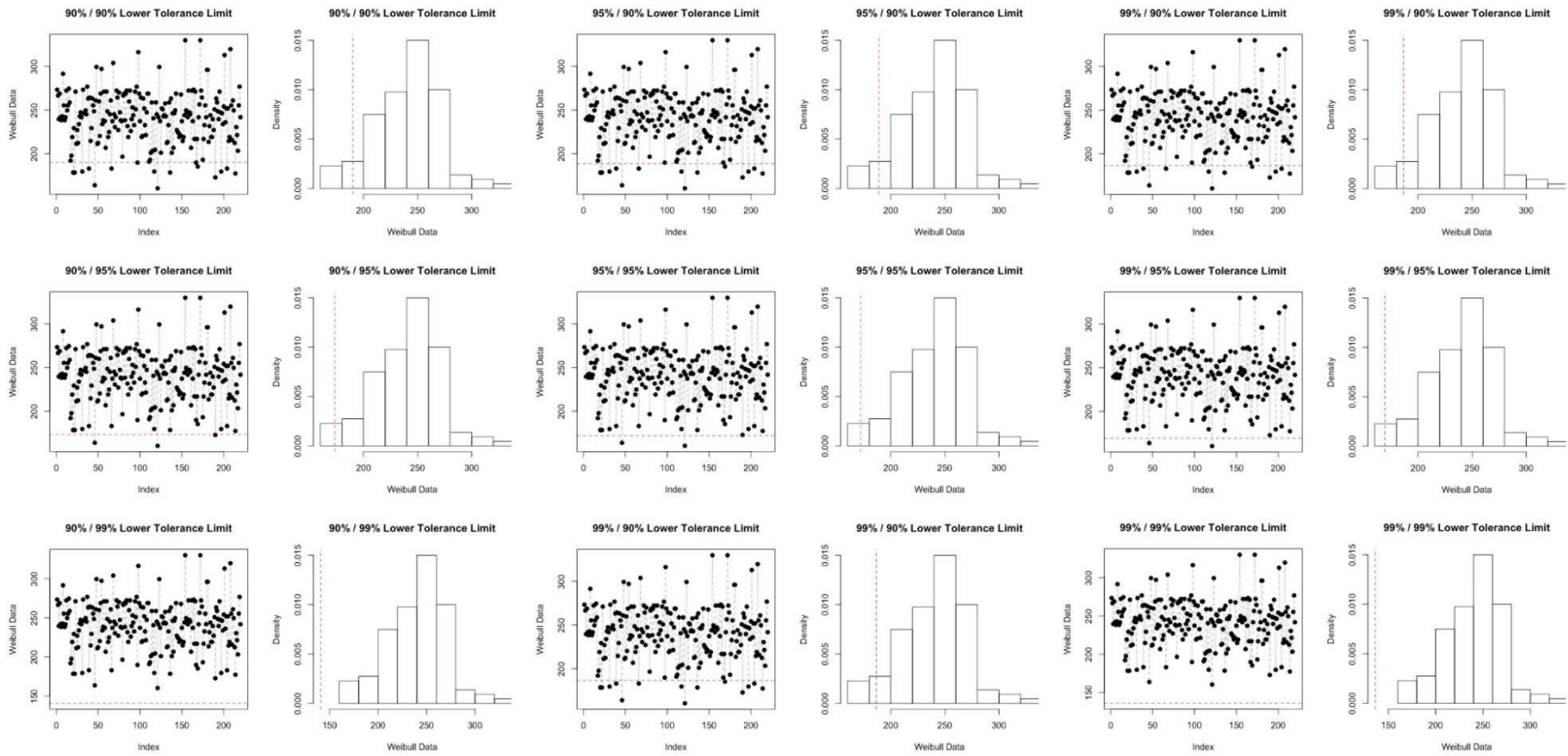


Figure 3.45 LTLs in Data Chart and Histogram of Dowel Joints Made of Red Oak

LTLs values for *bending strength of dowel joints made of white oak* are given in Figure 3.46, and its data distribution and histogram corresponding to LTLs values are depicted in Figure 3.47. The ratio of LTL value and average bending moment capacity and percentage of number of values below LTLs values are shown in Table 3.11. According to the test results, LTLs values for the 0.90/0.90, 0.95/0.90, 0.99/0.90, 0.95/0.90, 0.95/0.95, 0.95/0.99, 0.99/0.90, 0.99/0.95, and 0.99/0.99  $\gamma/P$  levels are 191.29, 189.95, 187.33, 177.15, 175.61, 172.59, 172.59, 150.47, 148.51, and 144.69 N.m, respectively.

As it can be seen in Figure 3.47 and Table 3.11, there is no violation for ratio of number of values below LTL value in tolerance analysis of dowel joints made of white oak. Also, there is no value below LTL value for 0.99/0.99  $\gamma/P$  level. LTL value (144.69 N.m) for 0.99/0.99  $\gamma/P$  level is 59.44% of average bending moment capacity of dowel joints made of red oak.

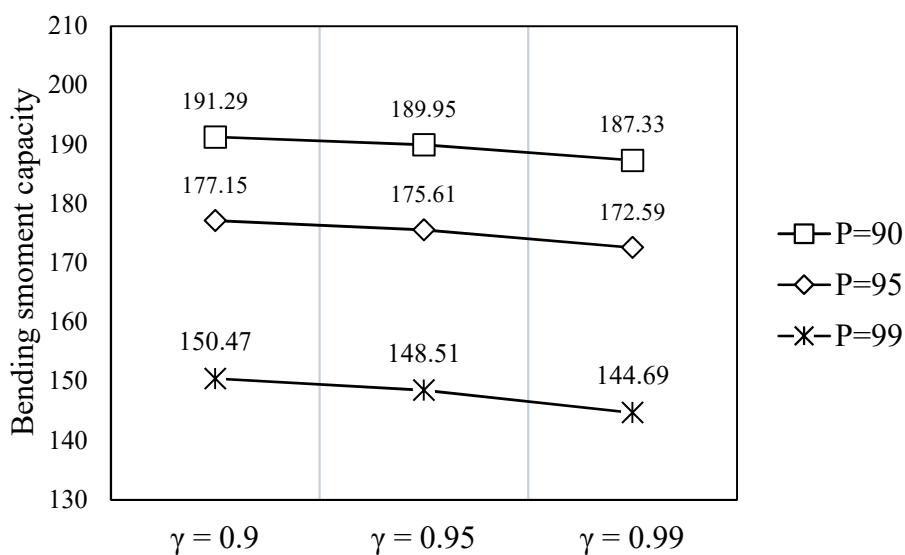


Figure 3.46 LTLs for Dowel Joints Made of White Oak

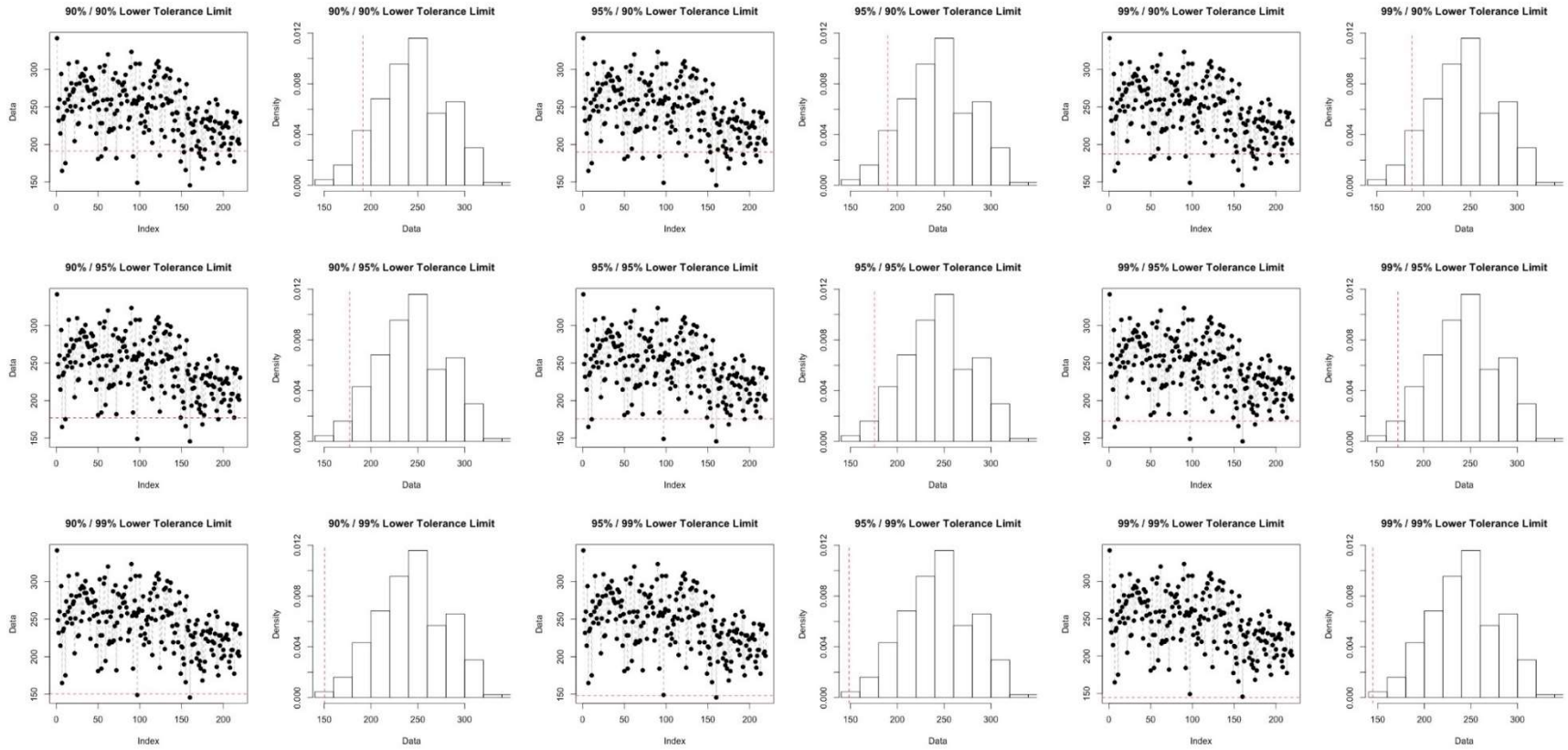


Figure 3.47 LTLs in Data Distribution of Dowel Joints Made of White Oak

Table 3.11 LTLs, Ratio of Mean and LTLs and, Number and Percentage of Values below LTLs Corresponding Confidence/Proportion Levels for RMT and Dowel Joints

Joint types	Wood Species	Mean (N.m)	P=0.90											
			$\gamma=0.90$				$\gamma=0.95$				$\gamma=0.99$			
			LTLs	LTLs/ Mean	No of values below LTL	% of values below LTLs	LTLs	LTLs/ Mean	No of values below LTL	% of values below LTLs	LTLs	LTLs/ Mean	No of values below LTL	% of values below LTLs
RMT	RO	350.56	277.6	79.19%	18	8.18%	275.89	78.70%	18	8.18%	272.61	77.76%	17	7.73%
	WO	341.17	256.53	75.19%	16	7.27%	254.34	74.55%	15	6.82%	250.09	73.30%	13	5.91%
Dowel	RO	240.81	190.04	78.92%	16	7.27%	188.86	78.43%	14	6.36%	186.61	77.49%	14	6.36%
	WO	243.44	191.29	78.58%	20	9.09%	189.95	78.03%	20	9.09%	187.33	76.95%	18	8.18%
			P=0.95											
			$\gamma=0.90$				$\gamma=0.95$				$\gamma=0.99$			
RMT	RO	350.56	253.39	72.28%	12	5.45%	251.42	71.72%	10	4.55%	247.58	70.62%	9	4.09%
	WO	341.17	233.57	68.46%	9	4.09%	231.06	67.73%	8	3.64%	226.18	66.30%	8	3.64%
Dowel	RO	240.81	173.42	72.02%	3	1.36%	172.07	71.45%	2	0.91%	169.43	70.36%	2	0.91%
	WO	243.44	177.15	72.77%	7	3.18%	175.61	72.14%	7	3.18%	172.59	70.90%	5	2.27%
			P=0.99											
			$\gamma=0.90$				$\gamma=0.95$				$\gamma=0.99$			
RMT	RO	350.56	205.98	58.76%	2	0.91%	203.63	58.09%	2	0.91%	199.04	56.78%	2	0.91%
	WO	341.17	190.27	55.77%	1	0.45%	187.09	54.84%	1	0.45%	180.88	53.02%	1	0.45%
Dowel	RO	240.81	140.89	58.51%	0	0.00%	139.28	57.84%	0	0.00%	136.14	56.53%	0	0.00%
	WO	243.44	150.47	61.81%	2	0.91%	148.51	61.00%	1	0.45%	144.69	59.44%	0	0.00%

LTLs values for *screw withdrawal strength in wood made of red oak from end-grain* are given in Figure 3.48, and its data distribution and histogram corresponding to LTLs values are shown in Figure 3.49. The ratio of LTL value and average bending moment capacity and percentage of number of values below LTLs values are demonstrated in Table 3.12. According to the test results, LTLs values for the 0.90/0.90, 0.95/0.90, 0.99/0.90, 0.95/0.90, 0.95/0.95, 0.95/0.99, 0.99/0.90, 0.99/0.95 and 0.99/0.99  $\gamma/P$  levels are 4492.74, 4459.45, 4394.83, 4143.43, 4105.26, 4030.94, 3484.59, 3436.24 and 3341.85 N, respectively.

As it can be seen in Figure 3.49 and Table 3.12, there is no violation for ratio of number of values below LTL value in tolerance analysis of screw withdrawal strength in wood made of red oak from end-grain. Also, there is no value below LTL value for 0.99/0.99  $\gamma/P$  level. LTL value (3341.85 N) for 0.99/0.99  $\gamma/P$  level is 57.81% of average screw withdrawal strength in wood made of red oak from end-grain.

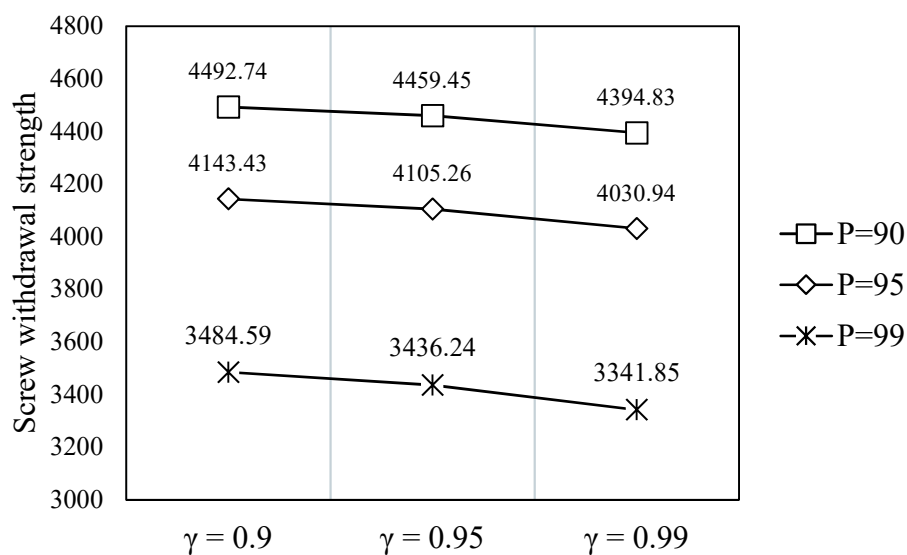


Figure 3.48 LTLs for Screw Withdrawal Strength in Wood Made of Red Oak from End-Grain

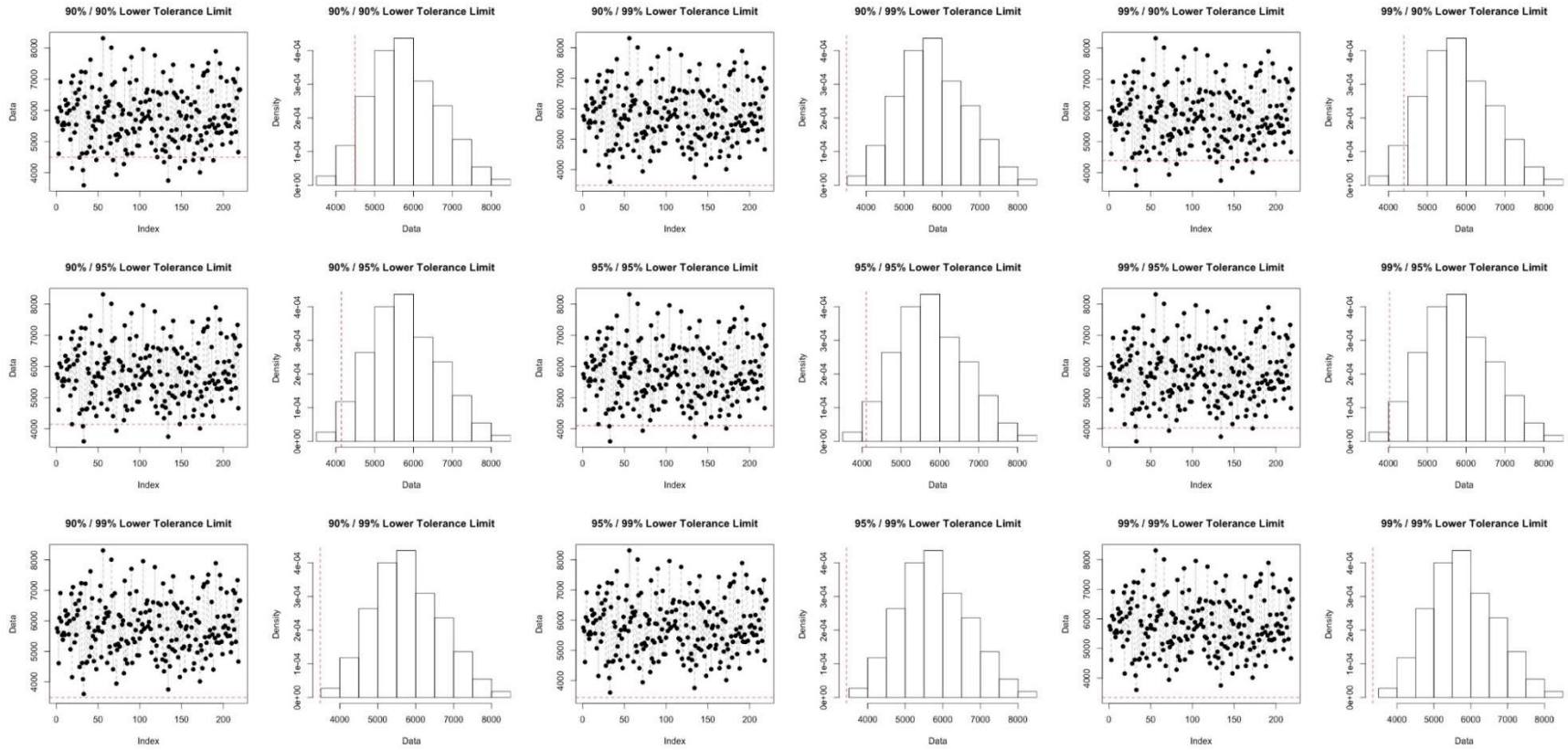


Figure 3.49 LTLs in Data Chart and Histogram of Screw Withdrawal Strength in Wood Made of Red Oak from End-Grain

LTLs values for *screw withdrawal strength of white oak from end-grain* are given in Figure 3.50, and its data distribution and histogram corresponding to LTLs values are shown in Figure 3.51. The ratio of LTL value and average bending moment capacity and percentage of number of values below LTLs values are tabulated in Table 3.12. According to the test results, LTLs values for the 0.90/0.90, 0.95/0.90, 0.99/0.90, 0.95/0.90, 0.95/0.95, 0.95/0.99, 0.99/0.90, 0.99/0.95 and 0.99/0.99  $\gamma/P$  levels are 4932.01, 4896.89, 4828.68, 4563.38, 4523.09, 4444.66, 3868.08, 3817.06 and 3717.44 N, respectively.

As it can be seen in Figure 3.51 and Table 3.12, there is no violation for ratio of number of values below LTL value in tolerance analysis screw withdrawal strength in wood made of white oak from end-grain. There are only two values (3611.96 and 3282.89 N) below LTL value for 0.99/0.99  $\gamma/P$  level. LTL value (3717.44 N) for 0.99/0.99  $\gamma/P$  level is 59.09% of average screw withdrawal strength in wood made of white oak from end-grain.

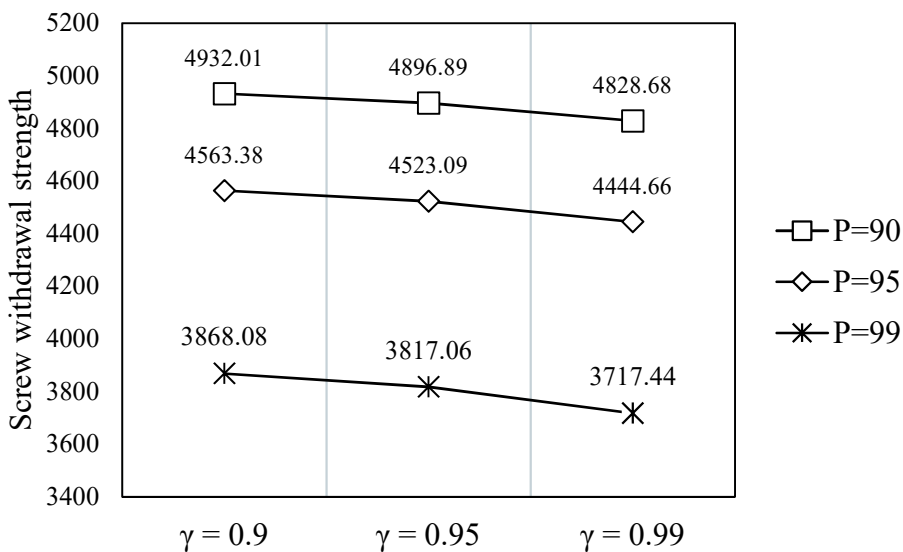


Figure 3.50 LTLs for Screw Withdrawal Strength in Wood Made of White Oak from End-Grain

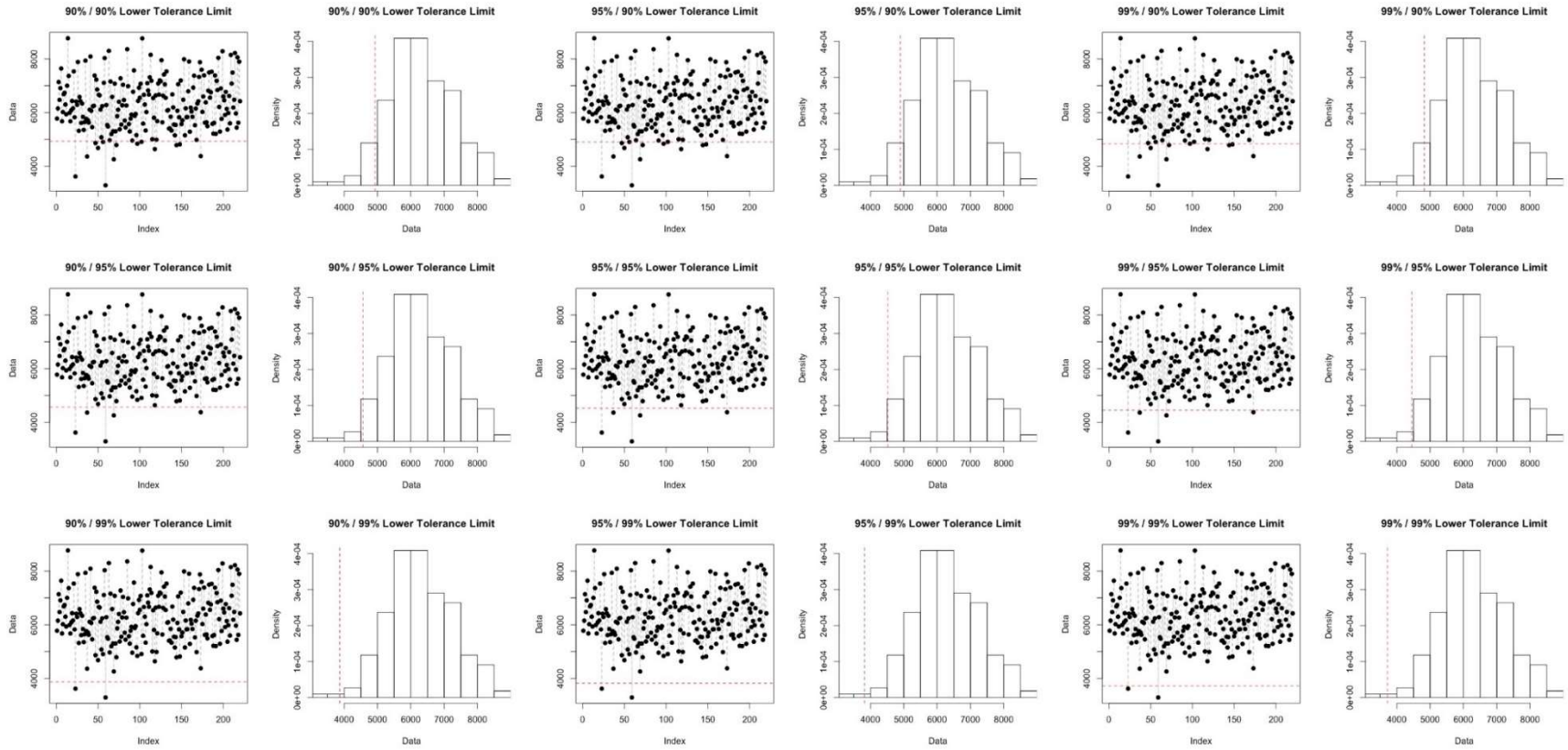


Figure 3.51 LTLs in Data Chart and Histogram of Screw Withdrawal Strength in Wood Made of White Oak from End-Grain

LTLs values for *screw withdrawal strength in red oak from edge-grain* are given in Figure 3.52. Its data distribution and histogram corresponding to LTLs values are demonstrated in Figure 3.53 and the ratio of LTL value, average bending moment capacity, percentage of number of values below LTLs values are shown in Table 3.12. According to test results, LTLs values for the 0.90/0.90, 0.95/0.90, 0.99/0.90, 0.95/0.90, 0.95/0.95, 0.95/0.99, 0.99/0.90, 0.99/0.95 and 0.99/0.99  $\gamma/P$  levels are 5537.01, 5507.33, 5450.14, 5233.29, 5201.14, 5139.08, 4705.06, 4668.47 and 4597.84 N, respectively.

As it can be seen in Figure 3.53 and in Table 3.12, there is no violation for ratio of number of values below LTL value in tolerance analysis of screw withdrawal strength in wood made of red oak from edge-grain. Also, there is no value below LTL value for 0.99/0.99  $\gamma/P$  level. LTL value (4597.84 N) for 0.99/0.99  $\gamma/P$  level is 66.71% of average screw withdrawal strength in wood made of red oak from edge-grain.

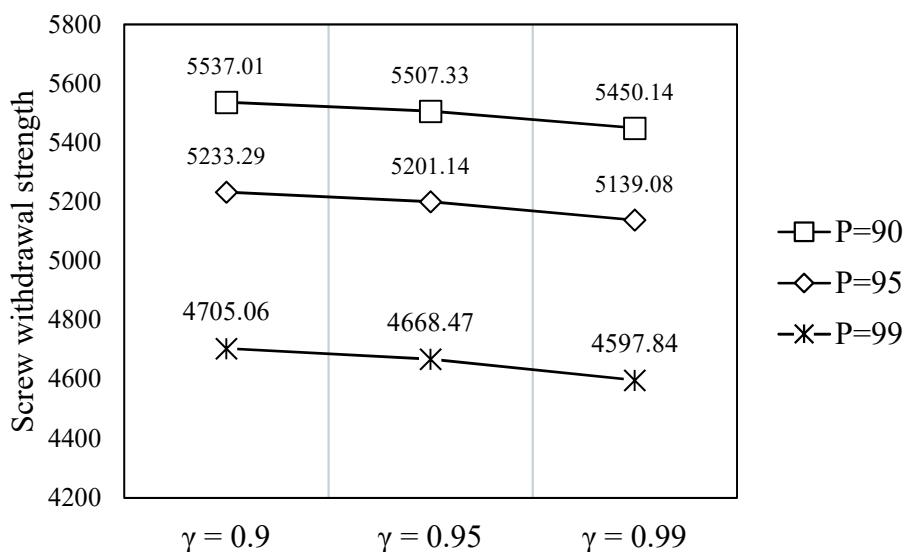


Figure 3.52 LTLs for Screw Withdrawal Strength in Wood Made of Red Oak from Edge-Grain

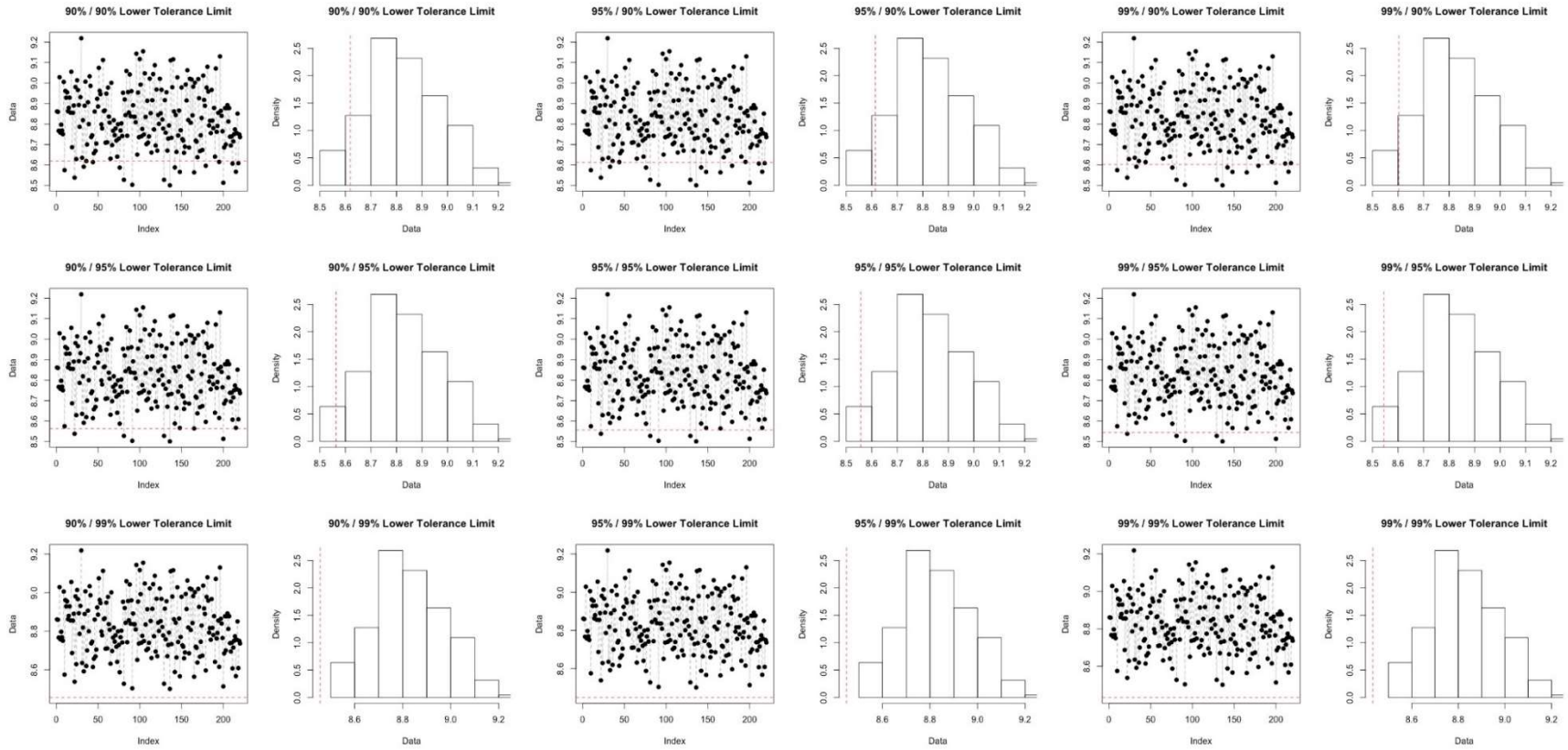


Figure 3.53 LTLs in Data Chart and Histogram of Screw Withdrawal Strength in Wood Made of Red Oak from Edge-Grain

LTLs values for screw withdrawal strength in wood made of white oak from edge-grain are shown in Figure 3.54, and its data distribution and histogram corresponding to LTLs values are depicted in Figure 3.55. The ratio of LTL value and average bending moment capacity and percentage of number of values below LTLs values are tabulated in Table 3.12. According to the test results, LTLs values for the 0.90/0.90, 0.95/0.90, 0.99/0.90, 0.95/0.90, 0.95/0.95, 0.95/0.99, 0.99/0.90, 0.99/0.95, and 0.99/0.99  $\gamma/P$  levels are 5828.11, 5784.34, 5697.41, 5359.28, 5307.94, 5207.98, 4473.13, 4408.11, and 4281.15 N, respectively.

As can be seen in Figure 3.55 and Table 3.12, there is no violation for ratio of number of values below LTL value in tolerance analysis of screw withdrawal strength in wood made of white oak from edge-grain. There is also no value below LTL value for 0.99/0.99  $\gamma/P$  level. LTL value (4281.15 N) for 0.99/0.99  $\gamma/P$  level is 56.62% of average screw withdrawal strength in wood made of white oak from edge-grain.

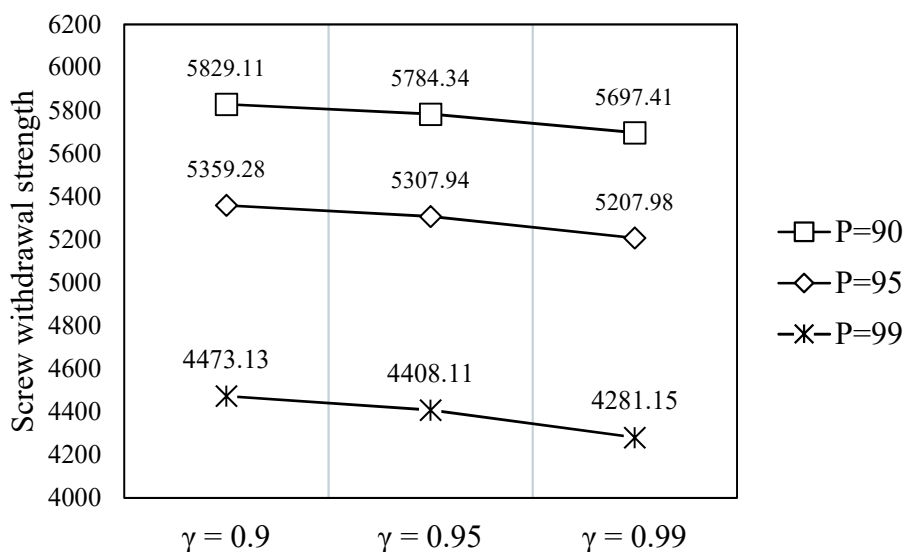


Figure 3.54 LTLs for Screw Withdrawal Strength in Wood Made of White Oak from Edge-Grain

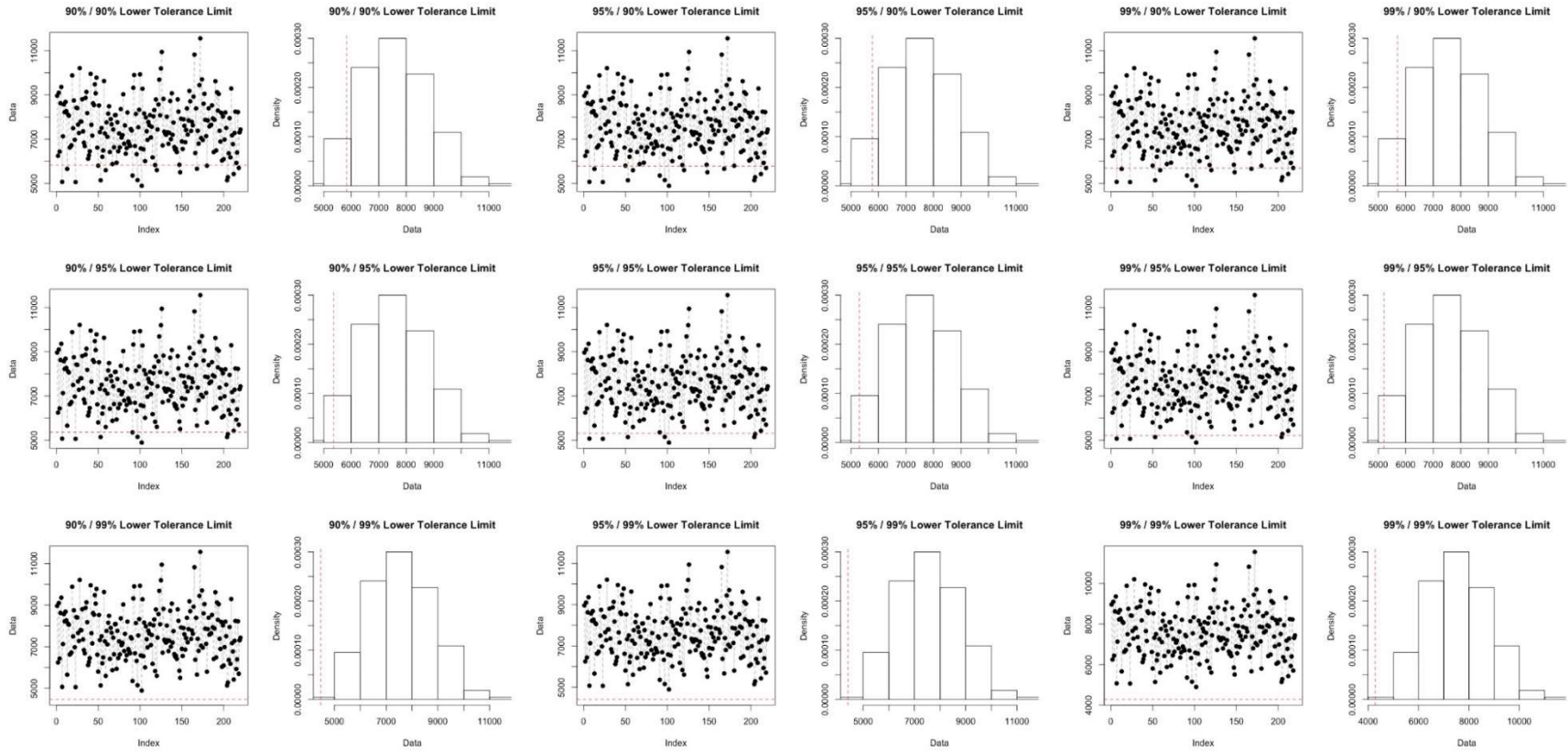


Figure 3.55 LTLs in Data Chart and Histogram of Screw Withdrawal Strength in Wood Made of White Oak from Edge-Grain

LTLs values for screw withdrawal strength in wood made of red oak from face-grain are given in Figure 3.56. Its data distribution and histogram corresponding to LTLs values are demonstrated in Figure 3.57, and the ratio of LTL value and average bending moment capacity and percentage of number of values below LTLs values are shown in Table 3.12. According to test results, LTLs values for the 0.90/0.90, 0.95/0.90, 0.99/0.90, 0.95/0.90, 0.95/0.95, 0.95/0.99, 0.99/0.90, 0.99/0.95, and 0.99/0.99  $\gamma/P$  levels are 5132.54, 5098.61, 5032.73, 4776.44, 4737.53, 4661.76, 4104.79, 4055.51, and 3959.28 N, respectively.

As can be seen in Figure 3.57 and in Table 3.12, there is no violation for ratio of number of values below LTL value in tolerance analysis of screw withdrawal strength in wood made of red oak from face-grain. There is also no value below LTL value for 0.99/0.99  $\gamma/P$  level. LTL value (3959.28 N) for 0.99/0.99  $\gamma/P$  level is 61.43% of average screw withdrawal strength in wood made of red oak from face-grain.

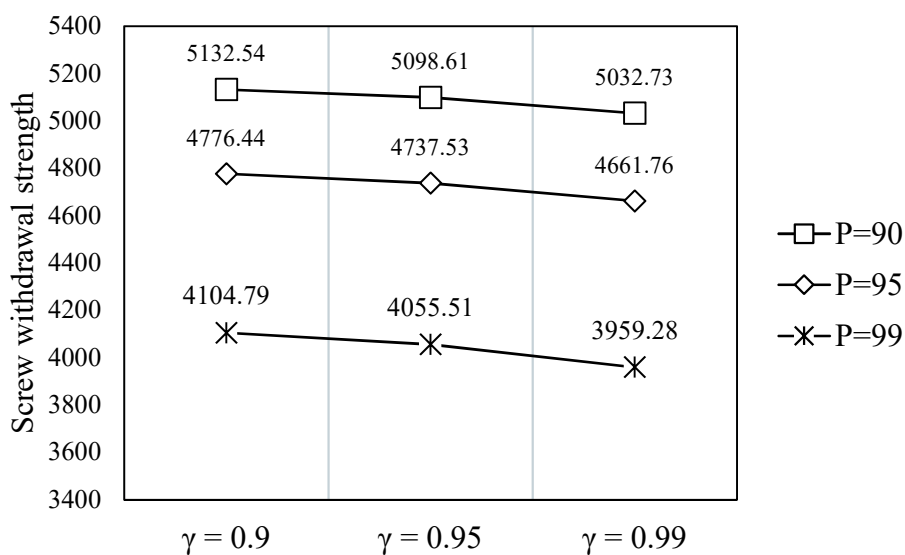


Figure 3.56 LTLs for Screw Withdrawal Strength in Wood Made of Red Oak from Face-Grain

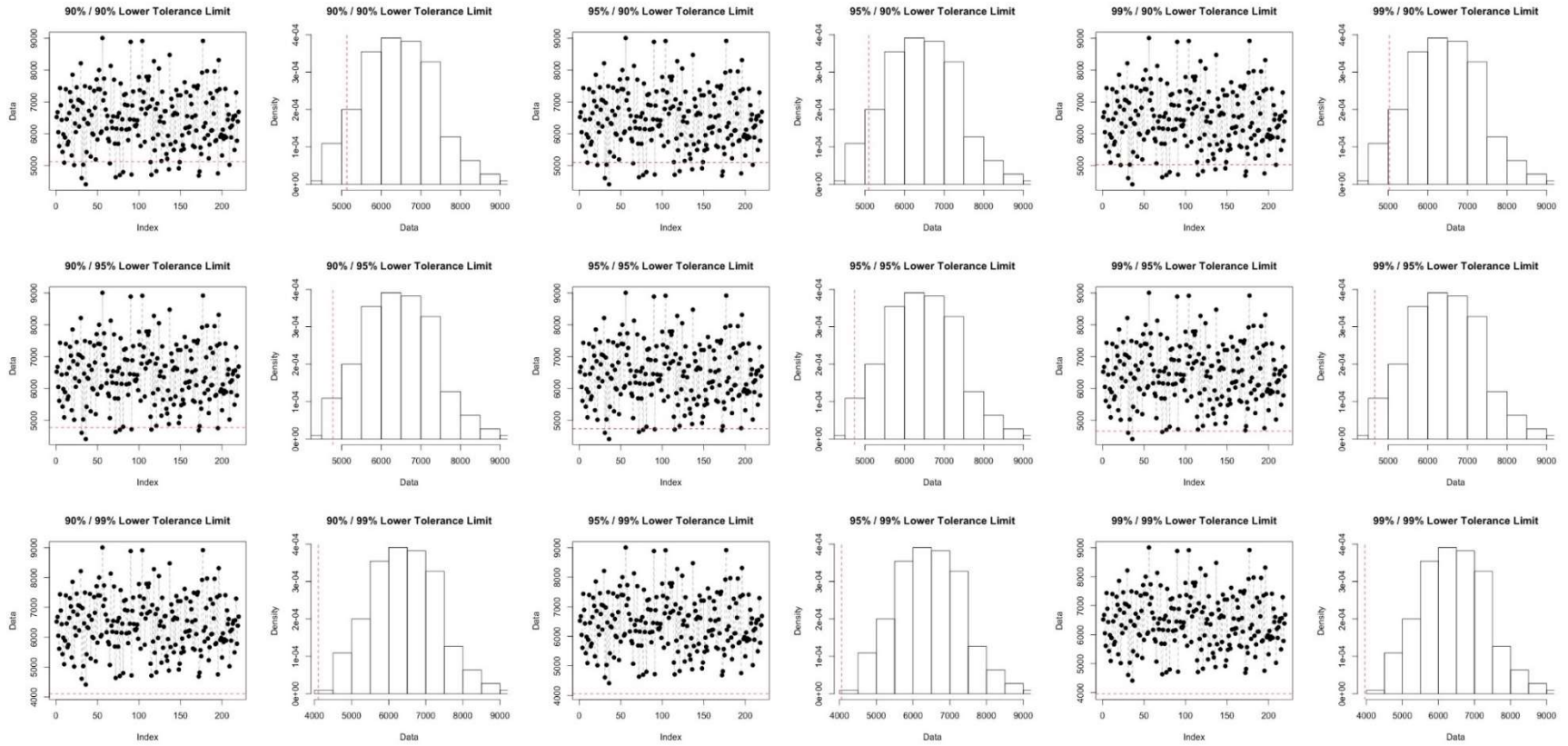


Figure 3.57 LTLs in Data Chart and Histogram of Screw Withdrawal Strength in Wood Made of Red Oak from Face-Grain

LTLs values for screw withdrawal strength in wood made of white oak from face-grain are given in Figure 3.58. Its data distribution and histogram corresponding to LTLs values are shown in Figure 3.59, and the ratio of LTL value and average bending moment capacity and percentage of number of values below LTLs values are shown in Table 3.12. According to test results, LTLs values for the 0.90/0.90, 0.95/0.90, 0.99/0.90, 0.95/0.90, 0.95/0.95, 0.95/0.99, 0.99/0.90, 0.99/0.95, and 0.99/0.99  $\gamma/P$  levels are 5341.09, 5313.11, 5259.17, 5054.52, 5024.17, 4965.55, 4555.19, 4520.56, and 4453.69 N, respectively.

As can be seen in Figure 3.59 and in Table 3.12, there is no violation for ratio of number of values below LTL value in tolerance analysis of screw withdrawal strength in wood made of white oak from face-grain. There is only one value (4163.54 N) below LTL value for 0.99/0.99  $\gamma/P$  level. LTL value (4453.69 N) for 0.99/0.99  $\gamma/P$  level is 67.34% of average screw withdrawal strength of wood made in white oak from face-grain.

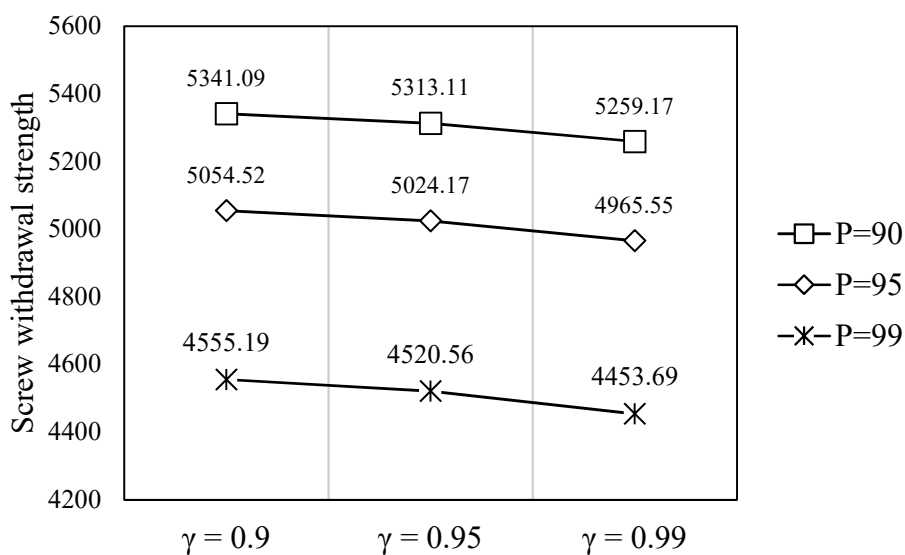


Figure 3.58 LTLs for Screw Withdrawal strength in Wood Made of White Oak from Face-Grain

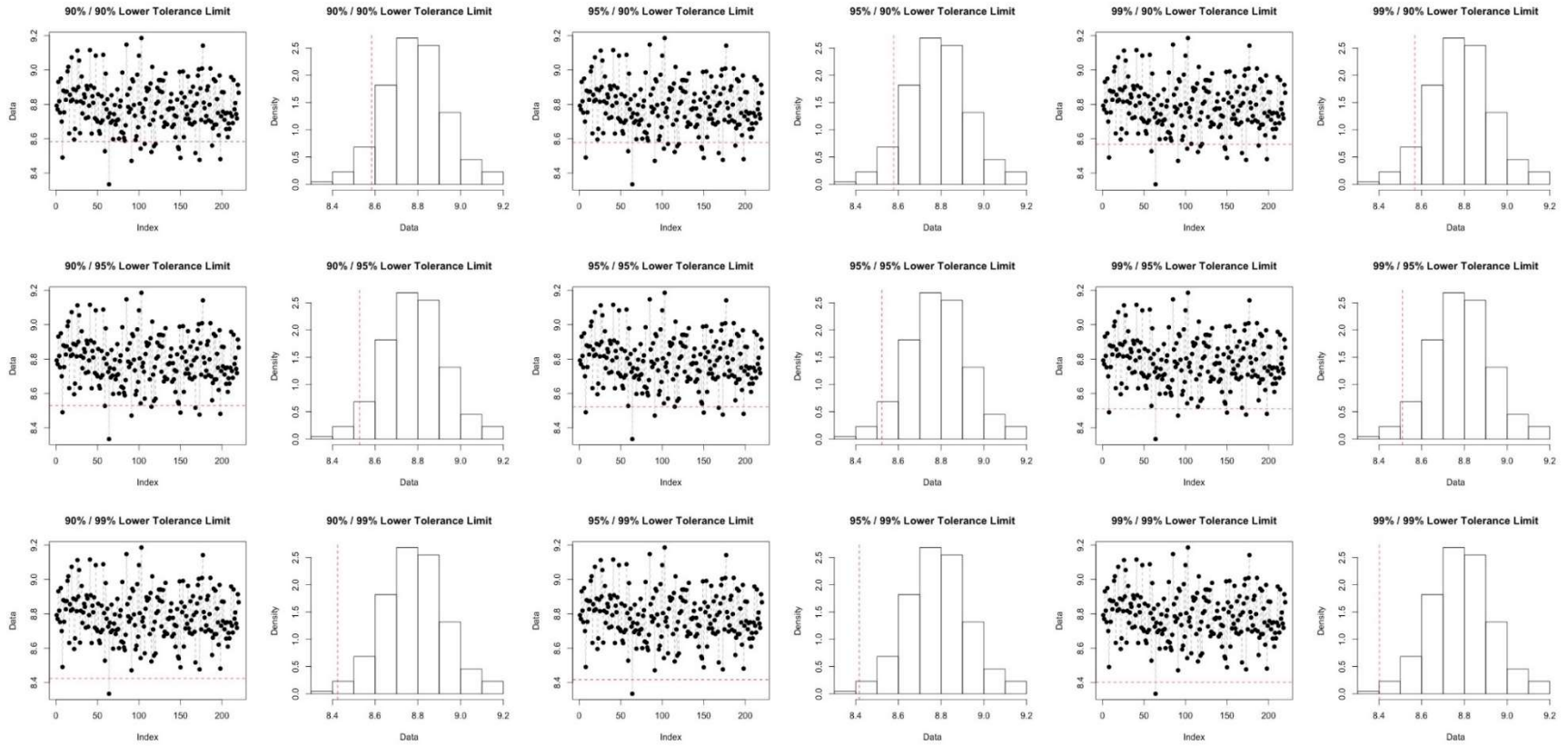


Figure 3.59 LTLs in Data Chart and Histogram of Screw Withdrawal Strength in Wood Made of White Oak from Face-Grain

Table 3.12 LTLs, Ratio of Mean and LTLs and, Number and Percentage of Values below LTLs Corresponding Confidence/Proportion Levels for Screw Withdrawal Strength in Wood

Screw Orientation	Wood Species	Mean (N)	P=0.90											
			$\gamma=0.90$				$\gamma=0.95$				$\gamma=0.99$			
			LTLs	LTLs/ Mean	No of values below LTL	% of values below LTLs	LTLs	LTLs/ Mean	No of values below LTL	% of values below LTLs	LTLs	LTLs/ Mean	No of values below LTL	% of values below LTLs
End	RO	5780.51	4492.74	77.72%	16	7.27%	4459.45	77.15%	15	6.82%	4394.83	76.03%	10	4.55%
	WO	6291.04	4932.01	78.40%	14	6.36%	4896.89	77.84%	12	5.45%	4828.68	76.75%	10	4.55%
Edge	RO	6892.14	5537.01	80.34%	18	8.18%	5507.33	79.91%	16	7.27%	5450.14	79.08%	14	6.36%
	WO	7561.17	5829.11	77.09%	17	7.73%	5784.34	76.50%	15	6.82%	5697.41	75.35%	14	6.36%
Face	RO	6445.35	5132.54	79.63%	20	9.09%	5098.61	79.11%	18	8.18%	5032.73	78.08%	16	7.27%
	WO	6614.08	5341.09	80.75%	16	7.27%	5313.11	80.33%	16	7.27%	5259.17	79.51%	14	6.36%
			P=0.95											
			$\gamma=0.90$				$\gamma=0.95$				$\gamma=0.99$			
End	RO	5780.51	4143.43	71.68%	5	2.27%	4105.26	71.02%	5	2.27%	4030.94	69.73%	4	1.82%
	WO	6291.04	4563.38	72.54%	5	2.27%	4523.09	71.90%	5	2.27%	4444.66	70.65%	5	2.27%
Edge	RO	6892.14	5233.29	75.93%	6	2.73%	5201.14	75.46%	6	2.73%	5139.08	74.56%	6	2.73%
	WO	7561.17	5359.28	70.88%	8	3.64%	5307.94	70.20%	7	3.18%	5207.98	68.88%	6	2.73%
Face	RO	6445.35	4776.44	74.11%	8	3.64%	4737.53	73.50%	7	3.18%	4661.76	72.33%	3	1.36%
	WO	6614.08	5054.52	76.42%	9	4.09%	5024.17	75.96%	7	3.18%	4965.55	75.08%	6	2.73%
			P=0.99											
			$\gamma=0.90$				$\gamma=0.95$				$\gamma=0.99$			
End	RO	5780.51	3484.59	60.28%	0	0.00%	3436.24	59.45%	0	0.00%	3341.85	57.81%	0	0.00%
	WO	6291.04	3868.08	61.49%	2	0.91%	3817.06	60.67%	2	0.91%	3717.44	59.09%	2	0.91%
Edge	RO	6892.14	4705.06	68.27%	0	0.00%	4668.47	67.74%	0	0.00%	4597.84	66.71%	0	0.00%
	WO	7561.17	4473.13	59.16%	0	0.00%	4408.11	58.30%	0	0.00%	4281.15	56.62%	0	0.00%

Table 3.13 continued LTLs, Ratio of Mean and LTLs and, Number and Percentage of Values below LTLs Corresponding  
Confidence/Proportion Levels for Screw Withdrawal Strength in Wood

<b>Face</b>	<b>RO</b>	6445.35	4104.79	63.69%	0	0.00%	4055.51	62.92%	0	0.00%	3959.28	61.43%	0	0.00%
	<b>WO</b>	6614.08	4555.19	68.87%	1	0.45%	4520.56	68.35%	1	0.45%	4453.69	67.34%	1	0.45%

The given LTLs values are used as reasonable design values for furniture joints. If these values should not exceed wood strength in joints after furniture is subjected to loading, failure probability can be reduced as much as the confidence/proportional levels that are used. In here, designers' expertise or company strategy will be critical to choose what level of confidence/proportion is used to construct design value of furniture joints. In literature review, 0.95/0.95 levels are generally selected because significance level is most likely 0.05 as hypothesis of test for experiments. However, there is no objection to use lower or higher confidence/proportion levels in the LTLs study. The following are suggested to use as confidence/proportional levels [155]:

1. If a lower tolerance limits is  $L_1$ , the desired area of probability is above  $L_1$  which is  $P=1-f(L_1)$ .  $f(L_1)$  is cumulative density function (CDF) of distribution.
2. Possible range for probability (proportion) is  $0 < (1-P) < \delta$ .  $\delta$  is relative content error and is usually selected 0.1, 0.05 and 0.01. Therefore,  $P$  is usually constructed as 0.90, 0.95 or 0.99.
3. The absolute range for confidence level is  $0 < 1-\alpha < 1$ . However, it is typically used as  $0.80 < 1-\alpha < 1$ . Therefore, one of the values for confidence level is usually 0.80, 0.90, 0.95 or 0.99.

In this study, confidence/proportion levels were chosen based on judgement on use of significance levels in academic studies in engineering and to obtain higher reliable design values. Therefore, one of the values for 0.90, 0.95 and 0.99 was used in the study.

The minimum sample size requirements for the tolerance interval were determined with modified Faulkenberry-Weeks method developed, although several sampling methods were defined in literature review. This method is easy to apply for sample size determination for tolerance intervals because practitioner(s) can choose their  $\delta$  and  $P'$  levels depending on how critical of studies are being addressed. There is only a small probability that a large proportion of sampled population falls within tolerance interval, so it was guaranteed that tolerance interval is not wider. If tolerance interval is wider, there could be too much variation in the population. Another factor is that sample size determination

depends on what  $\delta$  and  $P'$  levels are defined as. Therefore, if small sample sizes would like to be specified in a study then  $\delta$  and  $P'$  levels can be changed. However, sample sizes were constructed corresponding to confidence/proportion levels. Test results dictated what minimum sample size requirements were used. When confidence/proportion levels increase, tolerance interval requires larger sample sizes because both the level of proportion covered in sampled population and sample error in sampled data increase. Hence, the tolerance analysis required larger sample sizes. The proportion level ( $P$ ) pertained to population and is essentially acting like a parameter that reflects both sample error and sampling variance in population. On the other hand, the confidence level is reflecting only sampling error. Therefore, it will usually be the case that the sampling variability will cause the tolerance limits to grow faster in terms of the proportion level relative to confidence level. Thus, larger sample sizes are needed in increasing proportion level relative to confidence level.

Within the quality-control field, several ways are defined to construct such limits; namely, Six-sigma rule, confidence interval, and prediction interval. Six-sigma rule is the most significant and conservative method in manufacturing, which is developed by Bill Smith in the Motorola company. However, the tolerance intervals were selected to estimate reasonable design values of furniture joints. Six-sigma is considered extreme in the process that falls into specification limits and usually applied to Gaussian (normal) distribution. Another factor is that six-sigma rule aims to be set for process by company strategy, so it is an intended result. On the other hand, tolerance intervals have more specific interpretation and are calculated differently depending on the underlying distribution as covering a specific proportion of population. Tolerance intervals can be wider or narrower depending on the sample variation in data. Besides, confidence intervals rely on sampling error while tolerance intervals take into consideration both sampling error and the variance in population. When sample sizes approach the entire population, confidence interval is close to zero. On the other hand, sample error declines and estimated percentiles in tolerance interval approach the true population percentiles in tolerance intervals. Therefore, tolerance interval should be used if we have sampled data and would like to predict future outcomes.

In Table 3.12 and 3.13, LTLs values are given for bending strength of RMT and dowel joints, as well as screw withdrawal strength in wood from end-, edge- and face-grain. The question is how these LTLs values are used as a design value for furniture joints in design process of furniture. The given LTL values are given in bending moment and withdrawal force, which are both expressed as internal forces in structural analysis. Therefore, they pertain to member and joints sizes, wood species, and test set-up. Use of these LTLs values as an internal value may drive us the wrong way to design joints. For example, a designer would like to use screws in structure made of red oak and consider withdrawal strength from end-grain. In here, s/he will use LTLs for 0.95/0.95 (4105.26 N) and 0.99/0.99 (3341.85 N) confidence/proportion levels based on the experiment in this study. If s/he designs screws as using rational design of screws given in Table 2.7, internal force and screw dimensions are directly proportional to each other. Therefore, screw size would be larger according to calculation based on 0.95/0.95 confidence/proportional level compared to those of 0.99/0.99. Logically, screw dimension should be larger for higher reliable design values. In LTLs method in this study, the aim was not to exceed design value, so failure probability of joints can be reduced. Therefore, it is suggested to use internal stresses that are pertaining to wood species.

### 3.4 Conclusion

In this study, reasonable design values for selected furniture joints; namely, rectangular mortise and tenon, two-pin moment resisting dowel joints, and screw withdrawal strength in wood were predicted by using the lower tolerance limits (LTLs) methods. LTLs method is a probabilistic approach, pertaining to both sample error and variance in the population, and is used for the measurements of reliability and safety of products. Therefore, LTLs value given for  $\gamma/P$  level is accepted as a design value for joint strength and screw withdrawal strength.

In the tolerance analysis, normality assumption, randomness, and homogeneity in experiment are vital because its method may vary depending on violation of any assumption, randomness, and/or homogeneity. Therefore, all three assumptions were taken into consideration to make a reliable tolerance analysis in this study.

Firstly, minimum sample sizes requirements were determined by using a modified Faulkenberry-Weeks method. Previously sampled data was used as reference data to calculate sample sizes corresponding to confidence/proportional level. In reference data, 30 specimens were used to assume that data is normally distributed in each sample group according to CLT. Shapiro-Wilks normality test was conducted to check normality of the data-set and it was not observed that there was no normality violation in any sample group. However, in conducting power testing, 30 sample sizes were not enough to complete the test for RMT joints made of white oak (64%). Therefore, sample size increased to 40 for this sample group and any violation was discarded to make a reliable analysis. According to the minimum ample size requirements test, sample sizes varied from 9 to 216 for corresponding confidence/proportion levels. Therefore, the minimum sample size requirement for 0.99/0.99 confidence/proportion level was considered to ensure consistency in analysis for all confidence/proportion levels. Therefore, 220 specimens were constructed for each sample group to determine their LTLs values.

Sample sizes were increased based on considering randomness and homogeneity in the experiment if needed. After all tests were conducted, data was analyzed for each sample group whether it was normally distributed or not. If not, logarithmic normalizing transformation and Weibull distribution were used to calculate LTLs. In the study, six sample groups were normally distributed while normalizing transformation were used for two sample groups and data for two sample groups were fitted to Weibull distribution. After all of these considerations, LTL values were calculated for 9 different confidence/proportion levels by using one of the values from 0.90, 0.95, and 0.99. It was observed that LTLs values decrease more with an increase in proportion level relative to confidence level. Since proportion level pertains to sampling error and variance, it acts as a population parameter. Therefore, it is more effective to use LTLs than confidence level.

These LTL values are used as reasonable design values for furniture joints. If the LTL values are not exceeded after furniture is subjected to load, failure probability can be reduced depending on what confidence/proportion level is used. Confidence/proportion levels can be selected based on designers' judgement or company's manufacturing strategy.

If a company would like to produce low reliable but cheap furniture, they may use a lower confidence/proportional level such as a 0.90/0.90 level – which means that less than 10% of future products will lie beyond the LTLs value. Otherwise, 0.99/0.99 can be used to produce high reliable and durable furniture so, less than 1% of future products will lie beyond this level according to test results.

Further investigations are needed to prove the validity of design values obtained from LTLs method. For this purpose, how to design furniture joints by using LTLs values and performance testing of chairs constructed with these designed joints will be discussed in the following chapters.

## CHAPTER 4. DESIGN OF FURNITURE JOINTS

### 4.1 Introduction

The design of joints in furniture structures is the last but the most important step in furniture engineering design. If a joint is too weak, it does not matter how strong members in the structure are and the furniture itself will fail.

Rational design of furniture frames dictates that strength of the members and its joints are known, so that both can be designed to resist the internal forces imposed on them in service. Considerable information concerning joints is discussed in “Section 2.2 Joint Properties.” These studies indicated joint strength and provided a predictive equation for joint strength based on joint dimension, wood species, and adhesive type used. However, many of these results rely on point estimation (mean and standard deviation) which does not ensure reliability of a product. On the other hand, estimation of joint strength could be based on interval estimation, including tolerance interval (limits), and may ensure reliability of the product design. Therefore, lower tolerance limits can provide design values for furniture joints so that joints in furniture can be designed corresponding to the external applied loads.

In this chapter, the main objective is to determine joint dimensions based on design values estimated by LTLs method.

### 4.2 Materials and Method

#### 4.2.1 Structural Analysis of Chair Frame

A chair frame made of red oak wood species, obtained from an industry cooperator, was used to make the prototype in Figure 4.1. To simplify the structural analysis of this prototype in MATLAB using displacement method, its side frame was structurally analyzed by reducing number of degrees of freedom. Side frame was subjected to 1000 N vertical static load (the load is 2000N for full-frame chair). The internal forces – bending moment capacity, shear forces and axial forces – of joints in side rail to back post were attained as shown in Figure 4.2.

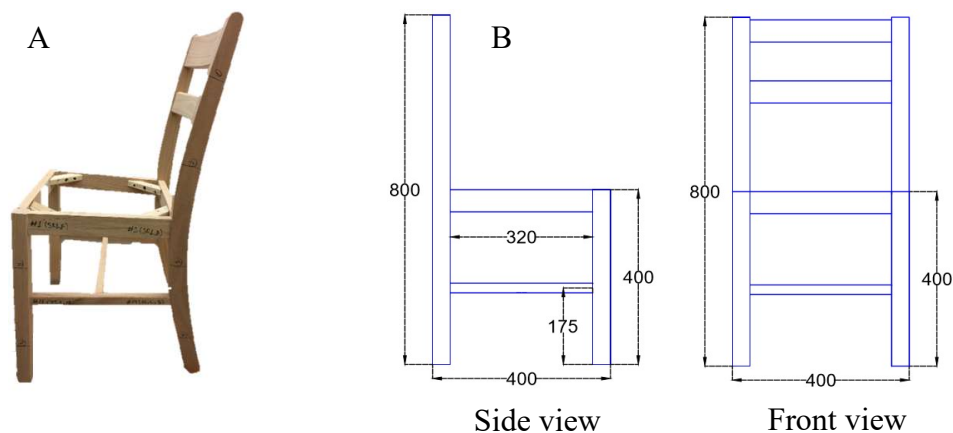


Figure 4.1 A. Chair Frame Obtained from Industry, B. Chair Model

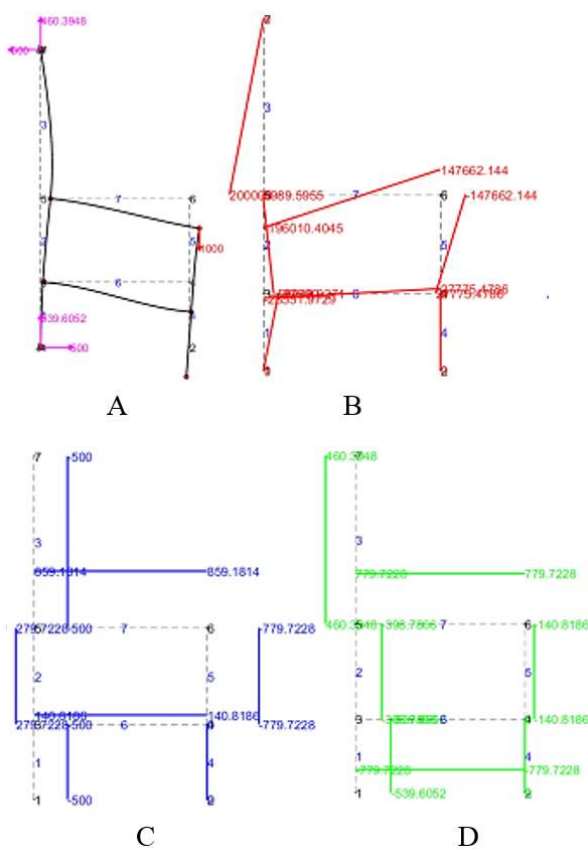


Figure 4.2 Configuration of Structural Analysis on Chair A. Deflected Shape and Reaction Forces, B. Bending Forces, D. Shear Forces and D. Axial Forces

#### 4.2.2 Design of Joints

*Rectangular mortise and tenon joints* – a round shouldered rectangular tenon fitting into a tight-fitting mortise, were selected to utilize in chair frame shown in Figure 4.1. This joint is considered as a mechanical joint and its strength is limited by the bending moment resistance of tenon itself. Therefore, its bending stress is calculated by [42]:

$$\sigma_{(bending)} = \frac{M \times \bar{y}}{I} \quad \text{Equation 4.1}$$

where,  $\sigma_{bending}$  is normal stress due to bending stress (N/mm<sup>2</sup>),  $M$  is bending moment capacity of joints (N.mm),  $\bar{y}$  is distance between centerline of tenon and bottom of the tenon (mm), and  $I$  is moment of inertia of tenon (mm<sup>4</sup>). Configuration of mortise and tenon joints in the cross section of rail is shown in Figure 4.3. The following equations were used to calculate moment of inertia for RMT joints.

$$M = F \times l \quad \text{Equation 4.2}$$

$$I_T = [I_1 + (A_1 \times d_1^2)] + [I_2 + (A_2 \times d_2^2)] + [I_3 + (A_3 \times d_3^2)] \quad \text{Equation 4.3}$$

$$I_1 = I_3 = \frac{\pi r^4}{8} \quad \text{Equation 4.4}$$

$$I_2 = \frac{(2r)d^3}{12} \quad \text{Equation 4.5}$$

$$A_1 = A_3 = \frac{\pi r^2}{2} \quad \text{Equation 4.6}$$

$$A_2 = b \times d \quad \text{Equation 4.7}$$

$$d_1 = |\bar{y} - y_1| \quad \text{Equation 4.8}$$

$$d_2 = |\bar{y} - y_2| \quad \text{Equation 4.9}$$

$$d_3 = |\bar{y} - y_3| \quad \text{Equation 4.10}$$

$$h = d + 2r \quad \text{Equation 4.11}$$

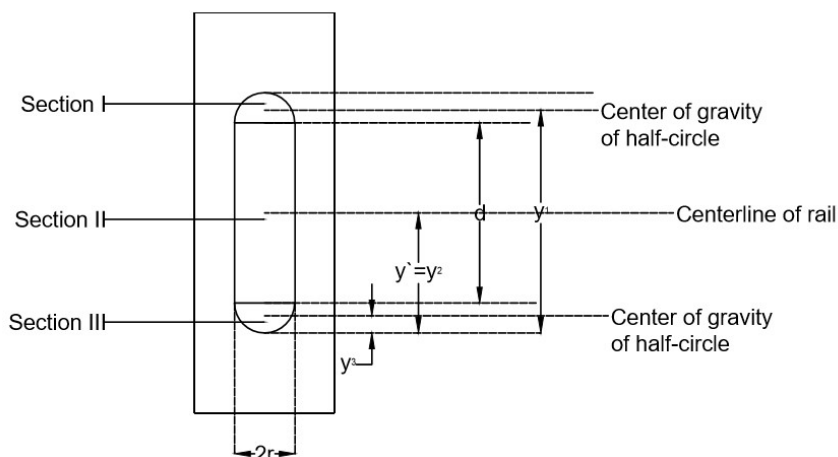


Figure 4.3 Configuration of RMT Joints in the Cross Section of Rail

In the consideration of mechanical joints, thickness and width of tenon can be calculated. The length of the tenon must be calculated because length of tenon affects joint strength as well. Therefore, this is calculated by using equation 4.12 after attaining the width and thickness of the tenon [4].

$$M = 0.7 \times \tau_{wood} \times A \times B \times C \times D \quad \text{Equation 4.12}$$

where  $\tau_{wood}$  is shear strength of wood (lb-in),  $A$  is tenon width and rail width factor,  $B$  is tenon length factor,  $C$  is an adhesive factor, and  $D$  is a tenon fit factor. In this equation, the unit should be pound-inch system owing to the factors in calculation. The results should be converted into the metric system after calculations are completed.

*Two pin moment-resisting dowel joints* – dowel pins in furniture construction are ordinarily subjected to axial and shear forces (Figure 4.4) although they resist to axial, shear and bending in-plane loads. Therefore, axial and shear strength on dowel joints in furniture frame should be also considered. This joint should be considered as a mechanical joint to determine dimensions in a cross-section of rails in Figure 4.5 by using equation 4.1 as RMT joints, but calculation of moment of inertia differs in dowel joints from those of RMT joints.

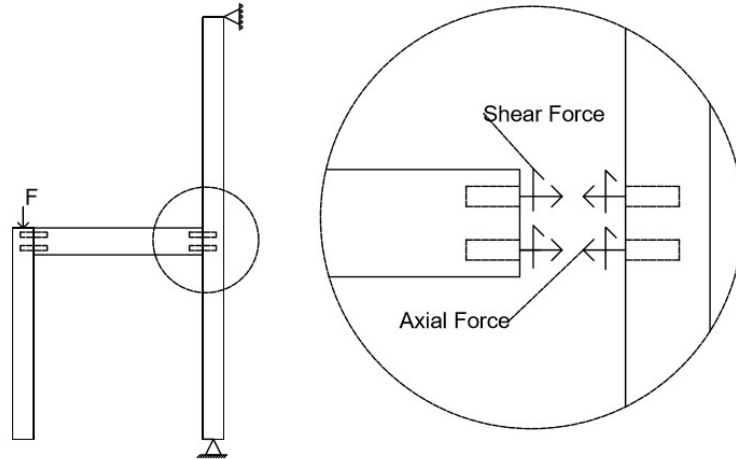


Figure 4.4 Configuration of Dowel Pins on Rail Cross-Section [4]

For bending stress of dowel joint, moment of inertia must be calculated as given equations 4.13 to 4.17 owing to the change in cross-section geometry.

$$I_T = [I_1 + (A_1 \times d_1^2)] + [I_2 + (A_2 \times d_2^2)] \quad \text{Equation 4.13}$$

$$I_1 = I_2 = \frac{\pi r^4}{4} \quad \text{Equation 4.14}$$

$$A_1 = A_2 = \pi r^2 \quad \text{Equation 4.15}$$

$$d_1 = |\bar{y} - y_1| \quad \text{Equation 4.16}$$

$$d_2 = |\bar{y} - y_2| \quad \text{Equation 4.17}$$

For axial stress, withdrawal strength of dowel must be taken into consideration so that dowel loaded in tension must be designed to have stronger joint.

$$\sigma_{axial} = \frac{F_T}{A_1} \quad \text{Equation 4.18}$$

$$F_T = \frac{M}{d_1 + d_2 + \frac{d_3}{2}} \quad \text{Equation 4.19}$$

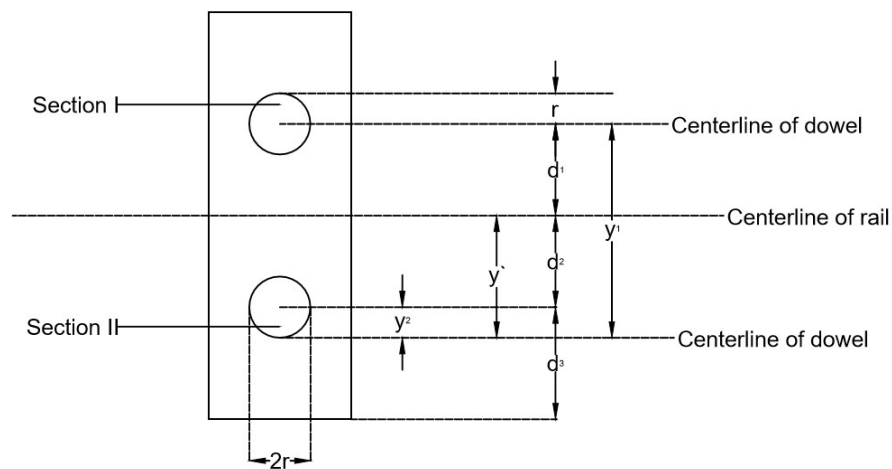
where,  $\sigma_{axial}$  is normal stress due to axial force (N/mm<sup>2</sup>),  $F_T$  is tensile force on dowel,  $d_1$  and  $d_2$  are distances between the rail center and the centerlines of the dowels loaded in tension and compression (mm), respectively, and  $d_3$  is distance between dowels in compression and the outside compression rail edge (mm).

For shear stress, shear force on dowel loaded in tension should be taken into consideration.

$$\tau = \frac{F_v \times Q}{I_T \times 2r} \quad \text{Equation 4.20}$$

$$Q = A_1 \times d_1 \quad \text{Equation 4.21}$$

where,  $\tau$  is shear stress on the dowel loaded in tension (MPa),  $F_v$  is shear force on all dowels (N),  $r$  is the radius of dowel (mm), and  $Q$  is centroid area of dowel in tension ( $\text{mm}^3$ ).



Equation 4.22 Configuration of Dowel on the Cross-Section of Rail

Length of dowel embedment into furniture member is a significant parameter to measure strength of dowel as much as dowel diameter. Therefore, the following equation is used to determine length of dowel embedment.

$$F_T = 0.834 \times D \times L^{0.89} \times [(0.95 \times \tau_{rail}) + \tau_{dowel}] \times a \times b \times c \quad \text{Equation 4.23}$$

where,  $D$  is dowel diameter (in),  $L$  is length of dowel embedment (in),  $\tau_{rail}$  is shear parallel to grain in wood for rail (psi),  $\tau_{dowel}$  is shear parallel to grain in wood for dowel (psi),  $a$  is adhesive factor,  $b$  is dowel tolerance factor, and  $c$  is dowel surface factor.

### 4.3 Results and Discussion

Dimensional parameters and internal forces are used to calculate bending stress for RMT joints and bending, and shear and axial stresses for dowel joints are tabulated in Table 4.1 and in Table 4.2, respectively. As with using corresponding equations, stresses are calculated and tabulated in Table 4.3. In here, the designer can select a design value at the desired reliability level and design joints in chair frames as shown in Figure 4.1b. For this purpose, joints on side rail to back post in the chair prototype is designed corresponding to design value for 0.99/0.99 confidence/proportional level in order to obtain high reliable joint.

For RMT joints,  $d$  was calculated to find width ( $h$ ) of tenon using equations 4.1 to 4.11. At this point, normal stress due to bending ( $\sigma_{bending}$ ) is the LTL value for the 0.99/0.99 confidence proportional level. In production, assuming a 9.525-mm diameter router-bit was used to cut mortises, tenon thickness is 9.525 mm. Equation to calculate dimension of “ $d$ ” for RMT joints corresponding to bending stress for 0.99/0.99 confidence/proportional level is expressed as:

$$\sigma_{bending_{0.99/0.99}} = \frac{M \times (4.7625 + (\frac{d}{2}))}{0.79375d^3 + 17.9534d^2 + 14.2286d + 697.5356} \quad \text{Equation 4.24}$$

Tenon length was calculated with equation 12, assuming rail width is 50.8 mm, and tenon fit is 0.12 mm with PVAc adhesive being used in construction. The factors and joint sizes are given in Table 4.4. According to the results, tenon width should be at least 38.1 mm and 41.0275 mm; in the case of tenons made of red oak and white oak, respectively. Those of length should be at least 22.225 mm and 19.05 mm, respectively.

Table 4.1 Dimensional Parameters for RMT Joints

<b>Wood Species</b>	<b>Moment (N.m)</b>	<b>y (mm)</b>	<b>y<sub>1</sub> (mm)</b>	<b>y<sub>2</sub> (mm)</b>	<b>y<sub>3</sub> (mm)</b>	<b>I<sub>1</sub>, I<sub>3</sub> (mm<sup>4</sup>)</b>	<b>I<sub>2</sub> (mm<sup>4</sup>)</b>	<b>A<sub>1</sub>, A<sub>2</sub> (mm<sup>2</sup>)</b>	<b>A<sub>2</sub> (mm<sup>2</sup>)</b>	<b>I<sub>t</sub> (mm<sup>4</sup>)</b>
<b>Red oak</b>	350.56	19.05	35.385	19.05	2.74	201.92	18764.2	35.6098	272.65	38142.6
<b>White Oak</b>	341.17									

Table 4.2 Dimensional Parameters for Dowel Joints

<b>Wood Species</b>	<b>Moment (N.m)</b>	<b>F<sub>v</sub> (N)</b>	<b>F<sub>t</sub> (N)</b>	<b>y (mm)</b>	<b>d<sub>1</sub>, d<sub>2</sub> (mm)</b>	<b>d<sub>3</sub> (mm)</b>	<b>I<sub>1</sub>, I<sub>2</sub> (mm<sup>4</sup>)</b>	<b>A<sub>1</sub>, A<sub>2</sub> (mm<sup>2</sup>)</b>	<b>I<sub>t</sub> (mm<sup>4</sup>)</b>	<b>Q (mm<sup>3</sup>)</b>
<b>Red oak</b>	240.81	948.071	6454.95	19.05	14.2875	17.4625	403.84	71.2196	29884.2	1017.55
<b>White oak</b>	243.44	958.425	6525.45	19.05	14.2875	17.4625	403.84	71.2196	29884.2	1017.55

Table 4.3 Internal Stresses for RMT and Dowel Joints (in MPa)

	<b>RMT</b>		<b>Dowel</b>					
	<b>Bending Stress</b>		<b>Bending Stress</b>		<b>Shear Stress</b>		<b>Axial Stress</b>	
	<b>Red Oak</b>	<b>White Oak</b>	<b>Red Oak</b>	<b>White Oak</b>	<b>Red Oak</b>	<b>White Oak</b>	<b>Red Oak</b>	<b>White Oak</b>
<b>Mean</b>	175.08	170.39	153.51	155.18	3.40	3.44	90.63	91.62
<b>0.90/0.90</b>	138.64	128.12	121.14	121.94	2.68	2.70	71.53	72.00
<b>0.95/0.90</b>	137.79	127.03	120.39	121.09	2.66	2.68	71.08	71.49
<b>0.99/0.90</b>	136.15	124.91	118.96	119.42	2.63	2.64	70.24	70.51
<b>0.95/0.90</b>	126.55	116.65	110.55	112.93	2.45	2.50	65.27	66.67
<b>0.95/0.95</b>	125.57	115.40	109.69	111.94	2.43	2.48	64.76	66.09
<b>0.99/0.95</b>	123.65	112.96	108.01	110.02	2.39	2.44	63.77	64.96
<b>0.99/0.90</b>	102.87	95.03	89.81	95.92	1.99	2.12	53.03	56.63
<b>0.99/0.95</b>	101.70	93.44	88.79	94.67	1.97	2.10	52.42	55.90
<b>0.99/0.99</b>	99.41	90.34	86.78	92.23	1.92	2.04	51.24	54.46

For *dowel joints*, the radius of the dowel was calculated corresponding to bending, shear, and axial stresses for 0.99/0.99 confidence/proportion level using equations 4.25, 4.26 and 4.27, which are expressed as:

$$\sigma_{bending_{0.99/0.99}} = \frac{M \times (19.05 + r)}{1.57^4 + 2279.0227r^2} \quad \text{Equation 4.25}$$

$$\tau_{0.99/0.99} = \frac{51393.653}{3.08r^3 + 4558.0454r} \quad \text{Equation 4.26}$$

$$\sigma_{axial_{0.99/0.99}} = \frac{5254.09025}{3.14^2} \quad \text{Equation 4.27}$$

Length of dowel embedment was calculated using equation 4.23, assuming rail width is 50.8 mm, clearance between dowel and dowel hole 0.12 mm (dowel-clearance factor was calculated by  $1 - (17.1 \times 0.12)$  (Eckelman, 2003)), and PVAc adhesive was used in construction. The factors and joint sizes are given in Table 4.5. According to the results, diameters of dowels made of red oak are 9.61, 11.45 and 11.38 mm in the case of the chair made of red oak. On the other hand, those of white oak are 9.30, 10.80 and 11.05 mm. To make reliable dowel joints, dowel diameter should be resistant to all internal forces so, largest diameter should be used in dowels. For this purpose, largest diameter was obtained in shear with 11.45 mm for chair made of red oak, while white oak chair was 11.05 mm in axial. In design process, the designers should not use a dowel diameter less than 11.45 mm for a chair made of red oak and 11.05 mm for a chair made of white oak. In the calculation of length of dowel embedment, the largest diameter should be considered. The length of dowel embedment was 36.475 mm (dowel length is 72.95 mm) for a chair made of red oak and 34.4 mm (dowel length is 68.8 mm) for a chair made of white oak.

Table 4.4 Factors in Equation and Joint Dimension for RMT Joints

Wood species used in chair	Thickness (mm)	Width (mm)	Shear parallel to grain (MPa)	Rail/Tenon width factor	Adhesive factor	Tenon fit factor	Length factor	Length (mm)
Red Oak	<i>0.9525</i>	<i>38.1</i>	14.15	1.335	1.17	0.89	0.825	<i>22.225</i>
White Oak		<i>41.275</i>	15.87	1.40625			0.696	<i>19.05</i>

Table 4.5 Factors in Equation and Joint Dimension for Dowel Joints

Wood species used in chair	Diameter (mm)			Shear parallel to grain (MPa)		Adhesive factor	Dowel clearance factor	Dowel surface factor	Length of dowel embedment (mm)
	In bending	In shear	In axial	Wood in dowel	Wood in rail				
Red Oak	9.61	<i>11.45</i>	11.38	14.15	14.15	0.9	0.9316	1	<i>36.475</i>
White Oak	9.30	10.80	<i>11.05</i>	-	15.87				<i>34.4</i>

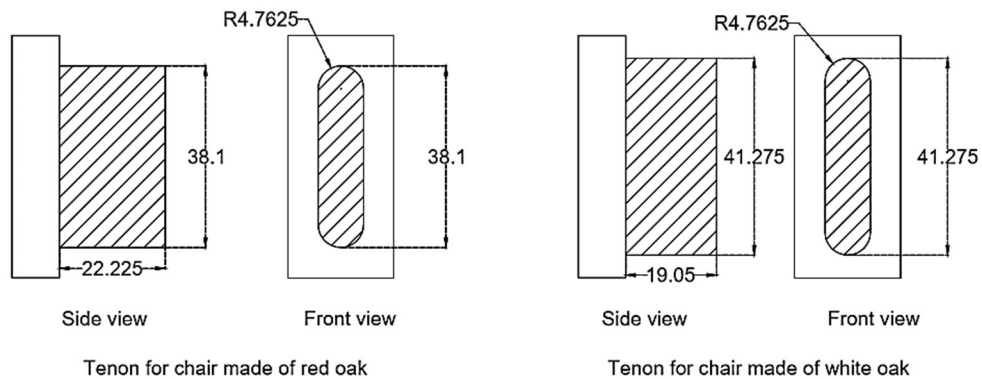


Figure 4.5 Tenon Dimensions

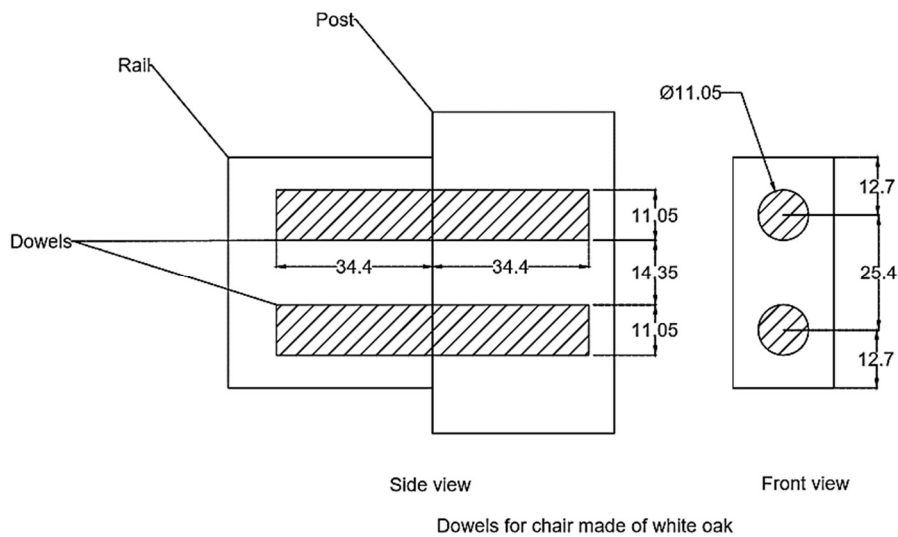
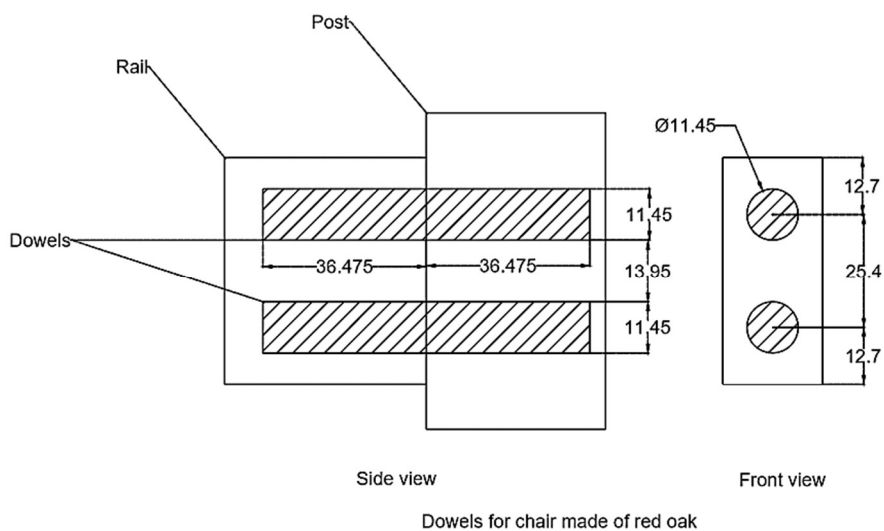


Figure 4.6 Dowel Dimensions

#### 4.4 Conclusion

In this chapter, the design of joints in furniture structure based on reasonable design values obtained from LTLs method was discussed. Both RMT and dowel joints were considered as mechanical joints so the tenon width and dowel diameter were determined. The semi-rigidity of the furniture joints was considered to calculate the length of tenon and dowel embedment.

Reasonable design values were obtained for 0.99/0.99 confidence/proportional level to construct the highest reliable joints according to this study. Tenon thickness was 9.525 mm for RMT joints made of red oak because 3/8 bits were used to cut matching mortises. Tenon thickness should be determined from what size of drill bits were used in the process. The tenon length and width values are 22.225 mm and 38.1 mm, respectively. Tenon sizes in a chair made of red oak and obtained from industry are 9.525 x 19.05 x 38.1 mm. On the other hand, tenon sizes for RMT joints made of white oak are 9.525 x 19.05 x 41.275 mm. Tenon sizes in designed joints are larger than those in chairs obtained from the industry. It is obvious that the chair strength may not be enough according to the design value for 0.99/0.99 confidence/proportion level. However, chairs in industry are reinforced with corner blocks to increase overall chair strength and ensure chair rigidity. The tenon width for joint made of white oak is also larger than those of red oak because of comparable design values for 0.99/0.99 confidence/proportion level. However, tenon length is shorter for white oak than red oak owing to its mechanical properties and inverse variation between tenon length and tenon width in equations.

In dowel joints, according to 0.99/0.99 confidence/proportion level, minimum dowel diameters are 11.45 and 11.05 mm while corresponding length of dowel embedment are 36.475 and 344 mm for chairs made of red oak and white oak, respectively. However, the change of dowel diameter also depends on what size drill bits are used to drill dowel holes. Table 4.6 shows the most widely used drill bit sizes in the industry. Therefore, dowel diameters can be selected as 11.51 and 11.11 mm for dowel joints made of red oak and white oak.

Table 4.6 Most Commonly Used Drill Bits Sizes (in mm)

1.59	4.37	7.14	9.92	10.32
1.98	4.76	7.54	10.32	10.72
2.38	5.16	7.94	10.24	11.11
2.78	5.56	8.33	8.73	11.51
3.18	5.95	8.73	9.13	11.91
3.57	6.35	9.13	9.53	12.30
3.97	6.75	9.53	9.92	12.70

## CHAPTER 5. PERFORMANCE TEST OF CHAIR FRAMES

### 5.1 Introduction

Performance test of a chair is described as an evaluation of its strength under expected loads in service. A chair is subjected to static, cyclic, and/or impact load during its service. Static and cyclic testing are widely used performance testing methods to evaluate chair strength. Static and cyclic load types for performance testing of chairs were discussed in Chapter 2.

In service, chair strength decreases over the course of time owing to fatigue behavior of material. Therefore, chair strength in cyclic performance testing is always lower than in static testing. Eckelman and Erdil [181] stated that chair strength in cyclic test should not be assumed to be more than 50% of its static load capacity. Likos *et al.* also found that the ratio between cyclic and static load capacities of chairs were 56.5%, 66.8%, and 69.2% for round, rectangular, and diamond tenons, respectively [60]. Kuskun [182] and Kasal *et al.* [69] indicated that cyclic load capacity of chairs was 56% of their static load capacity. Figure 5.1 shows the relationship between load steps in cyclic performance testing and chair strength. In testing, the chair fails when load level reaches the chair strength and it is called first-crossing point.

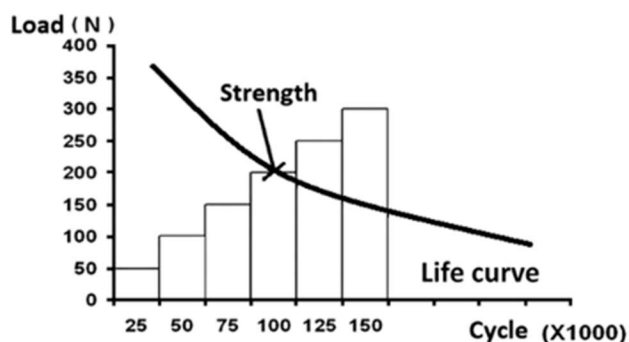


Figure 5.1 Relationship Between Load Steps and Chair Strength [14]

In literature, BIFMA defined acceptable static load capacity levels for functional load and service load. EN standards also described static load level for chairs. However, GSA specifications do not have such information available.

In this chapter, the aim is to evaluate performance of chairs of which joints were designed with reasonable design values (LTLs values). For this purpose, the chair model in Chapter 4 was used to construct chairs for performance testing to evaluate their static and cyclic load capacities. In static load testing, it is expected that chairs fail above 2000 N load levels. In cyclic load testing, chair strength was compared with ALA specifications.

## 5.2 Materials and Methods

### 5.2.1 Specimen Construction

In this study, 20 red oak chairs of simple configuration joined with RMT joints were produced in laboratory conditions (10 chairs for static vertical load test and 10 chairs for cyclic front-to-back load test). RMT joint sizes were determined as described in Chapter 4. RMT joints were used only in joints on side rails to back legs and front legs due to the fact that most failures occur in these joints. Dowels with diameter of 9.525 mm and 25.4 mm of length were used in the front and back rails to assemble side frames. Round mortise and tenon joints with 19.05 mm diameter and 22.225 mm length were used for side stretchers while screws with 4.3 mm diameter and 38.1 mm length were used for middle stretchers. Defect-free members at 7% MC were dimensioned according to the chair obtained from industry. Member dimensions are tabulated in Table 5.1. Chair configuration for performance tests is depicted in Figure 5.2.

Table 5.1 Member Dimensions Used in Chair (in mm)

<b>Member</b>	<b>Thickness</b>	<b>Width</b>	<b>Length</b>
<b>Front legs</b>	38.1	38.1	400
<b>Back legs</b>	38.1	38.1	800
<b>Rails</b>	22.225	50.8	323.8
<b>Side stretchers</b>	22.225	22.225	323.8
<b>Middle stretchers</b>	22.225	22.225	339.775

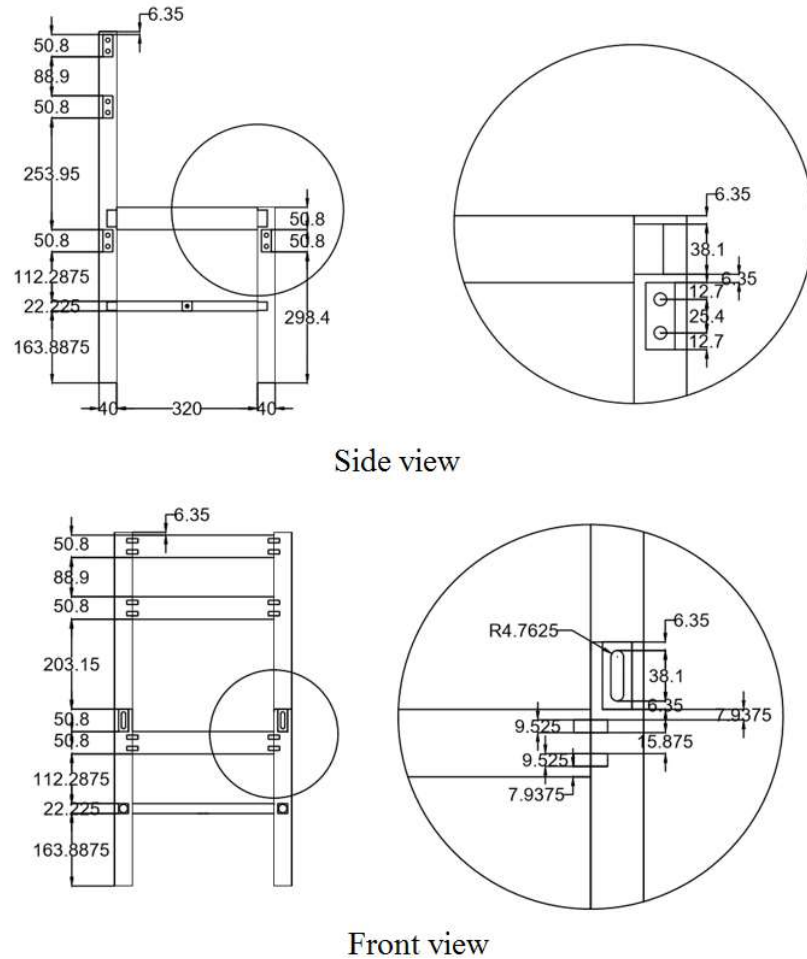


Figure 5.2 Configuration of Chair Samples

## 5.2.2 Test Procedure

### 5.2.2.1 Vertical Statically Load Test

All tests were conducted on a 4450 N load capacity MTS test machine. Figure 5.3 shows schematic configuration of test set-up for static vertical load testing of chairs. The load was applied mid-span of front legs with frequency of 12.7 mm/min. Tests were carried on until non-recoverable failure occurred in joints on side rail to back post [60].

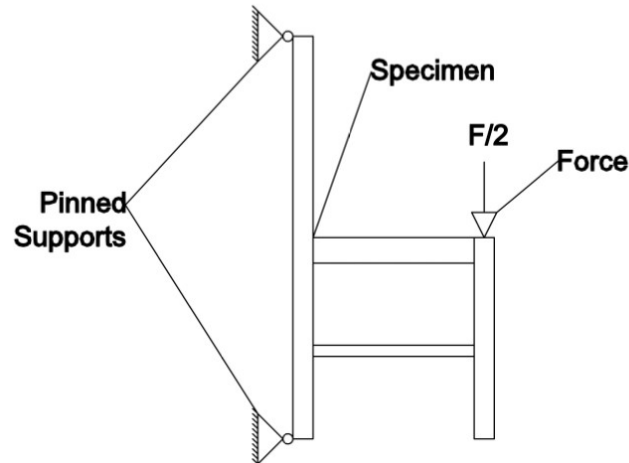


Figure 5.3 Configuration of Vertical Statically Load Test Set-Up

#### 5.2.2.2 Front-to-Back Cyclic Load Test

Studies by American Library Association (ALA) indicated that failures occur most commonly in joints on side rail to back post owing to front-to-back load of chairs when users sit down on a chair and push or tilt backwards. Therefore, front-to-back load performance test reported by ALA specifications were used to evaluate chair strength.

In the test procedure, a chair was mounted for test shown in Figure 5.4. Reaction brackets were used to prevent chair sliding on the platform. A chain was passed over the seat front-to-back, connected to load head on one end, and anchored to the platform on the other. In doing so, chairs were subjected to horizontal front-to-back load. Loads were applied on chairs with 20 cycles per minute. Initial load level was 445 N with 111.25 N load increments after each completed 25,000 cycles. When 1112.5 N load level was completed in the test, load increments were 222.5 N after 25,000 cycles were completed at each preceding load level. Test continued until one or both joint(s) on side rails to back post failed, or horizontal deflection in these joints exceeded 50.8 mm [46].

Ultimate failure load ( $F_{cyclic}$ ) for cyclic load test were calculated by the expression:

$$F_{cyclic} = F - F_i \times \left(1 - \frac{C_{failure}}{25000}\right) \quad \text{Equation 5.1}$$

where  $F$  is load level at failure (N),  $F_i$  is incremental load after 25,000 cycles are completed at preceding load level (N), and  $C_{failure}$  is load cycle at failure.

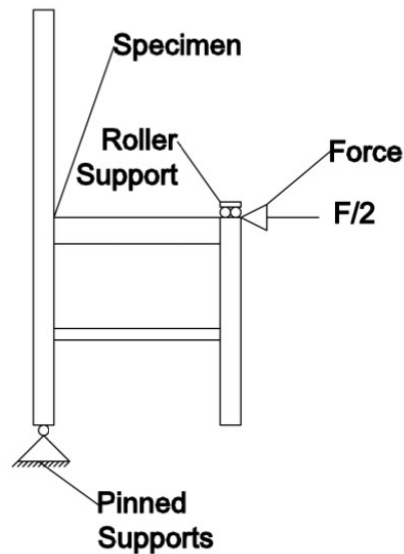


Figure 5.4 Configuration of Front-to-Back Cyclic Load Test Set-Up

### 5.3 Results and Discussion

Results for the performance testing of chairs made of red oak with RMT joints are given in Figure 5.5, Figure 5.6, and Table 5.2. According to test results, average ultimate static load capacity level for chairs are 2,458.63 N with a standard deviation of 232.84 N, while those of cyclic load is 1,435.19 N with 123.84 N. Chair strength in static load testing is 58.37% greater than chair strength in front-to-back cyclic load testing. Kuskun *et al.* indicated that 56% of static strength was recommended to predict cyclic load capacity level of chairs [183].

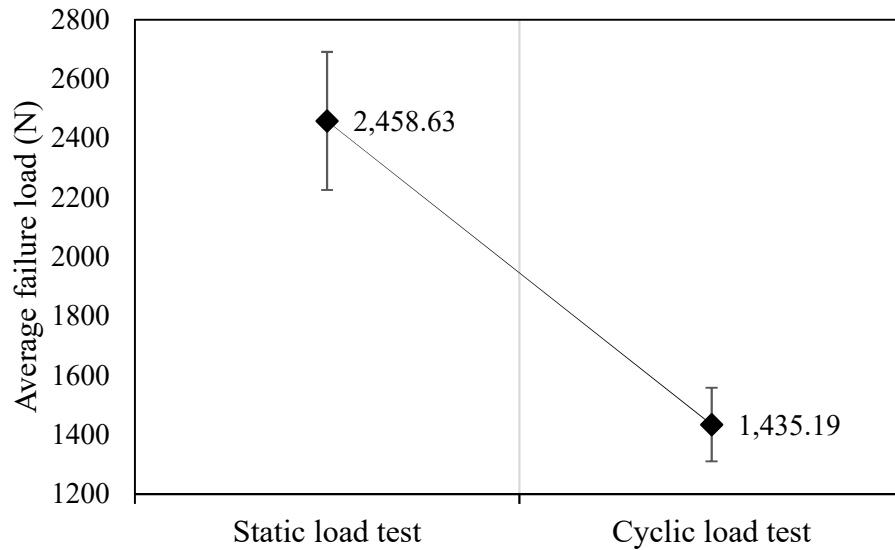


Figure 5.5 Average Failure Load of Chair Frames in Static and Cyclic Test

In Figure 5.6, individual failure loads for static and cyclic load test are presented. According to the design philosophy, failure strength for chairs was expected to be higher than 2000 N, which was the desired load level in the design process. Results show that all chairs subjected to static load test failed within this aforementioned desired load level. The highest load level capacity of a chair in static testing was 2,861.35 N (143.06% of 2000 N) while those of the lowest was 2,131.55 N (106.58% of 2000 N).

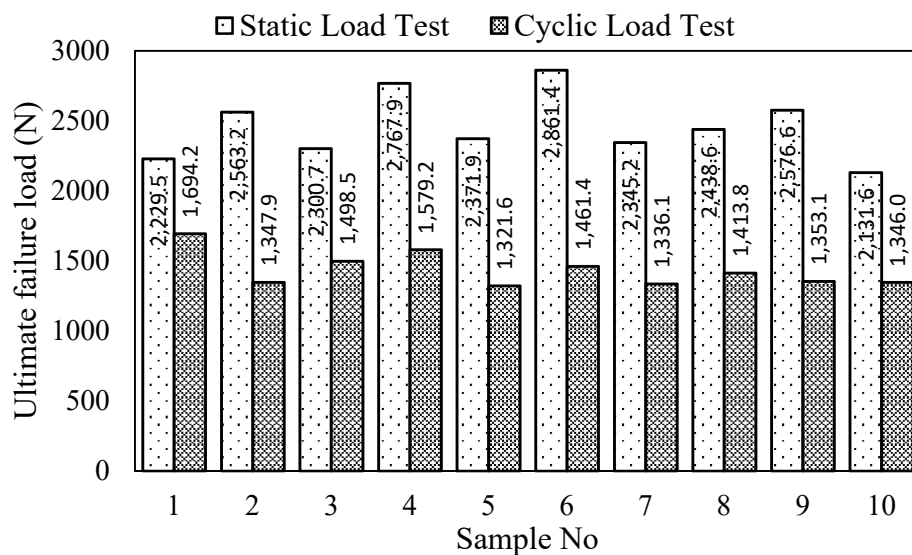


Figure 5.6 Individual Test Results for Failure Load of Chair Frames in Static and Cyclic Load Tests

Table 5.2 Performance Test Results of Chair Frames

	Static failure load	Cyclic failure load		
		Failure load level	Failure cycle	Ultimate load level
<b>1</b>	2229.45	1780.00	15363.00	1694.23
<b>2</b>	2563.20	1557.50	1453.00	1347.93
<b>3</b>	2300.65	1557.50	18369.00	1498.48
<b>4</b>	2767.90	1780.00	2442.00	1579.23
<b>5</b>	2371.85	1335.00	23493.00	1321.59
<b>6</b>	2861.35	1557.50	14205.00	1461.42
<b>7</b>	2345.15	1557.50	127.00	1336.13
<b>8</b>	2438.60	1557.50	8852.00	1413.78
<b>9</b>	2576.55	1557.50	2038.00	1353.14
<b>10</b>	2131.55	1557.50	1235.00	1345.99
<b>Mean</b>	2458.63			1435.19
<b>SD</b>	232.84			123.84

In Figure 5.7, bending stresses of joints in side rail to back post at the failure are given. According to the results, stress on joints at failures are above the design value (LTL value), which is 99.41 MPa. It is observed that joints have enough strength to carry applied loads, even if stress level exceeds design value.

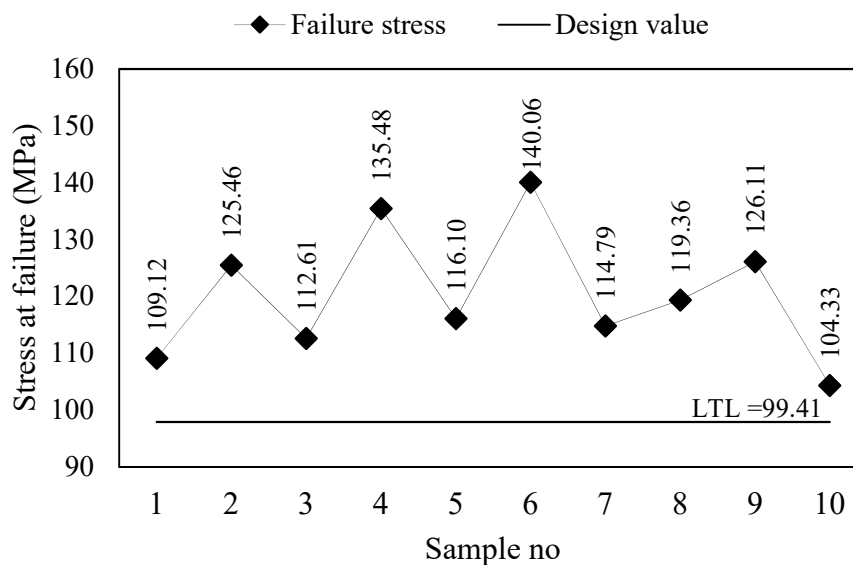


Figure 5.7 Failure Stress in Joints

Test results in front-to-back cyclic load test were compared to acceptable load levels given by [46]. According to ALA specifications, acceptable service load levels for front-to-back cyclic load test are i) 890 N for light duty service load for household chairs, ii) 1001.25 N for light duty service load for restaurant chairs, iii) 1335 N for light duty service load for library chairs, iv) 1557.5 N for medium duty service load for library chairs, and v) 2002.5 N for heavy duty service load for library chairs. The comparison results between specified acceptable load level and cyclic strength of chairs are given in Table 5.3. All chairs satisfied acceptable light duty service load for household and restaurant chairs while only one chair (1321.59 N) did not meet acceptable light-duty service load for library chairs. Its strength was 1% lower than the acceptable load level. Furthermore, only two chairs' strengths met acceptable medium duty service load for library chairs and no chairs met heavy duty load level. If chairs are utilized as household dining chairs, they will have enough strength in service, but they may not be suitable for service in libraries.

Table 5.3 Evaluation of the Cyclic Front-to-Back Load Test Results Corresponding to ALA Specifications

Chair no	Cyclic strength (N)	Acceptable light duty service load for house hold chairs	Results	Acceptable light duty service load for restaurants chairs	Results	Acceptable light duty service load for library chairs	Results	Acceptable medium duty service load for library chairs	Results	Acceptable heavy-duty service load for library chairs	Results
1	1694.23	890.00 N	Pass	1001.25 N	Pass	1335.00 N	Pass	1557.50 N	Pass	2002.50 N	Fail
2	1347.93		Pass		Pass		Pass		Fail		Fail
3	1498.48		Pass		Pass		Pass		Fail		Fail
4	1579.23		Pass		Pass		Pass		Pass		Fail
5	1321.59		Pass		Pass		Fail		Fail		Fail
6	1461.42		Pass		Pass		Pass		Fail		Fail
7	1336.13		Pass		Pass		Pass		Fail		Fail
8	1413.78		Pass		Pass		Pass		Fail		Fail
9	1353.14		Pass		Pass		Pass		Fail		Fail
10	1345.99		Pass		Pass		Pass		Fail		Fail

In contemporary furniture manufacturing, service load level is a critical measure for overall strength of the chair structure rather than joint strength. Therefore, recommended service loads for chair structures with BIFMA specifications were discussed in Chapter 2. In doing so, designers considered the overall strength of a chair structure. If a chair passes specified acceptable load levels, it also satisfies durability and reliability requirements. However, design of joints is neglected. Joints are solely a way to connect members rather than providing strength so the joint itself may not have enough strength to carry subjected loads. In this case, designers use reinforcements to increase overall strength of chair frames to satisfy specified acceptable load levels. On the other hand, if a design value for furniture joints is recommended, a chair can be designed with desired joint types according to subjected load level. In doing so, designer can theoretically estimate whether joint strength will meet specifications or not. This study is demonstrating that a chair of which joints are designed according to design values could resist subjected loads without any reinforcements.

#### 5.4 Conclusion

In this chapter, performance testing of chair frame was investigated. A chair was designed according to 2000 N vertical statically load level and subjected to static and cyclic front-to-back load.

In vertical static load testing, chairs were expected to fail above 2000 N load level. All chairs met specified load level. Failure loads in chairs are 106.58% to 143.06% greater than desired load level. It is observed that the chair has enough strength even if load exceeds its design value.

In front-to-back cyclic load testing, all chairs met acceptable light-duty service load for household and restaurant chairs according to ALA specifications. Cyclic strength of chairs is 58.37% of their static strength. According to other studies this recommended value could vary between 50% and 56% [63,181].

Consequently, if a chair is designed with recommended design values, overall strength of chairs can meet acceptable load levels and/or desired load level. Recommended standards, such as BIFMA, ALA, GSA etc., provide service and/or functional load levels in service. In the furniture design process, these service loads can be used to design the chair itself and its joint by using reasonable design value of joints to increase reliability of final products.

## CHAPTER 6. SUMMARY AND CONCLUSION

### 6.1 Summary

In this study, reasonable design values of selected furniture joints were estimated by using the Lower Tolerance Limits (LTLs) method in order to provide a systematic procedure in design of furniture itself and its joints. Studies concerning rational design of furniture have been conducted, but design values of furniture itself, its members, and /or its joints have not been well-addressed. Several attempts were conducted to determine allowable design values of furniture joints. However, the attempts considered point estimation rather than interval estimation.

Wood is a structural material and its design values were determined for structural purposes of large structures. However, wood material used in furniture structures are defect-free and clearer than those for structural purposes. Therefore, design values established for large structures may not work for furniture engineering. The establishment of design values for furniture members and joints were then investigated.

It was indicated that probabilistic approaches provided reliable results rather than deterministic approaches [10]. Probabilistic approaches ensure reliability of product by considering the variability in a data set. On the other hand, deterministic approaches use point estimation so that design values for a product relies on sample error. Therefore, in this study, tolerance intervals were used to estimate design values of furniture joints by using sample error and predicting future population variability. To ensure reliability and safety of products, one-sided lower tolerance limits were used.

In a tolerance analysis, normality assumption, randomness, and homogeneity in the experiment are significant. Normality assumes that continuous variables are normally distributed in data sets. Therefore, tolerance analysis can be made for univariate data. If the data is not normally distributed, other distribution methods should be sought to make a tolerance analysis. Otherwise, a non-parametric tolerance analysis must be done. If

normality assumption is violated, the tolerance analysis may be damaged. Furthermore, randomization is crucial for three points: to prevent bias, to make experiment accurate as much as possible, and to control lurking variables in experiment. Therefore, specimens must be randomly selected in experiment. Lastly, homogeneity of the experiment affects reliability of the tolerance analysis. Each sample group should be represented with identical specimens and test procedures during the duration of this experiment. However, [136] studied the tolerance limits of heterogeneous data and tolerance analysis can be done for heterogeneous data if appropriate assumptions are made.

Sample sizes in tolerance analysis are significant because k-tolerance factor for univariate tolerance intervals depends on sample sizes. [178–180] studied the effects of sample sizes on tolerance analysis. Studies showed that non-central t-distribution provided better and easier solutions to construct k-tolerance factor whether sample size is large or small. Modified Faulkenberry-Wilks methods was used to determine minimum sample size requirements for univariate tolerance intervals, albeit other methods, because they are easier and in compliance to make a tolerance analysis developed by [151]. The results showed that 215 to 216 specimens were enough to make a reliable tolerance analysis for 0.99/0.99 confidence/proportion level.

k-tolerance factor also depends on confidence/proportion levels because tolerance intervals use z-statistic, and their z-scores construct k-tolerance factor. It becomes greater with an increase in confidence/proportion level. Therefore, the selection of confidence/proportion level comes into prominence but there is no certain rule on how to select them. It depends on one's judgement. The recommended confidence/proportion level is between 0.80 and 0.99. In many studies, it was constructed as of 0.95/0.95 level because of the significance in level of test. As long as appropriate assumption is made, and appropriate sample size is used, there is no objection in what confidence/proportion levels are used. In this study, one of 0.90, 0.95 and 0.99 is used for confidence/proportion levels.

To obtain LTLs values, normality of data set was tested to figure out what type of tolerance analysis was made. According to the test result, RMT and dowel joints made of red oak

were fitted to Weibull distribution, while sample groups of screw withdrawal strength in wood made of red oak from edge-grain and white oak from face-grain were transformed by the logarithmic normalizing transformation. Univariate tolerance analysis was conducted for the others. The results showed that LTLs of sample groups for 0.99/0.99 confidence/proportional level were 53% to 66% of their means. It was also observed that there was no value below LTLs for 0.99/0.99 confidence/proportional levels unless there was an outlier in data sets.

Joints were designed based on 0.99/0.99 confidence/proportion levels of RMT and dowel joints to provide higher reliability. A chair frame was modelled and subjected to 2000 N load. Bending moments of joint in side rail to back post, where most of the failure occurs, were used to calculate width of the tenon due to considering the joints were a mechanical joint. Afterwards, the length of tenon was calculated owing to the semi-rigidity of furniture joints. Studies showed that width of tenon has more effect on joint strength rather than its length, as long as enough joint length was assured. In design of joints, there are some limitations because of tools used in production. For example, thickness of tenon should be determined according to what type of drill bits are used in production. Generally, the type of drill bits used is 3/8-inch bits with diameter of 9.525 mm. Templates are also used to cut tenons and conclude that recommended joint sizes should be matched with appropriate templates.

Performance testing is used to evaluate strength of chair frames. Therefore, chairs whose RMT joints were designed by using LTL values were tested under static and cyclic vertical front-to-back load. In static load testing, chairs were expected to resist 2,000 N load level. Results showed that all chairs failed above, so it proved that a chair of which joints designed with a design value could resist any specified external applied load and LTLs method provided a systematic procedure to estimate its design values. In cyclic load testing, the strength of chairs met ALA specification for light-duty household, restaurant, and library chairs. The purpose of the modelled chairs is to be used as dining chairs and these chairs meet recommended specifications.

## 6.2 Recommendations

Tolerance interval is a way to estimate lower and upper limits for future outcomes in the case of testing a sampled data. Therefore, a design value can be estimated from data set of tested specimens of furniture joint. However, each sample group of joint specimens will have its own data distribution, sample error, and population variation, so the designer should not draw a conclusion to estimate other types of joints from the perspective of one sample group. Therefore, each joint type and wood species should be tested individually to determine these values.

In the tolerance analysis, assumptions (normality, linearity, and constant variance) for experiment should be made accurately. Normality is the most significant assumption in tolerance intervals because it changes what type of distribution is used in the analysis. Therefore, if data is not normally distributed, (i) normalizing transformation should be done, (ii) Weibull distribution is used, or (iii) non-parametric tolerance analysis is made, respectively. The randomization and homogeneity in the experiment should also be considered to make a reliable analysis. Otherwise, the results of tolerance analysis may be inaccurate and drive designers to make inappropriate outcomes in the design process. In the case of homogeneity being violated, F-statistic test will be biased, and null hypothesis is falsely rejected. Therefore, sample sizes, construction of specimens, and test procedure should be maintained identically for all sample groups. If homogeneity of test was violated, then a non-parametric analysis should be made. Violation of randomness in the experiment also causes biased outcomes.

In the experiment, sample size is vital because sample error reduces with larger sample sizes. Determination of appropriate sample sizes causes a reduction of unreliable statistical analysis, as well as a reduction of sample cost and experiment time [151]. Accuracy of mean and standard deviation, for example, differs up to 0.012% and 60%, respectively, by using small sample sizes in experiment [184]. Furthermore, k-tolerance factor changes depending on sample sizes. If sample size is smaller, k-tolerance factor is larger. Therefore, variance for future population is estimated between larger limits in tolerance analysis. Therefore, appropriate sample sizes should be used in the tolerance analysis. Eckelman *et*

*al.* indicated how sample sizes affects cumulative means, standard deviation, and LTLs [13]. The study did not provide a tangible outcome on what sample sizes should be used but accuracy of mean, standard deviation, and LTLs is larger when the sample size is smaller than 100. On the other hand, modified Faulkenberry-Weeks method provides more conservative results about sample sizes.

The obtained LTLs value can be used as a reasonable design value of the furniture joints. In the design process of furniture joints, a designer's personal judgement determines what type of joint and joint sizes will be used in furniture construction. Such design values will be helpful for a designer to design joints rather than brain-storming with other designers or looking at empirical data from pass-fail joint tests. Designers can choose any level of confidence/proportion levels depending on the company's strategy. If a company is willing to produce high reliability furniture, they can choose 0.99/0.99 confidence levels. Future studies may also contribute to the higher confidence/proportion level.

In the design process, width of tenon and diameter of dowels should be obtained first since studies showed that they have more effect on joint strength than tenon length and dowel embedment. In doing so, the joints should be considered as mechanical joinery. The length of the joints should be attained with semi-rigidity of joints. A joint size should be designed to resist intended load capacity. Performance testing specified in standards should be evaluated for chair strength because all of the design considerations are theoretical, so chair strength may vary owing to the orthotropic properties of wood.

### 6.3 Limitations

LTLs value relies on previously sampled data, so the variation in data may have an effect. If sample error is large, k-tolerance factor will be also large and the LTLs value will be reduced. Therefore, statistical assumptions in experiment should be checked thoroughly. The sample sizes are also critical to obtain the LTLs value. If sample size is smaller, it prevents making a reliable tolerance analysis. Otherwise, the experiment becomes costly. Sample sizes are determined by using the modified Faulkenberry-Week method in this study. A pilot study is needed to determine the minimum sample size requirements for a

univariate tolerance analysis. In this study, sample sizes need to be increased at least 7 times more than sample sizes in the pilot study. In some cases, sample size in the pilot study may be enough to make a tolerance analysis for higher confidence/proportion levels [151].

Selection of confidence/proportion levels in tolerance analysis depends on personal judgement or designer's experience. 0.95/0.95 confidence/proportion level is generally used in literature for tolerance intervals. However, this level may increase the failure probability in joints.

In the designing of joints, the process is tedious because of numerous calculations. There is no tool to find joint sizes with inputs being external forces and design values. However, if joint sizes are known, joint strength can be obtained with computer software. Therefore, a tool can be developed for design of joints compatible with LTLs method.

The last but not least complication in furniture manufacturing is that there is no such design value for furniture joints. Therefore, it is a challenge to adapt this method into furniture manufacturing. Specifications for furniture strength dictates overall strength of furniture. If furniture can meet specifications for its intended purpose, the furniture can serve a long service life. However, the integration of this proposed method for design of joints will not be simple within the furniture industry. Test results were also obtained under laboratory conditions and not real-life applications. In the furniture industry, many parameters such as glue type, glue application, tolerance-fit, etc., are underestimated and joint strength may be lower than expected strength in laboratory conditions. Uysal and Haviarova [185] studied the joint strength obtained from industrial chairs. Test results showed that joint strength was very low and did not meet LTLs values.

#### 6.4 General Conclusion

Results of this study determined how to predict reasonable design values of RMT, dowel, and screw joints under static load test, how to design joints by using these design values, and how to evaluate performance testing of chairs of which joints were designed by the

proposed procedure in order to provide reliable furniture structures within the furniture industry.

The dissertation presents a systematic procedure to determine the implications of what strength capacity of joints is used for design purposes, which is discussed in Chapter 3. These design values will be beneficial to design reliable furniture since reasonable design values will be known under nominal conditions and these joints would be designed. The results of testing in Chapters 4 and 5 proved that the reliability of joints could be increased as long as internal stress in joints transferred by external loads do not exceed the design values.

The results of this study aim to (i) increase joint reliability, so that furniture would have a long service life for sustainable product design, (ii) reduce failure probability, so that number of injuries and deaths owing to furniture failure would be decreased, and (iii) reduce warranty cost by preventing probability of furniture failure in service and number of returned products.

## APPENDIX A. TABLES FOR RATIONAL DESIGN OF JOINTS

A-factor is related to both width of tenon and rail used in joints. It was derived from equation of  $(0.57T_w \times 0.24R_w)$  where,  $T_w$  is width of tenon and  $R_w$  is width of rail. A-factors for various width of tenons and rails are shown in Table A.1.

Table A.1 A-Factors for Rectangular Mortise and Tenon Joint [4]

Rail Width (in.)	Tenon Width (in.)													
	0.50	0.75	1.00	1.25	1.50	1.75	2.00	2.25	2.50	2.75	3.00	3.25	3.50	
1.00	0.525	0.668	0.810											
1.25	0.585	0.728	0.870	1.013										
1.50	0.645	0.788	0.930	1.073	1.215									
1.75	0.705	0.848	0.990	1.133	1.275	1.418								
2.00	0.765	0.908	1.050	1.193	1.335	1.478	1.620							
2.25	0.825	0.968	1.110	1.253	1.395	1.538	1.680	1.823						
2.50	0.885	1.028	1.170	1.313	1.455	1.598	1.740	1.883	2.025					
2.75	0.945	1.088	1.230	1.373	1.515	1.658	1.800	1.943	2.085	2.228				
3.00	1.005	1.148	1.290	1.433	1.575	1.718	1.860	2.003	2.145	2.288	2.430			
3.25	1.065	1.208	1.350	1.493	1.635	1.778	1.920	2.063	2.205	2.348	2.490	2.633		
3.50	1.125	1.268	1.410	1.553	1.695	1.838	1.980	2.123	2.265	2.408	2.550	2.693	2.835	
3.75	1.185	1.328	1.470	1.613	1.755	1.898	2.040	2.183	2.325	2.468	2.610	2.753	2.895	

B-factor is related to length of tenon. Unless length of tenon is enough, joint strength relies on glues strength, so failures at lower strength are observed. C-factor is related to adhesive type. In the case of enough glue is used in joint, PVAc with higher solid content provides higher joint strength. Furthermore, D-factor is related to tolerances between face of tenons and wall of mortises. If tolerance increases, joint strength relied on shear strength of glueline rather than wood strength so joint may not behave as mechanical joint. By doing so, joint strength reduces with increase in tolerance between face of tenon and wall of mortises.

Table A.2 B, C and D-Factors for Rectangular Mortise and Tenon [4]

<b>B-Factor</b>		<b>C-factor</b>	
<b>Tenon</b>		<b>Adhesive</b>	
<b>Length (in.)</b>	<b>Factor</b>	<b>Type</b>	<b>Factor</b>
0.500	0.48	Phenol-Resorcinol	1.00
0.625	0.68	Animal	1.05
0.750	0.80	UF	1.24
0.875	0.90	PVA - 62 % solids	1.32
1.000	1.00		
1.125	1.06	<b>D-factors</b>	
1.250	1.12	<b>Tenon fit</b>	
1.375	1.20	<b>Fit (in.)</b>	<b>Factor</b>
1.500	1.28	0.000 to 0.002	1.00
1.625	1.36	0.003 to 0.005	0.94
1.750	1.46	0.006 to 0.008	0.89
1.875	1.56		
2.000	1.66		

For two-pin bending resisting dowel joints, A-factor is given in Table A.3 while B-factor are shown in Table A.4

Table A. 3 A-Factors for Dowel Joints [4]

<b>Dowel Diameter (in.)</b>	<b>Depth of Dowel Embedment</b>						
	<b>1/2</b>	<b>3/4</b>	<b>1</b>	<b>1-1/4</b>	<b>1-1/2</b>	<b>1-3/4</b>	<b>2</b>
<b>1/4</b>	0.11	0.16	0.21				
<b>5/16</b>	0.14	0.20	0.26	0.32			
<b>3/8</b>	0.17	0.24	0.31	0.38	0.45		
<b>7/16</b>	0.20	0.28	0.36	0.44	0.52	0.60	
<b>1/2</b>	0.23	0.32	0.41	0.50	0.59	0.68	0.77

Table A.4 B-Factors for Dowel Joints [4]

<b>Dowel- Hole Clearance (in.)</b>	<b>Type of Adhesive</b>		
	<b>UF</b>	<b>PVA</b>	<b>Animal</b>
	<b>Adhesive Clearance Factor</b>		
0.000	1.00	0.90	0.85
0.001	0.99	0.88	0.85
0.002	0.98	0.87	0.85
0.003	0.97	0.85	0.84
0.004	0.96	0.84	0.84
0.005	0.96	0.82	0.84
0.006	0.95	0.81	0.84
0.007	0.94	0.79	0.84
0.008	0.93	0.78	0.84
0.009	0.92	0.76	0.84
0.010	0.91	0.75	0.83

**Table 7.** Length Diameter Factors for Screws Driven into the Side Grain of Solid Wood ( $3.2 \times D \times (L - D)^{3/4}$ ) [4]

Screw Gage	Length-Diameter Factors- Side Grain										
	Depth of Penetration (in.)										
	1/4	3/8	1/2	5/8	3/4	7/8	1	1 1/4	1 1/2	1 3/4	2
<b>1</b>	0.064	0.095	0.124	0.15	0.175	0.198	0.221	0.264	0.305	0.345	0.383
<b>2</b>	0.071	0.109	0.142	0.173	0.203	0.231	0.258	0.309	0.357	0.404	0.448
<b>3</b>	0.077	0.121	0.16	0.196	0.23	0.262	0.293	0.352	0.408	0.462	0.514
<b>4</b>	0.081	0.132	0.176	0.218	0.256	0.293	0.328	0.395	0.459	0.52	0.578
<b>5</b>	0.084	0.142	0.192	0.238	0.282	0.323	0.362	0.437	0.509	0.576	0.642
<b>6</b>	0.086	0.15	0.206	0.258	0.306	0.352	0.396	0.479	0.557	0.633	0.705
<b>7</b>	0.085	0.158	0.22	0.276	0.329	0.38	0.428	0.519	0.606	0.688	0.767
<b>8</b>	0.083	0.164	0.232	0.294	0.352	0.407	0.459	0.559	0.653	0.743	0.829
<b>10</b>	0.074	0.172	0.253	0.326	0.394	0.458	0.52	0.636	0.745	0.85	0.95
<b>12</b>	0.055	0.174	0.269	0.354	0.432	0.506	0.577	0.71	0.835	0.954	1.068
<b>14</b>	0.021	0.171	0.281	0.377	0.467	0.55	0.63	0.78	0.921	1.055	1.184
<b>16</b>	0.000	0.161	0.287	0.397	0.497	0.59	0.68	0.847	1.004	1.153	1.296
<b>18</b>	0.000	0.143	0.288	0.411	0.523	0.627	0.726	0.911	1.084	1.249	1.406
<b>20</b>	0.000	0.116	0.283	0.421	0.544	0.659	0.768	0.971	1.161	1.341	1.513

**Table 8.** Length Diameter Factors for Screws Driven into the End Grain of Solid Wood ( $8.75 \times D^{1.75} \times (L - D)^{0.75}$ ) [4]

Screw Gage	Length-Diameter Factors- Side Grain										
	Depth of Penetration (in.)										
	1/4	3/8	1/2	5/8	3/4	7/8	1	1 1/4	1 1/2	1 3/4	2
<b>1</b>	0.024	0.037	0.047	0.057	0.067	0.076	0.085	0.101	0.117	0.132	0.147
<b>2</b>	0.031	0.047	0.062	0.075	0.088	0.100	0.112	0.134	0.155	0.175	0.195
<b>3</b>	0.037	0.058	0.077	0.094	0.111	0.126	0.141	0.170	0.197	0.223	0.248
<b>4</b>	0.043	0.070	0.093	0.115	0.135	0.155	0.174	0.209	0.243	0.275	0.306
<b>5</b>	0.048	0.081	0.110	0.137	0.162	0.185	0.208	0.251	0.292	0.331	0.369
<b>6</b>	0.053	0.093	0.128	0.159	0.189	0.218	0.245	0.296	0.345	0.391	0.436
<b>7</b>	0.056	0.104	0.145	0.183	0.218	0.251	0.283	0.344	0.401	0.455	0.508
<b>8</b>	0.059	0.115	0.163	0.207	0.248	0.286	0.323	0.394	0.460	0.523	0.583
<b>10</b>	0.058	0.135	0.199	0.256	0.310	0.360	0.409	0.500	0.586	0.668	0.747
<b>12</b>	0.047	0.151	0.233	0.306	0.374	0.438	0.499	0.614	0.722	0.826	0.926
<b>14</b>	0.020	0.161	0.265	0.356	0.440	0.519	0.594	0.735	0.868	0.994	1.116
<b>16</b>	0.000	0.163	0.292	0.404	0.505	0.601	0.691	0.862	1.022	1.173	1.319
<b>18</b>	0.000	0.156	0.314	0.448	0.570	0.684	0.791	0.993	1.182	1.362	1.534
<b>20</b>	0.000	0.135	0.329	0.489	0.633	0.766	0.892	1.128	1.349	1.558	1.758

## APPENDIX B. SAMPLE PREPARATION AND TESTING

Samples for bending test of clear specimen were cut from heartwood to prevent variation in strength properties between heartwood and sapwood. On the other hand, this variation is not considered for joint specimens because both heartwood and sapwood may be consisted in furniture construction. Therefore, consistency of sapwood and heartwood is considered as lurking variable for joint strength in experiment.



Figure B.1 Wood Lumbers A. Red Oak, B. White Oak

Sample for bending test and depiction of test set up are shown in below:



Figure B.2 A. Red Oak Samples, B. White Oak Samples and C. Test Set-Up



Figure B.3 Chair Sample for Static Load Test and Typical Joint Failure

**APPENDIX C. TABLES FOR K-TOLERANCE FACTOR  
DEPENDING ON SMAPLE SIZES AND ASSUMPTION**

Table C.1 k-Tolerance Factors for One-Sided Tolerance Limits ( $\gamma$ , P) Given by [148]

n	$\gamma$	0.90			0.95			0.99		
	$\beta$	0.90	0.95	0.99	0.90	0.95	0.99	0.90	0.95	0.99
3		4.258	5.130	7.340	6.158	7.655	10.552			
4		3.187	3.957	5.437	4.163	5.145	7.042			
5		2.742	3.400	4.666	3.407	4.202	5.741			
6		2.494	3.091	4.242	3.066	3.707	5.062	4.408	5.409	7.334
7		2.333	2.894	3.972	2.755	3.399	4.641	3.856	4.730	6.411
8		2.219	2.755	3.783	2.582	3.188	4.353	3.496	4.287	5.811
9		2.133	2.649	3.641	2.454	3.031	4.143	3.252	3.971	5.389
10		2.065	2.568	3.532	2.355	2.911	3.981	3.048	3.739	5.075
11		2.012	2.503	3.444	2.275	2.815	3.852	2.897	3.557	4.828
12		1.966	2.448	3.371	2.210	2.736	3.747	2.773	3.410	4.633
13		1.928	2.403	3.310	2.155	2.670	3.659	2.677	3.290	4.472
14		1.895	2.363	3.257	2.108	2.614	3.585	2.592	3.189	4.336
15		1.866	2.329	3.212	2.068	2.566	3.520	2.521	3.102	4.224
16		1.842	2.299	3.172	2.032	2.523	3.463	2.458	3.028	4.124
17		1.820	2.272	3.136	2.001	2.486	3.415	2.405	2.962	4.038
18		1.800	2.249	3.106	1.974	2.453	3.370	2.357	2.906	3.961
19		1.781	2.228	3.078	1.949	2.423	3.331	2.315	2.855	3.893
20		1.765	2.208	3.052	1.926	2.396	3.295	2.275	2.807	3.832
21		1.750	2.190	3.028	1.905	2.371	3.262	2.241	2.768	3.776
22		1.736	2.174	3.007	1.887	2.350	3.233	2.208	2.729	3.727
23		1.724	2.159	2.987	1.869	2.329	3.206	2.179	2.693	3.680
24		1.712	2.145	2.969	1.853	2.309	3.181	2.154	2.663	3.638
25		1.702	2.132	2.952	1.838	2.292	3.158	2.129	2.632	3.601
30		1.657	2.080	2.884	1.778	2.220	3.064	2.029	2.516	3.446
35		1.623	2.041	2.833	1.732	2.166	2.994	1.957	2.431	3.334
40		1.598	2.010	2.793	1.697	2.126	2.941	1.902	2.365	3.250
45		1.577	1.986	2.762	1.669	2.092	2.897	1.857	2.313	3.181
50		1.560	1.965	2.735	1.649	2.065	2.863	1.821	2.296	3.124
$\infty$		1.282	1.645	2.326	1.282	1.645	2.326	1.282	1.645	2.326

Table C.2 Tolerance Factors for One Sided Tolerance Limits (0.90, P) by Using Equations Given by [148]

n	$\gamma$	0.90					
	$\beta$	0.90		0.95		0.99	
		1*	2**	1	2	1	2
3		3.8684	3.86979 ± 0.00351	4.82208	4.8242 ± 0.00415	6.65344	6.65625 ± 0.00533
4		2.95522	2.95601 ± 0.002	3.66814	3.66941 ± 0.0023	5.03994	5.04159 ± 0.00285
5		2.58586	2.58647 ± 0.00153	3.20679	3.20778 ± 0.00172	4.40128	4.40256 ± 0.00208
6		2.37819	2.3787 ± 0.00129	2.94976	2.95061 ± 0.00144	4.04842	4.04952 ± 0.00171
7		2.24209	2.24255 ± 0.00115	2.78252	2.7833 ± 0.00127	3.82042	3.82141 ± 0.0015
8		2.1446	2.14502 ± 0.00106	2.66343	2.66415 ± 0.00116	3.65897	3.65989 ± 0.00135
9		2.07058	2.07098 ± 0.00099	2.57345	2.57413 ± 0.00108	3.53758	3.53844 ± 0.00125
10		2.01204	2.01241 ± 0.00094	2.50257	2.50322 ± 0.00102	3.44234	3.44316 ± 0.00117
11		1.96431	1.96467 ± 0.0009	2.44498	2.44561 ± 0.00097	3.36523	3.36603 ± 0.00111
12		1.92448	1.92482 ± 0.00087	2.39706	2.39767 ± 0.00093	3.30126	3.30203 ± 0.00106
13		1.8906	1.89093 ± 0.00084	2.35642	2.35701 ± 0.0009	3.24716	3.2479 ± 0.00102
14		1.86135	1.86167 ± 0.00082	2.3214	2.32198 ± 0.00088	3.20066	3.20139 ± 0.00098
15		1.83578	1.83609 ± 0.0008	2.29086	2.29142 ± 0.00085	3.16018	3.16089 ± 0.00095
16		1.81318	1.81349 ± 0.00078	2.26392	2.26447 ± 0.00083	3.12455	3.12524 ± 0.00093
17		1.79304	1.79334 ± 0.00077	2.23993	2.24048 ± 0.00081	3.09288	3.09357 ± 0.0009
18		1.77493	1.77523 ± 0.00075	2.21841	2.21895 ± 0.0008	3.06451	3.06519 ± 0.00089
19		1.75855	1.75884 ± 0.00074	2.19897	2.1995 ± 0.00079	3.03892	3.03958 ± 0.00087
20		1.74363	1.74392 ± 0.00073	2.18129	2.18181 ± 0.00077	3.01568	3.01634 ± 0.00085
21		1.72999	1.73027 ± 0.00072	2.16513	2.16565 ± 0.00076	2.99446	2.99511 ± 0.00084
22		1.71743	1.71772 ± 0.00071	2.15028	2.1508 ± 0.00075	2.975	2.97564 ± 0.00082
23		1.70584	1.70612 ± 0.0007	2.13659	2.1371 ± 0.00074	2.95706	2.9577 ± 0.00081
24		1.6951	1.69537 ± 0.0007	2.12391	2.12441 ± 0.00072	2.94046	2.94109 ± 0.0008
25		1.6851	1.68538 ± 0.00069	2.11212	2.11262 ± 0.00069	2.92505	2.92568 ± 0.00079

Table C.2 continued Tolerance factors for one sided tolerance limits (0.90, P) by using equations given by [148]

<b>30</b>	1.64386	1.64412 ± 0.00066	2.06358	2.06406 ± 0.00069	2.86174	2.86235 ± 0.00075
<b>35</b>	1.61284	1.61309 ± 0.00064	2.02719	2.02766 ± 0.00067	2.81445	2.81503 ± 0.00072
<b>40</b>	1.58845	1.5887 ± 0.00062	1.99865	1.99911 ± 0.00065	2.77745	2.77802 ± 0.0007
<b>45</b>	1.56864	1.56888 ± 0.00061	1.97551	1.97596 ± 0.00064	2.74752	2.74808 ± 0.00068
<b>50</b>	1.55215	1.55239 ± 0.0006	1.95628	1.95672 ± 0.00062	2.72268	2.72324 ± 0.00066
$\infty$	1.28155	1.28173 ± 0.00045	1.64485	1.64521 ± 0.00045	2.32635	2.32679 ± 0.00045

\* When k-factor is calculated, z-scores are obtained by MS Excel equation (“*normsinv(probability)*”)

\*\* When k-factor is calculated, z-scores are obtained by using rational approximation for z-scores [177]

Table C.3 Tolerance Factors for One Sided Tolerance Limits (0.95, P) by Using Equations Given by [148]

n	$\gamma$ $\beta$	0.95					
		0.90		0.95		0.99	
		1*	2**	1	2	1	2
3		7.61994	7.62828 ± 0.01167	9.58397	9.59534 ± 0.01427	13.33195	13.34764 ± 0.01913
4		4.25452	4.25684 ± 0.00355	5.29317	5.2965 ± 0.00418	7.29074	7.29524 ± 0.00534
5		3.38067	3.38206 ± 0.00224	4.1903	4.19236 ± 0.00258	5.75041	5.75315 ± 0.0032
6		2.9624	2.96344 ± 0.00174	3.66698	3.66855 ± 0.00197	5.02495	5.02702 ± 0.00239
7		2.71113	2.71199 ± 0.00147	3.35485	3.35616 ± 0.00164	4.59505	4.59677 ± 0.00197
8		2.54084	2.54158 ± 0.0013	3.14457	3.14572 ± 0.00144	4.30704	4.30854 ± 0.00171
9		2.41646	2.41712 ± 0.00119	2.99175	2.99279 ± 0.00131	4.09874	4.10009 ± 0.00153
10		2.32087	2.32147 ± 0.0011	2.8748	2.87577 ± 0.00121	3.94	3.94125 ± 0.00141
11		2.24464	2.24521 ± 0.00104	2.78189	2.7828 ± 0.00114	3.81435	3.81551 ± 0.00131
12		2.18214	2.18267 ± 0.00099	2.70596	2.70682 ± 0.00108	3.71198	3.71308 ± 0.00123
13		2.12976	2.13026 ± 0.00095	2.6425	2.64332 ± 0.00103	3.62667	3.62772 ± 0.00117
14		2.08508	2.08556 ± 0.00092	2.58851	2.5893 ± 0.00099	3.55428	3.55529 ± 0.00112
15		2.04642	2.04689 ± 0.00089	2.5419	2.54267 ± 0.00096	3.49194	3.49291 ± 0.00108
16		2.01257	2.01301 ± 0.00086	2.50117	2.50191 ± 0.00093	3.43756	3.4385 ± 0.00104
17		1.98261	1.98305 ± 0.00084	2.4652	2.46592 ± 0.0009	3.38963	3.39055 ± 0.00101
18		1.95588	1.9563 ± 0.00082	2.43315	2.43385 ± 0.00088	3.347	3.3479 ± 0.00098
19		1.93184	1.93225 ± 0.00081	2.40437	2.40505 ± 0.00086	3.30879	3.30966 ± 0.00096
20		1.91007	1.91047 ± 0.00079	2.37835	2.37902 ± 0.00084	3.27429	3.27514 ± 0.00094
21		1.89025	1.89064 ± 0.00078	2.35468	2.35535 ± 0.00083	3.24296	3.2438 ± 0.00092
22		1.8721	1.87248 ± 0.00077	2.33305	2.3337 ± 0.00081	3.21435	3.21517 ± 0.0009
23		1.85541	1.85579 ± 0.00076	2.31317	2.31381 ± 0.0008	3.1881	3.18891 ± 0.00089
24		1.83999	1.84036 ± 0.00075	2.29483	2.29546 ± 0.00079	3.1639	3.1647 ± 0.00087
25		1.8257	1.82607 ± 0.00074	2.27785	2.27847 ± 0.00078	3.14152	3.1423 ± 0.00086

Table C.3 continued Tolerance Factors for One Sided Tolerance Limits (0.95, P) by Using Equations Given by [148]

<b>30</b>		1.76721	1.76755 ± 0.0007	2.20851	2.2091 ± 0.00074	3.05039	3.05113 ± 0.0008
<b>35</b>		1.72373	1.72405 ± 0.00067	2.15715	2.15771 ± 0.00071	2.98314	2.98385 ± 0.00077
<b>40</b>		1.68982	1.69013 ± 0.00065	2.11721	2.11776 ± 0.00068	2.93102	2.9317 ± 0.00074
<b>45</b>		1.66247	1.66277 ± 0.00064	2.08507	2.0856 ± 0.00067	2.88916	2.88983 ± 0.00072
<b>50</b>		1.63981	1.6401 ± 0.00063	2.05849	2.05901 ± 0.00065	2.85463	2.85528 ± 0.0007
$\infty$		1.28155	1.28173 ± 0.00045	1.64485	1.64521 ± 0.00045	2.32635	2.32679 ± 0.00045

\* When k-factor is calculated, z-scores are obtained by MS Excel equation (“*normsinv(probability)*”)

\*\* When k-factor is calculated, z-scores are obtained by using rational approximation for z-scores [177]

Table C.4 Tolerance Factors for One Sided Tolerance Limits (0.99, P) by Using Equations Given by [148]

n	$\gamma$	0.99								
	$\beta$	0.90			0.95			0.99		
		1*	2**		1	2		1	2	
6		5.28083	5.28409	± 0.00428	6.57194	6.57656	± 0.00504	9.05527	9.06154	± 0.00644
7		4.30043	4.30251	± 0.00289	5.33195	5.33497	± 0.00334	7.32052	7.32458	± 0.00417
8		3.75945	3.761	± 0.00224	4.65168	4.65398	± 0.00256	6.37345	6.37652	± 0.00315
9		3.41213	3.41339	± 0.00188	4.21717	4.21906	± 0.00212	5.77123	5.77374	± 0.00257
10		3.168	3.16908	± 0.00164	3.91313	3.91476	± 0.00184	5.35155	5.3537	± 0.00221
11		2.98573	2.98668	± 0.00148	3.68704	3.68849	± 0.00165	5.0406	5.04251	± 0.00196
12		2.84367	2.84453	± 0.00136	3.51145	3.51277	± 0.00151	4.79991	4.80164	± 0.00177
13		2.72934	2.73012	± 0.00127	3.37057	3.37179	± 0.0014	4.60738	4.60897	± 0.00163
14		2.63498	2.63571	± 0.00119	3.25465	3.25579	± 0.00131	4.4494	4.45088	± 0.00152
15		2.55556	2.55624	± 0.00113	3.15732	3.1584	± 0.00124	4.31708	4.31848	± 0.00143
16		2.48761	2.48825	± 0.00109	3.07425	3.07527	± 0.00118	4.20441	4.20574	± 0.00136
17		2.42868	2.4293	± 0.00104	3.00237	3.00335	± 0.00114	4.10713	4.10839	± 0.0013
18		2.377	2.37759	± 0.00101	2.93945	2.94039	± 0.00109	4.02214	4.02335	± 0.00125
19		2.33123	2.33179	± 0.00098	2.88383	2.88473	± 0.00106	3.94714	3.94831	± 0.0012
20		2.29035	2.2909	± 0.00095	2.83423	2.83511	± 0.00103	3.88039	3.88152	± 0.00116
21		2.25358	2.2541	± 0.00093	2.78969	2.79054	± 0.001	3.82052	3.82162	± 0.00113
22		2.22027	2.22078	± 0.00091	2.74941	2.75024	± 0.00097	3.76648	3.76755	± 0.0011
23		2.18995	2.19044	± 0.00089	2.71278	2.71359	± 0.00095	3.71739	3.71843	± 0.00107
24		2.16218	2.16267	± 0.00087	2.67929	2.68008	± 0.00093	3.67258	3.6736	± 0.00104
25		2.13666	2.13713	± 0.00085	2.64853	2.64931	± 0.00091	3.63147	3.63247	± 0.00102
30		2.03422	2.03465	± 0.00079	2.5255	2.52621	± 0.00085	3.46754	3.46845	± 0.00093
35		1.96007	1.96047	± 0.00075	2.43683	2.4375	± 0.0008	3.34995	3.3508	± 0.00087

Table C.4 continued Tolerance Factors for One Sided Tolerance Limits (0.99, P) by Using Equations Given by [148]

<b>40</b>	1.90337	1.90375 ± 0.00072	2.36927	2.36991 ± 0.00076	3.26068	3.26149 ± 0.00083
<b>45</b>	1.8583	1.85865 ± 0.0007	2.31571	2.31633 ± 0.00073	3.19014	3.19092 ± 0.0008
<b>50</b>	1.82141	1.82175 ± 0.00068	2.27199	2.27258 ± 0.00071	3.13269	3.13344 ± 0.00077
∞	1.28155	1.28173 ± 0.00045	1.64485	1.64521 ± 0.00045	2.32635	2.32679 ± 0.00045

\* When k-factor is calculated, z-scores are obtained by MS Excel equation (“*normsinv(probability)*”)

\*\* When k-factor is calculated, z-scores are obtained by using rational approximation for z-scores [177]

Table C.5 Error (%) between Tabulated k-Factors (in Table C.1) and Calculated k-Factors by Using Equation Given by [148]

n	$\gamma$	0.90			0.95			0.99		
	$\beta$	0.90	0.95	0.99	0.90	0.95	0.99	0.90	0.95	0.99
3		-9.15	-6.00	-9.35	23.74	25.20	26.35			
4		-7.27	-7.30	-7.30	2.20	2.88	3.53			
5		-5.69	-5.68	-5.67	-0.77	-0.28	0.16			
6		-4.64	-4.57	-4.56	-3.38	-1.08	-0.73	19.80	21.50	23.47
7		-3.90	-3.85	-3.82	-1.59	-1.30	-0.99	11.53	12.73	14.19
8		-3.35	-3.32	-3.28	-1.59	-1.36	-1.06	7.54	8.51	9.68
9		-2.93	-2.85	-2.84	-1.53	-1.30	-1.07	4.92	6.20	7.09
10		-2.56	-2.55	-2.54	-1.45	-1.24	-1.03	3.94	4.66	5.45
11		-2.37	-2.32	-2.29	-1.33	-1.18	-0.98	3.06	3.66	4.40
12		-2.11	-2.08	-2.07	-1.26	-1.10	-0.93	2.55	2.98	3.60
13		-1.94	-1.94	-1.90	-1.17	-1.03	-0.88	1.95	2.45	3.03
14		-1.78	-1.76	-1.73	-1.09	-0.98	-0.86	1.66	2.06	2.62
15		-1.62	-1.64	-1.61	-1.04	-0.94	-0.80	1.37	1.78	2.20
16		-1.56	-1.53	-1.50	-0.96	-0.87	-0.73	1.20	1.53	1.95
17		-1.48	-1.41	-1.37	-0.92	-0.84	-0.74	0.98	1.36	1.71
18		-1.39	-1.36	-1.34	-0.92	-0.81	-0.68	0.85	1.15	1.54
19		-1.26	-1.30	-1.27	-0.88	-0.77	-0.67	0.70	1.01	1.39
20		-1.21	-1.21	-1.19	-0.83	-0.74	-0.63	0.67	0.97	1.26
21		-1.14	-1.14	-1.11	-0.77	-0.69	-0.58	0.56	0.78	1.18
22		-1.07	-1.09	-1.06	-0.79	-0.72	-0.58	0.56	0.75	1.06
23		-1.05	-1.04	-1.00	-0.73	-0.68	-0.56	0.50	0.73	1.02
24		-0.99	-0.98	-0.96	-0.70	-0.61	-0.54	0.38	0.61	0.95
25		-0.99	-0.93	-0.91	-0.67	-0.62	-0.52	0.36	0.63	0.85
30		-0.79	-0.79	-0.77	-0.61	-0.52	-0.44	0.26	0.38	0.63
35		-0.63	-0.68	-0.65	-0.48	-0.41	-0.36	0.16	0.24	0.48
40		-0.60	-0.56	-0.56	-0.42	-0.41	-0.34	0.07	0.18	0.33
45		-0.53	-0.53	-0.52	-0.39	-0.33	-0.27	0.07	0.12	0.29
50		-0.50	-0.44	-0.45	-0.56	-0.32	-0.29	0.02	-1.05	0.28
$\infty$		-0.03	-0.01	0.01	-0.03	-0.01	0.01	-0.03	-0.01	0.01

Table C.6 Tolerance Factors for One Sided Tolerance Limits (0.90, P) by Calculating Using Given by [179]

n	$\gamma$	0.90					
	$\beta$	0.90		0.95		0.99	
		1*	2**	1	2	1	2
3		5.78373	5.78657 ± 0.00719	7.27181	7.27598 ± 0.00868	10.1119	10.1175 ± 0.01147
4		3.53139	3.53244 ± 0.00268	4.40261	4.40428 ± 0.00312	6.07483	6.07703 ± 0.00393
5		2.89298	2.8937 ± 0.00182	3.59757	3.59874 ± 0.00207	4.95125	4.95277 ± 0.00253
6		2.57953	2.5801 ± 0.00146	3.20567	3.20663 ± 0.00164	4.40833	4.40956 ± 0.00196
7		2.38891	2.3894 ± 0.00127	2.96902	2.96986 ± 0.0014	4.08259	4.08367 ± 0.00166
8		2.2588	2.25925 ± 0.00114	2.80844	2.80921 ± 0.00126	3.86277	3.86376 ± 0.00147
9		2.16333	2.16375 ± 0.00105	2.6912	2.69192 ± 0.00115	3.70304	3.70396 ± 0.00133
10		2.08973	2.09012 ± 0.00099	2.60119	2.60188 ± 0.00108	3.58091	3.58178 ± 0.00124
11		2.0309	2.03127 ± 0.00094	2.52952	2.53017 ± 0.00102	3.484	3.48483 ± 0.00116
12		1.98258	1.98294 ± 0.0009	2.47083	2.47146 ± 0.00097	3.40491	3.4057 ± 0.00111
13		1.94203	1.94238 ± 0.00087	2.42172	2.42233 ± 0.00094	3.3389	3.33967 ± 0.00106
14		1.90741	1.90775 ± 0.00084	2.37989	2.38048 ± 0.00091	3.28283	3.28358 ± 0.00102
15		1.87743	1.87775 ± 0.00082	2.34374	2.34432 ± 0.00088	3.23449	3.23522 ± 0.00098
16		1.85115	1.85147 ± 0.0008	2.31213	2.3127 ± 0.00086	3.19229	3.19301 ± 0.00096
17		1.82789	1.8282 ± 0.00078	2.2842	2.28476 ± 0.00084	3.15508	3.15578 ± 0.00093
18		1.80712	1.80742 ± 0.00077	2.25929	2.25984 ± 0.00082	3.12196	3.12265 ± 0.00091
19		1.78843	1.78873 ± 0.00076	2.23692	2.23747 ± 0.0008	3.09226	3.09294 ± 0.00089
20		1.7715	1.7718 ± 0.00074	2.21669	2.21723 ± 0.00079	3.06544	3.06611 ± 0.00087
21		1.75608	1.75637 ± 0.00073	2.19828	2.19881 ± 0.00078	3.04107	3.04173 ± 0.00085
22		1.74196	1.74225 ± 0.00072	2.18145	2.18197 ± 0.00076	3.0188	3.01946 ± 0.00084
23		1.72897	1.72925 ± 0.00071	2.16598	2.1665 ± 0.00075	2.99837	2.99902 ± 0.00083
24		1.71697	1.71725 ± 0.00071	2.1517	2.15221 ± 0.00074	2.97954	2.98018 ± 0.00082

Table C.6 continued Tolerance Factors for One Sided Tolerance Limits (0.90, P) by Calculating Using Given by [179]

<b>25</b>	1.70584	1.70612 ± 0.0007	2.13848	2.13898 ± 0.00074	2.96211	2.96274 ± 0.0008
<b>30</b>	1.66028	1.66055 ± 0.00067	2.08447	2.08495 ± 0.0007	2.89112	2.89173 ± 0.00076
<b>35</b>	1.6264	1.62665 ± 0.00065	2.04443	2.04491 ± 0.00068	2.8387	2.83929 ± 0.00073
<b>40</b>	1.59996	1.60021 ± 0.00063	2.0133	2.01376 ± 0.00066	2.79806	2.79864 ± 0.0007
<b>45</b>	1.57863	1.57887 ± 0.00062	1.98823	1.98868 ± 0.00064	2.76541	2.76598 ± 0.00068
<b>50</b>	1.56096	1.5612 ± 0.00061	1.9675	1.96795 ± 0.00063	2.73847	2.73903 ± 0.00067
$\infty$	1.28155	1.28173 ± 0.00045	1.64485	1.64521 ± 0.00045	2.32635	2.32679 ± 0.00045

\* When k-factor is calculated, z-scores are obtained by MS Excel equation (“*normsinv(probability)*”)

\*\* When k-factor is calculated, z-scores are obtained by using rational approximation for z-scores [177]

Table C.7 Tolerance Factors for One Sided Tolerance Limits (0.95, P) by Using Equations Given by [179]

n	$\gamma$ $\beta$	0.95					
		0.90		0.95		0.99	
		1*	2**	1	2	1	2
3		24.7969	24.8836 ± 0.11291	31.6167	31.7304 ± 0.14252	44.4841	44.6436 ± 0.19803
4		5.5906	5.59449 ± 0.00575	7.0006	7.00607 ± 0.00687	9.70012	9.70758 ± 0.00895
5		3.92507	3.92689 ± 0.00287	4.8842	4.88686 ± 0.00334	6.72806	6.73162 ± 0.0042
6		3.27793	3.27916 ± 0.00204	4.06847	4.07032 ± 0.00232	5.59003	5.59248 ± 0.00285
7		2.92518	2.92615 ± 0.00165	3.62692	3.6284 ± 0.00185	4.9777	4.97965 ± 0.00224
8		2.69952	2.70033 ± 0.00142	3.34611	3.34737 ± 0.00159	4.59036	4.59202 ± 0.00189
9		2.54094	2.54166 ± 0.00128	3.14979	3.15091 ± 0.00141	4.32083	4.32229 ± 0.00166
10		2.42243	2.42307 ± 0.00117	3.0037	3.00472 ± 0.00129	4.12109	4.12242 ± 0.0015
11		2.3299	2.3305 ± 0.0011	2.89008	2.89104 ± 0.0012	3.96631	3.96755 ± 0.00139
12		2.25529	2.25585 ± 0.00104	2.79877	2.79967 ± 0.00113	3.84233	3.84349 ± 0.0013
13		2.19361	2.19413 ± 0.00099	2.7235	2.72436 ± 0.00107	3.74043	3.74153 ± 0.00123
14		2.14158	2.14208 ± 0.00095	2.66019	2.66101 ± 0.00103	3.65494	3.65599 ± 0.00117
15		2.09699	2.09747 ± 0.00092	2.60605	2.60684 ± 0.00099	3.58202	3.58303 ± 0.00112
16		2.05825	2.05872 ± 0.00089	2.55913	2.55989 ± 0.00096	3.51895	3.51993 ± 0.00108
17		2.02423	2.02467 ± 0.00086	2.51799	2.51873 ± 0.00093	3.46377	3.46471 ± 0.00104
18		1.99404	1.99447 ± 0.00084	2.48156	2.48228 ± 0.0009	3.41499	3.41591 ± 0.00101
19		1.96704	1.96746 ± 0.00083	2.44903	2.44974 ± 0.00088	3.37151	3.37241 ± 0.00099
20		1.94272	1.94313 ± 0.00081	2.41977	2.42046 ± 0.00086	3.33246	3.33334 ± 0.00096
21		1.92066	1.92106 ± 0.00079	2.39328	2.39395 ± 0.00085	3.29716	3.29802 ± 0.00094
22		1.90055	1.90094 ± 0.00078	2.36915	2.36982 ± 0.00083	3.26506	3.2659 ± 0.00092
23		1.88212	1.88251 ± 0.00077	2.34707	2.34772 ± 0.00082	3.23571	3.23653 ± 0.0009
24		1.86516	1.86553 ± 0.00076	2.32677	2.32741 ± 0.0008	3.20876	3.20957 ± 0.00089

Table C.7 continued Tolerance Factors for One Sided Tolerance Limits (0.95, P) by Using Equations Given by [179]

<b>25</b>	1.84947	1.84984 ± 0.00075	2.30802	2.30865 ± 0.00079	3.1839	3.1847 ± 0.00087
<b>30</b>	1.78576	1.78611 ± 0.00071	2.23206	2.23266 ± 0.00075	3.08348	3.08423 ± 0.00082
<b>35</b>	1.73886	1.73919 ± 0.00068	2.17637	2.17694 ± 0.00072	3.01016	3.01088 ± 0.00078
<b>40</b>	1.70257	1.70288 ± 0.00066	2.13341	2.13396 ± 0.00069	2.95378	2.95447 ± 0.00075
<b>45</b>	1.67345	1.67375 ± 0.00064	2.09903	2.09956 ± 0.00067	2.90879	2.90946 ± 0.00072
<b>50</b>	1.64944	1.64974 ± 0.00063	2.07074	2.07126 ± 0.00066	2.87185	2.87251 ± 0.0007
∞	1.28155	1.28173 ± 0.00045	1.64485	1.64521 ± 0.00045	2.32635	2.32679 ± 0.00045

\* When k-factor is calculated, z-scores are obtained by MS Excel equation (“*normsinv(probability)*”)

\*\* When k-factor is calculated, z-scores are obtained by using rational approximation for z-scores [177]

Table C.8 Tolerance Factors for One Sided Tolerance Limits (0.99, P) by Using Equations Given by [179]

n	$\gamma$ $\beta$	0.99					
		0.90		0.95		0.99	
		1*	2**	1	2	1	2
6		6.42002	6.42476 ± 0.00603	8.02789	8.03452 ± 0.00717	11.1099	11.119 ± 0.0093
7		4.87353	4.87617 ± 0.00356	6.06299	6.06677 ± 0.00415	8.35101	8.35612 ± 0.00524
8		4.11753	4.11936 ± 0.0026	5.10778	5.11047 ± 0.00299	7.0158	7.0194 ± 0.0037
9		3.66328	3.66471 ± 0.0021	4.53671	4.53884 ± 0.00239	6.22093	6.22377 ± 0.00291
10		3.3572	3.35838 ± 0.0018	4.15364	4.15544 ± 0.00202	5.68985	5.69222 ± 0.00244
11		3.13532	3.13635 ± 0.00159	3.87708	3.87865 ± 0.00178	5.30779	5.30986 ± 0.00212
12		2.96614	2.96705 ± 0.00145	3.66695	3.66836 ± 0.00161	5.01846	5.02031 ± 0.0019
13		2.83225	2.83308 ± 0.00134	3.50119	3.50248 ± 0.00148	4.79091	4.7926 ± 0.00173
14		2.72324	2.72401 ± 0.00125	3.36664	3.36784 ± 0.00138	4.60671	4.60828 ± 0.00161
15		2.63249	2.63321 ± 0.00118	3.25492	3.25604 ± 0.0013	4.45416	4.45562 ± 0.0015
16		2.55557	2.55624 ± 0.00113	3.16044	3.16151 ± 0.00123	4.32545	4.32683 ± 0.00142
17		2.48938	2.49001 ± 0.00108	3.07933	3.08035 ± 0.00118	4.2152	4.21651 ± 0.00135
18		2.43171	2.43232 ± 0.00104	3.00882	3.00979 ± 0.00113	4.11954	4.12079 ± 0.00129
19		2.38094	2.38152 ± 0.00101	2.94685	2.94779 ± 0.00109	4.03562	4.03683 ± 0.00124
20		2.33583	2.33639 ± 0.00098	2.89189	2.89279 ± 0.00106	3.96133	3.9625 ± 0.0012
21		2.29543	2.29597 ± 0.00095	2.84275	2.84362 ± 0.00103	3.89501	3.89614 ± 0.00116
22		2.259	2.25952 ± 0.00093	2.79849	2.79935 ± 0.001	3.83538	3.83648 ± 0.00112
23		2.22594	2.22644 ± 0.00091	2.7584	2.75923 ± 0.00097	3.78144	3.7825 ± 0.00109
24		2.19578	2.19627 ± 0.00089	2.72187	2.72268 ± 0.00095	3.73235	3.73339 ± 0.00107
25		2.16813	2.16861 ± 0.00087	2.68842	2.68922 ± 0.00093	3.68747	3.68848 ± 0.00104
30		2.05796	2.05839 ± 0.00081	2.55559	2.55632 ± 0.00086	3.50979	3.51071 ± 0.00095
35		1.97897	1.97938 ± 0.00076	2.4608	2.46148 ± 0.00081	3.3836	3.38446 ± 0.00089

Table C.8 continued Tolerance Factors for One Sided Tolerance Limits (0.99, P) by Using Equations Given by [179]

<b>40</b>	1.919	1.91937 ± 0.00073	2.38908	2.38973 ± 0.00077	3.28851	3.28932 ± 0.00084
<b>45</b>	1.87156	1.87192 ± 0.0007	2.33254	2.33316 ± 0.00074	3.21377	3.21455 ± 0.0008
<b>50</b>	1.8329	1.83325 ± 0.00069	2.28657	2.28717 ± 0.00072	3.15317	3.15393 ± 0.00078
$\infty$	1.28155	1.28173 ± 0.00045	1.64485	1.64521 ± 0.00045	2.32635	2.32679 ± 0.00045

\* When k-factor is calculated, z-scores are obtained by MS Excel equation (“*normsinv(probability)*”)

\*\* When k-factor is calculated, z-scores are obtained by using rational approximation for z-scores [177]

Table C.9 Error (%) between Tabulated k-Factors (in Table C.1) and Calculated k-Factors by Using Equation Given by Link [179]

n	$\gamma$	0.90			0.95			0.99		
	$\beta$	0.90	0.95	0.99	0.90	0.95	0.99	0.90	0.95	0.99
3		35.83	41.75	37.76	302.68	313.02	321.57			
4		10.81	11.26	11.73	34.29	36.07	37.75			
5		5.51	5.81	6.11	15.21	16.24	17.19			
6		3.43	3.71	3.92	6.91	9.75	10.43	45.64	48.42	51.48
7		2.40	2.59	2.78	6.18	6.71	7.25	26.39	28.18	30.26
8		1.79	1.94	2.11	4.55	4.96	5.45	17.78	19.15	20.73
9		1.42	1.59	1.70	3.54	3.92	4.29	12.65	14.25	15.44
10		1.20	1.29	1.38	2.86	3.18	3.52	10.14	11.09	12.12
11		0.94	1.06	1.16	2.41	2.67	2.97	8.23	9.00	9.94
12		0.84	0.93	1.01	2.05	2.29	2.54	6.96	7.54	8.32
13		0.73	0.78	0.87	1.79	2.00	2.23	5.80	6.42	7.13
14		0.65	0.71	0.79	1.59	1.77	1.95	5.06	5.57	6.24
15		0.61	0.63	0.70	1.40	1.56	1.76	4.42	4.93	5.45
16		0.50	0.57	0.64	1.29	1.43	1.62	3.97	4.37	4.88
17		0.43	0.54	0.61	1.16	1.29	1.43	3.51	3.96	4.39
18		0.40	0.46	0.51	1.02	1.16	1.34	3.17	3.54	4.00
19		0.42	0.40	0.46	0.93	1.07	1.22	2.85	3.22	3.66
20		0.37	0.39	0.44	0.87	0.99	1.14	2.67	3.02	3.37
21		0.35	0.38	0.43	0.82	0.94	1.08	2.43	2.70	3.15
22		0.34	0.34	0.39	0.72	0.82	0.99	2.31	2.55	2.91
23		0.29	0.32	0.38	0.70	0.78	0.93	2.15	2.43	2.76
24		0.29	0.31	0.35	0.66	0.77	0.87	1.94	2.21	2.59
25		0.23	0.30	0.34	0.62	0.70	0.82	1.84	2.14	2.40
30		0.20	0.21	0.25	0.44	0.54	0.64	1.43	1.57	1.85
35		0.21	0.17	0.20	0.40	0.48	0.54	1.12	1.23	1.49
40		0.12	0.16	0.18	0.33	0.35	0.43	0.89	1.02	1.18
45		0.10	0.11	0.12	0.27	0.34	0.41	0.78	0.84	1.03
50		0.06	0.13	0.13	0.03	0.28	0.31	0.65	-0.41	0.93
$\infty$		-0.03	-0.01	0.01	-0.03	-0.01	0.01	-0.03	-0.01	0.01

Table C.10 Tolerance Factors for One Sided Tolerance Limits ( $\gamma$ , P) by Using Equation 3.19 [151]

n	$\gamma$	0.90			0.95			0.99		
	$\beta$	0.90	0.95	0.99	0.90	0.95	0.99	0.90	0.95	0.99
3		4.25816	5.31148	7.34044	6.15528	7.6559	10.5527			
4		3.18784	3.95657	5.43823	4.16193	5.14387	7.04236			
5		2.74235	3.39983	4.66598	3.40663	4.20268	5.74108			
6		2.49369	3.09188	4.2429	3.00626	3.70768	5.06199	4.41108	5.40554	7.33457
7		2.33265	2.8938	3.97202	2.75543	3.39947	4.64172	3.85913	4.72786	6.41194
8		2.21859	2.75428	3.78255	2.58191	3.18729	4.35386	3.49721	4.28525	5.8118
9		2.13287	2.6499	3.64144	2.45376	3.03124	4.14302	3.24041	3.97226	5.38888
10		2.06567	2.56837	3.53166	2.35464	2.91096	3.98112	3.04791	3.73831	5.07373

Table 14: Error (%) between Tabulated k-Factors (in Table C.1) and Calculated k-Factors by Using Equation 3.19 [151]

n	$\gamma$	0.90			0.95			0.99		
	$\beta$	0.90	0.95	0.99	0.90	0.95	0.99	0.90	0.95	0.99
3		0.02	18.15	0.04	-0.27	0.09	0.07			
4		0.08	-0.04	0.12	-0.11	-0.11	0.04			
5		0.03	-0.02	0.00	-0.04	0.07	0.01			
6		-0.03	0.09	0.09	-5.97	0.07	0.00	0.31	-0.35	0.06
7		-0.04	-0.02	0.00	0.04	0.05	0.07	0.31	-0.21	0.09
8		-0.04	-0.07	-0.05	-0.01	-0.07	0.09	0.12	-0.17	0.08
9		-0.01	0.09	0.04	-0.02	0.02	0.00	-1.16	0.13	-0.01
10		0.07	0.04	-0.03	-0.04	0.00	0.01	-0.01	-0.07	-0.13

## REFERENCES

- [1] Smardzewski, J. *Furniture Design*; Springer International Publishing: Poznan, **2015**; ISBN 9783319195322.
- [2] Eckelman, C.A. Chair stretchers and spindles prove tough after purdue testing. *Furnit. Des. Manuf.* **1970**, 200–202.
- [3] Ratnasingam, J.; Perkins, M.; Reid, H. Fatigue : it’s relevance to furniture. *Holz als Roh- und Werkst.* **1997**, 55, 297–300.
- [4] Eckelman, C.A. *Textbook of product engineering and strength design of furniture*; Purdue University: West Lafayette, **2003**.
- [5] Nelson, D.V. Prediction of fatigue life under irregular loadings. In Proceedings of the Probabilistic Mechanics and Structural Reliability; Tucson, Arizona, **1979**; pp. 1–5.
- [6] Klos, R.; Fabisiak, B. Possibilities of reliability theory application in the process of furniture design. *Wood Res.* **2013**, 58, 113–122.
- [7] Kececioglu, D.B. *Reliability engineering handbook*; DEStech Publications: Lancaster, **2002**; ISBN 8125565094.
- [8] Eckelman, C.A. Reasonable design stresses for woods used in furniture. *Purdue Univ. Agric. Exp. Stn. Res. Bull.* **1974**, 916, 1–7.
- [9] Eckelman, C.A.; Erdil, Y.Z.; Haviarova, E. School Chairs for Developing Countries: Designing for Strength and Durability, Simplicity and Ease of Construction. *For. Prod. J.* **2003**, 53, 1–8.
- [10] Smardzewski, J. The reliability of joints and cabinet furniture. *Wood Res.* **2009**, 54, 1–10.
- [11] Ratnasingam, J.; Ioras, F.; McNulty, T. Fatigue strength of mortise and tenon furniture joints made from oil palm lumber nad some Malaysian timber. In *Journal of Applied Sciences*; Intergovernmental Panel on Climate Change, Ed.; Cambridge University Press: Cambridge, **2010**; Vol. 10, pp. 2869–2874.
- [12] Wencheng, L. Principles for determining material allowable and design allowable values of composite aircraft structures. *Procedia Eng.* **2011**, 17, 279–285.

- [13] Eckelman, C.A.; Uysal, M.; Haviarova, E. Statistical Lower Tolerance Limits for Rectangular Mortise and Tenon Joints. *Bioresources* **2016**, *11*, 7162–7171.
- [14] Erdil, Y.Z.; Haviarova, E.; Eckelman, C.A. Product Engineering and Performance Testing in Relation. *Wood Fiber Sci.* **2004**, *36*, 411–416.
- [15] Ratnasingam, J.; Ioras, F.; McNulty, T. Fatigue strength of mortise and tenon furniture joints made from oil plam lumber and some Malaysian timbers. *J. Appl. Sci.* **2010**, *10*, 2869–2874.
- [16] Huber, H.A.; Eckelman, C.A. The role of wood science in invastigating furniture failures. *Wood Des. Focus J. Contempory Wood Enginering* **1999**, *10*, 15–18.
- [17] Echard, B.; Gayton, N.; Bignonnet, A. A reliability analysis method for fatigue design. *Int. J. Fatigue* **2014**, *59*, 292–300.
- [18] Fink, G.; Kohler, J. Probabilistic modelling of the tensile related material properties of timber boards and finger joint connections. *Eur. J. Wood Wood Prod.* **2015**, *73*, 335–346.
- [19] Zhao, Y.X.; Zhang, Y.; He, H.W. Improved measurement on probabilistic fatigue limits/strengths by test data from staircase test method. *Int. J. Fatigue* **2017**, *94*, 58–80.
- [20] Domljan, D.; Grbac, I.; Bogner, A. The role of design in developing of the school furniture. *Wood Ind. 55 77-90* **2004**, *55*, 77–90.
- [21] Bras, B. Incorporating Environmental Issues in Product Design and Realization. *United Nations Ind. Environ.* **1997**, *20*, 7–13.
- [22] Lagerstedt, J. Functional and environmental factors in early phases of product development, KTH, **2003**.
- [23] Hauschild, M.Z.; Jeswiet, J. Design for Environment — Do We Get the Focus Right? *CIRP Ann.* **2004**, *53*, 1–4.
- [24] Anon. United States Environmental Protection Agency, Wood : Material-Specific Data Available online: <https://www.epa.gov/facts-and-figures-about-materials-waste-and-recycling/wood-material-specific-data#WoodOverview> (accessed on May 4, 2019).
- [25] Parikka-Alhola, K. Promoting environmentally sound furniture by green public procurement. *Ecol. Econ.* **2008**, *68*, 472–485.

- [26] Anon. *United States Environmental Protection Agency, Advancing Sustainable Materials Management*; **2010**.
- [27] ANSI/BIFMA e3-2014e Furniture Sustainability Standard **2015**, 1–104.
- [28] Anon. Directive 2001/95/EC of the European Parliament and of the Council of 3 December 2001 on general product safety; **2002**.
- [29] Flecha, I.A.; Boja, J.W. *U. S. Consumer Product Safety Commission: Requirements for furniture Sold in the United States* Available online: [https://www.cpsc.gov/s3fs-public/pdfs/blk\\_pdf\\_furnreq032012\\_en.pdf](https://www.cpsc.gov/s3fs-public/pdfs/blk_pdf_furnreq032012_en.pdf) (accessed on April 15, 2019)
- [30] Goodden, R. Why companies are missing the mark on product recalls and liability, *Cooperate Counsel*. Available on: <https://jasperin.org/wp-content/uploads/2018/08/Articles-Seminar.pdf> (accessed on April 15, 2019).
- [31] Anon. 2018 Holiday Consumer Protection Guide Available online: [https://www.myfloridalegal.com/webfiles.nsf/WF/TDGT-B6PQF7/\\$file/2018+AG+Holiday+Guide+Final.pdf](https://www.myfloridalegal.com/webfiles.nsf/WF/TDGT-B6PQF7/$file/2018+AG+Holiday+Guide+Final.pdf) (accessed on April 4, 2019).
- [32] Anon. A KID Report : 2017 Children Product Recalls and 2016 Recall. **2017**.
- [33] Stull, M.R.; Soule, G.W. *Furniture Worl Magazine*. 2016,.
- [34] O'Brien, C.; Mills, A.; Marcy, N. *United States Consumer Product Safety Commission: Hazard Screening Report - Home Furnishes and Fixtures*; **2006**.
- [35] Trueman, M. Competing through Design. *Long Range Plann.* **1998**, *31*, 594–605.
- [36] Bucior, J. *The basis of reliability theory and engineering*; **2004**.
- [37] Avontuur, G.C. *Reliability Analysis in Mechanical Engineering Design*, 2003.
- [38] Gurel, U.; Cakmakci, M. Impact of reliability on warranty : A study of application in a large size company of electronics industry. *Measurement* **2013**, *46*, 1297–1310.
- [39] Murthy, D.N.. Product reliability and warranty: an overview and future research. *Producao* **2007**, *17*, 426–434.
- [40] Podolyakina, N. Estimation of the Relationship between the Products Reliability, Period of Their Warranty Service and the Value of the Enterprise Cost. *Procedia Eng.* **2017**, *178*, 558–568.
- [41] Anon. Building Materials Warranty Report Available online: <https://www.warrantyweek.com/archive/ww20180614.html> (accessed on April 4, 2019).

- [42] Hibbeler, R.C. *Structural Analysis*; Hortan, M.J., Ed.; 8th editio.; Pearson Prentice Hall: Upper Saddle River, New Jersey, **2012**.
- [43] Eckelman, C.A. Performance test of side chairs. *Holz als Roh-und Werkst.* **1999**, *57*, 227–234.
- [44] Ratnasingam, J.; Ioras, F. Static and Fatigue Strength of Oil Palm Wood Used in Furniture. *J. Appl. Sci.* **2010**, *10*, 986–990.
- [45] Zhang, J.L.; Quin, F.; Tackett, B. Bending strength and stiffness of two-pin dowel joints constructed of wood and wood composites. *For. Prod. J.* **2001**, *51*, 29–35.
- [46] Eckelman, C.A. Library Chairs: An Overview of the ALA Test Method with Test Reports on Side Chairs. *Libr. Technol. Rep.* **1995**, *31*, 117–214.
- [47] Palmgren, A. Die Lebensdauer von Kugellagern (The service life of vall bearings). *Zeitschrift des Vereines Dtsch. Ingenieure* **1924**, *68*, 339–341.
- [48] Miner, M.A. Cumulative Damage in Fatigue. *J. Appl. Mechnanics* **1945**, *12*, 159–164.
- [49] Kauzlarich, J.J. The Palmgren-Miner rule derived. *Tribol. Ser.* **1989**, *14*, 175–179.
- [50] Eckelman, C.A. Bending strength and moment-rotation characteristics of two-pin moment resisting dowel joints. *For. Prod. J.* **1971**, *21*, 35–39.
- [51] Anon. Wood Chair Failures – Expert Article Discusses the Cause of Most Wood Chair Collapse Incidents Available online: <https://www.robsonforensic.com/articles/wood-chair-failure-collapse-expert-witness> (accessed on Aug 3, 2018).
- [52] Erdil, Y.Z.; Kasal, A.; Eckelman, C.A. Bending moment capacity of rectangular mortise and tenon furniture joints. *For. Prod. J.* **2005**, *55*, 209–213.
- [53] Podlena, M.; Hysek, S.; Prochazka, J.; Bohm, M.; Bomba, J. Axial loading of different single-pin dowels and effect on withdrawal strength. *BioResources* **2018**, *13*, 5179–5192.
- [54] Eckelman, C.A.; Hill, M.D. Textured vs. plain dowel which are stronger. *Furnit. Des. Manuf.* **1971**.
- [55] Smardzewski, J. Strength of profile-adhesive joints. *Wood Sci. Technol.* **2002**, *36*, 173–183.

- [56] Tankut, A.N.; Tankut, N. The effects of joint forms (Shape) and dimensions on the strengths of mortise and tenon joints. *Turkish J. Agric. For.* **2005**, *29*, 493–498.
- [57] Eckelman, C.A.; Erdil, Y.Z.; Haviarova, E. Effect of shoulders on bending moment capacity of round mortise and tenon joints. *For. Prod. J.* **2006**, *56*, 82–86.
- [58] Eckelman, C.; Haviarova, E. Performance tests of school chairs constructed with round mortise and tenon joints. *For. Prod. J.* **2006**, *56*, 51–57.
- [59] Prekrat, S.; Smardzewski, J. Effect of glueline shape on strength of mortise and tenon joint. *Drv. Ind.* **2010**, *61*, 223–228.
- [60] Likos, E.; Haviarova, E.; Eckelman, C.A.; Erdil, Y.Z.; Ozcifci, A. Effect of tenon geometry, grain orientation, and shoulder on bending moment capacity and moment rotation characteristics of mortise and tenon joints. *Wood Fiber Sci.* **2012**, *44*, 462–469.
- [61] Prekrat, S.; Smardzewski, J.; Brezović, M.; Pervan, S. Quality of corner joints of beech chairs under load. *Drv. Ind.* **2012**, *63*, 205–210.
- [62] Kasal, A.; Haviarova, E.; Efe, H.; Eckelman, C.A.; Erdil, Y.Z. Effect of Adhesive Type and Tenon Size on Bending Moment Capacity and Rigidity of T-Shaped Furniture Joints Constructed of Turkish Beech and Scots Pine. *Wood Fiber Sci.* **2013**, *45*, 287–293.
- [63] Likos, E.; Haviarova, E.; Eckelman, C.A.; Erdil, Y.Z.; Ozcifci, A. Technical note: Static versus cyclic load capacity of side chairs constructed with mortise and tenon joints. *Wood Fiber Sci.* **2013**, *45*, 223–227.
- [64] Hajdarević, S.; Martinović, S. Effect of tenon length on flexibility of mortise and tenon joint. *Procedia Eng.* **2014**, *69*, 678–685.
- [65] Derikvand, M.; Ebrahimi, G.; Eckelman, C.A. Bending moment capacity of mortise and loose-tenon joints. *Wood Fiber Sci.* **2014**, *46*, 159–166.
- [66] Derikvand, M.; Ebrahimi, G. Strength performance of mortise and loose-tenon furniture joints under uniaxial bending moment. *J. For. Res.* **2014**, *25*, 483–486.
- [67] Oktaee, J.; Ebrahimi, G.; Layeghi, M.; Ghofrani, M.; Eckelman, C.A. Bending moment capacity of simple and haunched mortise and tenon furniture joints under tension and compression loads. *Turkish J. Agric. For.* **2014**, *38*, 291–297.

- [68] Kasal, A.; Eckelman, C.A.; Haviarova, E.; Erdil, Y.Z.; Yalcin, I. Bending moment capacities of L-shaped mortise and tenon joints under compression and tension loadings. *BioResources* **2015**, *10*, 7009–7020.
- [69] Kasal, A.; Kuskun, T.; Efe, H.; Erdil, Y.Z. Relationship between static front to back loading capacity of whole chair and the strength of individual joints. In Proceedings of the The 27th International Conference on Research for Furniture Industry; Ankara, Turkey, **2015**; pp. 422–429.
- [70] Zaborsky, V.; Boruvka, V.; Ruman, D.; Gaff, M. Effects of geometric parameters of structural elements on joint stiffness. *BioResources* **2017**, *12*, 932–946.
- [71] Acar, M.; Diler, H.; Erdil, Y.Z. Effects of cross-sectional shape on the bending strength in furniture joints. *Kastamonu Üniversitesi Orman Fakültesi Derg.* **2018**, 164–170.
- [72] Eckelman, C.A. Engineering concepts of single-pin dowel joint design. *Purdue Univ. Agric. Exp. Stn. Res. Bull.* **1969**, *3671*, 53–60.
- [73] Eckelman, C.A. Out-of-plane strength and stiffness of dowel joints. *For. Prod. Res. Soc.* **1979**.
- [74] Zhang, J.L.; Eckelman, C.A. The bending moment resistance of single-dowel Corner joints in case construction. *For. Prod. J.* **1993**, *43*, 19–24.
- [75] Zhang, J.-L.; Eckelman, C.A. Rational design of multi-dowel corner joints in case construction. *For. Prod. J.* **1993**, *43*, 52–58.
- [76] Erdil, Y.Z.; Eckelman, C.A. Withdrawal strength of dowels in plywood and oriented strand board. *Turkish J. Agric. For. J Agric* **2001**, *25*, 319–327.
- [77] Zhang, J.; Erdil, Y.Z.; Eckelman, C.A. Torsional strength of dowel joints constructed of plywood and oriented stranboard. *For. Prod. J.* **2002**, *52*, 89–94.
- [78] Altinok, M.; Taş, H.H.; Çimen, M. Effects of combined usage of traditional glue joint methods in box construction on strength of furniture. *Mater. Des.* **2009**, *30*, 3313–3317.
- [79] Çetin Yerlikaya, N.; Aktaş, A. Enhancement of load-carrying capacity of corner joints in case-type furniture. *Mater. Des.* **2012**, *37*, 393–401.
- [80] Kasal, A.; Erdil, Y.Z.; Demirci, S.; Eckelman, C.A. Shear force capacity of various doweled frame type furniture joints. *Kastamonu Univ. J. For. Fac.* **2013**, *13*, 60–71.

- [81] Yerlikaya, N.C.; Aktas, A. Enhancement of T-joints of Spruce wood reinforced by using glass-fiber composite laminate. *Acad. Journals* **2013**, *8*, 515–523.
- [82] Yerlikaya, N.Ç. Investigation of optimum dowel spacing for corner joints , which are reinforced with glass-fiber fabric in case-type furniture. *Wood Res.* **2014**, *59*, 191–200.
- [83] Derikvand, M.; Ebrahimi, G. Rotational stiffness of L-shaped dowel. In Proceedings of the The 27th International Conferance on Reseach for Furniture Industry; Ankara, Turkey, **2015**; pp. 18–27.
- [84] Tankut, N. The effect of adhesive type and bond line thickness on the strength of mortise and tenon joints. *Int. J. Adhes.* **2007**, *27*, 493–498.
- [85] Bomba, J.; Šedivka, P.; Böhm, M.; Devera, M. Influence of moisture content on the bond strength and water resistance of bonded wood joints. *BioResources* **2014**, *9*, 5208–5218.
- [86] Fairchild, I.. Holding power of wood screws. *U.S. Natl. Bur. Stand* **1929**, *319*, 553–580.
- [87] Eckelman, C.A. Holding strength of screws in wood and wood-based materials. *Purdue Univ. Agr. Exp. Sta. Res. Bul.* **1973**, *895*, 1–15.
- [88] Forest Products Laboratory - USDA *Wood handbook: Wood as an engineering material*; USDA - General Technical Report, **2010**; Vol. General Te; ISBN 1892529025.
- [89] Örs, Y.; Özen, R.; Doğanay, S. Screw holding ability (Strength) of wood materials used in furniture manufacture. *Turkish J. Agric. For.* **1998**, *22*, 29–34.
- [90] Semple, K.E.; Smith, G.D. Prediction of internal bond strength in particleboard from screw withdrawal resistance models. *Wood Fiber Sci.* **2005**, *38*, 256–267.
- [91] Efe, H.; Demirci, S. The effects of cutting section to the holding strength of screw nut on different wood materials. *G.U. J. Sci.* **2005**, *18*, 127–135.
- [92] Özçifçi, A. The effects of pilot hole, screw types and layer thickness on the withdrawal strength of screws in laminated veneer lumber. *Mater. Des.* **2009**, *30*, 2355–2358.

- [93] Efe, H.; Kasal, A.; Dizel, T.; Riza, A.A.; Erdem, H.E. Allen screw withdrawal strength of solid wood and laminated veneer lumber. *Kastamonu Univ. J. For. Fac.* **2009**, *9*, 95–105.
- [94] Yuksel, M.; Yildirim, N.; Kasal, A.; Erdil, Y.Z.; Demirci, S. Effect of the panel type and panel thickness on moment resistance of screw-jointed corner joints and stiffness of four-member cabinets. *BioResources* **2014**, *9*, 6340–6349.
- [95] Eckelman, C.A. Furniture mechanics: The analysis of paneled plate and carcass furniture. *Purdue Univ. Agr. Exp. Sta. Res. Prog. Rept.* **1967**, *274*, 1–12.
- [96] Yorur, H.; Tor, O.; Gunay, M.N.; Birinci, E. The effects of different variables on the screw withdrawal strength of plywood. *Kastamonu Üniversitesi Orman Fakültesi Derg.* **2017**, *17*, 325–333.
- [97] Nolan, R. Determining Allowable Design Values for Wood Determining Allowable Design Values for Wood Available online: [https://pdhonline.com/courses/s246/s246\\_new.htm](https://pdhonline.com/courses/s246/s246_new.htm) (accessed on April 4, 2019).
- [98] Tsai, K.T.; Ansell, M.P. The fatigue properties of wood in flexure. *J. Mater. Sci.* **1990**, *25*, 865–878.
- [99] Kommers, W.J. fatigue behavior of wood and plywood subjected to repeated and reverse bending stress. *USDA For. Serv. For. Prod. Lab. Madison, WI* **1943**, *1327*, 1–12.
- [100] Dietz, A.G.H.; Grinsfelder, H. Behaviour of plywood under repeated stresses. *Trans. Am. Soc. Mech. Eng.* **1943**, 187–191.
- [101] Sekhar, A.C.; Shukla, N.K.; Gupta, V.K. Effect of torsional stress and moisture content on the fatigue properties of timber. *Holz als Roh- und Werkst.* **1964**, *22*, 264–266.
- [102] Lewis, W.C. Fatigue resistance of quarter-scale bridge stringers in flexure and shear. *For. Prod- ucts Lab. Dep. Agric. For. Serv.* **1962**, *2236*.
- [103] Sekhar, A.C.; Shukla, N.K. Effect of specific gravity on fatigue properties of wood. *J. Indian Acad. Wood Sci.* **1979**, *10*.
- [104] Ibuki, Y.; Sasaki, H.; Kawamoto, M.; Maku, T. The plane bending fatigue strength of glued laminated wood. *Bull. Wood Res. Institute, Kyoto* **1962**, *31*, 11–22.

- [105] Maku, T.; Sasaki, H. The rotation bending fatigue test of glued laminated wood. *Bull. Wood Res. Institute, Kyoto* **1963**, *31*, 1–10.
- [106] Smith, I.; Foliente, G. Load and resistance factor design of timber joints: International practice and future direction. *J. Struct. Engineering* **2002**, *128*, 48–59.
- [107] Allen, T.; Nowak, A.S.; Bathurst, R.J. *Calibration to Determine Load and Resistance Factors for Geotechnical and Structural Design*; 2005;
- [108] Bao, Z.; Eckelman, C.A. Fatigue life and design stresses for wood composites used in furniture. *For. Prod. J.* **1995**, *45*, 59–63.
- [109] Bao, Z.; Eckelman, C.A.; Gibson, H. Fatigue strength and allowable design stress for some wood composite in furniture. *Holz als Roh-und Werkst.* **1996**, *54*, 377–382.
- [110] Ratnasingam, J.; Ioras, F. Bending and fatigue strength of mortise and tenon furniture joints made from oil palm lumber. *Eur. J. Wood Wood Prod.* **2011**, *69*, 677–679.
- [111] Ratnasingam, J.; Ioras, F. Load-bearing characteristics of heat-treated rubberwood furniture components and joints. *Eur. J. Wood Wood Prod.* **2013**, *71*, 287–289.
- [112] Ratnasingam, J.; Ioras, F. Fatigue strength and design stress of oil palm wood for furniture application. *Eur. J. Wood Wood Prod.* **2011**, *69*, 507–509.
- [113] *BS 4875: Specification for strength and stability of domestic and contract furniture*; London, **1972**; Vol. Part 1.
- [114] Sediva, B.; Vavra, F.; Toupal, T.; Marek, P. Statistical monitoring of failures - Methods and use. In Proceedings of the Proceedings of the 11th International Scientific Conference Electric Power Engineering **2010**, EPE 2010; 2010; pp. 1–9.
- [115] Papadrakakis, M.; Papadopoulos, V.; Lagaros, N.D. Structural reliability analysis of elastic-plastic structures using neural networks and Monte Carlo simulation. *Comput. Methods Appl. Mech. Eng.* **1996**, *136*, 145–163.
- [116] Chang, K.-H. Reliability Analysis. In *e-Design*; Elsevier, **2015**; pp. 523–595 ISBN 9780123820389.
- [117] Das, P.K.; Frieze, P.A.; Faulkner, D. Structural reliability modelling of stiffened components of floating structures. *Struct. Saf.* **1984**, *2*, 3–16.
- [118] Stewart, M.G. Structural reliability and error control in reinforced concrete design and construction. *Struct. Saf.* **1993**, *12*, 277–292.

- [119] Yunis, I.S.; Carney, K.S. Structural reliability techniques applied to plume impingement loading of the space-station-freedom photovoltaic array. *Struct. Saf.* **1994**, *15*, 85–110.
- [120] Zureick, A.; Asce, M.; Bennett, R.M.; Asce, M.; Ellingwood, B.R.; Asce, F. Statistical characterization of fiber-Reinforced Polymer Composite Material Properties for Structural Design. **2006**, *132*, 1320–1327.
- [121] Li, W.; Zhu, H.; Luo, H.; Xia, Y. Statistical damage detection method for frame structures using a confidence interval. *Earthq. Eng. Eng. Vib.* **2009**, 1–8.
- [122] Klemenc, J.; Fajdiga, M. Joint estimation of E-N curves and their scatter using evolutionary algorithms. *Int. J. Fatigue* **2013**, *56*, 42–53.
- [123] Liao, Y.H.; Zhang, L.D.; Wang, C. Reliability optimization design of mechanical parts involving confidence level of reliability. *Appl. Mech. Mater.* **2014**, *490–491*, 560–563.
- [124] Yan, W.M.; Yuen, K.V. On the proper estimation of the confidence interval for the design formula of blast-induced vibrations with site records. *Rock Mech. Rock Eng.* **2014**, *48*, 361–374.
- [125] Angelo, L.D.; Nussbaumer, A. Reliability based fatigue assessment of existing motorway bridge. *Struct. Saf.* **2015**, *57*, 35–42.
- [126] Klemenc, J. Influence of fatigue–life data modelling on the estimated reliability of a structure subjected to a constant-amplitude loading. *Reliab. Eng. Syst. Saf.* **2015**, *142*, 238–247.
- [127] Piric, K. Reliability analysis method based on determination of the performance function’s PDF using the univariate dimension reduction method. *Struct. Saf.* **2015**, *57*, 18–25.
- [128] Tolentino, D.; Ruiz, S.E. Time-dependent confidence factor for structures with cumulative damage. *Earthq. Spectra* **2015**, *31*, 441–461.
- [129] Xu, Y. Fatigue reliability evaluation using probability density evolution method. *Probabilistic Eng. Mech.* **2015**, *42*, 1–6.

- [130] Harun, D.; Efe, H.; Kasal, A.; Erdil, Y.Z.; Kuskun, T. Comparison of the performance of some household chairs manufactured in Turkey with allowable design loads. In Proceedings of the The 27. International Conference Research of Furniture Industry; Ankara, **2015**.
- [131] Li, C.-L.N. and B. A probabilistic approach for estimating plastic hinge length of reinforced concrete columns. *J. Struct. Eng.* **2016**, *142*, 1–15.
- [132] Wang, Z.; Chen, W. Time-variant reliability assessment through equivalent stochastic process transformation. *Reliab. Eng. Syst. Saf.* **2016**, *152*, 166–175.
- [133] Lee, Y.L.; Makam, S.; McKelvey, S.; Lu, M.W. Durability reliability demonstration test methods. *Procedia Eng.* **2015**, *133*, 31–59.
- [134] Little, R.E.; C., E.J. Review of statistical analyses of fatigue life data using one-sided lower statistical tolerance limits. *Am. Soc. Test. Mater.* **1981**, 3–23.
- [135] Willink, R. Confidence intervals and other statistical intervals in metrology. *Int. J. Metrol. Qual. Eng.* **2012**, *3*, 169–178.
- [136] Trindade, A.A.; Uryasev, S. Improved tolerance limits by combining analytical and experimental data : An information integration methodology. *Jourbal od Data Sci.* **2006**, *4*, 371–386.
- [137] Rajagopalan, S. Statistical tolerance limits for process capability. *Def. Sci. J.* **2004**, *54*, 303–306.
- [138] Saweeres, E.S.B.; Kuiper, J.; Evans, R.O.; Richardson, J.B.; White, S.H. Predicting in vivo clinical performance of anterior cruciate ligament fixation methods from In vitro analysis: Industrial tests of fatigue life and tolerance limits are more useful than other cyclic loading parameters. *Am. J. Sports Med.* **2005**, *33*, 666–673.
- [139] Nickens, D. Using tolerance limits to evaluate laboratory data. *Drug Inf. J.* **1998**, *32*, 261–269.
- [140] Silva, A.; Carvalho, F.; Mexia, J.; Fonseca, M. One-sided tolerance interval in a two-way balanced nested model with mixed effects. In Proceedings of the AIP Conference Proceedings; **2013**; Vol. 1558, pp. 818–820.
- [141] Emura, T.; Wang, H. Approximate tolerance limits under log-location-scale regression models in the presence of censoring. *Technometrics* **2010**, *52*, 313–323.

- [142] Zaslavsky, B.G. Calculation of tolerance limits and sample size determination for clinical trials with dichotomous outcomes. *J. Biopharm. Stat.* **2007**, *17*, 481–91.
- [143] Winn, T.J. Implementing digital data analysis using SAS Available online: <http://analytics.ncsu.edu/sesug/2001/P-411.pdf> (accessed on April 4, 2019).
- [144] Burrows, G.L. Statistical Tolerance limits-What Are They? *J. R. Stat. Soc.* **1963**, *12*, 133–144.
- [145] Kharoufeh, J.P.; Chandra, M.J. Statistical tolerance analysis for non-normal or correlated normal component characteristics. *Int. J. Prod. Res.* **2002**, *40*, 337–352.
- [146] Jordan, P. Estimation of tolerance limits from reference data. *Comput. Stat. Data Anal.* **1995**, *19*, 655–668.
- [147] Rae, J.N.K.; Subrahmaniam, K.; Owen, D.B.; Subrahmaniam, K.; Non-, D.B.O.E. Effect of non-normality on tolerance limits which control percentages in both tails of normal distribution. *Technometrics* **1972**, *14*, 571–575.
- [148] Ireson, W.G.; Smith, B.E.; Resnikoff, G.J. *Statistical Tolerance Limits*; **1960**.
- [149] Hu, X. Asymptotical distributions, parameters and coverage probabilities of tolerance limits. *Comput. Stat. Data Anal.* **2007**, *51*, 4753–4760.
- [150] Faulkenberry, G.D.; Weeks, D.L. Sample size determination for tolerance limits. *Technometrics* **1968**, *10*, 343–348.
- [151] Young, D.S.; Gordon, C.M.; Zhu, S.; Olin, B.D. Sample size determination strategies for normal tolerance intervals using historical data. *Qual. Eng.* **2016**, *28*, 337–351.
- [152] Stockinger, A.; Wartzack, S. Application of sampling methods for statistical tolerance analysis. In Proceedings of the The 7th Weimar Optimizzation and Stochastic Days; **2010**; pp. 1–17.
- [153] Beal, D. Sample size determination for a nonparametric upper tolerance limit for any order statistic. In Proceedings of the SESUG; **2012**; pp. 1–8.
- [154] Mckay, M.D.; Beckman, R.J.; Conover, W.J. A comparison of three methods for selecting values of input variables in the analysis of output from a computer code. *Technometrics* **2019**, *21*, 239–245.
- [155] Young, D. Normal tolerance interval procedures in the tolerance package. *R J.* **2016**, *8*, 200–212.

- [156] Goodman, J. On the definition of the “Best” confidence interval. *Reliab. Eng.* **1984**, 7, 213–228.
- [157] Calabria, R.; Pulcini, G. Confidence limits for reliability and tolerance limits in the inverse Weibull distribution. *Reliab. Eng. Syst. Saf.* **1989**, 24, 77–85.
- [158] Krishnamoorthy, K.; Lin, Y. Confidence limits for stress-strength reliability involving Weibull models. *J. Stat. Plan. Inference* **2010**, 140, 1754–1764.
- [159] Uysal, M. Furniture design and product development principles considering end-of-life options and design for environment strategies, **2014**.
- [160] Eckelman, C.A.; Haviarova, E.; Kasal, A.; Erdil, Y.Z. Lower tolerance limit approach to equation-based rational design values for T-shaped mortise and tenon joints. *Wood Fiber Sci.* **2017**, 49, 1–9.
- [161] Eckelman, C.A.; Haviarova, E.; Kasal, A.; Erdil, Y.Z. Lower tolerance limit approach to equation-based rational design values for L-shaped mortise and tenon joints. *Wood Fiber Sci.* **2017**, 49, 219–230.
- [162] Uysal, M.; Haviarova, E. Estimating design values for two-pin moment resisting dowel joints with Lower Tolerance Limit Approach. *BioResources* **2018**, 13, 5241–5253.
- [163] Cassens, D.. Red Oak. *Purdue Ext.* **2015**, FNR-288-W, 1–5.
- [164] Cassens, D.. White Oak. *Purdue Ext.* **2015**, FNR-292-W, 1–5.
- [165] Anon. Inside wood Available online: <http://insidewood.lib.ncsu.edu/search?1> (accessed on April 4, 2019).
- [166] Khan, U.; May, P.; Porwal, H.; Nawaz, K.; Coleman, J.N. Improved adhesive strength and toughness of polyvinyl acetate glue on addition of small quantities of graphene. *Appl. Mater. Interfaces* **2013**, 5, 1423–1428.
- [167] Ors, Y.; Atar, M.; Ozcifci, A. Bonding strength of poly (vinyl acetate )-based adhesives in some wood materials treated with impregnation. *J. Appl. Polym. Sci.* **2000**, 76, 1472–1479.
- [168] Eckelman, C.A. Wood moisture calculations. *Purdue Univ. For. Nat. Resour. Furnit. Manuf.* **1997**, FNR-156, 1–18.
- [169] ASTM D 143 – 94: Standard test methods for small clear specimens of timber. **2000**, 1–31.

- [170] Erdil, Y.Z.; Kasal, A.; Eckelman, C.A. Bending moment capacity of rectangular mortise and tenon furniture joints. *For. Prod. J.* **2005**, *55*, 209–213.
- [171] Young, D.S. tolerance : An R package for estimating tolerance intervals. *J. Stat. Softw.* **2010**, *36*, 1–39.
- [172] Young, D.S. Normal tolerance interval procedures in the tolerance package. **2014**, *XX*, 1–12.
- [173] Ghasemi, A.; Zahediasl, S. Normality tests for statistical analysis: A guide for non-statisticians. *Int. J. Endocrinol. Metab.* **2012**, *10*, 486–489.
- [174] Natrella, M.G. *National Bureau of Standards Handbook 91: Experimental Statistics*; **1963**.
- [175] Polhemus, N.W. Constructing Statistical Tolerance Limits for Non-Normal Data Available online: [http://www.statvision.com/webinars/Nonnormal Tolerance Limits.pdf](http://www.statvision.com/webinars/Nonnormal%20Tolerance%20Limits.pdf) (accessed on April 4, 2019).
- [176] Lane, D.M. Binomial Probability. In *Online Statistics Education: An Interactive Multimedia Course of Study*; **2019**; pp. 203–206.
- [177] Zelen, M.; Severo, N.C. Probability Functions. In *Handbook of Mathematical Functions With Formulas, Graphs, and Mathematical Tables*; Abramowitz, M., Stegun, I.A., Eds.; National Bureau of Standards: Washington, **1964**; pp. 925–997.
- [178] Lieberman, G.. Tables for one sided statistical tolerance limits. *Ind. Qual.* **1958**, *14*, 7–9.
- [179] Link, C.L. An equation for one-sided tolerance limits for normal distributions. *US Dep. Agric. For. Serv. For. Prod. Lab.* **1985**, *FPL 458*, 1–4.
- [180] Guttman, I. *Statistical tolerance regions.*; Darien, Conn., Hafner Pub. Co.: Darien, IL, **1970**; ISBN 3275406131666.
- [181] Eckelman, C.A.; Erdil, Y.Z. Joint design manual for furniture frames constructed of plywood and oriented strand board. In *Proceedings of the the International Furniture Congress*; Istanbul, **1999**; pp. 265–305.
- [182] Kuskun, T. Effect of the tenon size and loading type on chair strength and comparison of actual test and finite element analyses results., Mugla Sitki Kocman University, **2013**.

- [183] Kuskun, T.; Kasal, A.; Haviarova, E.; Kilic, H.; Uysal, M.; Erdil, Y.Z. Relationship between static and cyclic front to back load capacity of wooden chairs, and evaluation of the strength values according to acceptable design values. *Wood Fiber Sci.* **2018**, *50*, 1–9.
- [184] Stockinger, A.; Wartzack, S. Application of sampling methods for statistical tolerance analysis. **2010**, 1–17.
- [185] M, U.; Haviarova, E. A review based on reliability of furniture. In Proceedings of the the 61st International Convention of Society of Wood Science and Technology and Japan Wood Research Society; Nagoya, Japan, 2018; pp. 454–461.

## VITA

Mesut Uysal was born in Antalya, Republic of Turkey in 1988. He received his Bachelor of Science degree in Forest Product Engineering from Suleyman Demirel University in Isparta, Turkey in 2010.

In 2011, he won a scholarship supported by Ministry of National Education of Republic of Turkey to pursue Master of Science and Doctor of Philosophy in the field of Forest Products Engineering behalf of Bursa Technical University, in Turkey. In 2012, he was accepted for graduate program in Purdue University, West Lafayette, IN USA. In 2014, he got Master of Science degree in the field of Wood Products and Wood Products Manufacturing with a thesis titled “*Furniture design and product development principles considering End-of-Life options and Design for Environment strategies*”. Besides, in 2014, he was accepted for Ph.D program in Purdue University.

His main field of expertise is in investigation to (i) increase reliability of furniture itself and furniture joints, (ii) improve structural strength of furniture through physical prototype experiment, simulation and visualization techniques, and (iii) structural analysis of wood structure with instrumentation.

## PUBLICATIONS

**Uysal, M.**, Haviarova, E. and Eckelman, C.A. (2015). A compression of the cyclic durability, ease of disassembly, repair, and reuse of parts of wooden chair frames. *Materials and Design*, 87, 75-81.

Eckelman, C.A., **Uysal, M.** and Haviarova, E. (2016). Statistical lower tolerance limits for rectangular mortise and tenon joints. *Bioresources*, 11(3), 7162-7171.

**Uysal, M.**, Haviarova, E. (2018). Estimating design values for two-pin moment resisting dowel joints with lower tolerance limit approach. *Bioresources*, 13(3), 5241-5253.

Kuskun, T., Kasal, A., Haviarova, E., **Uysal, M.**, Kilic, H. and Erdil, Y.Z. (2018). Relationship between static and cyclic front to back load capacity of wooden chairs, and evaluation of the strength values according to acceptable design values. *Wood and Fiber Science*, 50(4), 402-410.

**Uysal, M.**, Tasdemir, C., Haviarova, E and Gazo, R. (2019). Manufacturing feasibility analysis and load carrying capacity of computer numerical control cut joints with interlocking assembly feature. *Bioresources*, 14(1), 1525-1544.